Modelling optimal plant carbon storage

By

Elisa Zofia Stefaniak

A thesis submitted in fulfilment of the requirements for the degree of Doctor of Philosophy

WESTERN SYDNEY UNIVERSITY

Hawkesbury Institute for the Environment

2021

Acknowledgments

I am grateful for all the support provided to me by my family, friends, and mentors in helping me reach this goal.

My sister, parents and grandparents for their constant presence and cheering.

My aunt for always supporting my education.

Alexie for pushing me through the hard times.

All my friends for being wonderful humans.

Poisson and Silk for providing much needed furry cuddles.

My supervisors and mentors, past and present for their support and guidance. My supervisors Prof. Belinda Medlyn and David Tissue for their patience. My previous supervisors Dr. Remko Duursma and Dr. Roderick Dewar for their help and advice. To all the others who helped, inspired, and welcomed me along the way: Dr. Daniel Falster, Prof. Christopher Kellett, my Society for Mathematical Biology accountability group and the ISWG group.

I want to give special thanks to Prof. Andy Jarvis, who put me on this path, for providing a constant source of inspiration.

Accredited professional editor Mary-Jo O'Rourke AE provided copyediting and proofreading services for the Introduction and Discussion chapters according to the national university-endorsed 'Guidelines for editing research theses' (Institute of Professional Editors, 2019).

Statement of Authentication

The work presented in this thesis is, to the best of my knowledge and belief, original except as acknowledged in the text. I hereby declare that I have not submitted this material, either in full or in part, for a degree at this or any other institution.

Elisa Zofia Stefaniak (11-10-2021)

Table of Contents

ACKNOWLEDGMENTS ..... **I**

STATEMENT OF AUTHENTICATION ..... **II**

LIST OF FIGURES **5**

LIST OF TABLES **8**

ABSTRACT **9**

1 GENERAL INTRODUCTION **11**

1.1 OVERVIEW 11

1.1.1 Plant response to environmental stress *11*

1.1.2 Modelling of carbon storage *12*

1.2 LITERATURE REVIEW 14

1.2.1 Role of non-structural carbohydrates in plant stress response *14*

1.2.2 Investigating whole-plant carbon storage coordination *17*

1.2.3 Carbon source and sink relationships *19*

1.2.4 Progress in modelling NSC *20*

1.2.5 Optimisation modelling *21*

1.2.6 Modelling long-term community dynamics *22*

1.2.7 Modelling optimal carbon storage under changing conditions *24*

1.3 AIMS OF THE STUDY AND STRUCTURE OF THE THESIS 24

2 DYNAMIC OPTIMISATION OF STORAGE IN STRESSED PLANTS **27**

ABSTRACT 27

2.1 INTRODUCTION 27

2.2 METHODS 32

2.2.1 Toy Model *32*

2.2.2 Environment *34*

2.2.3 Parameter Estimation *35*

2.2.4 Fitness Objective *37*

2.2.5 Solution for MaxS ... *39*

2.2.6 Solution for MaxM ... *44*

2.2.7 Numerical Solution of Optimal Switch Time ... *46*

2.3 RESULTS ... 46

2.3.1 Storage Schedule ... *46*

2.3.2 Environmental Conditions ... *51*

2.3.3 Fitness Strategy and Environmental Variability ... *53*

2.4 DISCUSSION ... 57

2.4.1 Active carbon storage explains observed responses of plant growth to drought ... *57*

2.4.2 Factors controlling the optimal allocation trajectory ... *58*

2.4.3 Model limitations ... *61*

2.4.4 Implications for modelling and observations ... *63*

2.5 CONCLUSIONS AND FUTURE WORK ... 65

2.6 APPENDIX: DERIVATION OF OCT SOLUTION ... 66

2.6.1 General solution ... *66*

2.6.2 Detailed solution ... *70*

2.6.3 Special Case: MaxS (kf = 0) ... *81*

2.6.4 Special Case: MaxM (kf = 1) ... *81*

3 EXAMINING THE LONG-TERM IMPACTS OF STORAGE ALLOCATION STRATEGIES IN PLANTS UNDER STOCHASTIC STRESS ... 82

ABSTRACT ... 82

3.1 INTRODUCTION ... 83

3.2 METHODOLOGY ... 89

3.2.1 Model ... *89*

3.2.2 Parameter Estimation ... *97*

3.2.3 Simulations ... *106*

3.2.4 Analysis of Simulation Results ... *107*

3.3 RESULTS ... 108

3.3.1 Effect of stress on final basal area 108

3.3.2 Environment treatment effect on final basal area 111

3.3.3 Drivers of competitive outcome 114

3.3.4 Stress and Mortality 118

3.4 Discussion 121

3.4.1 Effect of environmental stress 124

3.4.2 Modelling Carbon Storage Parameters 125

3.5 Conclusions 128

3.6 Appendix: List of Functions 129

3.7 Appendix: Smoothing piecewise step functions 132

4 ITERATIVE PREDICTIVE OPTIMISATION OF CARBON STORAGE ALLOCATION 133

Abstract 133

4.1 Introduction 133

4.2 Methodology 137

4.2.1 Plant model 138

4.2.2 Environment model 138

4.2.3 Control Framework 141

4.2.4 Simulations 143

4.3 Results 145

4.3.1 Comparison of prediction methods 145

4.3.2 Equivalence of Goal Functions 152

4.3.3 Storage Buffer 153

4.4 Discussion 156

4.4.1 Comparing strategies: capturing realism and CF/MPC viability 157

4.4.2 Parameter sensitivity: storage buffer response 158

4.4.3 Limitations 159

4.5 Conclusions and future work 160

5 SYNTHESIS AND FUTURE DIRECTIONS 162

5.1 SHAPE OF THE OPTIMAL STORAGE UTILISATION TRAJECTORY: RECOMMENDATIONS FOR THE REPRESENTATION OF CARBON STORAGE IN MODELS 162

5.2 LINKING CARBON STORAGE STRATEGIES WITH PLANT FUNCTIONAL TRAITS AND OTHER PROCESSES 164

5.3 REPRESENTING PLANT FUNCTION AS AN EMERGENT CONTROL PROCESS 166

BIBLIOGRAPHY 169

List of Figures

Figure 1-1 Yearly publication numbers of studies on non-structural carbohydrates (NSC) to 8 September 2021. 15

Figure 2-1 Conceptual model of a plant. 32

Figure 2-2 A: Trajectory of the adjunct values over the three phases of optimal growth: growth, storage and stress. B: Values of the storage utilisation rate ut *and the photosynthesis parameter* kp *throughout the three phases of optimal growth.* 42

Figure 2-3 Carbon and water pool trajectories using different switch times (A: $ts \quad 10d$*; B:* $ts \quad 20d$ *and C:* $ts \quad 30d$*) and an initial water availability of* $W0 \quad 1000 kgH2O$*.* 48

Figure 2-4 A: The value of final biomass, MT*, and final storage,* ST*, as a function of switch time* ts *for different initial soil water availabilities.* 49

Figure 2-5 Optimal carbon and water pool trajectories for plants under differing goal strategies (maximising Biomass, A and C, and maximising Storage, B and D) and initial water conditions ($W0 \quad 1000 \ kgH2O$*, A and B, and* $W0 \quad 3000 \ kgH2O$*, C and D).* 50

Figure 2-6 . The relationship between the optimal switch time and time of water depletion and initial water content for (A) maximising storage and (B) maximising biomass. 52

Figure 2-7 The optimal switch time, $ts*$*, and resulting time of water depletion,* $tcrit$*, for the spectrum of fitness proxy parameters* kf *for two initial soil water availabilities:* $W0 \quad 1000 \ kgH2O$ *and* $W0 \quad 3000 \ kgH2O$*.* 54

Figure 2-8 The optimal swtich time ($ts*$*) as determined by the fitness proxy parameter* kf *and initial soil water availability* $W0$*.* 55

Figure 2-9 Point of shift in strategy behaviour between the MaxS safe behaviour and the MaxM risky behaviour as determined by the initial water availability. 56

Figure 2-10 Approximate shape of the solution for the terminal constraint 1a. 73

Figure 2-11 Approximate shape of the solution for the terminal constraint 1b. 78

Figure 2-12 Approximate shape of the solution for the terminal constraint 2b. 80

Figure 3-1 The carbon allocation scheme used in the model. 91

Figure 3-2 The probability density function of for two potential environments: low-stress medium-stochasticity and medium-stress low-stochasticity. 96

Figure 3-3 Sensitivity analysis of a simulated individual to the switch time parameter ts for a range of initial plant heights and storage mass proportions and three values of αs. 102

Figure 3-4 Sensitivity of growth of an individual plant for one year to the storage utilisation rate parameter for different environmental stress treatments, switch time parameters, and initial heights. 103

Figure 3-5 Trajectory of plant height for a single plant using each allocation trajectory and growing without competition under different deterministic stress regimes over a 100 year period. 104

Figure 3-6 Illustration of variability in intra-annual height growth (A) and storage concentration (B) between strategies for a sample year. 105

Figure 3-7 Storage-Growth Trade-offs as represented by the four strategies. 106

Figure 3-8 Final yield as determined by the basal area averaged first across each time point in years 90-100 of data and then by environmental repetition. 110

Figure 3-9 Effect of the stress stochasticity (A) and intensity (B) on the final basal area for different strategies and all strategies combined. 112

Figure 3-10 Height distribution of individuals over 100 years on a 100 m^2 patch 115

Figure 3-11 Total Net Carbon Uptake (NCU) summed across all individuals in a patch of a given strategy across a 100-year time scale on a 100m2 patch. 116

Figure 3-12 Number of individuals of each strategy living on the 100 m^2 patch over time.. 117

Figure 3-13 Stored carbon concentration in individual plants as a rolling 2-year average. 118

Figure 3-14 Proportion of population dying during a stress period (all simulations), as a function of stress duration. 120

Figure 3-15 Relationship between population mortality and light competition for all simulations. 121

Figure 3-16 Summary of model outcomes by plant strategy.. 123

Figure 3-17 A representation of the dynamic function that determines the stress factor for a hypothetical year. 132

Figure 4-1 The Chi-Square distribution determining the likelihood of the amount of rain input in a day. 139

Figure 4-2 An illustration of the Rain Model for the Rain Season and the Dry Season. 140

Figure 4-3 A: Randomly generated rainfall used in evaluating simulations. B: Cumulative water available to the plant with random rainfall. 146

Figure 4-4 Carbon and water pool trajectories obtained from running simulations for the OCT, brute-force optimisation and control frameworks. 147

Figure 4-5 Fitness output evaluation for different model settings with four different goal functions. 148

Figure 4-6 Biomass pool size as a daily average over the simulation (A) and at the end of the simulation (B) for different models and with different fitness goals..... 149

Figure 4-7 Shape of the storage utilisation trajectory over time computed for different models used in the study and across different values of kf..... 150

Figure 4-8 Shape of the storage utilisation trajectory over the simulated period computed for different control framework parameters..... 152

Figure 4-9 Proportion of MaxM-like behaviour predicted for different goal functions kf 153

Figure 4-10 Storage pool size as a daily average over the simulation (A) and at the end of the simulation (B) for different models and with different fitness goals..... 155

Figure 4-11 Storage pool concentration at the end of the simulation, for the MaxM fitness goal..... 156

List of Tables

Table 2-1 Table of variables and parameters used in the model. 36

Table 3-1 Parameters used in the model.. 97

Table 3-2 Summary of Environmental Treatments.. 107

Table 3-3 Effect of stochasticity on the log of the final basal area (m2/ha) for each strategy. 112

Table 3-4 Effect of stress mean on the log of the final basal area per hectare (m2/ha) for each strategy. 113

Table 3-5 List of functions used in the model with references to where they are introduced in the chapter. 129

Table 4-1: The Markov chain used for the rainy season with two states: SD and$R$. 141

Table 4-2: The Markov chain used for the dry season with two states: SD and SR.. 141

Table 4-3 List of parameters and variables used in simulation. 144

Abstract

As sessile organisms, plants are especially vulnerable to a wide range of abiotic and biotic pressures. Moreover, anthropogenic climate change has been causing increased intensity and frequency of stress events. To predict how environmental stress modifies vegetation function, we need to better understand plant stress tolerance mechanisms. One such mechanism is carbon storage: storage of non-structural carbohydrates provides plants with reserves during a stress period and expedites post-stress recovery. However, storing carbon requires an *a priori* action that only has a positive effect on survival during future stress, and may be detrimental, in the short-term, by re-directing carbon from other crucial processes such as growth. In this thesis, I focus on exploring the growth-storage trade-off involved in plant carbon storage in the presence of stress. I employ a range of modelling techniques to mathematically characterise the response of the optimal storage utilisation trajectory (OSUT).

In Chapter 2, I explore the shape of OSUT during a single stress period. It is commonly observed that, during a drought stress period, growth stops before photosynthesis, and storage increases. This pattern is used to infer that storage occurs passively, as an outcome of limitations to photosynthesis and growth. I examine whether this pattern could also be explained as an optimal process that maximises plant fitness and survival under stress (termed "active storage"). Using optimal control theory for a plant with limited soil water availability, I characterise the OSUT for two potential fitness outcomes: maximum biomass (MaxM) or maximum storage (MaxS) at the end of the stress period. In all cases, the OSUT consists of three discrete phases: "growth", "storage without growth", and a "stress" phase where there is no carbon uptake. The OSUT can be defined by the time point when the plant switches from growing to storing. This time point always occurs before the cessation of photosynthesis. These results imply that the common observation that growth always stops before photosynthesis can be interpreted as an optimal trade-off between carbon storage and growth, and that carbon storage may be an active process in a carbon-limited plant.

In Chapter 3, I explore the long-term success of alternative storage strategies for a community of plants experiencing stochastic stress events. I use a gap model to simulate the

outcome of competition among tree species differing in two carbon storage-related traits: the switch time, which emerges from Chapter 2 (risky-safe spectrum), and the storage utilisation rate (fast-slow spectrum). All four possible combinations of the storage traits were used in 100-year simulations of environments differing in stress stochasticity (variance of stress duration) and intensity (average stress duration). In an environment with stress, only the slow-safe and slow-risky strategies survived; mortality caused primarily by depletion of carbon reserves prevented the other strategies from being successful. Increasing stress duration and stochasticity shifted community dominance towards the slow-safe strategies. These findings highlight the importance of carbon storage strategies in the survival of plants during stochastic annual stress and suggest that climate change will impact community composition, favouring trees with storage-prioritising strategies.

Whilst Chapter 2 assumed that the evolved strategy is static, that is unrealistic. Hence in Chapter 4, I explore the acclimation of carbon storage to a stochastic environment. The framework applies model predictive control (MPC) that iteratively computes a short-term OSUT, adopts the first step and updates its prediction to respond to changing environmental conditions. The MPC framework is applied to a simple plant model, coupled with an environmental model consisting of semi-random rainfall modelled as a Markov Process, and results are compared with the OCT model from Chapter 2. Overall, the MPC framework successfully imitated the optimisation framework, but, when maximising biomass, MPC maintained a significant storage buffer, increasing the potential survival of the plant. This chapter demonstrates that the MPC framework can be used to model biological acclimation of time-sensitive processes and is, therefore, a valuable new tool for modelling the effects of climate change in trees and other organisms.

The results presented in this thesis identify candidate storage-related allocation traits that can link carbon storage strategies with other observable plant traits and processes. Such work would be vital in improving the representation of carbon storage in models. Therefore, the findings from this thesis provide new insights into how optimal carbon storage may be modelled and, further, underline the importance of capturing the trade-offs of growth-storage and the effects of stochasticity when exploring the process of carbon storage.

1 General Introduction

1.1 Overview

1.1.1 Plant response to environmental stress

Plants, especially trees as long-lived and sessile organisms, have evolved numerous mechanisms of resilience to stress (Craine et al., 2012). However, increased temperatures, land-use change and anthropogenic climate change are exacerbating the stress regimes experienced by plants (IPCC, 2021; Sheffield & Wood, 2008). Simultaneous stress events are increasingly common (Coumou & Rahmstorf, 2012), leading to increased negative effects on plants (Anderegg et al., 2015; Kayler et al., 2015). For example, higher temperatures can lead to heatwaves, which can amplify drought stress (Alexander, 2016), increase insect breeding (Anderegg et al., 2015) and increase the likelihood and intensity of fires (Adams, 2013; Brando et al., 2019). On the other end of the temperature spectrum, delayed springtime frost events are more common (Zohner et al., 2020) and these events are more likely to co-occur with droughts (Charrier et al., 2021). Tree mortality due to extreme stress events has also been increasing (Adams et al., 2010), while those plants that survive may suffer prolonged damage from stress (Anderson et al., 2018; Birami et al., 2018; Ruehr et al., 2019), leading to higher susceptibility to future stresses and herbivore attacks, and potentially to mortality (Blum & Tuberosa, 2018; Dietze, Matthes, et al., 2014; Trugman et al., 2018).

In turn, these widespread effects can lead to trophic and demographic changes in local plant and animal populations (Mueller et al., 2005; Nadeau & Urban, 2019) with further impacts on the local and regional water, nutrient and CO_2 cycling (Anderegg et al., 2020; Batllori et al., 2020; Kannenberg et al., 2020). This potentially leads to a large positive feedback impacting on the global climate and CO_2 levels (Bahn et al., 2014; Bonan, 2008; Chapin et al., 2008; Field et al., 2007; Reichstein et al., 2013), with increased likelihood of future stresses (Laurance & Williamson, 2001). In extreme cases, particularly in large vegetative regions such as the Amazon basin, boreal forests and the Arctic permafrost, the effects of increased stress can lead to positive climate feedback at a global scale (Bradshaw & Warkentin, 2015; Feldpausch et al., 2016; Field et al., 2007; McLaughlin & Webster, 2014;

Phillips et al., 2009). Stress-induced decreases in plants' carbon (C) uptake, as caused by fires, droughts or heatwaves, can be large enough to turn a region from a C sink into a temporary source of C (Ma et al., 2012; Qie et al., 2017; Yang et al., 2018).

Plants have evolved a wide range of both specialised and general mechanisms for stress resilience and resistance. The study of physiological and biochemical mechanisms for tolerance of stress has enhanced our understanding of stress impacts on plants over the last few decades; for example, Doerner (2020) has investigated the effects of extreme environments, Janni *et al.* (2020) have studied heat stress and Liao and Bassham (2020) have explored the role of hormones. Likewise, in order to improve the accuracy of climate-change projections (Bastos et al., 2020), vegetation-modelling efforts have increasingly focused on improving the understanding of plant responses to stressors such as fires (e.g., WMFire, Bart et al., 2020), droughts (Drewniak & Gonzalez-Meler, 2017; Hartmann, Moura, et al., 2018; Sperry & Love, 2015) and heatwaves (Bastos, 2020; Cochard, 2019; Yiou & Viovy, 2020).

In addition to discovering the biochemichal mechanisms responsible for plant stress responses, it is crucial to understand the plant system and its interaction with the environment at the macro scale (De Kauwe et al., 2017), which can be facilitated by looking at overall plant fitness. As shown by general economic theory, the timing of allocation of scarce resources in plants is crucial (Chapin et al., 1990; Iwasa, 2000; Lerdau, 1992). Plants that can optimise resource use for a particular context, such as drought or winter stress, are more likely to gain a competitive advantage for themselves and their offspring. However, there is a long-term cost to plant fitness associated with defending against stress (e.g., Albrecht & Argueso, 2016; Fine et al., 2006; J. Huang et al., 2019) and response to potential stress must always be balanced against short-term gains.

1.1.2 Modelling of carbon storage

Stored C facilitates the maintenance, recovery and resilience of plants during periods of stress (Chapin et al., 1990). The C assimilated in photosynthesis may be stored as non-structural carbohydrates (NSC) throughout the plant (Kozlowski, 1992) and may remain in storage for periods of a few hours up to several years prior to utilisation (Carbone et al., 2013; Richardson et al., 2013). The size of stored pools of C in plants changes seasonally

(Barbaroux & Breda, 2002; Brum et al., 2021) and varies both between species (Myers & Kitajima, 2007; Würth et al., 2005) and within species from different environments (Bansal & Germino, 2010; Blumstein & Hopkins, 2021; Cao et al., 2018). Moreover, since C storage is a highly dynamic process that is sensitive to phenological as well as environmental stimuli, the timing of processes associated with NSC accumulation and utilisation may be of particular importance (Hartmann & Trumbore, 2016).

Plant coordination of the storage and mobilisation of C is complex and not currently well understood. Landmark review papers published over the last two decades have repeatedly called for increased attention to and improvement of C-storage modelling (Dietze, Sala, et al., 2014; Franklin et al., 2012; Le Roux et al., 2001; Litton et al., 2007; Merganičová et al., 2019). While the versatile nature of stored C is what makes it useful for plant growth and stress response, this is also what makes it a difficult and complex subject to model. Although the number of modelling efforts has been on the rise – with many dynamic global vegetation models (DGVM) increasingly including C storage processes (Merganičová et al., 2019) – there is still no consensus on how C storage should be modelled. One problem is a lack of appropriate data for model development (Dietze, Sala, et al., 2014; Fatichi et al., 2014; Quentin et al., 2015). In addition, modelling the asynchronous nature of storage accumulation and use is especially challenging (Hartmann & Trumbore, 2016; Piper, 2020). Including stored C in models disconnects the source of C in plants (photosynthesis) from the ultimate sinks for C (growth, respiration, reproduction, defence, etc.) by considering the use of C independently from its uptake (Gough et al., 2009). While this separation is important for improving the accuracy of modelling, it also increases the degrees of freedom in a model and ultimately the difficulty of modelling vegetation dynamics.

One way of improving our understanding of how to model carbon storage dynamics is to examine how integrated, whole-plant C storage may be optimised over time in response to stress. Optimisation modelling is a mathematical technique which seeks to describe how the outcomes of certain macro-scale mechanisms (e.g., evolutionary processes) have led to micro-scale mechanisms (e.g., the allocation of C) to meet an optimality criterion such as maximising the Darwinian fitness of the individual (Smith &

Maynard, 1978). The concept of Darwinian fitness is difficult to define, measure and model for long-lived organisms such as trees, so a proxy (or 'optimisation goal') is used instead (Franklin et al., 2012). Outcomes of optimisation modelling can complement the design of experiments and models by identifying a mathematically rational underlying evolutionary reasoning behind the observed or modelled behaviours. Crucially, such optimisation studies can extend our ability to extrapolate process dynamics beyond the limitations of available data.

With respect to C storage dynamics, high concentrations of NSC storage within plants have been theorised to have evolved as a way of enhancing plant fitness in seasonally and stochastically stressful environments by maximising the likelihood of plant survival (Wiley & Helliker, 2012). Dynamic optimisation methodologies (e.g. optimal control theory, OCT) from the calculus of variations (Lenhart & Workman, 2007) provide a mathematical approach to examining temporal dynamics such as C storage.

In the literature review below, I outline current research on the role of NSC in plant responses to stress and on the variation in observed patterns (Section 1.2.1), whole-plant carbon storage coordination (Section 1.2.2), the carbon source and sink dynamics (Section 1.2.3) and highlight progress in the modelling of C storage (Section 1.2.4). I then describe studies showing how optimisation modelling of C resources can enhance the modelling of C storage (Section 1.2.5). Finally, I describe modelling approaches to complement optimisation modelling of C storage: gap models (Section 1.2.6) and model predictive control (Section 1.2.7). I conclude the chapter with an overview of the thesis structure and the research questions that are addressed in this study and outline the approaches I have used to address these in the subsequent chapters (Section 1.3).

1.2 Literature review

1.2.1 Role of non-structural carbohydrates in plant stress response

Two seminal papers (Chapin et al., 1990; McDowell et al., 2008) have triggered an increase in the number of studies on NSC over the last 3 decades (Figure 1-1). The first of these papers presented a theoretical model of the temporal dynamics and trade-offs associated with plant resource storage (Chapin et al., 1990), while the second paper explored plant dynamics during drought, including the role of C storage in resilience to drought (McDowell

et al., 2008). Consequently, the period 1990–2008 saw an increase in the number of studies addressing the role of C storage in relation to other trade-offs such as fast-slow growth (Kobe, 1997) and shade tolerance (Kitajima, 1994; Myers & Kitajima, 2007). Since 2008, however, the focus in the field has been primarily on the role C storage plays during periodic stress such as drought. Below I outline the dynamics of NSC within the plant, followed by a description of their role during and after stress, before addressing some of the questions that still remain about NSC dynamics.

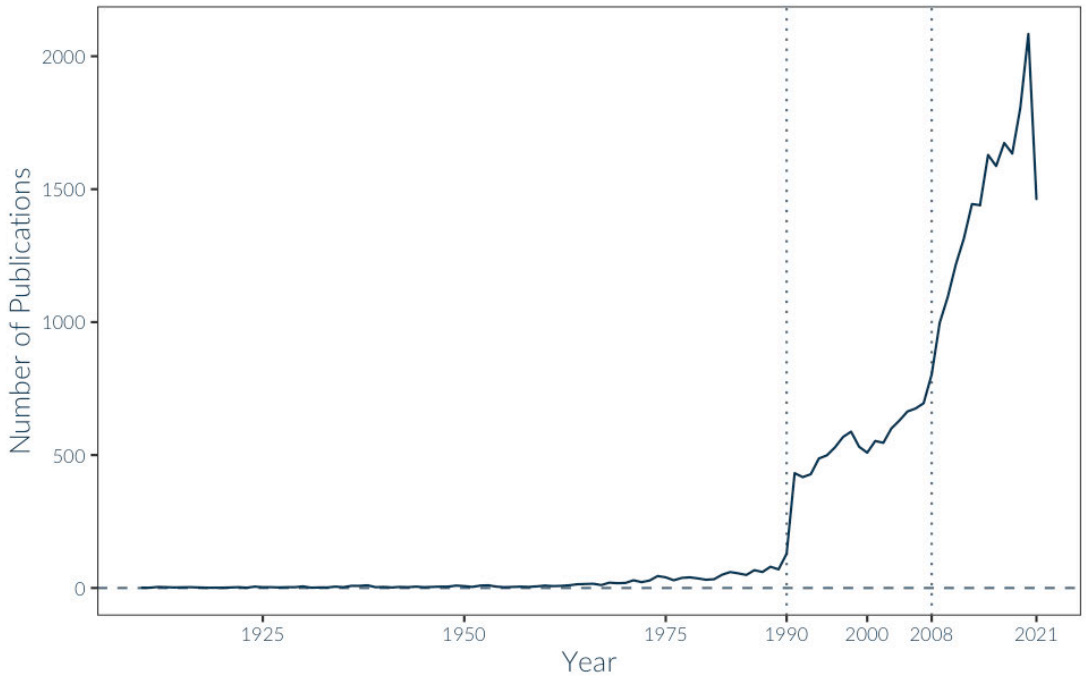

Figure 1-1 Yearly publication numbers of studies on non-structural carbohydrates (NSC) to 8 September 2021. Publication data obtained from Web Of Science using the search query: '((ALL=(non-structural carbohydrate) OR ALL=(carbohydrate) OR ALL=(NSC)) AND (ALL=(plant) OR ALL=(tree)))' and by restricting the results to the top 20 plant-science-related WoS categories. Total number of publications: 31,048. Two marked increases in publication numbers can be observed after the publications of Chapin et al. (1990) and McDowell et al. (2008). Analysed using the bibliometrix R-package (Aria & Cuccurullo, 2017).

Plants store C in the form of NSC, in contrast to structural C within the plant. The use of carbohydrates produced by photosynthesis is twofold: a small portion is used for building tissues within the leaf, while the majority is transported to other organs in the form of highly mobile sugars (Kozlowski, 1992). Once the sugars reach their targets, they are synthesised into long-chained structural carbohydrates such as cellulose to build tissue

outside of the leaf, kept in the form of soluble sugars (SS) or converted into starch. NSC represents the sum of SS and starch. Sugars are the substrates for primary and secondary metabolism, and are thus often stored for use in short-term respiration (Martínez-Vilalta et al., 2016). Starch, a much larger compound, is generally more suitable for long-term storage due to its osmotically inactive nature (Hoch, 2015). NSC, especially starch, are widely accepted as the main proxy for measuring C storage in trees (Dietze, Sala, et al., 2014). Other compounds, such as hemicellulose and lipids, can also function as C storage depending on their mobility (Hoch, 2007). Nevertheless, most studies focus only on the contribution of starch – or more often NSC – to storage, as the contributions of other compounds are generally negligible for most species (Chapin et al., 1990; Hoch et al., 2002).

C storage supplies plants with their energy and construction needs during periods of reduced or suspended photosynthetic activity due to stress. While photosynthesis can generally acclimatise to a wide range of abiotic conditions, it becomes strongly inhibited when the plant experiences conditions outside its tolerance limits. Plant photosynthesis is greatly reduced in most plants in temperatures below 5 °C (Linder & Troeng, 1980). Similarly, heatwaves can inhibit photosynthesis (O'Sullivan *et al.*, 2017). Water stress also inhibits photosynthesis by disrupting the water supply to leaves, causing the plant to close stomata (McDowell et al., 2008). Plants vary in their tolerance to drought (Choat et al., 2012; Zhu et al., 2013) and in the extent to which they regulate their stomata throughout drought in response to hydrological and chemical activity within the plant (an/isohydricity; Tardieu and Simonneau, 1998). Stress can also cause physical damage to plants such as leaf burning during heatwaves (Ruehr et al., 2019). In addition, plants may abscise their leaves when under stress (Munné-Bosch & Alegre, 2004; Wilkinson & Davies, 2002) as a means of avoiding potential energy costs and damage. Recovery from physical damage is initially supported by the mobilisation of NSC (Ruehr et al., 2019) and increased NSC levels are potentially associated with faster post-stress recovery (Tomasella et al., 2017, 2019).

In addition to their energy and construction functions, NSC, chiefly SS, play an important role in enhancing the resistance of plants to stress. Under both drought stress and cold stress, air bubbles called embolisms can form in the transpiration stream. Embolisms disrupt the flow of water, affecting the plant's ability to capture and transport

resources, and can eventually lead to hydraulic failure and mortality (McDowell et al., 2008; Sperry & Sullivan, 1992). Plants accumulate SS to adjust their osmotic properties with the aim of increasing resistance to stress. For example, under water stress, osmotic potential along the water column and within organs is increased in order to improve resistance to embolism (Tomasella et al., 2020). Higher levels of sugar in plant cells decrease their freezing point and make the plant more resistant to damage from cold temperatures (Ruelland et al., 2009). Solute-induced osmotic adjustment also aids in the salt resistance of salt-acclimatised plants (Chaves et al., 2009). Although less studied, differences in the composition of NSC between flood-tolerant and flood-intolerant species suggest that NSC may also play a role in mitigating extreme water stress, if only to support energy needs (Camisón et al., 2020; Delgado et al., 2018). This use of sugars during stress is mediated by the regular transformation between starch and sugar. Most commonly, plants will increase their sugars before winter so as to better tolerate cold and then convert them to starch in spring (Graham & Patterson, 1982). Furthermore, when stressed to the point of mortality, plants may retain high SS concentrations in order to maintain metabolic function, although this can significantly deplete their starch pools (e.g., Dickman et al., 2015; Marler & Cascasan, 2018; Wiley et al., 2017).

1.2.2 Investigating whole-plant carbon storage coordination

Thus, there have been significant advances recently in understanding the biochemical and physiological roles of C storage during plant stress. However, it is more difficult to investigate the temporal dynamics that control whole-plant C storage in anticipation of, during and after periods of stress. Designing experiments that can reveal C storage dynamics is not straightforward, in part due to the destructive nature of sampling and the complexity of integrating whole-tree dynamics (Hartmann et al., 2020; Ryan, 2011). This is further complicated by methodological issues when measuring stored C that can lead to divergent results across labs (Piper & Reyes, 2020; Quentin et al., 2015). Moreover, it is not fully understood how readily stored C is accessible in different plant growth forms or across different organs (Sala et al., 2012). Trees generally tend to use more recently stored C for new root growth (Gaudinski et al., 2009) and bud burst (Ichie et al., 2013) but less recently stored C for recovery from stresses and disturbances (Dietze, Sala, et al., 2014). Clipping

studies suggest that some stored C is sequestered or unavailable to plants (Chapin et al., 1990) but radioisotope measurements revealed that 11-year-old C was used by trees in the Amazon to produce new tissues following severe drought (Vargas et al., 2009). Older C is less likely to be available to plants, due to its location, and can be mobilised only when newer stores become unavailable or depleted, or under extreme abiotic conditions (Galiano et al., 2011). A plant generally utilises the C from the storage location closest to where it is needed, but dieback may occur before the plant is able to mobilise C from more distant locations (Munné-Bosch & Alegre, 2004; Wiley et al., 2017).

A recent synthesis (Martínez-Vilalta et al., 2016) found that plants maintain a minimum level of NSC throughout the year, with no clear differences between organs, plant functional types or biomes. While there is no simple way to measure the minimum amount of NSC, which may be dependent on plant phenology, abiotic conditions and other factors, consistent minimum NSC concentrations support the hypothesis that maintaining C storage is crucial for plant survival and fitness (Wiley & Helliker, 2012).

Data from experimental manipulations and observations of plants under natural stress conditions shows that the responses of plants to abiotic stress and the temporal variations in these responses differ. The responses may be influenced by a number of factors, as explored below. Firstly, the intensity of the stress may influence the response. Drought-stressed plants have been observed to decrease their levels of starch (Mitchell et al., 2013) and total NSC (O'Brien et al., 2015) under conditions of gradual drought and infrequent watering, respectively, as well as during natural drought (Rosas et al., 2013). In contrast, increased total NSC was observed during an extreme drought (O'Brien et al., 2015). Changes in NSC with drought also vary significantly between species: in an experiment involving 5 species, *Quercus rubra* and *Acer rubrum* seedlings subjected to drought showed no change in their NSC concentrations over time, while the remaining 3 species showed decreases (Maguire & Kobe, 2015). Moreover, the dynamics of C storage can also change during a period of stress: *Robinia pseudoacacia* seedlings increased their NSC in the first 10 days of extreme drought stress, but showed significant decrease soon after with NSC levels returning to pre-drought conditions after 20 days and continuing to decrease thereafter (Yang et al., 2019). A similar pattern was also observed in SS in

Eucalyptus globulus subjected to an extreme drought (Mitchell, O'Grady, Tissue, et al., 2014). The stress response may also vary between experimental and natural conditions, although this comparison has not been systemically analysed. However, in natural environments stressed trees generally have a reduced NSC level compared to non-stressed individuals (Piper & Paula, 2020). NSC dynamics also differ between seedlings and mature plants (Hartmann, Adams, et al., 2018 and the studies within). *Quercus virginiana* and *Quercus hemisphaerica* seedlings had much greater fluctuations in diurnal NSC concentration than their mature counterparts (Baber et al., 2014). Another study comparing the drought responses of seedlings and mature trees in 4 subtropical species showed that seedlings generally decreased their NSC pools, while mature individuals kept their NSC levels static (Zhang et al., 2020). Finally, stress responses may vary due to an individual's local adaptation. Gradients of stress suggest that plants are locally adapted to stress (Bansal et al., 2011; Cao et al., 2018; Dolezal et al., 2021), implying potentially significant intra-specific variations in species responses to stress. Furthermore, NSC dynamics may also change following multiple stress events (Atkinson et al., 2014; Galiano et al., 2017), suggesting that plants adjust their storage strategies to new conditions.

1.2.3 Carbon source and sink relationships

Explaining and consolidating these divergent responses in relation to plant NSC dynamics requires the use of conceptual models. Consideration of C source and sink relationships can help to explain the observed patterns. Briefly, the C source refers to the rate of photosynthetic uptake, while the C sink is the demand for C by plant processes such as biomass growth and respiration. Two primary dynamics of storage can be defined which refer to the relationship between C sources and sinks (Chapin et al., 1990). When the C source is larger than the C sink, the plant passively accumulates the excess Carbon in a process termed 'passive storage'. On the other hand, when C is allocated to storage despite demand by the sink, competition for C is observed in a process termed 'active storage'.

To determine the triggers of NSC dynamics, researchers often manipulate either the sink or source strengths of the plant, for example, by manipulating access to light and CO_2 (source manipulation) or by subjecting the plant to abiotic stress such as high and low temperature and drought (sink manipulation). Source limitation can be achieved by

increased shading (e.g., Bahn et al., 2013), decreased CO_2 (e.g., Duan et al., 2018) or defoliating of plants (e.g., Deslauriers et al., 2015) to decrease the amount of C entering the plant. Alternatively, increased CO_2 may be provided to increase the C source (e.g., Bachofen et al., 2018; Clarke et al., 2016), particularly in studies which combine this treatment with sink limitation. Sink limitation can be achieved by lowering the temperature (although primarily explored through field studies, e.g., Li et al., 2018) or decreasing water availability (e.g., da Costa et al., 2010). Alternatively, sink strength can be decreased by limiting rooting volume through pot-size restriction (Mahmud et al., 2018).

However, storage of C, as a transitory compound, can be both a sink and a source at different timescales (Hartmann & Trumbore, 2016), which may contribute to further difficulty in interpreting results. When treated entirely as a sink, C storage is generally considered to be of lowest priority in a plant (Minchin, 2007). Stressed plants often stop growing before they stop photosynthesising, so the accumulation of NSC under stressful conditions is considered a fully passive process (Fatichi et al., 2014; Körner, 2003, 2015). However, studies that have manipulated C sink and source strength observed both passive (Bachofen et al., 2018) and active C storage (Li et al., 2018). Resolving questions about storage dynamics requires models which can fully explore C storage and consolidate its changing behaviours over time.

1.2.4 Progress in modelling NSC

Models are crucial in the endeavour to reconcile the available data on NSC response to stress. Studies which compare model schemes with and without storage pools have invariably shown that a storage pool significantly improves model accuracy (Mahmud et al., 2018; Richardson et al., 2013). As such, C storage is increasingly included in C allocation schemes (Merganičová et al., 2019). However, only just over half of DVGMs include a storage pool (Merganičová et al., 2019), although labile C was used in theoretical models as early as the 1970s in a C allocation model (Thornley, 1972) and in whole-plant and ecosystem models in the late 1980s (Running & Coughlan, 1988) and the 1990s (Friend et al., 1997; Grossman & DeJong, 1994; e.g., Weinstein et al., 1991; Wermelinger et al., 1991).

Due to the lack of consensus on how to model C storage allocation (Dietze, Sala, et al., 2014), there are many approaches to modelling this process. While models

predominantly adopt a single C storage pool (e.g., Fisher et al., 2010), some make a distinction between labile C used for immediate purposes and storage C used for long-term buffering (e.g., Richardson et al., 2013). Another approach is to implement local C storage pools for different plant components (e.g., Allen et al., 2005). Stored C is used exclusively for respiration and growth (Dietze, Sala, et al., 2014) and is occasionally a mortality trigger, for example, relating mortality to low carbohydrate rates in the TRIPLEX model (Liu *et al.*, 2021). The role of storage in osmotic processes is generally ignored even in C allocation models with a greater hydraulic focus (e.g., the TREES model, Mackay et al., 2015). Finally, some models of plant hydraulics use sugar concentration to capture phloem dynamics (De Schepper & Steppe, 2011), but these detailed process representations are generally not adopted in whole-tree models (Hartmann et al., 2020).

Models also vary in the mechanisms posited to govern the allocation and use of C storage. In some models, the accumulation of C storage occurs as a consequence of passive storage and is thought of as a simple overflow buffer (McDowell et al., 2013). Alternative schemes use an active storage allocation model in which storage competes with growth (Richardson et al., 2013). Active storage may be represented as a fraction of the total plant biomass (Fisher et al., 2010) or may be more dynamic, with variable storage-allocation rates (Mahmud et al., 2018). Increasingly, storage dynamics are also being integrated with sink controls. Sink strength is usually defined by the order in which sinks are prioritised, leaves being the top priority and storage the lowest (Guillemot et al., 2017). Environmental controls are placed on the sink strength to increase the realism of the storage model (Jones et al., 2020).

1.2.5 Optimisation modelling

While modelling of C storage is important for improving the accuracy of modelling vegetation, including C storage processes increases the degrees of freedom in the model by increasing the number of model parameters and variables. If there are no clear guidelines as to the whole-tree processes that control C storage such an increase in model complexity may not necessarily increase the accuracy of representing whole-tree C cycling. Optimisation modelling can help address this gap. In biology, optimisation modelling helps explain how a natural process does occur out of the many ways it can occur (Rosen, 2000, p.

201) by providing a powerful constraint on the relationship between available resources and their effects on the plant (Raupach, 2005). To do this, optimisation modelling assumes the overarching goal of maximising plant fitness with respect to the observed variables as constrained by physical limitations. Plant fitness is usually represented by a proxy, or objective function, which is more comprehensible and at times measurable (Franklin et al., 2012). With the appropriate constraints and objective function, optimisation models have been shown to explain a variety of plant behaviours such as the trade-off between photosynthesis and water use (Cowan & Farquhar, 1977), allocation dynamics between roots and shoots (Reynolds & Thornley, 1982) and leaf nitrogen (N) allocation (Field, 1983). Optimisation modelling creates a feedback loop between the objective function and the targeted variables, creating powerful coupling between otherwise unlinked processes.

In modelling of C storage, dynamic optimisation creates a relationship between current plant behaviour and projected plant fitness. In other words, dynamic optimisation using OCT (Lenhart & Workman, 2007) provides a method for finding an optimal behaviour trajectory over time with respect to a future goal. Thus, the temporal asynchronicity between storage accumulation and use can be resolved by linking C allocation over an observed period with a future fitness proxy such as plant size or photosynthetic gain at the end of the period. Dynamic optimisation models which include storage have most often been used to explain reproductive behaviours: finding the optimal time for switching to reproductive behaviour in an annual plant (Chiariello & Roughgarden, 1984) and exploring perennial dormancy and eventual reproduction at maturity using a storage pool to survive through winter (Iwasa & Cohen, 1989). Examining such dynamics further to look at optimal responses to drought stress, a task I undertake in Chapter 2, would greatly aid in helping determine storage dynamics.

1.2.6 Modelling long-term community dynamics

In addition to stress, carbon storage dynamics are further affected by community dynamics and long-term processes. Competition for resources can impose additional stress on already stressed plants and lead to more complex NSC dynamics (Deng et al., 2019) and potentially earlier mortality (Piper & Fajardo, 2016). Moreover, NSC can mitigate the long-term effects of stress, by improving recovery following stress (Ruehr et al., 2019). As such, while a carbon

storage strategy may be optimal in a short-term drought scenario, the combined effects of competition and long-term effects of stress may reduce the efficacy of the strategy with respect to the fitness over a lifetime of an individual.

Gap models, which simulate interspecific population dynamics within a patch of forest subject to a stochastic environment (Bugmann, 2001), can be used to help understand the community dynamics in specific environmental conditions (Bugmann, 1996). In gap models, individual trees are modelled explicitly based on species-specific traits. Therefore, competition for resources, such as light or nutrients, can limit growth and survival of smaller individuals. Plant behaviour and relevant feedback mechanisms can, therefore, be explored and community dynamics and individual fitness become emergent properties of the simulations. Gap models have been used to study mixed-age and mixed-species dynamics, reproducing climate-dependent species coexistence and dynamics in several New Hampshire forest plots (Botkin et al., 1972), effects of fire and high altitude on Australian Eucalyptus-dominated forest ecosystems (Shugart & Noble, 1981) and more recently allowing for short-term forecasts of community dynamics in a range of forest ecosystems in France (Morin et al., 2021).

In addition to reproducing community dynamics of real species and ecosystems, gap models can be used to examine long-term trait- and size- dynamics on emergent community properties (Falster et al., 2016). For example, Falster et al. (2011) examined the effect of varying four plant traits (leaf economic strategy, height at maturation, wood density, and seed size) on commonly observed vegetation properties (average height of leaf area, leaf-area index, net primary productivity and biomass density). In addition to individual-level plant traits the study also looked at landscape properties such as disturbance probability to examine the effect of the environment on emergent properties. Through this study, Falster et al. (2011) were able to determine the contribution of specific traits on the plant community and determine their importance.

Similarly, gap models can be used to bridge the gap between the knowledge on short-term storage dynamics and long-term success. By specifying alternative traits related to a carbon storage strategy, individual strategies can be formulated and simulated over the long-term using gap models. Moreover, in addition to modelling alternative individual

strategies, landscape conditions can be examined to determine the effect of stress intensity on the community. This is undertaken in Chapter 3 to determine the effect of individual strategies on long-term community dynamics in stochastic environments.

1.2.7 Modelling optimal carbon storage under changing conditions

As stress cannot be fully predicted, the optimal response of carbon storage to stress will also be affected by stochasticity. Accounting for variable stress risk is likely to have a notable effect on predicted carbon allocation strategies. For example, models using stochastic dynamic programming (SDP) – an extension of OCT that allows for stochasticity – showed that relationships between stochastic and destructive local events, such as fire, affected the optimal storage-to-foliage ratio (Iwasa & Kubo, 1997), which, in turn, determined the capacity of the plant to recover. However, the statistical tools embedded in SDP focus on the average individual tree response to average environmental conditions. Therefore, SDP makes assumptions about equilibrium dynamics which may not be valid under climate change.

To model the acclimation of tree carbon storage strategy to changing conditions a new framework may be required. Instead of approaching optimal response as dependent "average" conditions, the optimal trajectory may be found by repeatedly computing and updating the optimal trajectory to account for stochastic changes in the environment. This can be achieved by using a method called model predictive control (MPC) which has been successfully applied to engineering (García et al., 1989), economic (Nordhaus, 1993) and policy systems (An et al., 2021) but never before to plant dynamics. MPC can simultaneously simulate plant acclimation to changing conditions and approximate optimal dynamics, allowing us to examine how an optimal carbon storage allocation model may change when stochastic conditions are introduced. The development of a new framework using MPC is undertaken in Chapter 4 of this thesis.

1.3 Aims of the study and structure of the thesis

Finding the optimal allocation trajectory with respect to given environmental conditions and stressors is an important step in determining the asynchronous drivers of C allocation. In this study, I undertake a multifaceted approach to modelling C allocation to storage under stress through the use of different but complementary modelling approaches. I use OCT to

find the optimal storage dynamics for plants subjected to stress (Chapter 2). The OCT results are then used to explore the stochastic effects of stress on individuals in competitive environments (Chapter 3) and how the optimal dynamics may change and adapt to a changing environment (Chapter 4).

I first apply OCT in order to calculate the optimal storage utilisation trajectory (OSUT) in the simple situation of a single drought to predict optimal C storage strategies for plants facing drought (Chapter 2). Moreover, in order to capture variable life history strategies, I look at alternative formulations of the optimisation function to look at plants that maximise their storage pool and plants that maximise their biomass pool, as well as strategies which maximise a particular ratio of biomass to storage size. Finally, to better understand the impact of stress intensity on the plant I vary the water availability to subject the plant to more intense drought conditions to explore how stress intensity controls the allocation trajectory. The insights obtained from this analysis forms the basis for the remaining parts of this work.

One major challenge in applying OCT is in identifying the appropriate objective function to represent plant fitness. I have explored alternative objective functions, but needed a framework within which to understand the outcome of competition that determines fitness. Therefore, in Chapter 3 I use a gap model to model outcomes of competition across species and explore the success of different strategies under different stress regimes. I use OCT predictions to inform an individual-based model of C storage allocation and simulate a stochastic environment in which plants can compete. Since competition imposes an additional stress on individuals by constraining access to resources, individual interaction may be an important factor to consider.

A second major challenge in applying OCT is that it finds a single optimal trajectory which cannot adapt to changing conditions. Therefore, OCT results should be interpreted as the outcome of an evolutionary process adapted to specific conditions, rather than as a continuous system of adaptation. Thus, in Chapter 4 I apply a new method to the field, model predictive control (MPC), which models an updating OCT solution which can adapt to stochastic conditions through simulations, in order to explore MPC's potential for adaptive modelling.

In summary, these approaches to modelling are used in this thesis study to investigate the following 3 research questions:

1. What is the optimal storage strategy for plants faced with drought?
2. How does the optimal storage strategy perform in a stochastic and competitive environment?
3. How might a plant adapt its optimal storage strategy under uncertain future conditions?

2 Dynamic Optimisation of Storage in Stressed Plants

Abstract

Allocation of non-structural carbohydrates (NSC) to storage allows plants to maintain a labile carbon pool in anticipation of future stresses. However, to do so, plants must forego use of the carbon for growth, creating a trade-off between storage and growth. There is debate as to whether carbon storage is an active process, meaning plants have evolved strategies to optimise this trade-off, or a passive process in which carbon storage occurs only once other needs are satisfied. To help distinguish whether carbon storage is an active process, one can predict an optimal storage utilisation trajectory (OSUT) and compare the predictions with appropriate experimental data.

Here, I use optimal control theory to calculate the OSUT over a single drought stress period. I examine two fitness objectives representing alternative life strategies: prioritisation of growth (MaxM) and prioritisation of storage (MaxS), as well as strategies in between these extremes. I show how soil water availability at the start of the stress period affects the OSUT. I find OSUT consists of three discrete phases: "growth", "storage without growth", and the "stress" phase where there is no carbon source. The OSUT can be defined by the time point when the plant switches from growing to storing. Growth-prioritising plants switch later and fully deplete their stored carbon over the stress period while storage-prioritising plants either do not grow or switch early in the drought period. The switch time almost always occurs before soil water is depleted, meaning that growth stops before photosynthesis. Experiments that observe drought-exposed plants cease growth prior to photosynthesis are often taken as evidence for passive storage and a lack of carbon source limitation. However, the results derived here imply that carbon storage during drought can be interpreted as an active process that optimises plant performance during stress.

2.1 Introduction

Carbon storage is a crucial mechanism of plant stress tolerance. When a plant is subjected to abiotic stress, such as drought or cold stress, photosynthetic carbon uptake is limited

(Ferner et al., 2012; McDowell et al., 2008), and the energy required for survival and post-stress recovery must be supplied by non-structural carbohydrates (NSC) stored before the onset of stress (Hartmann & Trumbore, 2016). However, the opportunity cost of storage can be substantial. If carbon is stored rather than allocated to increasing structural or productive biomass, the plant misses the opportunity to increase light capture and photosynthetic capacity (Lerdau, 1992). While carbon that is stored may often be used for growth later, the compounding benefits of early investment in growth are not realised (Bloom et al., 1985).

Growth comes with additional costs: bigger plants have larger metabolic maintenance costs (Mori et al., 2010), while faster growth is often associated with less resistant tissues, such as lower wood density (Eller et al., 2018) or leaf mass per area (Blumenthal et al., 2020; Wright et al., 2004), which are more vulnerable during stress (Onoda et al., 2017). Faster growth means less carbon is kept in storage (Atkinson et al., 2014), which increases plant susceptibility during stress periods, including an increased risk of significant tissue damage (Kreuzwieser & Rennenberg, 2014; Ruehr et al., 2019) and potential mortality (Adams et al., 2017; Allen et al., 2010; Bojórquez et al., 2019; McDowell et al., 2008). To predict the effects of climate change on forest dynamics, it is important to reliably model carbon storage during stress (Ceballos-Núñez et al., 2018; Merganičová et al., 2019; Richardson et al., 2013).

Several approaches to modelling carbon storage have been developed over time. Some models represent the environmental effects of stress on photosynthesis and growth, with storage acting as a passive buffer between these two processes (Fatichi et al., 2012; Leuzinger et al., 2013; Weinstein et al., 1991). Another approach is to assume plants maintain a fixed concentration of stored carbon in live biomass during non-stress periods, with storage accessed during stress periods (De Schepper & Steppe, 2010; R. Fisher et al., 2010; Jones et al., 2020; Medvigy et al., 2009). In more complex models, the utilisation of stored carbon can be primarily sink (growth) dependent rather than source (photosynthesis) dependent (Jones et al., 2020). This approach is equivalent to the assumption of “passive” storage (Chapin et al., 1990), in which the rate of storage emerges as the outcome of environmentally-controlled photosynthesis and growth processes. For example, following

the onset of stress, storage may accumulate because photosynthesis has higher tolerance to abiotic stress than growth; if photosynthesis continues after growth is inhibited, non-structural carbohydrates accumulate in the plant (Ayub et al., 2011).

However, the idea behind passive storage dynamics minimises the role of the trade-off between growth and storage. Models rely on purely environmental triggers for growth and storage dynamics. In reality, there is increasing evidence for complexity in storage dynamics (D'Andrea et al., 2021; Mund et al., 2020) and the existence of a growth-storage trade-off. An alternative theory, called "active" storage, is that plants actively manage the timing of growth to ensure adequate storage during stress periods (Bond & Midgley, 2000; Sala et al., 2012; Wiley & Helliker, 2012). Because the processes of carbon uptake and subsequent storage utilisation are asynchronous (Hartmann & Trumbore, 2016), an understanding of how plants economise the use of carbon over time is crucial for examining this trade-off. Therefore, an alternative approach to predicting storage during stress may be to assume plants are actively managing storage to optimise the growth-storage trade-off.

One way of doing this is to use dynamic optimisation modelling to predict carbon allocation to storage under stress. Rather than assuming *a priori* values for parameters that determine model behaviour, optimisation modelling finds the values of the parameters that maximise a pre-defined goal function over some observed period. Assumptions are, therefore, moved from an empirical framework to an evolutionary one. One example of the successful application of optimisation theory has been to predict plant stomatal conductance from the hypothesis that stomata are regulated to maximise daily photosynthetic gain for a given amount of water loss (Cowan & Farquhar, 1977). Cowan and Farquhar's analysis led to an explanation of diurnal stomatal behaviour, including the observation that photosynthetic activity dips around midday. This behaviour could not previously be explained by responses to abiotic conditions: photosynthetic assimilation is highest during midday when temperatures and transpiration are highest. It follows, therefore, that midday photosynthesis would be preferred if the process were evaluated instantaneously, independent of diurnal dynamics. Instead, when water costs are evaluated against photosynthetic gain over a diurnal scale, dynamic optimisation models predict peak activity in the morning and evenings, thereby explaining the observed patterns of stomatal

behaviour (Buckley, 2005; Damour et al., 2010; Medlyn, Duursma, Eamus, et al., 2011). Theoretical advances such as these have led to the development of more accurate photosynthetic models, as well as assisting in experimental design to explore the effects of stress on plant function (e.g., Manzoni et al., 2011; Wolf et al., 2016).

In the same way that optimisation modelling has helped explain physiological processes, it can be used to provide insight into carbon allocation, storage, and utilisation. One simple theory of optimal resource allocation suggests that plants should allocate carbon towards growing the organ responsible for the most limiting resource, e.g. allocation towards roots when nutrient uptake is limiting (Bloom et al., 1985; Chapin et al., 1987). This "functional balance" hypothesis is supported by data for numerous species (Buckley, 2021; Qi et al., 2019; van der Werf et al., 1993). Optimal response models have also been developed to predict biomass allocation by assuming plants maximise photosynthetic uptake (McMurtrie et al., 2008), growth (Franklin, 2007) or net primary production (NPP, Mäkelä, Valentine, and Helmisaari 2008), using annual to decadal time-steps.

A model to optimise the carbon storage and utilisation rate needs to consider time explicitly because carbon storage decouples growth from photosynthesis (Hartmann & Trumbore, 2016), and because the benefits of carbon storage only become apparent under future stress. The optimal time course can be identified using a method from the Calculus of Variations called optimal control theory (OCT, Lenhart & Workman, 2007). The OCT method can be used to calculate the optimal trajectory of selected variables, such as allocation parameters, which optimise fitness outcomes over a time course, rather than at a given point in time. For example, Cowan & Farquhar's optimisation approach used OCT to maximise the sum of photosynthesis over a day. Theoretical analysis of plant allocation patterns using OCT has mostly focused on using reproductive efforts as a proxy for plant fitness. For example, OCT has been applied to determine the optimal balance between root and shoot allocation that maximises reproductive output (Iwasa & Roughgarden, 1984; McMorris, 2020), and to determine the optimal time course of storage in both annual and perennial plants (Chiariello & Roughgarden, 1984; Iwasa & Cohen, 1989). Another example of OCT application found the optimal allocation of carbon to fungal partners in a mutualist

relationship with plants that maximised plant growth (Moeller & Neubert, 2016). OCT is a promising technique to examine active storage utilisation trajectories.

Fitness is traditionally associated with reproductive output (Johansson et al., 2018) which is difficult to quantify and model (Obeso, 2002; Oddou-Muratorio et al., 2018, 2020). In nature, plants use a number of different life history strategies that maximise their fitness (Bryant, 1971). For example, seed size (Muller-Landau, 2010), rate of growth (Rose et al., 2009), and colonization strategy (Rüger et al., 2018, 2020) all contribute to the overall fitness of an individual over its lifetime. At shorter timescales, proxies that do not directly contribute to reproduction, must be considered. For example, when a single drought event is considered, the plant may prioritise survival over reproductive effort. To do that, a plant can vary its carbon storage versus utilisation rate, otherwise referred to as the growth-storage trade-off (Myers & Kitajima, 2007). Therefore, plants may maximise growth or storage during stress as a proxy for their life history strategy.

Depending on the complexity of the modelled problem, OCT can provide either a tractable, analytical solution to the dynamics of carbon allocation to storage, or a numerical solution. A toy model can be used with OCT to examine the dynamics of active carbon storage. A toy model is a simplified model that captures some dynamics of carbon allocation to storage under stress, but with reduced complexity to make solution of the problem more tractable. The aim of this work is to provide insight into the optimal active storage allocation under stress. By applying OCT to a toy model representing a plant subjected to a simple drought stress regime, the optimal dynamic allocation patterns can be calculated for a range of environmental conditions and fitness assumptions. The aims of this chapter are therefore to:

1. Create a toy model that describes plant carbon storage and growth under drought stress
2. Apply OCT to predict the optimal pattern of optimal storage utilisation trajectory (OSUT) under drought stress
3. Examine how the optimal pattern of storage utilisation varies with different fitness objectives and environmental conditions

2.2 Methods

2.2.1 Toy Model

The purpose of a "toy" model is to examine a physiological process by restricting a model to only those elements that are necessary to explore the process. Therefore, the approach taken is not to describe the process comprehensively, or precisely, in physiological or molecular terms, but to capture the main features as simply as possible. Here, I use a simple representation of plant carbon uptake and use, including stored carbon accumulation and utilisation. Crucially, all processes captured are modelled as linear processes which allows for the creation of a tractable model.

The plant is represented simply, with only two carbon pools: biomass (M) and storage (S), which are affected by the biological processes of photosynthesis (A), respiration (R), and growth (G). There is also a single soil water pool (W) which is reduced by evapotranspiration (E; see Equation 2-1 and Figure 2-1).

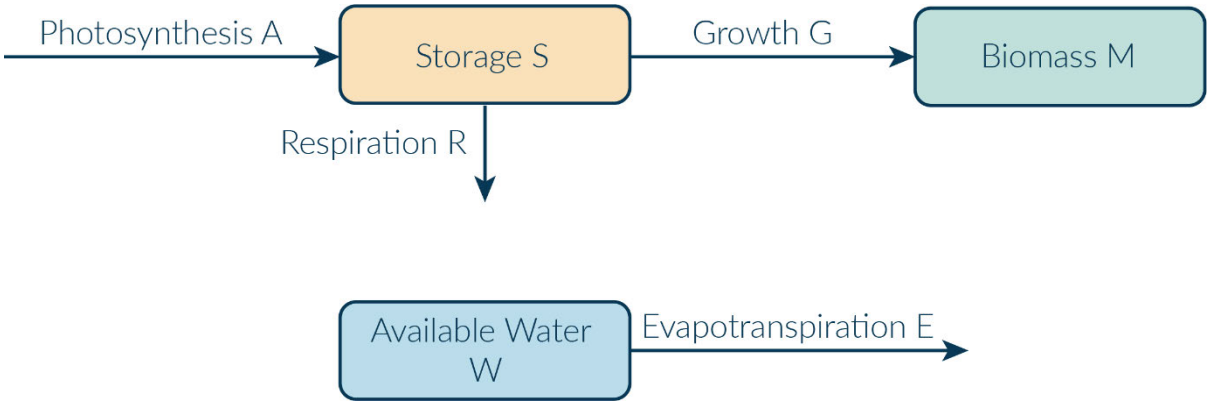

Figure 2-1 Conceptual model of a plant. The model consists of two carbon pools (storage, yellow and biomass, green) and a single water pool (blue). Storage (S) represents available labile carbon that can be used for respiration (R) or growth (G) of the plant. Photosynthetic uptake (A) is first delivered to storage to later be utilised for respiration and growth of biomass. The Available Water pool is depleted through evapotranspiration as the plant photosynthesises.

The model represents photosynthesis, water use, and growth during a drought period. The soil water pool W is defined as the amount of water available for use by the plant. There is no water input during the drought and, therefore, the only water available to the plant is the initial available water, W_0. The lower this initial value is, the less water is available to the plant during the drought period and, thus, the higher the stress applied to the plant.

For simplicity, plant biomass, M, is represented as a single pool, and not differentiated into different tissue. The storage pool S consists of the labile carbon, which can be used for respiration or building biomass. The maintenance respiration rate depends on biomass. Biomass growth depends on the size of the storage pool and size of the storage utilisation rate u_t which determines the proportion of stored carbon utilised for growth. The time course of "utilisation of stored carbon to biomass" is flexible, and can be optimised, using OCT, once the fitness objective is defined.

The storage pool can be increased through photosynthesis (A), can be used for respiration (R), or utilised for growing biomass (G). This is captured in Equation 2-1:

$$f_S = \dot{S} = A - R - G \tag{2-1}$$

Further, the model specifies that biomass M is changed only through increases in biomass G:

$$f_M = \dot{M} = G \tag{2-2}$$

Briefly, the individual processes are modelled as linear processes based on the size of the biomass M and the storage pool S. Specifically, photosynthesis A is directly proportional (by the photosynthesis parameter k_p) to the amount of biomass M:

$$A = k_p M \tag{2-3}$$

Likewise, the model specifies respiration R to be directly proportional to the amount of biomass M with a respiration parameter k_r:

$$R = k_r M \tag{2-4}$$

The plant moves carbon from the storage pool S to biomass G at the storage utilisation rate u_t:

$$G = u_t S \tag{2-5}$$

The maximum of the storage utilisation rate u_t is given by the maximum storage utilisation parameter k_s:

$$0 \leq u_t \leq k_s \leq 1 \tag{2-6}$$

A plant is considered alive only while its storage pool S is greater than or equal to zero, which in turn is equivalent to final storage size being greater than or equal to zero (further explained in Appendix 2.6):

$$S_t \geq 0 \Rightarrow S_T \geq 0 \quad (2\text{-}7)$$

If a plant's storage pool S goes below zero, it is considered dead.

2.2.2 Environment

At the outset, the plant enters a deterministic drought period of length T with a specified initial soil water pool (W_0). No additional water is supplied during the observed period and post-drought conditions are ignored. The plant uses up the soil water as it photosynthesises through the water use parameter k_w:

$$f_W = \dot{W} = -\mathrm{E} = -k_w A = -k_w k_p M \quad (2\text{-}8)$$

k_w can be considered as the inverse of the water use efficiency (Bierhuizen & Slatyer, 1965; Sinclair et al., 1984). The soil water pool is constrained within the model to always be positive:

$$W_t \geq 0 \quad (2\text{-}9)$$

Photosynthesis is dependent on the water availability. The photosynthesis parameter k_p is a constant when the available soil water is positive and becomes zero when W goes to zero:

$$k_p = \begin{cases} 0 \text{ when } W = 0 \\ k_p^* \text{ when } W > 0 \end{cases} \quad (2\text{-}10)$$

The time at which the available water goes to zero is denoted t_{crit}.

In order to satisfy the plant's metabolic requirements when the plant is photosynthesising, the photosynthetic gain must be greater than metabolic costs. This is implemented by constraining the value of k_p^*:

$$k_p^* > k_r \quad (2\text{-}11)$$

2.2.3 Parameter Estimation

Table 2-1 lists the relevant parameters, with units and baseline values. Values are derived from a study by Drake et al. (2019) in which young *Eucalyptus tereticornis* trees were exposed to factorial warming x rainfall reduction treatments in whole-tree chambers for 15 months. Parameters were obtained from the control treatment trees. The drought length T was set to 150 d.

From height and diameter increments reported in the experiment, together with data for the final dry matter (12 kg mass approximated to 6 kg C), a linear growth rate was approximated (305 g C/month) resulting in an estimation of a plant size at the start of the observation of 3.85 kg C. This total plant size was then distributed between the storage pool S and the biomass pool M. The total NSC concentration varies greatly both within and among *Eucalyptus* tree components: between 6% and 31% in leaves (e.g., Aspinwall et al., 2016; Chen et al., 2020); 5% and 12% in stem wood (e.g., Chen et al., 2020; Mitchell, O'Grady, Tissue, et al., 2014); and up to 22% in below-ground organs (e.g., Mitchell, O'Grady, Tissue, et al., 2014; Smith et al., 2018). Here, a ratio of 1:6 for the initial S: M was estimated as an average that accounts for this variability in pool concentrations and the contribution of individual pools to the total biomass.

In Drake et al. (2019), respiration per unit mass varied between 0.02 g C g^{-1} C d^{-1} and 0.12 g C g^{-1} C d^{-1}. It exhibited a linear relationship with relative growth rate. The respiration range, in this case, includes both growth and maintenance respiration, but the model does not differentiate between respiration types. A conservative value of $k_r = 0.06$ gC g^{-1}C d^{-1} was chosen as the respiration parameter. In the same study, the total plant respiration was approximately 0.3 of GPP. Since, in the model, both respiration and photosynthesis are linear functions of biomass, the photosynthetic parameter, k_p^*, was derived as $k_p^* = \frac{k_r}{0.3} = 0.2$ gC g^{-1}C d^{-1}.

The maximum storage utilisation parameter, k_s, is derived from the relative growth rate (RGR) value and the aforementioned 1:6 ratio between the storage and biomass pools. With the RGR value in the Drake et al. (2019) study estimated between 5 and 15 mg C g C^{-1}

d^{-1}, the mid-point of this rate is taken and further divided by the ratio between storage and biomass (1/6) to give a value of $k_s = 0.06\ \mathrm{gC\ gC^{-1}\ d^{-1}}$.

The values for the initial water availability, W_0, and the water utilisation parameter, k_w are derived from the water use during the experiment. In the Drake et al. (2019) study, plants in the drought treatment used an average of 1,000 kg H_20 in the first 4 months. Thus, the simulation used a value of $W_0 = 1{,}200\ \mathrm{kgH_2O}$ to account for the additional month. The water utilisation parameter was calculated by dividing the water loss rate by the carbon uptake rate using results from the period of the experiment when the plant was not stressed. This yielded a value of $k_w = 0.4\ \mathrm{kg\ H_2O\ g^{-1}C}$.

Table 2-1 Table of variables and parameters used in the model.

Symbol	Units	Value (if applicable)	Description
Carbon and Water Pools			
S_t	$\mathrm{gC\ plant^{-1}}$	-	Storage carbon pool
S_0	$\mathrm{gC\ plant^{-1}}$	550	Initial storage carbon pool
M_t	$\mathrm{gC\ plant^{-1}}$	-	Biomass carbon pool
M_0	$\mathrm{gC\ plant^{-1}}$	3,300	Initial biomass carbon pool
W_t	$\mathrm{kg\ H_2O\ plant^{-1}}$	-	Available soil water pool
W_0	$\mathrm{kg\ H_2O\ plant^{-1}}$	1,200	Initial soil water pool
Time parameters			
T	d	150	Simulated drought length
t_s	d	-	Time of switch from allocating carbon to biomass to allocating carbon to storage
t_{crit}	d	-	Time at which soil water pool runs out
Process parameters			
k_p	$\mathrm{gC\ g^{-1}C\ d^{-1}}$	-	Photosynthesis parameter (Equation 2-10)
k_p^*	$\mathrm{gC\ g^{-1}C\ d^{-1}}$	0.2	Maximum value of the photosynthetic parameter
k_r	$\mathrm{gC\ g^{-1}C\ d^{-1}}$	0.06	Respiration parameter
k_w	$\mathrm{kg\ H_2O\ g^{-1}C}$	0.4	Water use parameter
k_s	$\mathrm{gC\ g^{-1}C\ d^{-1}}$	0.06	Maximum storage utilisation parameter

u_t	$gC\ g^{-1}C\ d^{-1}$	-	Storage utilisation rate
k_f	-	0 - 1	Fitness proxy parameter

2.2.4 Fitness Objective

Evolutionary theory posits that, given sufficient time, species will evolve that maximise evolutionary fitness (Parker & Smith, 1990). Fitness in this case is defined as the overall reproductive success, which includes the survival of all offspring produced in their lifetime. However, because reproductive success is exceptionally challenging to estimate for long-living species such as trees, use of a proxy is common (Franklin et al., 2012). Here, I consider two fitness proxies: maximising biomass and maximising storage at the end of period T.

One potential optimisation target is the biomass at the end of the stress period (Φ_M; herein MaxM):

$$\Phi_M = M_T \tag{2-12}$$

This proxy can be taken to represent fitness because the plant with the largest biomass at the end of the stress period can potentially outcompete its neighbours and provide increased carbon to reproduction. However, this optimisation target must be subject to the plant maintaining a sufficiently large storage pool such that the storage pool S does not become negative during the stress period (in which case, as stated above, the plant would be considered dead). This proxy may best represent fitness when plants experience a short stress period and rely on a continued supply of immediate carbon through photosynthesis for reproduction (sometimes referred to as “income breeding”, Stearns, 1989). Maintaining a large biomass pool would, therefore, increase current assimilates that can be redirected to reproduction post-stress. It would also enhance fitness in environments where plants experience “predictable” stress (e.g., seasonal) and the plant can maintain a sufficiently large storage pool buffer to survive. Storing additional carbon may be detrimental to fitness when the approximate length and intensity of stress is unlikely to vary much year to year. Therefore, carbon that is not used will incur a cost to potential competitive and reproductive effort.

However, the total biomass at the end of a stress period may not represent fitness in environments which experience more intense, or uncertain, stress. An alternative fitness

proxy considered here is, therefore, to the final storage at the end of the stress period (Φ_S; herein MaxS):

$$\Phi_S = S_T \tag{2-13}$$

The final size of the storage pool can be taken to represent fitness because a large storage pool at the end of the stress period can be used to recover after the stress event and may increase carbon available for reproductive effort following stress. Post-stress, plants can redirect stored carbon to reproduction (a strategy referred to as "capital breeding", Stearns, 1989) thus increasing their evolutionary fitness (Kozlowski, 1992). However, reproduction is not explicitly included in the model, which focuses on survival during a single stress period. Increased growth can become detrimental to the plant as additional biomass will increase costs, thus decreasing storage and potential carbon for reproduction. However, while a smaller plant might have increased survival chances as a result of this strategy, it is less likely to perform competitively against plants with strategies maximising their competitive output through growth. Thus, the MaxS strategy is more advantageous when the stress risk is significant enough to warrant a large storage pool and benefits to reproduction can accumulate over a lifetime.

The two alternative fitness proxies may represent fitness in different environments, but they may also be thought of as representing different life-history strategies. Variations in life-history strategies are often observed within a single environment, both in terms of individual traits, but also the individual position on a trade-off spectrum (Clark et al., 2007; Rüger et al., 2020). The MaxM and MaxS strategies differ in their trade-offs to stress risk, survival, and overall benefits to lifetime reproduction. Hence, we can consider MaxM to be a "risky" strategy and MaxS to be a "safe" one. In the following chapter, I examine the competitive interactions among these different strategies. However, in this chapter I examine one long-term overall fitness objective at a time and identify the allocation strategy that maximises that fitness objective. In addition to MaxM and MaxS, I also consider fitness objectives that are linear combinations of these two objectives:

$$\Phi_{k_f} = k_f M_T + \left(1 - k_f\right) S_T \tag{2-14}$$

Where k_f is the fitness parameter taking on a value between 0 and 1. Clearly, MaxM and MaxS are special cases of Φ_{k_f} with $k_f = 1$ and $k_f = 0$, respectively. This work examines the special cases as well as the effect of intermediate range of k_f values.

2.2.5 Solution for MaxS

The approach taken here is to initially find the optimal allocation trajectory (u_t) which maximises the final storage pool ($J = \Phi_S$; where J refers to the function being maximised). I solve it using the Pontryagin Maximum Principle (Boltyanskii et al., 1960) from optimal control theory (Lenhart & Workman, 2007; Stengel, 2012). Following the definition of the analytical expressions which form a solution for the MaxS problem a simulation (numerical solution) approach is undertaken.

Below, I explain how the Hamiltonian, the state dynamics, and the optimal trajectory are defined. Full derivation of the solutions is given in Appendix 2.6.

The three state dynamics (f_S, f_M and f_W , Equations 2-1, 2-2 and 2-8 respectively) are referred to in optimal control vernacular as "dynamic constraints". They are used to define the Hamiltonian as:

$$\mathcal{H} = \lambda_M f_M + \lambda_S f_S + \lambda_W f_W + \mu_W c_{eff_W} \begin{cases} \mu_W = 0 \text{ if } c_{eff_W} < 0 \\ \mu_W \geq 0 \text{ if } c_{eff_W} = 0 \end{cases} \quad (2\text{-}15)$$

The three adjunct variables (λ_M, λ_S and λ_W) each correspond to one of the dynamic constraints. The water constraint is represented by the last term in Equation 2-15, in which μ_W is the Lagrange multiplier corresponding to the water constraint "in effect" (i.e., the constraint is being satisfied), c_{eff_W}:

$$c_{eff_W} = -W_t \leq 0 \quad (2\text{-}16)$$

A partial derivative of the Hamiltonian, with respect to the corresponding state variable, can be used to find the dynamics of the adjunct variables. As such, the dynamics for the adjuncts are:

$$\dot{\lambda_M} = -\frac{\partial \mathcal{H}}{\partial M} = -\lambda_S(k_p - k_r) + \lambda_W k_w k_p \quad (2\text{-}17)$$

$$\dot{\lambda_S} = -\frac{\partial \mathcal{H}}{\partial S} = u_t(\lambda_S - \lambda_M) \quad (2\text{-}18)$$

$$\dot{\lambda_W} = -\frac{\partial \mathcal{H}}{\partial W} = \mu_W \begin{cases} \mu_W = 0 \text{ if } -W_t < 0 \\ \mu_W \geq 0 \text{ if } -W_t = 0 \end{cases} \quad (2\text{-}19)$$

Moreover, the terminal adjuncts can be found by partially differentiating the goal function by the corresponding state:

$$\lambda_{M_T} = \left.\frac{\partial \Phi_S}{\partial M}\right|_{t=T} = 0 \quad (2\text{-}20)$$

$$\lambda_{S_T} = \left.\frac{\partial \Phi_S}{\partial S}\right|_{t=T} = 1 \quad (2\text{-}21)$$

$$\lambda_{W_T} = \left.\frac{\partial \Phi_S}{\partial W}\right|_{t=T} = 0 \quad (2\text{-}22)$$

When possible, the optimal trajectory for u_t is estimated in a similar way to the adjunct dynamics: a partial derivative of the Hamiltonian with respect to u_t set to 0 ($\frac{\partial \mathcal{H}}{\partial u_t} = 0$), which will give a value for maximising the Hamiltonian with respect to u_t. Therefore, unless u_t appears only in linear functions, this expression can be used to derive an expression for optimal u_t.

However, because u_t only appears in *linear* relationships in the model, I apply the Pontryagin Maximum Principle: I find the conditions under which $\mathcal{H}$ is maximised through observing the Hamiltonian dependence on u_t directly, rather than through a partial derivative. This involves finding the part of the Hamiltonian which is dependent on the control u_t and choosing boundary values that will maximise the result:

$$u_t^* = \arg \max_{u_t\ S,M,W,\lambda_S,\lambda_M,\lambda_W} \mathcal{H} \Rightarrow \arg \max_{u_t\ S,\lambda_S,\lambda_M} u_t S(\lambda_M - \lambda_S) \Rightarrow u_t^* = \begin{cases} k_s & \text{if} \quad \lambda_M > \lambda_S \\ 0 & \text{if} \quad \lambda_S > \lambda_M \end{cases} \quad (2\text{-}23)$$

This indicates that the behaviour of the trajectory follows the so-called “bang-bang” behaviour (Lenhart & Workman, 2007), where the control variable (the optimal storage utilisation rate, u_t^*) takes on only the minimal or maximal value within the allowed bounds.

Following on from Equation 2-23, I can find the optimal solution by solving the adjuncts backwards. Three scenarios must be considered. First, either water is limiting, and therefore the soil water pool is depleted at or before the end of the simulated period ($W_T = 0$). Second, water is not limiting, and the soil water pool is not depleted at the end of the simulation ($W_T > 0$). Finally, water availability is inadequate, and the plant “dies” during the simulation. In such a case, water is depleted before the end of the season ($W_t = 0$),

photosynthesis ceases, and the storage pool is insufficient to support the plant ($S_T < 0$). This scenario breaks the constraints of the model but a boundary value of W_{0min} can be defined such that water is limiting ($W_T = 0$) and storage is depleted at the end of the simulation ($S_T = 0$).

When explaining the solution (see Results, below), I first consider the water limiting scenario ($W_T = 0$) and then discuss the implications for the non-limiting water scenario and the inadequate water scenario as well as other implications which emerge from the analysis.

Because the adjuncts inform the value of u_t^*, we can start with calculating the adjuncts backwards. Equations 2-20, 2-21 and 2-22 specify the terminal conditions of the adjuncts. From Equation 2-23 we know that $u_t^* = 0$. Because $W_T = 0$ we can also deduce that $k_p = 0$. This indicates that the adjunct dynamics for the final period of the simulation are:

$$\dot{\lambda_M} = -\frac{\partial \mathcal{H}}{\partial M} = k_r \tag{2-24}$$

$$\dot{\lambda_S} = -\frac{\partial \mathcal{H}}{\partial S} = 0 \tag{2-25}$$

$$\dot{\lambda_W} = -\frac{\partial \mathcal{H}}{\partial W} = \mu_W \begin{cases} \mu_W = 0 \text{ if } -W_t < 0 \\ \mu_W \geq 0 \text{ if } -W_t = 0 \end{cases} \tag{2-26}$$

Thus, both λ_M and λ_W are increasing and λ_S remains constant for the duration of this period. Since, at the end of this phase, λ_S is higher than the other two adjuncts, at no point during this phase will λ_S meet λ_M, a condition for a change in the behaviour of u_t^*. Instead, the only thing that can happen is that the beginning of this period is marked by water availability going to zero with the onset of stress, t_{crit}. The boundary for the final, stress, period is, therefore, $t_{crit} < t \leq T$. Figure 2-2 illustrates the behaviour of the adjuncts throughout the simulation.

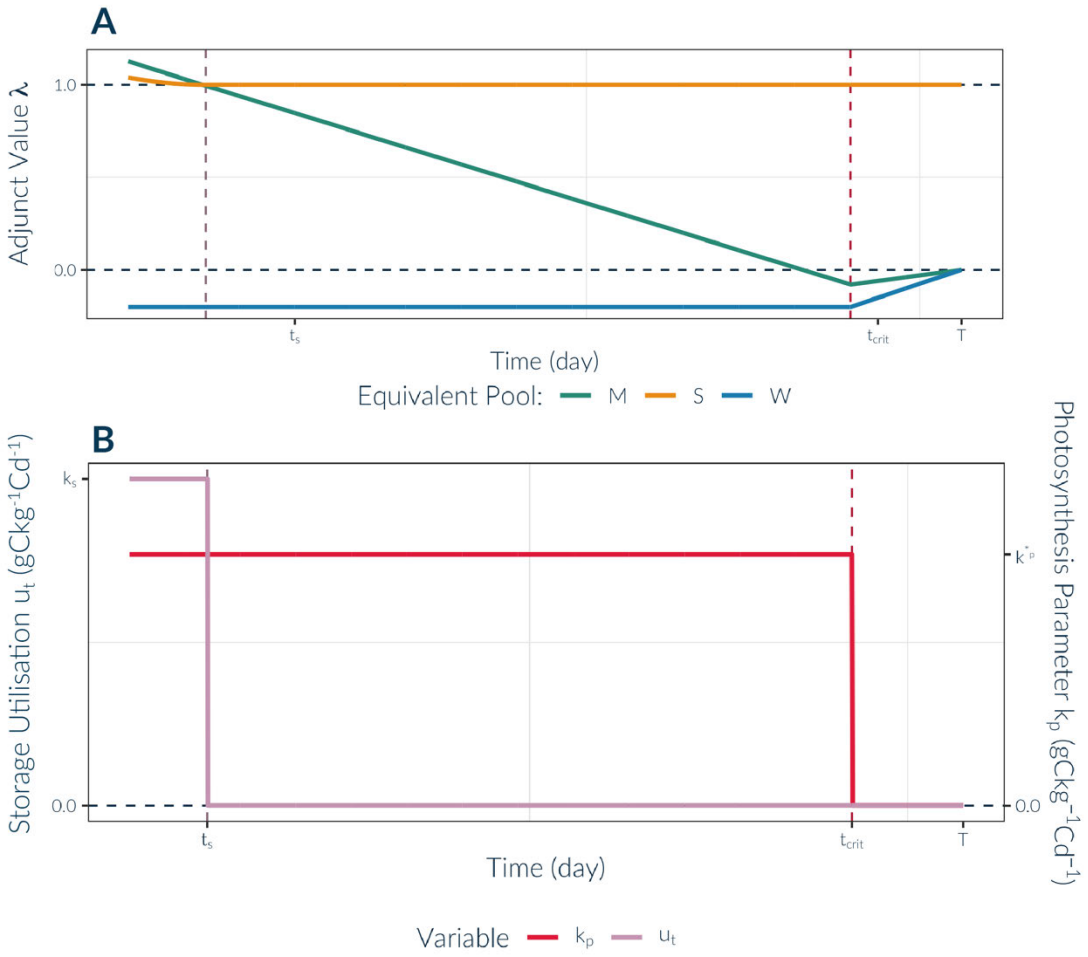

Figure 2-2 A: Trajectory of the adjunct values over the three phases of optimal growth: growth, storage and stress. B: Values of the storage utilisation rate $\boldsymbol{u_t}$ and the photosynthesis parameter $\boldsymbol{k_p}$ throughout the three phases of optimal growth.

Immediately prior to the stress period is the period during which the plant depletes the soil moisture. For the duration of this period, the plant has sufficient water and therefore $k_p = k_p^*$. Since $\lambda_S > \lambda_M$ we can further deduce that $u_t = 0$. Therefore, the adjunct dynamics for this period are:

$$\dot{\lambda_M} = -\frac{\partial \mathcal{H}}{\partial M} = \left(k_p^*(\lambda_W k_w - 1) + k_r\right) \tag{2-27}$$

$$\dot{\lambda_S} = -\frac{\partial \mathcal{H}}{\partial S} = 0 \tag{2-28}$$

$$\dot{\lambda_W} = -\frac{\partial \mathcal{H}}{\partial W} = 0 \tag{2-29}$$

Again, the trajectories of the adjuncts, specifically λ_S and λ_M, must be determined since they determine the control parameter. While λ_S remains constant for this period, λ_M

decreases linearly (as λ_W is negative and $k_r < k_p^*$). Therefore, at the beginning of this middle period λ_S and λ_M are equal. The boundary for this middle period is: $t_s < t \leq t_{crit}$. In this middle period, the plant has access to soil moisture but does not grow; I therefore call this period the storage period.

Prior to the storage period, $\lambda_S < \lambda_M$ and carbon allocation can occur ($u_t^* = k_s$). I call this period the growth period. The adjunct dynamics are:

$$\dot{\lambda_M} = -\frac{\partial \mathcal{H}}{\partial M} = -\lambda_S\left(k_p^* - k_r\right) + \lambda_W k_w k_p^* \quad (2\text{-}30)$$

$$\dot{\lambda_S} = -\frac{\partial \mathcal{H}}{\partial S} = k_s(\lambda_S - \lambda_M) \quad (2\text{-}31)$$

$$\dot{\lambda_W} = -\frac{\partial \mathcal{H}}{\partial W} = 0 \quad (2\text{-}32)$$

No other changes occur within the adjunct dynamics that would suggest the crossing of the two storage and biomass adjuncts. Therefore, it can be determined that there are no further stages within the simulation.

In general, therefore, there are three periods that can be distinguished in the optimal trajectory: growth, storage, and stress. They can be characterised as:

- Growth: $t < t_s$, $u_t^* = k_s$, $W_t > 0$
- Storage: $t_s < t \leq t_{crit}$, $u_t^* = 0$, $W_t > 0$
- Stress: $t_{crit} < t < T$, $u_t^* = 0$, $W_t = 0$

This is the general solution for the optimal trajectory. As explained above, there are two special cases where the trajectory differs from this three-stage trajectory: 1) water is never limiting ($W_T > 0$); 2) initial water availability is insufficient to support the plant, and death occurs. Moreover, there also may be a third alternative trajectory: there is enough water for the plant to survive but not to support any growth if the fitness goal is to maximise storage.

In the first special case, only the first two stages of the three-stage growth will be observed: growth and storage. The value of W above which water is not limiting for the MaxS fitness goal (herein $W_{0,Smax}$) can be found by looking for the value of t_s where there is

no additional benefit to storing ($t^*_{s,Smax}$; this value can be found numerically) and solving for the required water:

$$W_{0,Smax} = k_p k_w \int_0^{t^*_{sSmax}} M_t \mathrm{dt} + M_{t^*_{sSmax}} k_p k_w (T - t^*_{sSmax}) \quad (2\text{-}33)$$

In the second case, no growth is observed. The minimum initial water availability, W_{0min}, below which the plant is not viable can be found by solving for the W_0 that gives rise to $S_T = 0$ while not supporting any growth to the plant ($t_s = 0$):

$$W_{0min} = k_w(k_r M_0 T - S_0) \quad (2\text{-}34)$$

In the third case, the optimal $t_s = 0$, in which case there will be no growth stage, only the storage and stress stages. The value of the initial water availability below which this special case occurs can be calculated by looking at the amount of water required to satisfy the plant's photosynthetic demand if it remains at its initial size for the entire period of the simulation, given by:

$$W_{0store} = k_p k_w M_0 T \quad (2\text{-}35)$$

The Appendix 2.6 contains the detailed derivation of this value and further details of the derivation of the optimal control trajectory for the MaxS and other Φ_{k_f} strategies.

2.2.6 Solution for MaxM

The MaxM is solved in a similar fashion as MaxS but two changes must be applied:

First, the storage constraint (Equation 2-7) must be explicitly adjoined onto the MaxM goal function, J'_M, as a Lagrange multiplier:

$$J'_M = M_T + \nu S_T \quad (2\text{-}36)$$

where ν is the Lagrange multiplier corresponding to constraint in Equation 2-31, noting that ν is positive.

While the adjunct dynamics remain the same (i.e., there are no changes to the dynamic constraints or the constraint during the simulation run), the terminal adjunct values will be different to account for the changes in the goal function and the end point constraint:

$$\lambda_{M_T} = \left.\frac{\partial \Phi_S}{\partial M}\right|_{t=T} = 1 \quad (2\text{-}37)$$

$$\lambda_{S_T} = \left.\frac{\partial \Phi_S}{\partial S}\right|_{t=T} = \nu \quad (2\text{-}38)$$

$$\lambda_{W_T} = \left.\frac{\partial \Phi_S}{\partial W}\right|_{t=T} = 0 \quad (2\text{-}39)$$

In order to see if the solution to this problem follows a similar trajectory to the MaxS trajectory, the relationship between λ_{S_T} and λ_{M_T} must be established. Again, I first consider the case where there is no water at the end of the simulation. In this case, no photosynthesis can be enforced in the last period. If $\lambda_{M_T} > \lambda_{S_T}$ and the plant is allocating to biomass during the last period, little benefit is given to the plant, but its metabolic costs are increased. Instead, it's more likely that $\lambda_{M_T} < \lambda_{S_T}$ and the three-stage growth pattern is observed as per the MaxS solution. With regards to the dynamics of the adjuncts, the final solution will also include the same three phases: growth, storage and stress separated by t_s and t_{crit}.

As with the MaxS solution, alternative trajectories can be described based on initial water availability for which the behaviour of the system may vary from the 3-phase growth pattern (growth – storage – stress). These cases are: 1) initial water availability is insufficient to support the plant, and death occurs; 2) there is enough water for the plant to survive but the amount of water is insufficient to support any growth with respect to the goal of maximising final biomass; 3) water is limiting ($W_T = 0$) but growth is supported from stored carbon such that the time of water depletion (t_{crit}) and growth cessation (t_s^*) is reversed ($t_{crit} < t_s^* < T$) but a plant must still experience a storage phase; 4) water is limiting ($W_T = 0$) but the plant is able to grow throughout the entire simulation ($t_{crit} < t_s^* = T$); and, finally, 5) water is never limiting ($W_T > 0$);

Firstly, if the initial water availability is too low, the plant will not survive; the minimum water availability for survival (W_{0min}) can be found as per Equation 2-34. W_{0min} also satisfies special case (2) and any value above W_{0min} will follow the established 3-phase growth pattern.

For initial water availability above W_{0min}, cases (3), (4) and (5) can be found by defining the boundary conditions in terms of the relationships between t_s^*, t_{crit} and T. The

first of these values I term W_{0rev} to indicate the time point at which t_s^* and t_{crit} become reversed. The second, the necessary water for which the plant grows for the entirety of the simulation, is referred to W_{0grow}. Both W_{0rev} and W_{0grow} must be obtained numerically.

The final case, the value above which the plant is no longer stressed, $W_{0,Mmax}$, can be found analytically by looking at the water value necessary for the plant to sustain growth for the entirety of the simulation ($t_s^* = T$):

$$W_{0Mmax} = k_p k_w \int_0^T M_t \mathrm{dt} \tag{2-40}$$

2.2.7 Numerical Solution of Optimal Switch Time

The analytical solution described above demonstrates that the optimal trajectory consists of maximum storage utilisation up to an optimal switch time t_s^* followed by zero storage utilisation. Thus, the optimal trajectory can be summarised in terms of the value of t_s^*. Here, I solve the value of t_s^* numerically, using a simulation approach applied to the simplified model (Equations 2-1 to 2-11). The classic Runge-Kutta method is explicitly implemented to solve the model in continuous time using a time-step size of $\Delta t = 0.1d$. The approach generates storage and biomass trajectories for all possible values of t_s (0 – 150 days). From these results, I find the t_s value that gives the maximum value of the goal function. Given the bang-bang solution obtained analytically, this t^* value will give the optimal trajectory within the given time resolution. The source code for this simulation is freely available at the repository https://github.com/foxeswithdata/StoringForDrought.

2.3 Results

2.3.1 Storage Schedule

2.3.1.1 Description of the general solution

The emergence of the two dividing time points, the time switch t_s and the time of water depletion t_{crit}, leads to a three-phase storage utilisation strategy, illustrated for a range of t_s values in (Figure 2-3). In the first phase ($0 < t < t_s$), i.e., the *growth* period, the plant uses a proportion of the storage it has available to growing its biomass, thus increasing subsequent photosynthate production (A). During this time, biomass and storage grow exponentially while water is being used up at an increasing rate as the biomass growth leads to exponential water loss.

During the second stage ($t_s < t < t_{crit}$), the *storage* period, the utilisation rate goes to zero thereby halting any biomass growth. Respiration costs are continuous throughout this period but are smaller than photosynthetic uptake, leading to a linear increase in storage. The available water also decreases linearly.

At $t = t_{crit}$ the water runs out and photosynthesis stops. For the remainder of the simulation ($t_{crit} < t < T$), the *stress* period, the plant must support its respiration requirement by drawing on any stored carbon. The storage pool decreases linearly for the remainder of the simulated period.

2.3.1.2 Effect of t_s on the final biomass and storage pool sizes

The time of the switch, t_s, dictates the plant's final biomass pool size, storage pool size, time of water depletion, and ultimate survival. A plant which switches to storing earlier has a higher final storage pool but lower final biomass (e.g., $t_s = 10\mathrm{d}$, Figure 2-3A) compared to a plant that switches later (e.g., $t_s = 20\mathrm{d}$, Figure 2-3B). On the other hand, switching to storing too late leads to the plant dying (e.g., $t_s = 30\mathrm{d}$, Figure 2-3C) as the storage pool is insufficient to support respiration through the stress period.

The effect of the switch time on the fitness objective (as described by Equation 2-14) is further illustrated in Figure 2-4 for a range of values of the k_f life strategy parameter and two different stress regimes (initial water availability of $1000\ \mathrm{kg\ H_2O}$ and $3000\ \mathrm{kg\ H_2O}$). The fitness objective for the MaxM strategy, ($k_f = 1$), the final biomass size, increases as the switch time increases. The fitness objective for the MaxS strategy, $k_f = 0$, the final size of the storage pool, decreases as the switch time increases for lower values of the initial water availability (e.g., $W_0 = 1000\mathrm{kgH_2O}$ in Figure 2-4A). However, for higher initial water availabilities (e.g., $W_0 = 3000\mathrm{kgH_2O}$ in Figure 2-4B), there is a small initial increase in final storage as switch time increases before the decrease in final storage. Goal outcomes for combinations of final biomass and final storage ($0 < k_f < 1$) lie in between these two extremes. Moreover, a later switch time also decreases the time it takes for the plant to run out of water (Figure 2-4C).

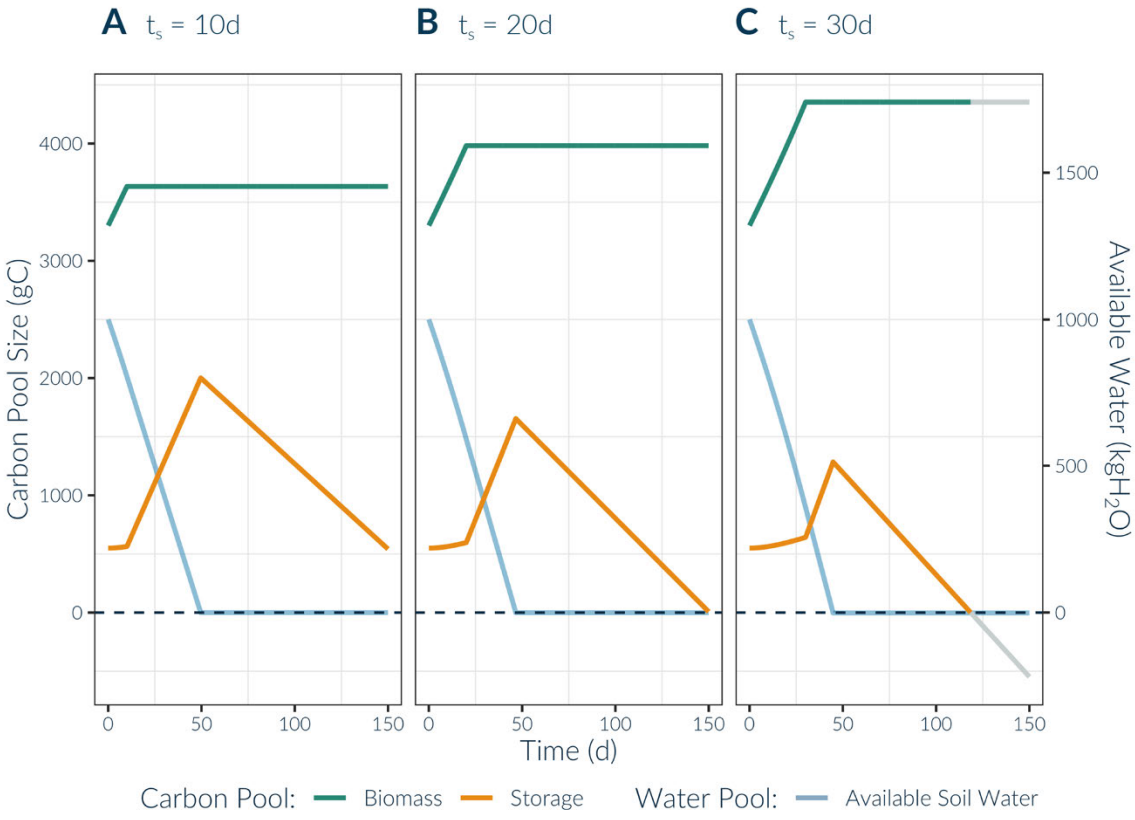

Figure 2-3 Carbon and water pool trajectories using different switch times (A: $t_s = 10\text{d}$; B: $t_s = 20\text{d}$ and C: $t_s = 30\text{d}$) and an initial water availability of $W_0 = 1000\text{kgH}_2\text{O}$. The biomass pool (green line) increases until the switch time and then remains constant for the rest of the simulation. The storage pool (yellow line) increases gradually before the switch time. After the switch time, it increases linearly until the point at which the water runs out. It then decreases at a constant rate until the end of the simulation. With an early switch time (A, $t_s = 10\text{d}$), some storage remains available to the plant at the end of the simulation. A later switch time (B, ($t_s = 20\text{d}$) leads to all the stored carbon being used up. Finally, in the third case (C, $t_s = 30\text{d}$) there is not enough storage to keep the plant alive until the end of the simulation. The plant dies once the storage is used up (gray line).

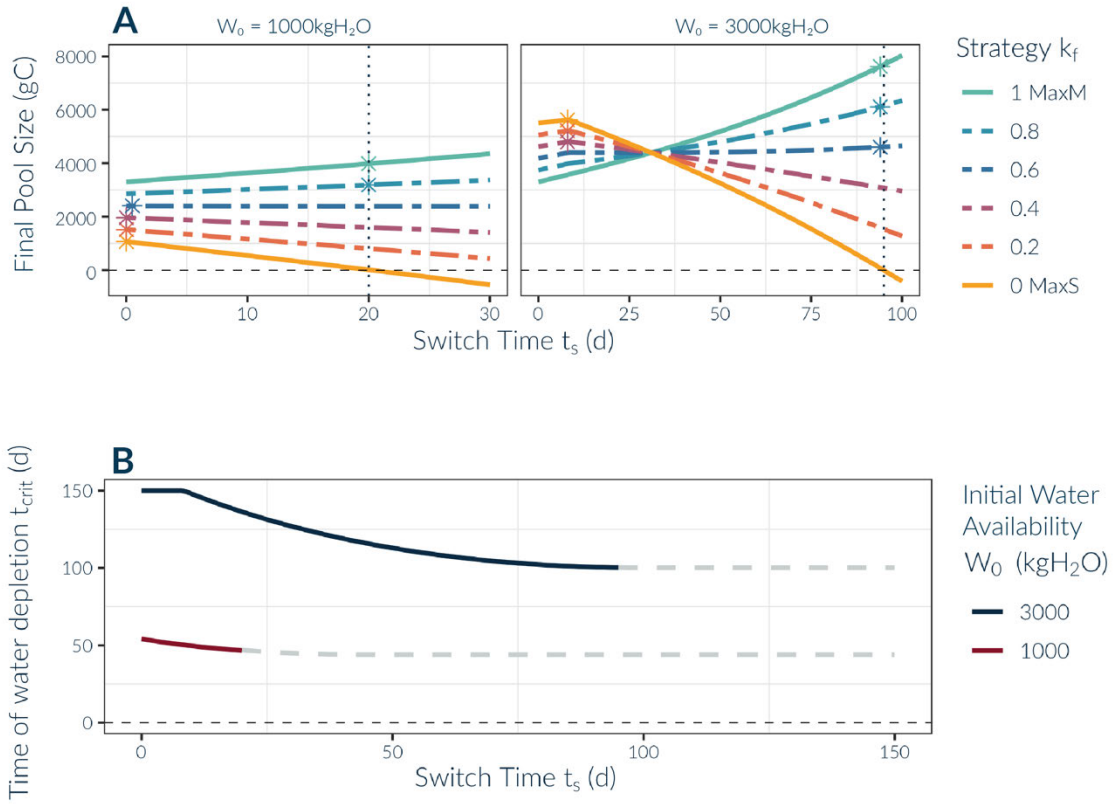

Figure 2-4 A: The value of final biomass, M_T, (solid green; $k_f = 1$) and final storage, S_T, (solid yellow; $k_f = 0$) as a function of switch time t_s for different initial soil water availabilities ($1000\text{kgH}_2\text{O}$; $3000\text{kgH}_2\text{O}$). Each dot-dashed line represents an intermediate strategy Φ_{k_f}, where $\Phi_{k_f} = k_f M_T + (1 - k_f) S_T$. Vertical dotted line represents the point beyond which the switch time will cause plant death ($S_T < 0$). Stars indicate the optimal switch point for each strategy. B: relationship between time of switch and time of water depletion for two different values of initial soil water availability. Gray dashed line indicates values of switch time for which the plant cannot survive.

2.3.1.3 Optimal Storage Schedule: MaxM and MaxS cases

A value of $t_s = t_s^*$ can be found that satisfies the constraints of the model (Equations 2-7, and 2-9) and maximises the final value of the biomass pool, MaxM, or the storage pool, MaxS, thereby giving the optimal solution with respect to each fitness goal (Figure 2-5).

For the MaxM strategy, the optimal schedule involves high values of t_s^* and fast water depletion. A later allocation switch means there is more time for the plant to accumulate biomass, which increases the risk of storage pool depletion by the end of the simulation. This behaviour is inherent to the optimal solution: if a given switch time has leftover carbon in storage at the end of simulation, this carbon is "wasted" (in simulation terms) as it could have been allocated to increase growth instead and thus delaying the allocation switch time. Thus, in general, the optimal schedule has zero storage at the end of

the simulation. One exception to this is when there is some carbon stored at the end of the simulation but the remaining time in the observed period is too short to deplete it.

Increasing the initial water availability, W_0, leads to a later optimal switch time (e.g., 20.1 days versus 94.9 days for $W_0 = 1000\text{kgH}_2\text{O}$ and $W_0 = 3000\text{kgH}_2\text{O}$) and a significant increase of the final biomass size due to the extended exponential growth. It can also be observed that the optimal storage period decreases with increased initial water availability (Figure 2-5A and C).

A different optimal behaviour is observed for the MaxS strategy. The growth period is minimised; for lower initial water availabilities no time is allocated for growing, $t^* = 0$, (eg. Figure 2-5B). This implies only a two-phase growth is observed: the plant immediately stops growing, and the two phases involved are storage and stress.

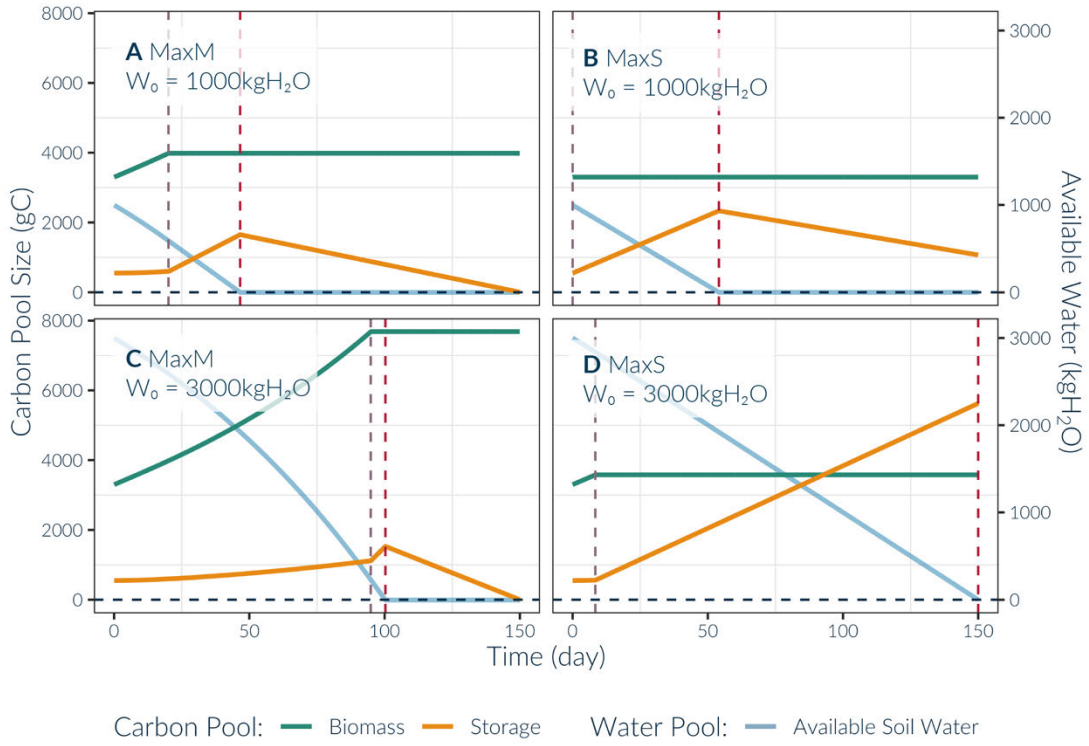

Figure 2-5 Optimal storage utilisation and water pool trajectories for plants under differing goal strategies (maximising Biomass, A and C, and maximising Storage, B and D) and initial water conditions ($W_0 = 1000\ \text{kgH}_2\text{O}$, A and B, and $W_0 = 3000\ \text{kgH}_2\text{O}$, C and D). Vertical purple dashed lines indicate the optimal switch time, t_s^*, and the red vertical dashed lines indicate the time the water runs out, t_{crit}.

Once water availability becomes high enough ($W_{0store} = 2772\text{kgH}_2\text{O}$, Equation 2-35) a two-phase growth is observed with the final (stress) phase omitted. The plant first

grows and then stores for the rest of the simulation period; water is depleted at the end of the simulation ($t_{crit} = T$; Figure 2-5D).

2.3.2 Environmental Conditions

When t_s^* is used as the one-dimensional proxy for the optimal allocation schedule of individual life strategies, it is possible to find how the initial water availability (W_0) impacts this optimal allocation trajectory (Figure 2-6).

There is a minimum initial water availability, W_{0min}, that is required for the plant to survive the drought period, as defined in Equation 2-34. This threshold is the minimum water required for the plant to survive given no allocation to biomass ($t_s = 0$) and with no stored carbon leftover at the end of the drought period ($S_T = 0$). For the parameter values in Table 2-1, $W_{0min} = 572\ \mathrm{kgH_2O}$.

For the MaxM strategy, there are five different cases depending on the initial water availability. In the first case ($W_0 < W_{0min}$), the plant cannot survive because the initial water availability is below the minimum required. Therefore, there is no viable optimal schedule.

In the second case ($W_{0_{min}} < W_0 < W_{0_{rev}}$), a three-phase growth is observed: 0 < $t_s^* < t_{crit} < T$. In this case the plant grows for a period and then switches to storing before running out of water and becoming stressed. In the optimal storage schedule, the stored carbon is depleted at the end of the simulation ($S_T = 0$; Figure 2-6B). $W_{0_{rev}}$ can be calculated numerically to be $W_{0rev} = 3700\ \mathrm{kgH_2O}$. In the third case ($W_{0_{rev}} < W_0 < W_{0growth}$), there is a three-phase growth, but stress and storage switch times are reversed ($t_{crit} < t_s^* < T$) and a phase of growth during stress can be observed. It can also be observed that the stored carbon is still depleted at the end of the simulation ($S_T = 0$; Figure 2-6B). $W_{0growth}$ can be calculated numerically to be $W_{0growth} = 4700\ \mathrm{kgH_2O}$.

The fourth case ($W_{0growth} < W_0 < W_{0Mmax}$) sees the growth period extended over the entirety of the growing period ($t_s^* = T$) and overlapping with the stress period ($t_{crit} < T$). This implies a 2-phase growth period: growth and growth during stress with no storage period observed. Additionally, storage is no longer depleted at the end of the simulation ($S_T > 0$).

For the fifth case ($W_0 > W_{0Mmax}$), no more changes in final storage and biomass pools are observed and both time of switch, t_s, and water loss, t_{crit} are at their maximum, meaning $t_{crit} = t_s^* = T$. This value of W_{0Mmax} can be found numerically to be $W_{0Mmax} = 5808\ \mathrm{kgH_2O}$.

The MaxS strategy has 4 cases (Figure 2-6A). The first case is the same as the MaxM case: $W_0 < W_{0_{min}}$ in which the plant cannot survive. In the second case ($W_{0min} < W_0 < W_{0store}$), a two-phase growth is observed with the plant not allocating any C to biomass ($t_s^* = 0$) and water is depleted by the end of the simulation ($t_{crit} < T$). W_{0store} can be found to be $W_{0store} = 2772\ \mathrm{kgH_2O}$.

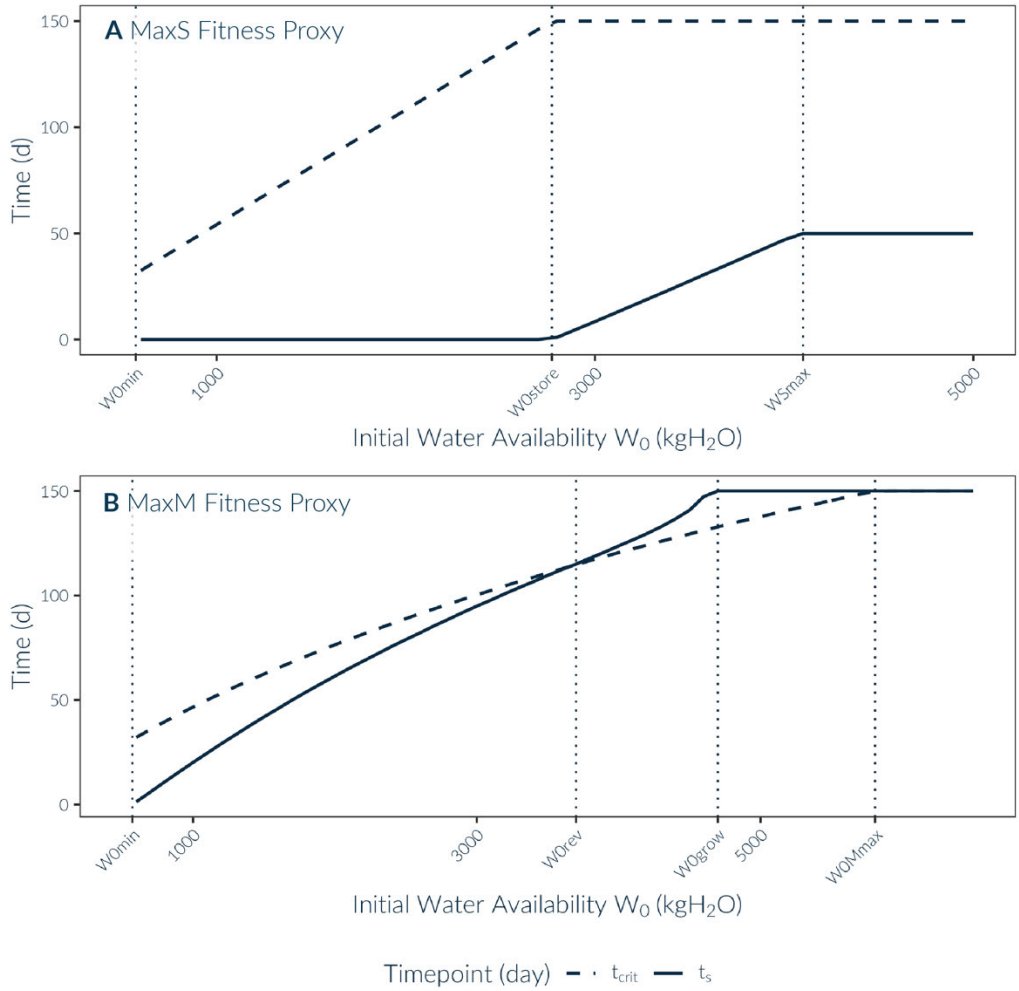

Figure 2-6 . The relationship between the optimal switch time (solid line) and time of water depletion (dashed line) and initial water content for (A) maximising storage and (B) maximising biomass. Vertical dotted lines indicate the values of initial water content that demarcate different model behaviours for each strategy. Note that the x-axis limits are different between the two plots.

The third case ($W_{0store} < W_0 < W_{0Smax}$) has a three-phase growth ($t_s^* > 0$) and the available water is depleted at the end of the simulation ($t_{crit} = T$). In the fourth case ($W_0 > W_{0Smax} = 4075\ \mathrm{kgH_2O}$), the plant no longer runs out of water ($W_T > 0$) and thus was considered not stressed. However, unlike the "not stressed" case with the MaxM strategy, the plant will still stop growing at some value of $t_s^* < T$ because additional growth might lead to decreased storage (see Figure 2-4B). The value of this time of switch, t_s^*, is 49.9d. However, the benefit of the extra growth at the beginning of the simulation period is small. For water availabilities above W_{0Smax}, when comparing between the optimal trajectory which switches at $t_s^* = 49.9\mathrm{d}$ and one that does not grow at all ($t_s^* = 0\mathrm{d}$), there is only an 8% increase in the final storage size.

2.3.3 Fitness Strategy and Environmental Variability

Other intermediate strategies lie between the boundary strategies MaxM and MaxS. These fitness strategies are denoted by the fitness proxy parameter k_f. The solutions for these intermediate strategies are shown in Figure 2-7 for two different initial water availabilities ($W_0 = 1000\mathrm{kgH_2O}$ and $W_0 = 3000\mathrm{kgH_2O}$). These optimal solutions don't fall on a spectrum, but rather follow either the trajectory for the MaxM or the MaxS strategy. This outcome suggests that although there is a range of fitness strategies, k_f, there are essentially only two optimal storage schedules: to either allocate as much as possible and deplete the storage ("risky" schedule) or allocate little to biomass and accumulate storage ("safe" schedule).

As the initial water availability increases, the border between the two optimal storage schedules shifts: risky schedules are optimal for a wider range of fitness goals. This outcome is further examined in Figure 2-4A, where Φ_{kf} result (that is the final carbon pool given by Equation 2-14) are presented for a range of switch time values. The pool sizes either increase with lengthened growing time or decrease depending on the proportion of final storage and biomass size in the final carbon outputs. For larger values of W_0, the size increases first peaked at the MaxS optimal t_s^*. Later, size decreased for strategies that followed MaxS and increased for strategies that followed MaxM behaviour.

These trends are consistent for the entire spectrum of W_0 values that encompass the drought conditions (Figure 2-8) and it can be further seen that the border between the two

alternative strategies decreases with higher W_0 but stays within the range of $0.5 < k_f < 0.7$ (Figure 2-9).

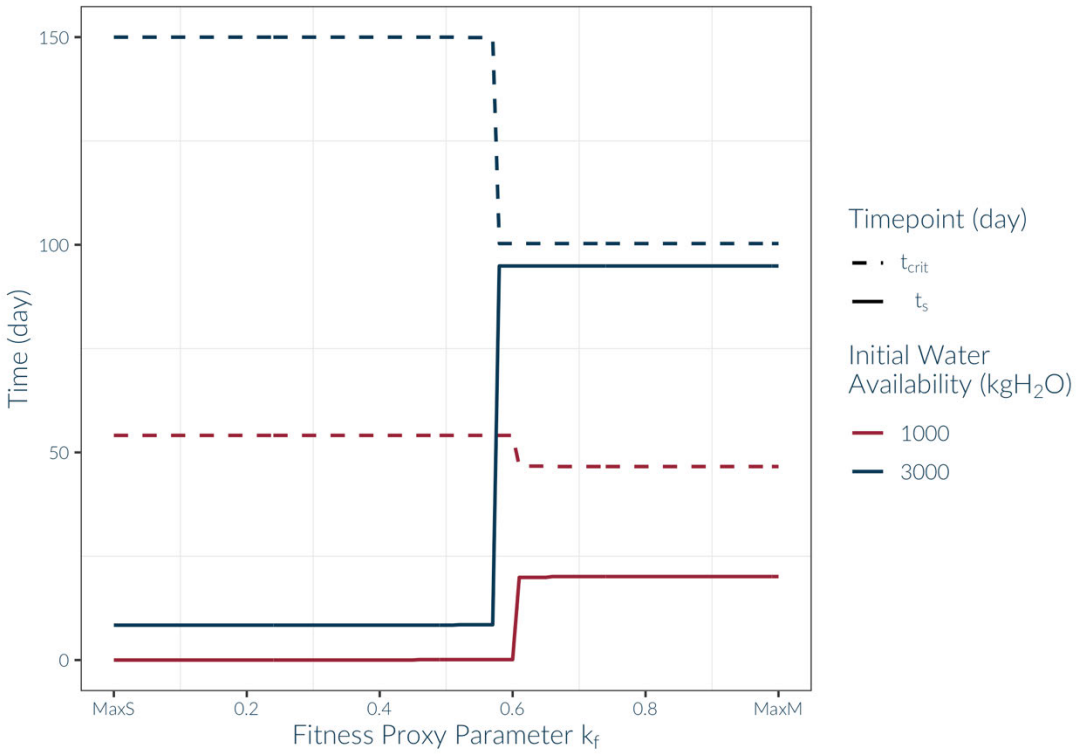

Figure 2-7 The optimal switch time, t_s^* (solid line), and resulting time of water depletion, t_{crit} (dashed line), for the spectrum of fitness proxy parameters k_f for two initial soil water availabilities: $W_0 = 1000\ \mathrm{kgH_2O}$ (red) and $W_0 = 3000\ \mathrm{kgH_2O}$ (blue).

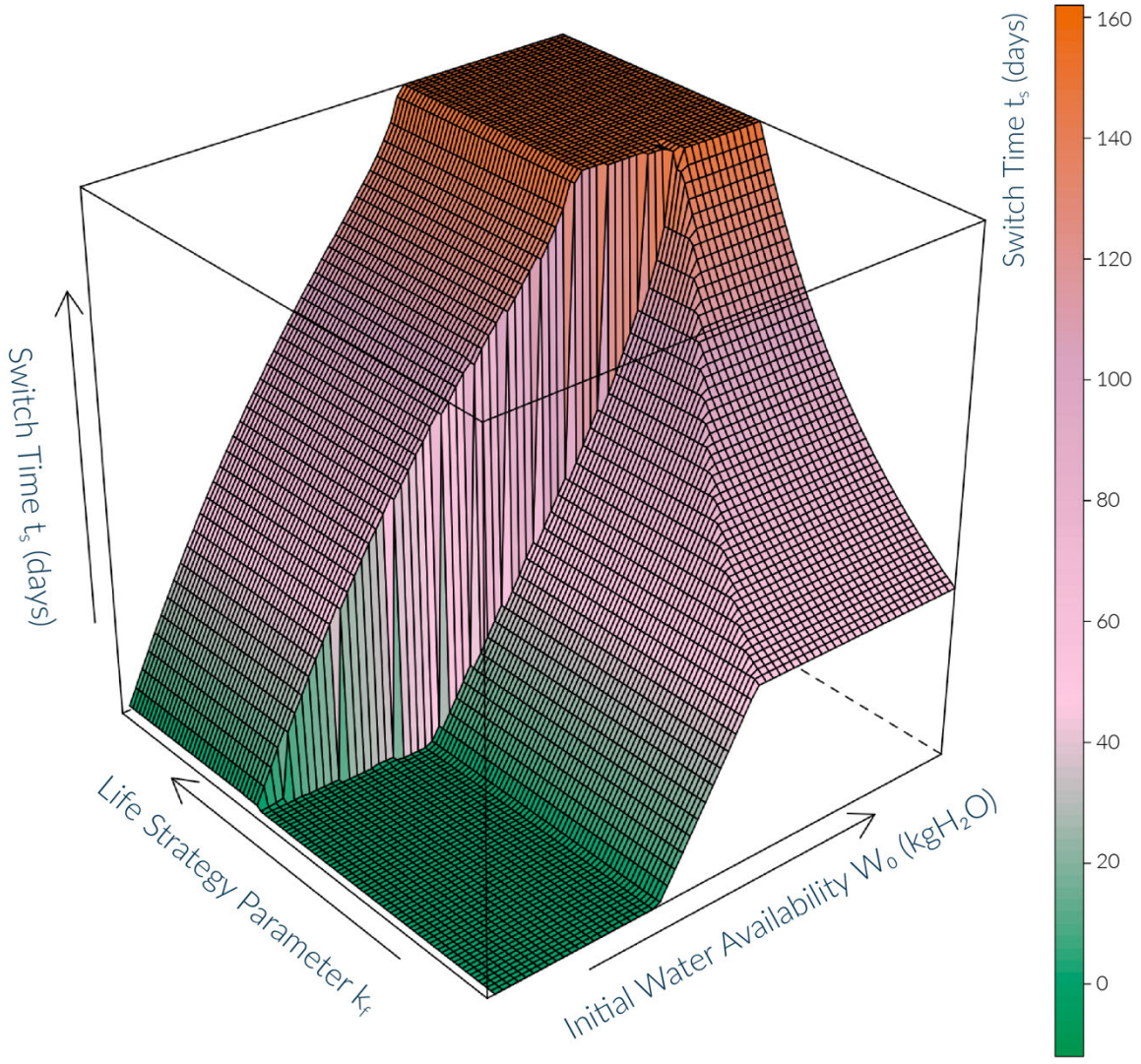

Figure 2-8 The optimal swtich time (t_s^*) as determined by the fitness proxy parameter k_f and initial soil water availability W_0. Colour is to assist the reader with the gradient following the vertical axis and indicating the value of the optimal switch time (t_s^*).

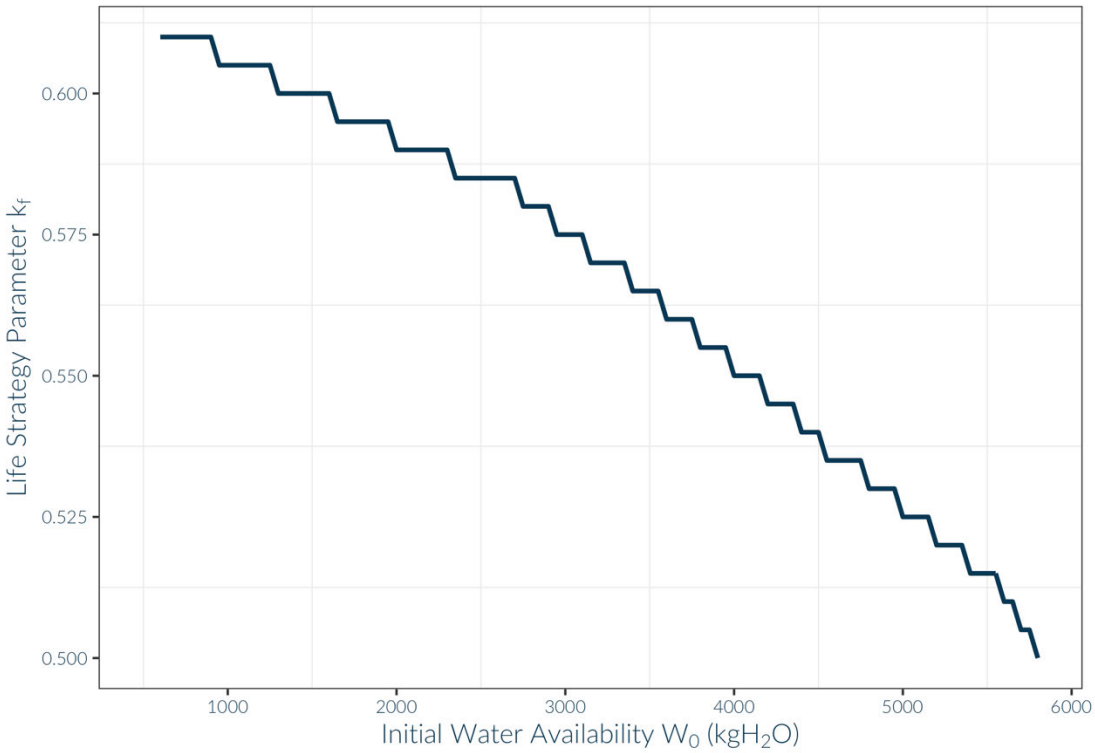

Figure 2-9 Point of shift in strategy behaviour between the MaxS safe behaviour (below line) and the MaxM risky behaviour (above line) as determined by the initial water availability. The fitness proxy parameter k_f determines the proportion of biomass versus storage prioritised in the calculation of optimal trajectory. The stepwise discontinuity is an artefact of the resolution of simulation.

2.4 Discussion

The key outcome of the optimisation model analysis is that the optimal storage utilisation trajectory during a drought is a three-phased strategy: (1) an initial period, when soil moisture is high, when storage is utilised at the maximum rate, increasing growth and future carbon gain; (2) an intermediate period, when carbon is stored and no growth occurs; and (3) finally the stress period when photosynthesis is inhibited and stored carbon must be available for respiration. While there are some alternative optimal storage utilisation trajectories, these usually are a simplification excluding one of the three phases, and the optimal pattern remains consistent for a wide range of initial water conditions and fitness proxies. Crucially, in almost all cases the optimal point for growth to stop occurs before the plant is fully stressed, leading to storage accumulation, irrespective of the objective function being maximised. This behaviour is often observed in droughted plants (Mitchell, O'Grady, Tissue, et al., 2014), but it is commonly associated with passive storage allocation (Körner, 2003). The results presented here suggest that this pattern could also arise if there is active storage allocation.

2.4.1 Active carbon storage explains observed responses of plant growth to drought

The modelled optimal response shown in this paper may represent how plants have adapted to drought in nature. The tendency for non-structural carbohydrate content to increase at the onset of drought before later decreasing has been observed in many studies (Adams et al., 2017; McDowell, 2011). It is also species-specific, with species responding to similar conditions with different NSC dynamics. For example, a study of seasonal drought in nut trees showed large NSC seasonality and a big spike in NSC concentration following the cessation of growth in almond, but a smaller response in walnut and pistachio with NSC concentrations remaining fairly stable throughout the year (Tixier et al., 2020). Similarly, (Mitchell, O'Grady, Tissue, et al., 2014) showed that after subjecting *Eucalyptus globulus* seedlings to drought, the plants grew for a time before stopping and accumulation of NSC until photosynthesis stopped. In the same experiment, *Pinus radiata* seedlings, grew for a longer time and accumulated much less NSC before photosynthesis ceased. The time between the cessation of growth, t_s, and the cessation of photosynthesis, t_{crit}, is referred

to in physiological literature as the Carbon Safety Margin, (Mitchell, O'Grady, Tissue, et al., 2014).

The model results suggest that the growth – storage – stress pattern is a result of adopting an active, not passive, carbon storage strategy by plants. However, the observation of a more rapid decline of growth as compared to photosynthesis following water stress has generally led to the theory that plants passively accumulate carbon (Körner, 2003, 2015). Not only does growth cease at a higher soil water potential (lower water stress) than photosynthesis does, the decline of growth is much more rapid (Fatichi et al., 2014). This is generally attributed to physiological factors which limit growth. Growth is affected by water stress through its effect on cell turgor (Muller et al., 2011) which is needed to support cell division and expansion (Tardieu et al., 2011). Therefore, water stress, which decreases turgor in plant cells, leads to physiological inhibition of plant growth. However, soluble sugar, one of the forms stored carbon takes, plays a significant role in maintaining cell turgor and contributes to the plasticity of turgor to water stress (Bartlett et al., 2014). Moreover, the turgor loss point, that is the soil water potential at which wilting is observed, is variable across species and biomes (Bartlett et al., 2012) and is positively correlated with drought tolerance (Zhu et al., 2018). In the above-mentioned study by Mitchell et al. (2014), both *Eucalyptus globulus* and *Pinus radiata* seedlings stopped growth at similar water potential values (approximately -1.4MPa) but only in *Pinus radiata* this value was close to its turgor loss point (-1.41MPa). In *Eucalyptus globulus*, the more drought-tolerant of the two species, the turgor loss point was more negative (-2.03MPa), suggesting that growth decline was not consistent with a water-stress physical limitation. It is, therefore, likely that the regulation of carbon storage in droughted plants is actively controlled, at least in more drought-tolerant species.

2.4.2 Factors controlling the optimal allocation trajectory

The optimal solution is defined by two time points: the switch to storage, t_s, and the time of water depletion, t_{crit}, which is dependent on the first point. The switch time is a function of 1) the optimisation goal defined as the fitness parameter k_f, 2) the environment: the initial water availability and the length of the stress season, and finally 3) the plant size and traits (including the maximum storage utilisation rate, k_s). Each aspect affects the plant response on a different level, from species- to individual- level. I discuss these properties now in turn.

At the species level, the optimal trajectory is determined by the optimisation goal. While most optimisation studies consider a single fitness proxy and vary plant parameters to maximise fitness here, I consider an alternative approach. Since OCT reveals dynamic behaviours rather than static ones, varying static plant traits in addition to allocation patterns may be more difficult to interpret. However, static plant traits often reveal important trade-offs such as slow-fast growing or stature-recruitment. By examining a range of fitness proxies, including the two edge cases of MaxS and MaxM, different life-history strategies which represent such trade-offs may be examined. Most importantly, MaxS represents risk-averse species while MaxM represents risk-taking species. Risk-averse behaviour may be exhibited by slow-growth and higher shade-tolerance (Kitajima, 1994, 2002; Poorter & Kitajima, 2007) or by increased focus on survival as opposed to reproduction (Rüger et al., 2018, 2020) or recovery (Barry et al., 2012; Galiano et al., 2011). In turn, risk-taking behaviour may be exhibited by the opposite of the above life-history strategies: fast growth, low shade tolerance, pioneering and potentially higher mortality risk during and post-stress (Trugman et al., 2018). This is exhibited by the lower carbon safety margin of MaxM plants versus MaxS plants which has implications for future plant recovery, competition, and reproductive success. Most data on the link between NSC and other life-history trade-offs focused on the slow-fast growth spectrum and shade-tolerance proving in fact that slow-growing and shade-tolerant plants do, in fact, show higher carbon stores than fast-growing plants (Atkinson et al., 2012; Rose et al., 2009). Moreover, when recovery patterns are examined, higher carbon stores are proven to aid in recovery from stress (Tomasella et al., 2017). Further studies examining the link between carbon storage strategies and life-history trade-offs may be useful in exploring these relationships further.

Intermediate fitness proxies were also considered to examine strategies that may potentially highlight life-history strategies, which occur between the extremes that trade-offs usually exhibit. However, in this model intermediate goals defaulted to either MaxS or MaxM behaviour. Hence, it may be sensible to consider just two potential fitness goals which represent different strategies. However, this phenomenon is also a limitation of the modelling approach: examining trade-offs often leads to the “biodiversity paradox”, the emergence of a limited number of strategies which do not capture real observed ranges of

behaviour (Clark et al., 2007). In fact, plants show a wide variety of carbon storage responses (Hartmann et al., 2015; Martínez-Vilalta et al., 2016). The model used in this study examines trade-offs only on one axis (fitness proxy) which may be insufficient to fully capture carbon storage phenomena. While more detailed examination of population dynamics and its modelling is beyond the scope of this chapter it must be acknowledged that no model can recreate all possible trade-off axes in a comprehensive manner but further work examining linked dynamics may prove useful in explaining storage life-history strategies further.

On local and regional scales, the strategy adopted is dependent on the initial water availability and length of stress season. The model relies on a significant simplifying assumption: the drought can be fully predicted, and the plant can predict of both the length (T_{end}) and water availability (W_0). Because a plant is not aware and is not capable of reliably predicting these environmental properties, this assumption leads to the conclusion that both $W_0$and T_{end} must, therefore, relate to regional and local adaptations to environmental conditions. One way of achieving this may be through genetic and epigenetic controls which would have evolved in and have adapted to a local climate. Given a sufficiently predictable environment, such as monsoonal rainfall dynamics, the local population may have optimised their response to these dynamics. However, few studies have shown that plant carbon allocation strategies are genetically adapted to their environment; one exception is the work by Blumstein & Hopkins (2021) who showed that intraspecific variation in NSC stores can be attributed to local adaptation of different *Populus trichocarpa* provenance trees grown in a common garden experiment. Another provenance study looked at the carbon storage dynamics of individuals from increasingly drier climates. Seedlings from drier provenances show a slightly higher starch concentration to those from a wetter environment (Bachofen et al., 2018). Although less studied, controls due to hormonal or genetic expression may further help explain the differences in responses (Mund et al., 2020; Vacchiano et al., 2018) and elucidate the role of provenance and triggers of drought response (Bogeat-Triboulot et al., 2007; Liao & Bassham, 2020; Roy & Mathur, 2021).

Finally, at the individual level, the size of the plant and its physiological properties will also affect the optimal switch time. The sensitivity of the model to these aspects has not been explored here, but future work would benefit from such an examination.

2.4.3 Model limitations

Several simplifying assumptions had to be made to keep the model tractable. Firstly, the model represents only two carbon pools: storage and biomass. In reality, many plant organs have different responses to drought; root growth may increase while shoot growth slows or stops in response to drought (Eziz et al., 2017). Plants may reduce leaf area during drought to reduce loss of water through transpiration (Munné-Bosch & Alegre, 2004), and increase root surface area to increase water uptake, although the effectiveness of larger root systems in taking up more water has been debated (Bennett et al., 2015). Additionally, the model assumes that photosynthetic uptake is directly proportional to total biomass, whereas there is likely to be a saturating response as photosynthetic leaf area typically does not increase in proportion with biomass. A more realistic model would include different plant organs, and their roles in carbon and water uptake, explicitly. However, while increasing the number of pools could provide additional realism, it would need to be done in such a way as to capture the desired process characteristics, as increased model complexity does not always provide an improved degree of insight (McNickle et al., 2016).

Secondly, the carbon safety margin is suggested to be physiologically related to hydraulic safety margin (Meir et al., 2015), which is thought to be a good predictor for plant mortality during drought (Anderegg et al., 2016). While water relations were not explicitly modelled in this study, it is possible that the optimal allocation trajectory may be associated with species-specific properties of the plant hydraulic system. Stomatal controls on plant photosynthesis were not represented in the model, other than through a complete shutdown of photosynthesis when soil water goes to zero. In nature, plants can control water loss during drought by reducing stomatal conductance as drought progresses, and the rate at which this occurs is linked to the plant's hydraulic architecture. The term an/isohydricity refers to the plant's ability to maintain photosynthetic activity during drought through control of stomatal conductance. Anisohydric species are able to keep their stomata open and active in higher leaf water stress and, therefore, keep C assimilation

positive longer into stress (Tardieu & Simonneau, 1998). An/isohydricity can be explained by optimality models of plant response to drought (Mrad et al., 2019) and falls reliably on the hydraulic safety versus carbon assimilation trade-off scale (Skelton et al., 2015). Integrating a model of stomatal conductance into this work may, therefore, further assist in defining the relationship between plant carbon strategies and hydraulic properties.

In this model I focused only on a single, predictable, stress period, and ignored the possibility of stochastic variation in the duration of stress. In reality, plants experience not only stochastic variation of abiotic stress which may lead to increased carbon storage pools (Wiley & Helliker, 2012) but also biotic stress through competition which may also lead to alternative storage allocation strategies (Guo et al., 2016; Wu et al., 2020). Including stochasticity and competition will likely increase the potential stress on the plant and may lead to more conservative strategies. In a deterministic environment, the optimal storage trajectory for maximising biomass leads the exhaustion of storage pools at the end of the stress period. If the same strategy were to be used in a stochastic environment, a random decrease in the amount of water available (W_0) or an increase in duration of stress (T_{end}) would lead to increased stress and plant mortality. It may, therefore, be better for the plant to adopt a more conservative, MaxS, strategy to decrease the likelihood of mortality. However, in a competitive environment, this strategy is likely to suffer due to decreased resource acquisition when outcompeted by neighbouring plants. It, thus, follows that while the general shape of the solution may be similar in a stochastic and competitive environment, whether a “safe” or “risky” strategy survives may not be easily determined.

In optimisation modelling, stochasticity can be tackled using stochastic dynamic programming (SDP). One modelling study which used SDP to compare the allocation trajectory of plant allocation to conceptually different environmental stochasticity models, did in fact show that plant allocation strategy changed drastically between different stochastic models (Iwasa, 1991). When the environmental stochasticity model changed from a fully random model of stress to a Markov model, which captures some predictable patterns, the optimal plant carbon allocation changed from a fixed strategy to one which responded to the environment. In order to model a stochastic environment in an optimisation framework, one approach would be to model consider an objective function as

an expectation value given some rain probability (Mäkelä et al., 1996) and such an approach may be considered in further examination of this problem.

When considering optimal behaviour in competition, such a dynamic can be examined by looking at emergent evolutionary stable strategies (Dybzinski et al., 2011) although ESS models are more complex and can be difficult to solve. To my knowledge no ESS model has examined carbon storage dynamics.

An alternative approach to including stochastic dynamics and competition is to use an Individual-Based Modelling approach, such as a gap model, which explicitly model individual behaviour and examine emergent behaviours after a period of time. This approach is further examined in Chapter 3.

Finally, the use of linear functions to describe processes, while useful in creating a tractable analysis, is an unrealistic assumption. It may also be contributing to the dual contrasting results of intermediate fitness proxy strategies resulting in an either MaxM or MaxS behaviour. This can be remedied by the use of saturating functions which better capture processes, such as photosynthesis, modelled in this study (Thornley, 1972; Wenk & Falster, 2015). The use of numerical solution algorithms can then be used to examine the model and better capture process realism (e.g. Mäkelä & Sievänen, 1992).

2.4.4 Implications for modelling and observations

Three aspects of the optimality approach used in this study may be important in expanding our understanding of how to model carbon storage allocation dynamics under stress. Firstly, the emergence of the bang-bang behaviour in this model highlights the importance of modelling phenology, that is the switch between behaviours. Phenological events may be affected by stress events (e.g., Adams et al., 2015; Ogaya & Peñuelas, 2004) though they are most often modelled as static in models (e.g., Thomas & Williams, 2014) or controlled by environmental conditions (e.g., Leuzinger et al., 2013). In this model the phenological event was the cessation of growth, which emerges in other optimal control models as well (summarised in Iwasa, 2000). When reproductive effort is maximised, a switch between allocating to vegetative and reproductive pools occurs as demonstrated in annual plants. This dynamic is also shown in annual dynamics of perennial plants. Leaf phenology also

emerges as a strategy for optimal carbon gain (Caldararu et al., 2014) as a function of climatic factors and length of the growing season which determine leaf phenology as a function of either leaf age (in tropics) or temperature constraints (in higher latitudes).

Secondly, though less clear in this modelling exercise, modelling control mechanisms using marginal return values may provide a fruitful method for exploring stress responses. The underlying mechanism for the emergence of phenology in OCT is the relationship between the marginal return values for different pools. The marginal return value can be described as the expected gain with respect to some optimisation goal per unit of a resource invested in a specific pool (Bloom, 1986), for example, the return on carbon gain per unit invested into shoots or roots. The optimal strategy is to invest in the component with the highest return value (Vincent & Pulliam, 1980) or balance allocation to competing resources if the returns are equal (Iwasa & Roughgarden, 1984). These values provide crucial information and show success in models where applied (e.g., Thomas & Williams, 2014). Adopting marginal returns may be especially useful when plants are stressed. For example, a strategy which allocates resources to the most limiting component according to its marginal return value (Chapin et al., 1987) may be an appropriate alternative to allometric balance allocation models which determine the allocation patterns based on set relationships between plant components. In nature, plants will have partitioned resources in a way that reflects past resource availability and stress, which may be better captured by models capturing marginal return values.

Finally, using dynamic optimisation modelling to assist with data interpretation and model-data comparison may prove crucial in exploring plant drought response. Specifically, measurements of NSC and hydraulic conductance involve labour-demanding and destructive sampling (Quentin et al., 2015) while mechanistic modelling of plant carbon storage is still under way (Fatichi et al., 2019). High resolution time-series data of carbon allocation and storage dynamics are relatively scarce, with many studies measuring NSC at a single time point to compare between a treatment and control pool (e.g., Palacio et al., 2020). When time-series data is produced the resolution of measurement rarely exceeds twice a month (e.g., Tixier et al., 2020). Extrapolating carbon storage patterns during drought, based on a small number of time points, would be highly beneficial. This can

potentially be done using more realistic dynamic optimisation models which incorporate carbon and hydraulic processes. Coupled with other, easier to measure, carbon and hydraulic measurements, such as photosynthesis, stomatal conductance and leaf and soil water potentials, carbon storage trajectories could then be predicted from low resolution data using such dynamic optimisation models to further explore plant drought response.

2.5 Conclusions and Future Work

In this work I have shown that a modelled optimal carbon storage allocation trajectory can explain some of the observed patterns of carbon storage dynamics in response to water stress. The cessation of growth before photosynthesis may be an active storage response rather than a purely passive outcome of physiological growth limitation. Following from this work, the use of phenological observations such as growth cessation or NSC maxima during stress may assist in explaining observed variability in drought tolerance and allocation strategies of different species. Although many important processes were omitted in this simplified model approach, the dynamics observed in this model can further aid in developing mechanistic models of carbon storage processes. Future work would be aided by exploring the resulting dynamics of optimal carbon allocation in simulated environments using more detailed modelling, as well as exploring the connection to optimal modelling of plant carbon and hydraulic dynamics during drought.

2.6 Appendix: Derivation of OCT solution

In this appendix I derive the solution to the optimal control problem of the toy model. In order to solve an OCT problem, one must first write an extended goal function and the Hamiltonian function which define the problem and incorporate constraints at the terminal point and during the observed period. Next, a set of adjuncts is derived from these functions and the problem is solved backwards for the adjuncts and forwards for the dynamic constraints. From the combination of these two, a full solution to an OCT problem can be found.

I first derive the Hamiltonian and adjunct functions, then derive the solution to the dynamic constraints. Next, I consider different terminal conditions and a set of solutions is then found.

Finally, the special cases of MaxM ($k_f = 1$) and MaxS ($k_f = 0$) are considered separately.

2.6.1 General solution

2.6.1.1 Setting out the problem

I consider here the general solution in which the goal is expressed as:

$$\Phi = k_f M_T + \left(1 - k_f\right) S_T \qquad (2\text{-}41)$$

Once this general solution is analysed, I then consider the special cases of $k_f = 1$ (MaxM) and $k_f = 0$ (MaxS).

Dynamic constraints are given as:

$$\dot{f_M} = \dot{M} = u_t S \qquad (2\text{-}42)$$

$$\dot{f_S} = \dot{S} = (k_p - k_r) M - u_t S \qquad (2\text{-}43)$$

$$\dot{f_W} = \dot{W} = -k_p k_w M \qquad (2\text{-}44)$$

With the following static constraints enforced on the states, control, and parameters:

$$W_t \geq 0 \qquad (2\text{-}45)$$

$$S_t \geq 0 \qquad (2\text{-}46)$$

$$0 \leq u_t \leq k_s \leq 1 \qquad (2\text{-}47)$$

$$k_p = \begin{cases} 0 & \text{if} \quad W = 0 \\ k_p^* & \text{if} \quad W > 0 \end{cases} \qquad (2\text{-}48)$$

$$k_p^* > k_r \qquad (2\text{-}49)$$

If storage reaches zero and there is no additional photosynthetic gain the plant is assumed to have died.

The general form of the Hamiltonian is given as:

$$\mathcal{H}(t) = \boldsymbol{\lambda}^T(t)\boldsymbol{f}(t) - \boldsymbol{\mu}^T\boldsymbol{c_{eff}}(t) \quad (2\text{-}50)$$

where $\boldsymbol{\lambda}(t)$ is the vector of adjunct variables, $\boldsymbol{f}(t)$ are the dynamic constraints, $\boldsymbol{\mu}^T$ are the Lagrange multiplier and $\boldsymbol{c_{eff}}(t)$ are the constraints in effect. In this model the Hamiltonian is therefore:

$$\mathcal{H}(t) = \lambda_M(u_t S) + \lambda_S\Big(\big(k_p - k_r\big)M - u_t S\Big) - \lambda_W k_w k_p M + \mu_S\, c_S + \mu_W c_W \quad (2\text{-}51)$$

where μ_S and μ_W take on a positive value when their respective pools (storage and water) are 0, and are 0 otherwise.

Moreover, we can expand the terminal goal function to consider the terminal constraints:

$$\Phi_A = k_f M_T + \big(1 - k_f + \nu_S\big)S_T + \nu_W W_T \quad (2\text{-}52)$$

Once again, ν_S and ν_W take on positive values only when the borderline terminal constraints are met (i.e. $S_T = 0$ or $W_T = 0$).

Both the $\boldsymbol{\mu}$ and $\boldsymbol{\nu}$ values are Lagrange multipliers which only become important in the analysis when differential equations are used. Otherwise, they don't have any influence over the full form of the function.

We can first find the terminal values of the adjunct values by looking at the respective derivatives of the terminal goal function with respect to the individual pools.

$$\lambda_M(T) = \frac{\partial \Phi_A}{\partial M_T}\Big|_{t=T} = k_f \quad (2\text{-}53)$$

$$\lambda_S(T) = \frac{\partial \Phi_A}{\partial S_T}\Big|_{t=T} = 1 - k_f + \nu_S \quad (2\text{-}54)$$

$$\lambda_W(T) = \frac{\partial \Phi_A}{\partial W_T}\Big|_{t=T} = \nu_W \quad (2\text{-}55)$$

The dynamic adjunct equations are also then defined as:

$$\dot{\lambda_M} = -\frac{\partial \mathcal{H}}{\partial M_t} = -\lambda_S(k_p - k_r) + \lambda_W k_p k_w \quad (2\text{-}56)$$

$$\dot{\lambda_S} = -\frac{\partial \mathcal{H}}{\partial S_t} = u_t(\lambda_S - \lambda_M) - \mu_S \quad (2\text{-}57)$$

$$\dot{\lambda_W} = -\frac{\partial \mathcal{H}}{\partial S_t} = \mu_W \quad (2\text{-}58)$$

Finally, the control can be found to be:

$$u_t = \max_{u_t, \lambda_M, \lambda_S} \mathcal{H} = u_t(\lambda_M(t) - \lambda_S(t)) \quad (2\text{-}59)$$

As such the solution to u_t can be defined as:

$$u_t = \begin{cases} 0 & \text{if} \quad \lambda_S(t) > \lambda_M(t) \\ k_s & \text{if} \quad \lambda_S(t) < \lambda_M(t) \end{cases} \qquad (2\text{-}60)$$

2.6.1.2 Constraints

Importantly, I don't need to consider both the terminal and state controls for both pools. Since $W_t \geq 0$ is enforced by μ_W and W only decreases, the end point constraint and its lagrange multiplier, ν_W, become superfluous and can be removed.

In the case of $S_t \geq 0$ the opposite can be argued. The $S_t = 0$ is unlikely to occur unless photosynthetic gains and costs are balanced which becomes intractable in the analysis. As such the μ_S lagrange multiplier can be ignored.

During the course of the analysis three distinct scenarios can be recognised. These will be further expanded upon for individual terminal constraints but the general patterns and considerations are described below.

Let's consider first the case in which there is no photosynthetic gain. The following can be inferred:

- Water is depleted: $W_t = 0$
- Therefore, S can only be decreasing: $\dot{S} < 0$
- If $S_t = 0$ and $t < T$ the plant has reached mortality and the $S_t \geq 0$ constraint is violated.

The second case is one in which there is photosynthetic gain but no growth. The following can then be inferred:

- Water is depleted: $W_t = 0$
- Therefore, S is changing at a rate of: $\dot{S} = \left(k_p^* - k_r\right)M$
- Since $k_p^* - k_r > 0$ is positive S cannot reach zero

The final case is one in which there is both photosynthesis and growth. The following can be inferred:

- Water is depleted: $W_t = 0$
- Therefore, S is changing at a rate of: $\dot{S} = \left(k_p^* - k_r\right)M - k_s S$
- As storage decreases $\lim_{S \to 0} k_s S = 0$ and case 2 comes into effect

Thus I rewrite the terminal goal function and the Hamiltonian:

$$\mathcal{H}(t) = \lambda_M(u_t S) + \lambda_S((k_p - k_r)M - u_t S) - \lambda_W k_w k_p M + \mu_W c_W \qquad (2\text{-}61)$$

$$\Phi_A = k_f M_T + \left(1 - k_f + \nu_S\right)S_T \qquad (2\text{-}62)$$

2.6.1.3 Solution to the dynamic constraints $\dot{\boldsymbol{f}}(t)$

The dynamic constraints can be solved by taking advantage of the fact that the M and S dynamic constraints can be rewritten in terms of M only:

$$\dot{S} = (k_p - k_r)M - u_t S = (k_p - k_r)M - \dot{M} \quad (2\text{-}63)$$

If the second derivative of M is taken the above can be substituted into Equation 2-42 to get a *homogeneous second-order linear differential equation* with constant coefficients:

$$\ddot{M} = u_t \dot{S} = u_t(k_p - k_r)M - \dot{M} \quad (2\text{-}64)$$

And this can be further rewritten into the classic quadratic equation format:

$$0 = \ddot{M} + u_t \dot{M} - u_t(k_p - k_r)M \quad (2\text{-}65)$$

The solution for M, $M = e^{rt}$, can be substituted in the above to get:

$$0 = r^2 e^{rt} + u_t r e^{rt} - u_t\big(k_p - k_r\big)e^{rt} \quad (2\text{-}66)$$

And the solution to r can be found through finding the roots of the function above:

$$r_1 = \frac{-u_t + \sqrt{u_t^2 - 4u_t(k_p - k_r)}}{2} \quad (2\text{-}67)$$

$$r_2 = \frac{-u_t - \sqrt{u_t^2 - 4u_t(k_p - k_r)}}{2} \quad (2\text{-}68)$$

Since there are two real distinct roots these can be combined to give a solution of the form of:

$$M(t) = C_1 e^{r_1 t} + C_2 e^{r_2 t} \quad (2\text{-}69)$$

C_1 and C_2 can be found by substituting M_0 and S_0. I start with the S_0:

$$M_0 = M(0) = C_1 e^0 + C_2 e^0 = C_1 + C_2 \quad (2\text{-}70)$$

Therefore:

$$C_1 = C_2 - M_0 \quad (2\text{-}71)$$

Using S_0 and $\dot{M} = u_t S$:

$$S_0 = \frac{M(0)}{u_t} = \frac{C_1 r_1 e^0 + C_2 r_2 e^0}{u_t} = \frac{(C_2 - M_0)r_1 + C_2 r_2}{u_t} \quad (2\text{-}72)$$

Therefore C_1 and C_2 can be defined as:

$$C_1 = M_0 - \frac{u_t S_0 - M_0 r_1}{r_1 - r_2} \quad (2\text{-}73)$$

$$C_2 = \frac{u_t S_0 - M_0 r_1}{r_1 - r_2} \quad (2\text{-}74)$$

As for the water pool W this can be found by substituting the equation for $M(t)$ into the dynamic constraint:

$$\dot{W} = -k_p k_w (C_1 e^{r_1 t} + C_2 e^{r_2 t}) \quad (2\text{-}75)$$

The integral of this expression is (using Equation 2-69):

$$W(t) = -k_p k_w \left(\frac{C_1}{r_1} e^{r_1 t} + \frac{C_2}{r_2} e^{r_2 t}\right) + C \quad (2\text{-}76)$$

C can by found by W_0 at $W(t=0)$ into the formula above to get:

$$W(t) = W_0 + k_p k_w \left(\frac{C_1}{r_1}(1 - e^{r_1 t}) + \frac{C_2}{r_2}(1 - e^{r_2 t})\right) \quad (2\text{-}77)$$

The full set of solutions is therefore:

$$M(t) = C_1 e^{r_1 t} + C_2 e^{r_2 t} \quad (2\text{-}78)$$

$$S(t) = \frac{C_1 r_1 e^{r_1 t} + C_2 r_2 e^{r_2 t}}{u_t} \quad (2\text{-}79)$$

$$W(t) = W_0 + k_p k_w \left(\frac{C_1}{r_1}(1 - e^{r_1 t}) + \frac{C_2}{r_2}(1 - e^{r_2 t})\right) \quad (2\text{-}80)$$

With the constants being:

$$r_1 = \frac{-u_t + \sqrt{u_t^2 - 4u_t(k_p - k_r)}}{2} \quad (2\text{-}81)$$

$$r_2 = \frac{-u_t + \sqrt{u_t^2 - 4u_t(k_p - k_r)}}{2} \quad (2\text{-}82)$$

$$C_1 = M_0 - \frac{u_t S_0 - M_0 r_1}{r_1 - r_2} \quad (2\text{-}83)$$

$$C_2 = \frac{u_t S_0 - M_0 r_1}{r_1 - r_2} \quad (2\text{-}84)$$

2.6.2 Detailed solution

The detailed solutions are found by analysing the adjunct dynamics backwards and then the dynamic constraints forwards to find the equations. Even with just the adjunct functions, guides can be found about the behaviour of u_t and a solution can be found by combining analytical and numerical solutions.

A total of 8 terminal conditions need to be considered. In the first instance the values of the terminal storage ($S_T = 0$ and $S_T > 0$) and water ($W_T = 0$ and $W_T > 0$) pool sizes need to be considered. Final water pool size determines the value of k_p whereas a positive value of the storage pool will eliminate the terminal storage constraint ν_S. Moreover, to determine the value of the storage allocation parameter u_t the relationships between terminal values of λ_M and λ_S are examined (as per Equation 2-60). When storage is positive this will depend only on the value of k_f ($(1 - k_f) \gtrless k_f \Rightarrow k_f \gtrless 0.5$) but when storage is zero then the Lagrange multiplier ν_S will need to be considered ($\nu_S + (1 - k_f) \gtrless k_f \Rightarrow \nu_S \gtrless 2k_f - 1$). The 8 terminal conditions are:

1. $S_T = 0$ and $W_T = 0$
   a. $\nu_S > 2k_f - 1$
   b. $\nu_S < 2k_f - 1$

2. $S_T = 0$ and $W_T > 0$
    a. $\nu_S > 2k_f - 1$
    b. $\nu_S < 2k_f - 1$
3. $S_T > 0$ and $W_T = 0$
    a. $k_f > 0.5$
    b. $k_f < 0.5$
4. $S_T > 0$ and $W_T > 0$
    a. $k_f > 0.5$
    b. $k_f < 0.5$

I look at each of these conditions in turn and where appropriate I solve an analytical solution. Alternatively, I describe the general solution to give insight into the solution but I do not follow through with a full solution. Moreover, some solution stages will be repeated across different terminal conditions and whenever that happens the previously described stage will be referenced.

2.6.2.1 Terminal Condition 1a

Final Stage Backwards: Stress

I first consider the case in which both constraints are enforced, and the storage terminal constraint is large enough to make $\lambda_S(T) > \lambda_M(T)$ and therefore enforce the lack of storage in the final stage.

The terminal pool values are:

$$S(T) = 0 \quad (2\text{-}85)$$

$$W(T) = 0 \quad (2\text{-}86)$$

The terminal adjunct values are:

$$\lambda_M(T) = k_f \quad (2\text{-}87)$$

$$\lambda_S(T) = 1 - k_f + \nu_S \quad (2\text{-}88)$$

$$\lambda_W(T) = 0 \quad (2\text{-}89)$$

And finally, the values of u_t and k_p are:

$$\lambda_S(T) > \lambda_M(T) \Rightarrow u_t = 0 \quad (2\text{-}90)$$

$$W(T) = 0 \Rightarrow k_p = 0 \quad (2\text{-}91)$$

These final conditions can be illustrated in Figure 2-10A.

The adjunct dynamics can thus be simplified:

$$\dot{\lambda_M} = -\lambda_S(-k_r) = k_r\left(\nu_S + 1 - k_f\right) \quad (2\text{-}92)$$

$$\dot{\lambda_S} = 0 \quad (2\text{-}93)$$

$$\dot{\lambda_W} = \mu_W \quad (2\text{-}94)$$

A solution can be found by integrating and substituting the terminal values of the adjuncts.

$$\lambda_M(t) = k_f + k_r\left(v_S + 1 - k_f\right)(t - T) \quad (2\text{-}95)$$

$$\lambda_S(t) = (v_S + 1 - k_f) \quad (2\text{-}96)$$

$$\lambda_W(t) = -\mu_W(T - t) \quad (2\text{-}97)$$

All the above are linear and either steady or increasing. Figure 2-10A shows the extended dynamics of the adjuncts and states.

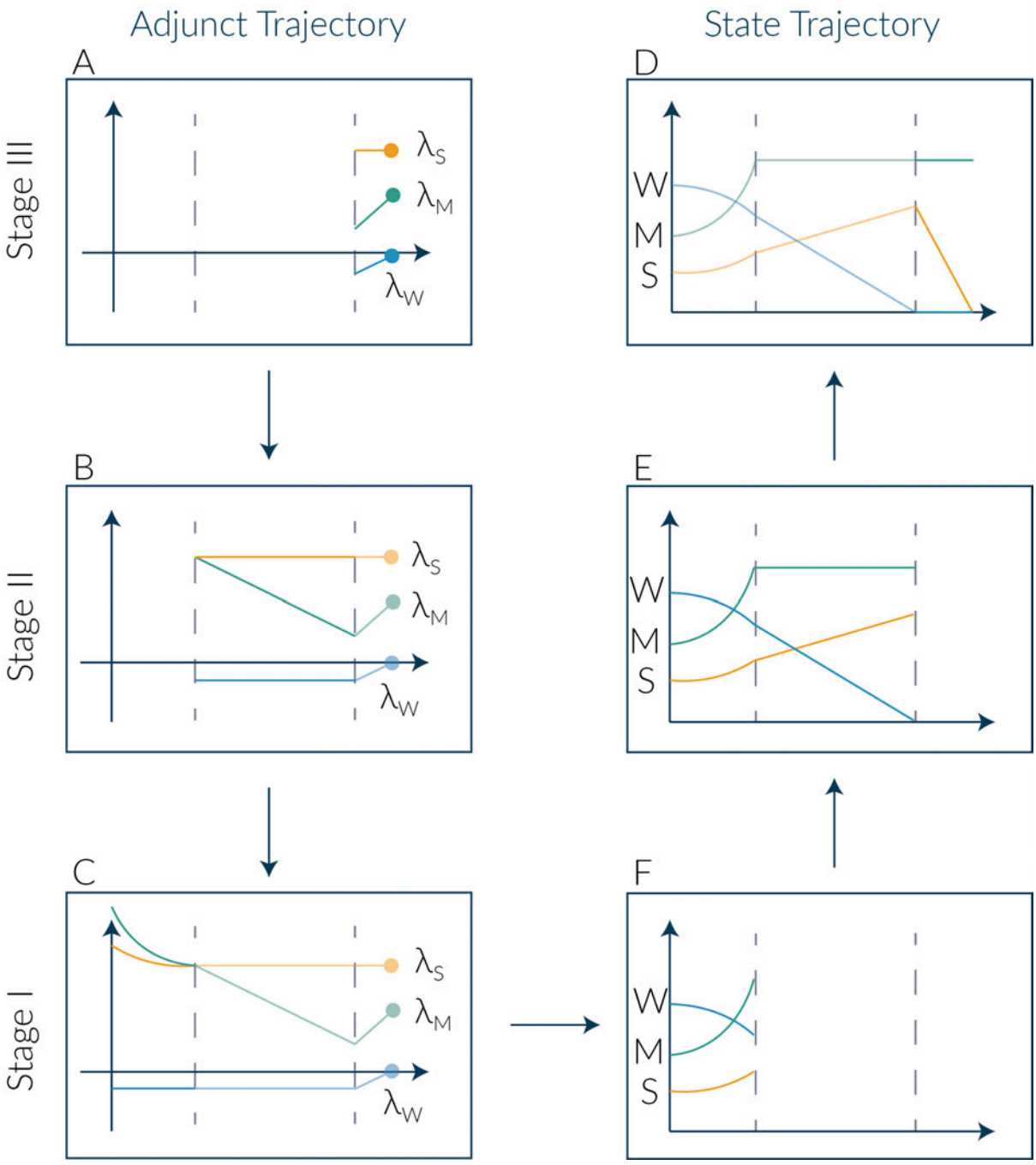

Figure 2-10 Approximate shape of the solution for the terminal constraint 1a.

Middle Stage Backwards: Storage

Unless there is a change in the conditions the model will continue without any changes. However, moving backwards at some point in the timeline the point at which the water has ran out will be reached (from here on labelled t_{crit}). Ultimately, I expect that this value will depend on the optimal strategy and initial conditions and thus it should be possible to estimate this value at the end of the analysis.

At this junction the adjuncts take the following values:

$$\lambda_M(t_{crit}) = k_f + k_r(\nu_S + 1 - k_f)(t_{crit} - T) \quad (2\text{-}98)$$

$$\lambda_S(t_{crit}) = \nu_S + 1 - k_f \quad (2\text{-}99)$$

$$\lambda_W(t_{crit}) = -\mu_W(T - t_{crit}) \quad (2\text{-}100)$$

When water is available the value of k_p changes. The following conditions are now taking place:

$$\lambda_S(T) > \lambda_M(T) \Rightarrow u_t = 0 \quad (2\text{-}101)$$

$$W(T) > 0 \Rightarrow k_p = k_p^* \quad (2\text{-}102)$$

Since k_p is now positive and the water Lagrange multiplier is no longer in effect the adjunct dynamics can be now defined as:

$$\dot{\lambda_M} = -\lambda_S\left(k_p^* - k_r\right) + \lambda_W k_p^* k_w = -(\nu_S + 1 - k_f)(k_p^* - k_r) - \mu_W(T - t_{crit})k_p^* k_w \quad (2\text{-}103)$$

$$\dot{\lambda_S} = 0 \quad (2\text{-}104)$$

$$\dot{\lambda_W} = 0 \quad (2\text{-}105)$$

Integrating these equations and solving for t_{crit} leads to the following set of equations:

$$\lambda_M(t) = k_f + \left(\nu_S + 1 - k_f\right)\left(k_p^* t_{crit} - k_r T\right)t + t_{crit}\left(\mu_W(T - t_{crit})\right)k_p^* k_w t \quad (2\text{-}106)$$

$$\lambda_S(t) = \nu_S + 1 - k_f \quad (2\text{-}107)$$

$$\lambda_W(t) = -\mu_W(T - t_{crit}) \quad (2\text{-}108)$$

Since λ_M is decreasing I can illustrate the next stage of the analysis in Figure 2-10B.

First Stage Backwards: Growth

The next change in the solution behaviour occurs when $\lambda_M(t) = \lambda_S(t)$ at which is the point at which the behaviour of the control switches. I label this point as t_s (switch time). The overall trajectory is now defined in the final part of the progress Figure 2-10C.

The conditions in this stage can now be defined as:

$$\lambda_S(T) < \lambda_M(T) \Rightarrow u_t = k_s \quad (2\text{-}109)$$

$$W(T) > 0 \Rightarrow k_p = k_p^* \quad (2\text{-}110)$$

The adjunct dynamics can be now defined as:

$$\dot{\lambda_M} = -\lambda_S\left(k_p^* - k_r\right) + \lambda_W k_p^* k_w = -(\nu_S + 1 - k_f)(k_p^* - k_r) - \mu_W(T - t_{crit})k_p^* k_w \quad (2\text{-}111)$$

$$\dot{\lambda_S} = u_t(\lambda_S - \lambda_M) \quad (2\text{-}112)$$

$$\dot{\lambda_W} = 0 \quad (2\text{-}113)$$

The exact value of these don't need to be found. What is most important is finding the value for t_s should then determine the optimal trajectory. The value of t_s can be found by solving $\lambda_S(t_s) = \lambda_M(t_s)$:

$$t_s = (\alpha - k_f)/(\beta(\alpha + k_w(\mu_w(T - t_{crit})) - k_r T\alpha) \quad (2\text{-}114)$$

Where:

$$\alpha = \nu_S + 1 - k_f \quad (2\text{-}115)$$

$$\beta = k_p^* t_{crit} \quad (2\text{-}116)$$

First Stage Forwards: Growth

In the first stage the standard solution to the dynamic constraints can be substituted. I repeat the solution to this stage below:

$$M_I(t) = C_1 e^{r_1 t} + C_2 e^{r_2 t} \quad (2\text{-}117)$$

$$S_I(t) = \frac{C_1 r_1 e^{r_1 t} + C_2 r_2 e^{r_2 t}}{k_s} \quad (2\text{-}118)$$

$$W_I(t) = W_0 k_p k_w \left(\frac{C_1}{r_1}(1 - e^{r_1 t}) + \frac{C_2}{r_2}(1 - e^{r_2 t})\right) \quad (2\text{-}119)$$

With the constants being:

$$r_1 = \frac{-k_s + \sqrt{k_s^2 - 4k_s(k_p - k_r)}}{2} \quad (2\text{-}120)$$

$$r_2 = \frac{-k_s + \sqrt{k_s^2 - 4k_s(k_p - k_r)}}{2} \quad (2\text{-}121)$$

$$C_1 = M_0 - \frac{k_s S_0 - M_0 r_1}{r_1 - r_2} \quad (2\text{-}122)$$

$$C_2 = \frac{k_s S_0 - M_0 r_1}{r_1 - r_2} \quad (2\text{-}123)$$

Middle Stage Forwards: Storage

In the second stage the plant will stop growth but continue photosynthesis. The values for the control and photosynthetic parameters are, therefore:

$$\lambda_{S,II}(T) > \lambda_{M,II}(T) \Rightarrow u_t = 0 \quad (2\text{-}124)$$

$$W(T) > 0 \Rightarrow k_p = k_p^* \quad (2\text{-}125)$$

Since there is no growth during this period the biomass remains constant, and the remaining dynamics will become linear. The solution to the dynamic constraints can be easily simplified. If we define the values at time $t = t_s$ to be:

$$M_I(t_s) = C_1 e^{r_1 t_s} + C_2 e^{r_2 t_s} \quad (2\text{-}126)$$

$$S_I(t_s) = \frac{C_1 r_1 e^{r_1 t_s} + C_2 r_2 e^{r_2 t_s}}{k_s} \quad (2\text{-}127)$$

$$W_I(t_s) = W_0 k_p k_w \left(\frac{C_1}{r_1}(1 - e^{r_1 t_s}) + \frac{C_2}{r_2}(1 - e^{r_2 t_s}) \right) \quad (2\text{-}128)$$

Then these values can be used to find the solution to the simplified dynamic constraints:

$$\dot{f_M} = \dot{M} = 0 \quad (2\text{-}129)$$

$$\dot{f_S} = \dot{S} = (k_p - k_r) M_I(t_s) \quad (2\text{-}130)$$

$$\dot{f_W} = \dot{W} = -k_p k_w M_I(t_s) \quad (2\text{-}131)$$

Thus, the solution to this period can be defined as:

$$M_{II}(t) = M_I(t_s) \quad (2\text{-}132)$$

$$S_{II}(t) = (k_p - k_r) M_I(t_s)(t - t_s) + S_I(t_s) \quad (2\text{-}133)$$

$$W_{II}(t) = W_I(t_s) + k_p k_w M_I(t_s)(t_s - t) \quad (2\text{-}134)$$

Final Stage Forwards: Stress

The next stage occurs when water runs out and the plant is stressed. The control and photosynthetic parameters are, therefore:

$$\lambda_S(T) > \lambda_M(T) \Rightarrow u_t = 0 \quad (2\text{-}135)$$

$$W(T) = 0 \Rightarrow k_p = 0 \quad (2\text{-}136)$$

The pool values at time t_{crit} when the water runs out are:

$$M_{II}(t_{crit}) = M_I(t_s) \quad (2\text{-}137)$$

$$S_{II}(t_{crit}) = (k_p - k_r) M_I(t_s)(t_{crit} - t_s) + S_I(t_s) \quad (2\text{-}138)$$

$$W_{II}(t_{crit}) = W_I(t_s) + k_p k_w M_I(t_s)(t_s - t_{crit}) \quad (2\text{-}139)$$

The dynamic constraint in the last period can be described as:

$$\dot{f_M} = \dot{M} = 0 \quad (2\text{-}140)$$

$$\dot{f_S} = \dot{S} = -k_r M_I(t_s) \quad (2\text{-}141)$$

$$\dot{f_W} = \dot{W} = 0 \quad (2\text{-}142)$$

Thus, the pool solution to this period can be found to be:

$$M_{III}(t) = M_I(t_s) \quad (2\text{-}143)$$

$$S_{III}(t) = k_p M_I(t_s)(t_{crit} - t_s) - k_r M_I(t_s)(t - t_s) + S_I(t_s) \quad (2\text{-}144)$$

$$W_{III}(t) = 0 \quad (2\text{-}145)$$

And, finally, the terminal values can be found:

$$M_{III}(T) = M_I(t_s) \quad (2\text{-}146)$$

$$S_{III}(T) = k_p M_I(t_s)(t_{crit} - t_s) - k_r M_I(t_s)(T - t_s) + S_I(t_s) = 0 \quad (2\text{-}147)$$

$$W_{III}(T) = 0 \quad (2\text{-}148)$$

Meaning the solution to the problem can be defined as:

$$\Phi = k_f M_{III}(T) \quad (2\text{-}149)$$

The progress of the state trajectory can be found in Figure 2-10E-F.

Final Remarks

In order to now find the exact solutions, the values for ν_s and μ_W have to be found.

This can be done by looking at $S_T = 0$ and $W(t_{crit}) = 0$. If these conditions are insufficient, it is then possible to use the expressions and constraints to simulate an optimal solution as I have done in the chapter.

2.6.2.2 Terminal Condition 1b

I now consider the situation in which both terminal constraints are enforced and the Storage terminal constraint $\nu_S < 2k_f + 1$ which leads to storage allocation over the last period. Depending on the size of the parameters and lagrange multipliers, there are upwards of 2 stages in this solution.

Final Stage Backwards: Stress + Growth

The terminal values are given in Equations 2-87-89. The terminal conditions imply that:

$$\lambda_S(T) < \lambda_M(T) \Rightarrow u_t = k_s \quad (2\text{-}150)$$

$$W_T = 0 \Rightarrow k_p = 0 \quad (2\text{-}151)$$

The values for the adjunct dynamics can thus be found and described.

$$\dot{\lambda_M} = \lambda_S k_r \quad (2\text{-}152)$$

$$\dot{\lambda_S} = k_s(\lambda_S - \lambda_M) \quad (2\text{-}153)$$

$$\dot{\lambda_W} = \mu_W \quad (2\text{-}154)$$

The $\dot{\lambda_M}$ and $\dot{\lambda_S}$ can be found by taking a second-order derivative of λ_S and finding the second-order linear differential equation with constant coefficients:

$$\ddot{\lambda_S} = k_s(\dot{\lambda_S} - k_r \lambda_S) \quad (2\text{-}155)$$

$\lambda_S(t)$ can be expressed as $\lambda_S(t) = e^{r_s t}$ and the roots and coefficients need to be found to define the function as:

$$\lambda_S(t) = C_{S1}e^{r_{s1}t} + C_{S2}e^{r_{s2}t} \quad (2\text{-}156)$$

$$\lambda_M(t) = \lambda_S(t) - \frac{C_{S1}r_{S1}e^{r_{S1}t} + C_{S2}r_{S2}e^{r_{S2}t}}{k_s} \quad (2\text{-}157)$$

The roots can be found to be:

$$r_{S1} = \frac{\left(k_s + \sqrt{k_s^2 - 4(k_s k_r)}\right)}{2} \quad (2\text{-}158)$$

$$r_{S2} = \frac{\left(k_s - \sqrt{k_s^2 - 4(k_s k_r)}\right)}{2} \quad (2\text{-}159)$$

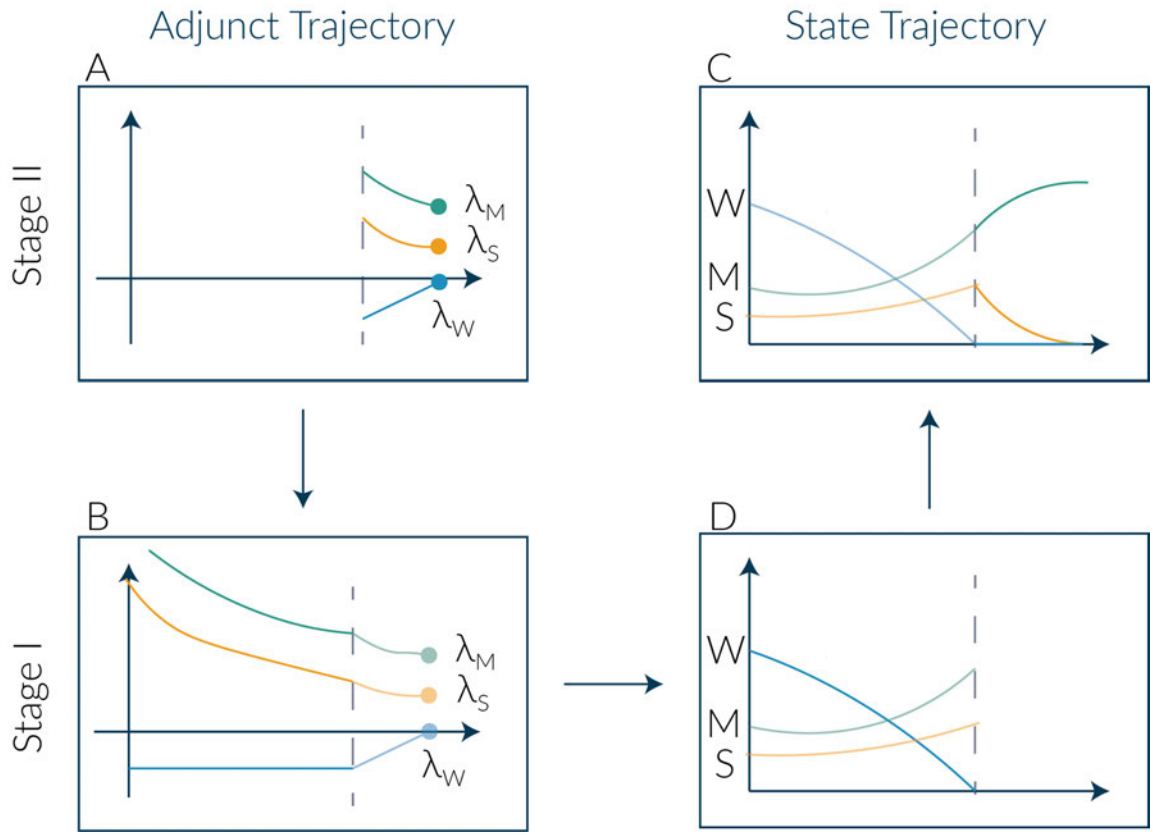

Figure 2-11 Approximate shape of the solution for the terminal constraint 1b.

And the coefficients can be found by looking at the terminal constraints:

$$C_1 = \frac{(1 - k_f + v_S - C_{S2}e^{r_{S2}T})}{e^{r_{S2}T}} \quad (2\text{-}160)$$

$$C_2 = \frac{k_s k_f + (1 - k_f + v_s)(r_{S1} - k_s)}{e^{r_{S2}T}(r_{S1} - r_{S2})} \quad (2\text{-}161)$$

This solution is shown in Figure 2-11A.

First Stage Backwards: Growth

In the next stage, water becomes available before the two adjuncts may meet the plant will continue to grow. This is illustrated in Figure 2-11B.

The exact value of the adjuncts once again does not need to be found and the solution can be determined from finding the value of t_{crit} and finding the forward conditions.

First Stage Forwards: Growth

This analysis follows the same analysis as Terminal Condition 1a, but finishing at the value of t_{crit} instead of t_s (i.e., $M_I(t_{crit})$ needs to be determined).

Final Stage Forwards: Stress + Growth

In this stage the stress phase must be adjusted to allow for growth during the stress period. The value of (k_p) may be removed from the formulas for r_1 and r_2:

$$r_1 = \frac{-k_s+\sqrt{k_s^2+4k_sk_r}}{2} \quad (2\text{-}162)$$

$$r_2 = \frac{-k_s-\sqrt{k_s^2+4k_sk_r}}{2} \quad (2\text{-}163)$$

Further the value of t_{crit} can be found by solving for $W(t_{crit}) = 0$, and the values of $M_I(t_{crit})$ and $S_I(t_{crit})$ can be substituted into the constants C_1 and C_2 in place of M_0 and S_0 to get:

$$C_1 = M_I(t_{crit}) - \frac{k_sS_I(t_{crit})-M_I(t_{crit})r_1}{r_1-r_2} \quad (2\text{-}164)$$

$$C_2 = \frac{k_sS_I(t_{crit})-M_I(t_{crit})r_1}{r_1-r_2} \quad (2\text{-}165)$$

These can be used in equations 2-126 and 2-127 for $M(t)$ and $S(t)$ respectively and Equation 2-148 for $W(t)$.

The solution to the problem can be defined as:

$$\Phi = k_f M_{III}(T) \quad (2\text{-}166)$$

The progress of the state trajectory can be found in Figure 2-11C-D.

Final Remarks

This solution is a boundary solution, meaning that it can be obtained for specific parameters only. It can be found by looking at conditions under which $S_T = 0$ and $W(t_{crit}) = 0$ for the above forward solution. As such, this solution is not fully considered in the analysis in the chapter.

2.6.2.3 Terminal Condition 2a

This condition is impossible to achieve. If storage is reduced to zero at the end of the simulation the implication is that storage must be decreasing in the final stage. However, with no loss to growth and photosynthesis still active (water is available throughout the entire period) under constraint 2-49 storage change becomes: $\dot{S} = (k_p - k_r)M$>0 which is positive and leads to a contradiction.

2.6.2.4 Terminal Condition 2b

In this condition only one stage is present: growth. It is another case of a boundary solution only present under specific parameters and can be found by solving Stage I of terminal condition 1a with the conditions of $t_s = T$ and $S_T = 0$. Figure 2-12 illustrates this solution.

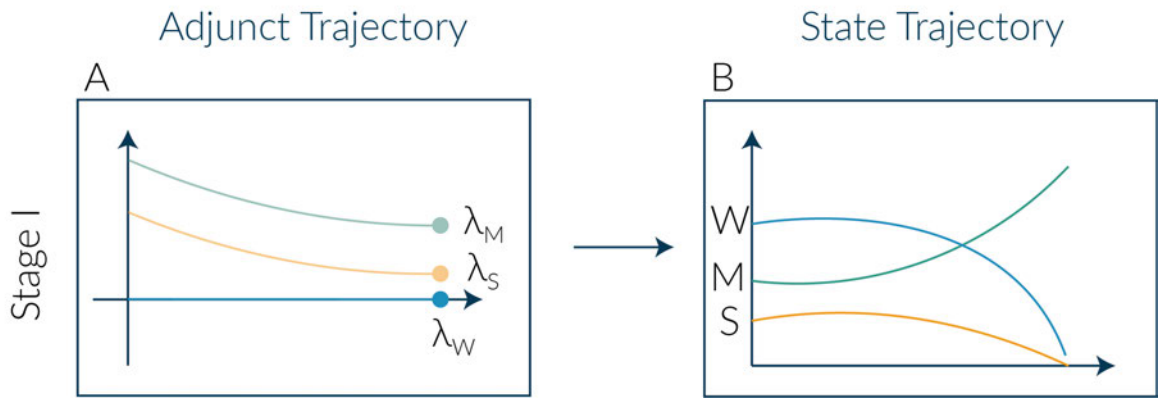

Figure 2-12 Approximate shape of the solution for the terminal constraint 2b.

2.6.2.5 Terminal Condition 3a

This solution is equivalent to terminal condition 1b and can be found by removing the Lagrange multiplier ν from the solution of terminal condition 1b.

2.6.2.6 Terminal Condition 3b

This condition is equivalent to terminal condition 1a (three stages: growth-storage-stress) and can be found by removing the Lagrange multiplier ν from the solution of terminal condition 1a. Note that it is also possible for $t_s = 0$ under some conditions leading to two-phases being observed (storage-stress).

2.6.2.7 Terminal Condition 4a

This solution has only one observed phase: growth equivalent to stage 1 in terminal condition 1b.

2.6.2.8 Terminal Condition 4b

This solution has 2 observed phases: growth and storage equivalent to stages 1 and 2 in terminal condition 1a.

2.6.3 Special Case: MaxS (kf = 0)

The special case MaxS can be found by removing the k_f from the above analysis. Moreover, cases in which $S_T = 0$ and $k_f > 0.5$ can be ignored and thus only solutions 3a and 4a need to be accounted for.

2.6.4 Special Case: MaxM (kf = 1)

The special case MaxM can be found by substituting $k_f = 1$ into the above analysis. Moreover, cases in which $k_f < 0.5$ and $\nu < 2k_f + 1$ can be ignored and thus only solutions 3b and 4b need to be accounted for.

3 Examining the long-term impacts of storage allocation strategies in plants under stochastic stress

Abstract

With the progression of global climate change, forests will experience more frequent and more variable extreme weather, including droughts and heatwaves, leading to potentially lethal stress. To mitigate stress, plants store carbon as non-structural carbohydrate reserves, which they can access when necessary. However, storing carbon limits the immediate benefits of growth, thereby creating a trade-off between growth and storage. In this chapter, I investigate the success of alternative growth vs storage strategies in stochastic (random) environments under competition. Using a gap model, I explore the outcome of competition among tree species differing in carbon storage-related traits: carbon utilisation rate (fast-slow spectrum) and switch time between growth and storage (risky-safe spectrum), in environments differing in stress stochasticity (variance of stress duration) and intensity (average stress duration). Four combinations of traits (utilisation rate-growth period) were used in the gap model: fast-risky, fast-safe, slow-risky, and slow-safe. I found that only the slow-safe and fast-safe strategies were still alive after 100 years when stress was present. When stress was absent, plants with the fast-risky and slow-risky strategies were dominant. Increasing the stochasticity and intensity of stress resulted in community dominance shifting from the slow-risky to the slow-safe strategy, with changes in stress stochasticity having a larger effect than changes in stress intensity. Mortality due to the depletion of carbon reserves was the major driver of the shift in community composition. Species with a faster carbon utilisation rate had lower carbon storage minima and higher mortality risk under competition-induced shading, while species with a later switch time (longer growth period) had higher mortality risk during stress events due to lower carbon availability during the stress period. These findings suggest that changing stress regimes towards increased stress intensity, and increased stress stochasticity, will likely impact future community composition, favouring trees with storage-prioritising strategies. The approach undertaken here shows that simulation models that consider

storage allocation and stochasticity may provide novel insights into the effects of stress on forest function and composition.

3.1 Introduction

Trees, as long-lived and sessile organisms, can be especially susceptible to environmental stress, such as drought, extreme temperatures, and herbivory. As climate changes and environmental stresses increase in frequency and severity (IPCC, 2021) there is an increasing need to understand how plants cope during stress periods.

Abiotic stresses such as drought, frost and heatwaves affect plant metabolism, reducing carbon uptake via photosynthesis. They can also impact plant structure through xylem embolism and/or direct tissue damage (Cailleret et al., 2014; Tyree & Sperry, 1989). Senescence may be caused by tissue damage or may be facultative as a form of protection (Munné-Bosch & Alegre, 2004). These effects can last beyond the stress period and have long-lasting effects on plants that survive, affecting their metabolic performance and future growth rates (Ruehr et al., 2019). Moreover, mortality induced by stress can also manifest after several years (Dietze, Matthes, et al., 2014; Trugman et al., 2018). In turn, stress-induced mortality has significant consequences for community composition (Bennett et al., 2015; Engelbrecht et al., 2007; McMahon et al., 2019) and, therefore, succession (Vieira et al., 2021; Walters & Reich, 1996) including local extinction of co-evolved species (Harrison, 2001).

Climate change is expected to result in more extreme and frequent droughts (Dai, 2013), and more extreme temperatures (Bojórquez et al., 2019; Reichstein et al., 2013). The resultant increased stress on plants can also increase the risk from herbivores (Huang et al., 2020) and pathogens (Aguade et al., 2015). Moreover, co-occurring stresses lead to more complex and potentially exacerbated effects on plants (Anderegg et al., 2015; Charrier et al., 2021; Williams et al., 2013). Despite increased scientific studies of plant response to stress, the mechanisms enabling plant survival are generally unresolved (Hartmann et al., 2020; Sala et al., 2010) .

Survival during and after stress depends on carbon availability. Uptake of carbon via photosynthesis is limited during stress periods (Muller et al., 2011) and may also be limited

following stress because of stress-induced damage to photosynthetic structures (Carnicer et al., 2011; Schwalm et al., 2017). Recovery requires investment into new structures and it can require several months (MacAllister et al., 2019; Ruehr et al., 2019) to several years (Huang et al., 2018) for metabolic activity and growth rates to return to pre-stress levels. Thus, storing carbon in the form of non-structural carbohydrates (NSC) is an essential strategy for plants that allows them to access carbon substrates during periods when carbon assimilation is limited (Adams, Germino, et al., 2013; Tixier et al., 2019; Wiley, 2020).

Stored NSC, often as starch, can be converted into soluble sugars and readily mobilised (Chapin et al., 1990) to ameliorate the potential effects of environmental stress and help with post-stress recovery (Tomasella et al., 2019). One theory is that plants have adapted to optimise their long-term survival in uncertain environments through storing carbon (Wiley & Helliker, 2012). However, storing carbon reduces investment of carbon in growth, including leaf area which contributes to higher whole-plant photosynthetic capacity (Poorter & Kitajima, 2007; Silpi et al., 2007), thereby constituting a trade-off between growth and storage carbon allocation (Atkinson et al., 2014; Hinman & Fridley, 2018). The success of different allocation strategies (storage vs growth) may be affected by competition with other species. If a plant is growing alone, the optimal strategy may be to delay growth in favour of storing carbon for defence against biotic attack or alleviating abiotic stress. In contrast, a slow-growing plant in a competitive environment may be shaded out by a faster-growing neighbouring tree. In order to outcompete its neighbours, and gain more resources by growing taller, a plant may exhibit faster growth at the cost of lower carbon stores and higher vulnerability to mortality (Atkinson et al., 2014; Myers & Kitajima, 2007). Some studies find that larger trees are more susceptible to stress mortality due to increased hydraulic and metabolic demand (Rose et al., 2009; Rowland et al., 2015; Trugman et al., 2018). However, higher growth rates may also increase the speed of recovery (Myers & Kitajima, 2007) and support larger resource uptake rates which in turn can lead to larger carbon stores.

Strategies for NSC storage allocation and mobilisation in plants vary among species and environments (see Martínez-Vilalta et al., 2016 for an overview of some of the differences). Different species' strategies can manifest in the size of the carbon pool (slow-

growing seedlings can have larger NSC stores compared to fast-growing ones; Myers and Kitajima 2007; Duan et al. 2019), minimum NSC values (Martínez-Vilalta et al., 2016), allocation between different organs (Bazot et al., 2013; Tixier et al., 2020) and seasonal amplitude (Hoch et al., 2003; Tixier et al., 2020). In addition to differences among species, plants can also display intraspecific variability in relation to climate (Ahrens et al., 2020, 2021) dependent on the dryness of the site or individual provenance (Bachofen et al., 2018; Hao et al., 2021). Thus, plants vary in the mechanisms – or 'strategies' - that they use for accumulation and mobilisation of NSC.

It has been suggested (Wiley & Helliker, 2012) that the allocation strategy adopted is a consequence of a plant seeking to optimise its survival likelihood versus growth. Optimisation models have been used to explore the storage strategies of plants in different conditions. However, the optimisation target in these models differs. Some models optimise storage in the short-term (instantaneously, or on a daily timescale). For example, Trugman et al. (2018) took the approach of maximising the Net Primary Production (NPP) during recovery from drought by balancing the rate of C allocation to storage as a function of the size of xylem, roots and shoots against the phloem loading rate. However, they found that this strategy, while optimal in the short-term, could lead to delayed mortality if the predicted recovery was too fast to be supported by the plant's current structure. It is more common for optimisation approaches to consider storage over a prolonged time-scale due to the asynchronicity between its use, and the cost and benefits incurred by storage (Hartmann & Trumbore, 2016).

Longer-term optimisation can be achieved by using dynamic allocation models, which identify a trajectory of carbon storage allocation or utilisation that maximises some fitness goal, commonly taken to be reproduction. Several models, which considered perennial plants maximising their reproductive output over several years punctuated by stress periods, have found that the optimal growth schedule typically follows a three-phase pattern within a single year: a period of growth (at maximum growth-rate), followed by storage or reproductive output (growth fully ceased), and finally the stress period (Iwasa & Cohen, 1989; Kozłowski & Uchmanski, 1987; Kozłowski & Wiegert, 1987; Pugliese & Kozlowski, 1990). Due to the shape of the response (the allocation parameter assuming the

value of either the lower or upper constraint), this pattern is also referred to as bang-bang dynamics (Johansson et al., 2018; Koshkin et al., 2021). Alternative goal formulations such as maximising storage or growth under a stress period of limited resources result in similar optimal allocation patterns (see Chapter 2, p 37). For annual plants maximising reproduction, the dynamic optimisation approach predicted a similar bang-bang dynamic to three carbon pools: vegetative, storing and reproductive carbon pools (Chiariello & Roughgarden, 1984). The solution determined several possible pathways for optimal C allocation which followed the general pattern of growth, followed by storage (under specific initial conditions), followed by reproductive allocation from current photosynthesis, and, finally, current reproductive allocation from both photosynthesis and stores. When the model was parameterised and tested against data using two ecotypes of *Hemizonia luzulifolia*, phenological data, including flowering time, for one of the ecotypes aligned with the predicted optimal time-course (Chiariello & Roughgarden, 1984).

However, there are several limitations to using optimisation models to explore NSC allocation. Firstly, it is unclear which optimisation target to use as a proxy for fitness (Franklin et al., 2012). Optimisation models that allocate carbon to storage may use a range of different targets, primarily reproduction (Iwasa, 2000; Iwasa & Cohen, 1989; Iwasa & Kubo, 1997) but also biomass size or storage size (Chapter 2). While some optimisation targets may agree and complement each other on varying spatial and time scales (Dewar et al., 2009), the use of different targets can also lead to differing conclusions (Chapter 2). Secondly, environmental stochasticity is difficult, though not impossible, to incorporate in an optimisation model. Stochastic dynamic programming has been used to evaluate allocation schedules under stochastic environment (Iwasa, 1991) and optimal storage size for recovery from disturbance (Iwasa & Kubo, 1997). However, the analytical approach taken in these studies relies on the use of “normal” variability of the stochastic events, an approach which fails to acknowledge predicted extremes in climate variability (Ghil et al., 2011). Finally, when dynamic optimisation approaches consider competition it is most often in the form of implicit intra-specific competition, which does not allow for the competition between several strategies (e.g., Koshkin et al., 2021).

An alternative approach to identifying the fittest strategies in a given environment is to explicitly simulate competitive interactions between individuals with different strategies in stochastic environments using gap models. Gap models simulate interspecific population dynamics within a patch of forest (Bugmann, 2001). Individuals are modelled explicitly and competition for resources, often light, limits growth and survival of smaller individuals. Gap model simulations can capture a significant breadth of plant behaviour and relevant feedback mechanisms, while community dynamics become an emergent property which can be further examined. Crucially, gap models focus on long-term rather than short-term community dynamics allowing for the examination of the successional status, that is success in differently aged ecosystems, of a species in a given environmental regime (Morin et al., 2021; Norby et al., 2001). For example, JABOWA (Botkin et al., 1972), the first such model to examine mixed-age and mixed-species dynamics, reproduced climate-dependent species coexistence and dynamics in several New Hampshire forest plots. As their development progressed, gap models have shown success in their ability to reproduce behaviour of different tree genera and environments. For example, the BRIND model (Shugart & Noble, 1981), successfully reproduced forest structure of a high-elevation eucalyptus forest subject to fire risk. More recently, trait-, size-, and patch-structured models (TSPMs) have expanded on the functionality of gap models to focus on trait dynamics (Falster et al., 2011). In contrast to reproducing observations of real forests, the original model developed by Falster et al. (2011) has examined the response and sensitivity of community composition to variations in individual-level functional traits. Since then, the TSPM modelling approach has been made available as a package (plant, Falster et al., 2016) making both the traditional gap model functionality and TSPM functionality more accessible.

In this chapter, I expand the existing model, *plant*, introduced by Falster et al. (2016) to examine the growth-storage trade-off under competition and environmental stochasticity. The goal of this work is to understand long-term fitness of different growth/storage allocation strategies in different environments. Use of a gap model allows the exploration of the impact of competition on the growth-storage trade-off and avoids the need to specify a particular proxy to represent fitness. In order to describe the spectrum of growth / storage allocation strategies, I examine two key parameters: 1) the switch time,

between growing and storing, which emerged from the optimisation models in Chapter 2; and 2) the rate of carbon utilisation (from storage compartment) in growth as a reflection of the plant growth rate (Eller et al., 2018). By considering four combinations of these two traits, this work investigates a more complex growth-storage trade-off spectrum than in Chapter 2.

In this chapter, environmental stress is characterised as an annual period during which photosynthesis is zero. Stress intensity is represented by the average duration of the stress period, and stochasticity is represented by the variability of that duration.

The objective is to address the following questions:

A. The baseline question: How does introducing stress and NSC storage to the model affect the success of species with different allocation strategies, as compared to a simulation with no stress and no storage-related mortality?
B. How does the stochasticity and intensity of stress affect the success of different strategies, and how does it change community dominance?
C. If species dominance is altered in (A) or (B), what are the primary drivers of such a change?

In this modelling study, I first explore the impact of stress (objective A) in the model. The yield will be lower in stressed environments, due to the decrease in total carbon gain from lower photosynthetic activity, but the proportional reduction in yield could be smaller or larger than the reduction in photosynthetic period. If increased stress promotes overall higher competition or mortality of individuals, the decrease in yield may be larger than the direct decrease due to annual stress limitation on carbon uptake. Alternatively, the decrease in yield may be smaller than the direct decrease if stress decreases competition between species by promoting long-lived individuals which can survive in more stressful environments.

I then explore the dominance of species in control vs stressed environments. I expect that growth-prioritising trees will be dominant in the control environment (no stress), but it is unclear whether dominance shifts to storage-prioritising trees in the stressed environment.

I then explore how stress stochasticity and intensity (objective B) affects the community composition. A priori, I expect that increasing stochasticity might increase the presence of the 'conservative' species and increase species diversity by allowing for a buffer of less 'risky' species to establish sufficient growth in a competitive environment.

3.2 Methodology

3.2.1 Model

The gap model was implemented in the *plant* package (Falster et al., 2016). The original *plant* package was developed to simulate the behaviour of plants using trait-based plants in a meta-community competing for light in a patch. The package has both deterministic and stochastic functionality, the latter of which allows it to be used as a traditional gap model. The default strategy for plant growth (FF16) relies on allometric scaling for carbon allocation. *Plant* allows the user to extend the software with their own models of plant growth adapting FF16 or using an entirely new strategy. The package has several computational advantages: *plant* uses a combination of the faster language, C++ for the model implementation and the slower statistical software R (R Core Team, 2018) to interface with the model. Also, *plant* uses an adaptive time solver, which finds the largest time-step capturing the required accuracy of computation, and thus, increases speed, robustness, and accuracy in obtaining the model solutions. Prior to using *plant*, I identified errors or limitations in the code ('bugs') and re-coded them to provide a greater degree of modularisation so that a variety of plant traits – beyond the default plant height - could be considered. This was done in co-ordination with the developers and all code was contributed back to them.

To implement the carbon storage allocation scheme, I created a new strategy, called ES20, which expands on the FF16 strategy by including a stored carbon pool in the core of the carbon allocation model. I also adjusted the remainder of the model to account for the effect of stress and storage-based mortality.

To introduce environmental stress, I created a new environment model, $ES20_{env}$ which extends the $FF16_{env}$ model. The model retains the mechanisms of light competition among species from $FF16_{env}$ and introduces an annual stress period of stochastically varying

length. Each year, the environment is characterised by a period of no stress followed by a period of stress. The time of the switch between no-stress and stress each year is derived from a normal distribution. The implementation of the model and model runs can be found in the following repository: https://github.com/foxeswithdata/plant.

Below I describe how the model was modified to allow for the abovementioned changes. Additional functions that were retained from the original FF16 model are given in Appendix 3.6.

3.2.1.1 Plant strategy

The overall structure of the carbon pools and flows of the model is shown in Figure 3-1.

Photosynthesis and respiration are derived from the FF16 model with new functionality introduced for the stress period. The average photosynthesis per leaf area for a plant with traits x, height H, living in a light environment of E_a and a stress environment of E_s, at time t can be given as:

$$\bar{p}\big(x, H, E_a, E_s(t)\big) = E_s(t) \int_0^H p\big(x, E_a(z)\big) q(z, H) \mathrm{d}z \qquad (3\text{-}1)$$

where, $E_s(t)$ is the experienced stress, $p(x, E_a(z))$ is the leaf photosynthesis at height *z* and $q(z, H)$ is the leaf area distribution. The experienced stress is a value between 0 and 1, where 0 is the highest level of stress which fully impedes photosynthesis and 1 is unstressed. Likewise, total maintenance respiration, R, is comprised of respiration rates of each component multiplied by the fraction r_{min}, which leads to decreased respiration during stress:

$$R = \left(r_{min} + \frac{E_s(t)}{2}\right) \sum_{i=l,b,s,r} M_i r_i \qquad (3\text{-}2)$$

where M_i is the mass of plant component i (*l* = leaf, *b* = bark, *s* = sapwood and *r* = fine roots) and r_i is the specific rate of respiration of that component.

The model was modified by including a storage pool. The storage utilisation scheme assumes that incoming carbon first enters the storage pool before being utilised for growth and reproduction (Figure 3-1). This representation is commonly used in optimal allocation

models (see this thesis' Chapter 2; Chiariello & Roughgarden, 1984; Iwasa & Cohen, 1989; Iwasa & Levin, 1995) and in some mechanistic models (e.g., Jones et al., 2020; Mahmud et al., 2018). Models differ, however, in how they represent the use of stored carbon. Here, we use an active storage utilisation scheme which is controlled by two traits: the switch time from growth to storage, t_s, and the storage utilisation parameter, α_s.

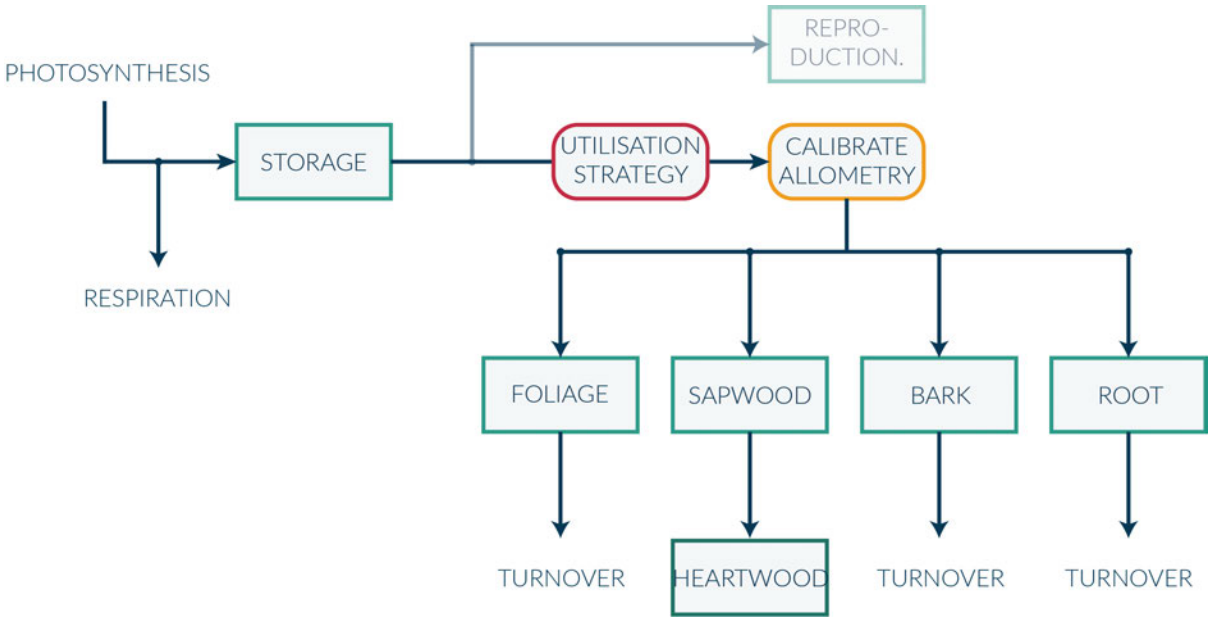

Figure 3-1 The carbon allocation scheme used in the model. Net carbon uptake (NCU; Photosynthesis - Respiration) first enters the storage pool before being utilised for growth of functional components and reproduction. The input to storage can be either positive or negative, depending on whether respiration exceeds photosynthesis. The amount of carbon utilised for growth is controlled by the utilisation strategy (red box) which is defined by the two trait parameters (the switch time from growth to storage, t_s, and the storage utilisation parameter, α_s). The allocation of growth among foliage, sapwood, bark, and root is controlled by allometric relationships with height and leaf area. Loss to turnover is kept at constant rates throughout the years. Litter carbon from foliage, bark, and root is lost from the plant, while the carbon from sapwood turnover is converted to heartwood. Reproduction is included in the model at a nominal amount kept for realism of carbon costs but not function. Reproduction only occurs when the utilisation of carbon is positive.

The rate of NSC utilisation U as controlled by the utilisation strategy (Figure 3-1, red box) is given by:

$$U = \begin{cases} \mathrm{t} < t_s & \Longrightarrow \quad a_s M_{st} \\ \mathrm{t} \geq t_s & \Longrightarrow \quad 0 \end{cases} \tag{3-3}$$

where t is the time of year, t_s is the switch time parameter, α_s is the storage utilisation rate parameter and M_{st} is the size of the storage pool. Note that Equation 3-3 allows for the plant to continue growing in some cases despite being stressed, if t_s is later than the onset of stress that year. Equation 3-3 is implemented as a series of logistic step

functions to assist with the model-solving (see Appendix 3.7) but is represented as a piecewise step function here for simplicity.

The growth-storage strategy is represented by the two parameters t_s and α_s.

The switch time parameter, t_s, corresponds to the outcome of an optimal carbon allocation model which predicts the time-point at which it is optimal to switch from growing to storing (Chapter 2; Engen & Saether, 1994; Iwasa & Cohen, 1989; Wenk & Falster, 2015). In the optimisation model, the value of t_s is predicted to vary with the plant size and the environment and represents the switch to storage *after* the onset of drought. Here, for each strategy, the value of t_s is a fixed time of the year, independent of the drought onset. The reason for this is twofold: firstly, to simplify calculation; and secondly, to capture an annual C allocation cycle which evolved in response to the occurrence of a predictable annual stress. Variation in the onset of stress thus results in yearly fluctuations in stored C and a surplus in one year can help a deficit in another year. Moreover, the plant may begin to store carbon prior to the onset of stress. In this case, an alternative approach, one in which t_s is dependent on the onset of stress rather than a fixed time of year, would require an assumption about the plant's ability to predict the onset of stress or a model in which storage always occurs following the onset of stress.

The storage utilisation parameter, α_s, is also present in optimisation models but its value usually takes on some constant maximum when the plant is growing or 0 when the plant is not growing. Here, the value of α_s is varied between different strategies.

The allometry scheme is based on the *FF16* height-based allometry, which is based on the Pipe Model Theory (Shinozaki et al., 1964). The scheme assumes a relationship between height growth and leaf area and in turn between leaf area and the size of the tree needed to support the desired leaf area. The allometric change in height is given by:

$$\frac{\mathrm{d}H}{\mathrm{d}t} = \frac{\mathrm{d}H}{\mathrm{d}A_l} \times \frac{\mathrm{d}A_l}{\mathrm{d}U} \times U \tag{3-4}$$

where the change in leaf area with respect to mass (unchanged from the original model) is given by:

$$\frac{\mathrm{d}A_l}{\mathrm{d}U} = \left(\frac{\mathrm{d}M_l}{\mathrm{d}A_l} + \frac{\mathrm{d}M_r}{\mathrm{d}A_l} + \frac{\mathrm{d}M_s}{\mathrm{d}A_l} + \frac{\mathrm{d}M_r}{\mathrm{d}A_l}\right)^{-1} \tag{3-5}$$

The size of the component i is given by:

$$\frac{\mathrm{d}M_i}{\mathrm{d}t} = \frac{\mathrm{d}M_i}{\mathrm{d}A_l} \times \frac{\mathrm{d}A_l}{\mathrm{d}U} \times U - k_i M_i \quad (3\text{-}6)$$

where k_i is the turnover rate for component i. The introduction of stress would cause a loss of the allometric balance between components because U is zero during storage periods and the size of a component i can decrease. To address this issue, the change in size of component i was made dependent on a calibration factor c_i:

$$\frac{\mathrm{d}M_i}{\mathrm{d}A_l} = c_i(H, A_l, M_i) \frac{\mathrm{d}M_i{}'}{\mathrm{d}A_l} \quad (3\text{-}7)$$

where $\frac{\mathrm{d}M_i{}'}{\mathrm{d}A_l}$ is the original allometric function from Falster et al. 2016 (supplementary table) and the calibration factor is given by:

$$c_i(H, A_l, M_i) = \frac{2}{1+\exp\left(-c_k(M_i'(H,A_l)-M_i\right)} \quad (3\text{-}8)$$

c_k is the calibration rate parameter, $M_i{}'(H, A_l)$ is the allometrically correct pool size for a plant of height H and leaf area A_l and M_i is the actual pool size. If the calibration is correct the growth rate stays constant ($c_i = 1$); if it is too small for the current size of the plant the growth to that part is prioritised to aid with recovery (up to double the usual speed of growth), and if the component is too big, growth is slowed down for the benefit of other components. c_k controls the speed of the prioritisation with a higher value leading to a larger increase in priority and faster calibration, and a low value leading to slow calibration and longer periods of adjustment. Height allometry is adjusted in the same way as pool biomass (Table 3-5).

Finally, carbon is also lost from storage to reproduction $\frac{\mathrm{d}F}{\mathrm{d}t}$ (Table 3-5) which only occurs during plant growth (when $U > 0$).

The total change in storage is therefore:

$$\frac{\mathrm{d}M_{st}}{\mathrm{d}t} = B - U - \frac{\mathrm{d}F}{\mathrm{d}t} \quad (3\text{-}9)$$

where B is the net carbon uptake (NCU), given by:

$$B = \alpha_{bio}\alpha_y(A_l\bar{p} - R) \quad (3\text{-}10)$$

with α_{bio} being the conversion factor from mol C to kg biomass, and α_y a factor that accounts for efficiency losses due to conversion of carbon into storage and growth respiration.

Mortality is controlled by three factors that work in tandem: (1) a constant, independent mortality rate (d_I) which represents the random chance of death due to events unaccounted for in the model (retained from original model); (2) productivity-dependent mortality (d_P) which represents the effect of light stress (adjusted to account for environmental stress); and (3) storage-dependent mortality (d_S) which represents the effect of low NSC reserves (newly introduced). The mortality rate, which is afterwards used to compute the probability, is given by:

$$d(x, H, M_{st}, E_a, E_s, t) = d_I + d_P(x, H, E_a, E_s, t) + d_S(x, M_{st}) \quad (3\text{-}11)$$

d_P is given by:

$$d_P(x, H, E_a, E_s, t) = E_s(t)\alpha_{dP1}\exp(-\alpha_{dP2}X) \quad (3\text{-}12)$$

where $X = B/A_l$, that is the net carbon uptake per unit leaf area. When the plants are stressed ($E_s(t) = 0$) photosynthesis goes to zero and B becomes negative. To avoid all plants dying during this period, the productivity-dependent mortality is multiplied by the stress factor E_s. α_{dP1} and α_{dP2} control the mortality function and can be adjusted for individual strategies.

The storage-dependent mortality follows the same structure, with the mortality rate decreasing as the storage concentration increases:

$$d_S(x, H, M_{st}) = \alpha_{dS1}\exp(-\alpha_{dS2}X) \quad (3\text{-}13)$$

where $X = M_{st}/M_a$ is the storage concentration in live biomass, $M_a = M_l + M_s + M_b + M_r$. α_{dS1} and α_{dS2} control the shape of the mortality function and can be adjusted for individual strategies.

Given that the number of trees is $\frac{dN}{dt} = -d(t)N$ such that the number of surviving trees is $N(t) = N_0 e^{-\int_0^t d(\tau)d\tau}$, the probability of mortality, p_D at time t, in model is then given by:

$$p_D(t) = 1 - \exp(-k\, d\,(x, H, M_{st}, E_a, E_s, t)) \quad (3\text{-}14)$$

where k is a constant. Full details of the deterministic model derivation are given in Falster et al. (2016).

Germination is dependent on the potential productivity of the new plant (Falster et al. 2016). The process has been adjusted to account for stress with germination halting throughout the stress period and introducing an initial storage pool.

New plants arrive at the patch with height H_0, correct allometry scaling of the strategy for live biomass ($M_{a0}(H_0)$) and a storage pool of size M_{st0}:

$$M_{st0} = \beta_s \, M_{a0}(H_0) \tag{3-15}$$

where β_s is the initial storage concentration for a new plant.

3.2.1.2 Environment

The model remains unchanged with regards to the light environment (based on the solar regime experienced in Sydney: Falster et al. 2011) and changes are only made to introduce environmental stress. For simplicity, there is no temperature response, and the light environment is assumed to be constant when no environmental stress is present. Outside of the annual stress period, the only factor affecting individual tree photosynthesis is light competition within the patch, which is based on the tree's height. The model assumes a uniform horizontal leaf area distribution with all the leaves at height *z* equally shaded (Bugmann, 2001) but leaf area is distributed vertically. Because patches are kept small to allow for computational performance, this scheme is deemed adequate for the model. For bigger patches, however, a crown projection area implementation that includes spatially heterogeneous interaction would be more appropriate (Lexer & Hönninger, 2001).

When the plant is stressed by the environment, photosynthesis, germination and productivity-driven mortality are all halted, and respiration is reduced.

This is achieved by introducing the stress factor $E_s(t)$ which is used to adjust plant functionality in response to the environment:

$$E_s(t) = \begin{cases} t < t_{crit} & \Longrightarrow \quad 1 \\ t \geq t_{crit} & \Longrightarrow \quad 0 \end{cases} \tag{3-16}$$

where t is the time of the year (between 0 and 1), and t_{crit} is the onset of stress in that year.

The annual time of stress onset t_{crit} is stochastic in the model.

The generation of the t_{crit} value for each environment is controlled by a normal distribution function $\mathcal{N}_s(\mu, \sigma^2)$ (see Figure 3-2). The smaller the t_{crit} for a given year, the longer the stress. The mean of the distribution can be used to increase or decrease the intensity of the stress and the standard deviation value to change the stress stochasticity, with a higher value increasing the likelihood of extremes. A t_{crit} value that is larger than 1 indicates a lack of stress in that year.

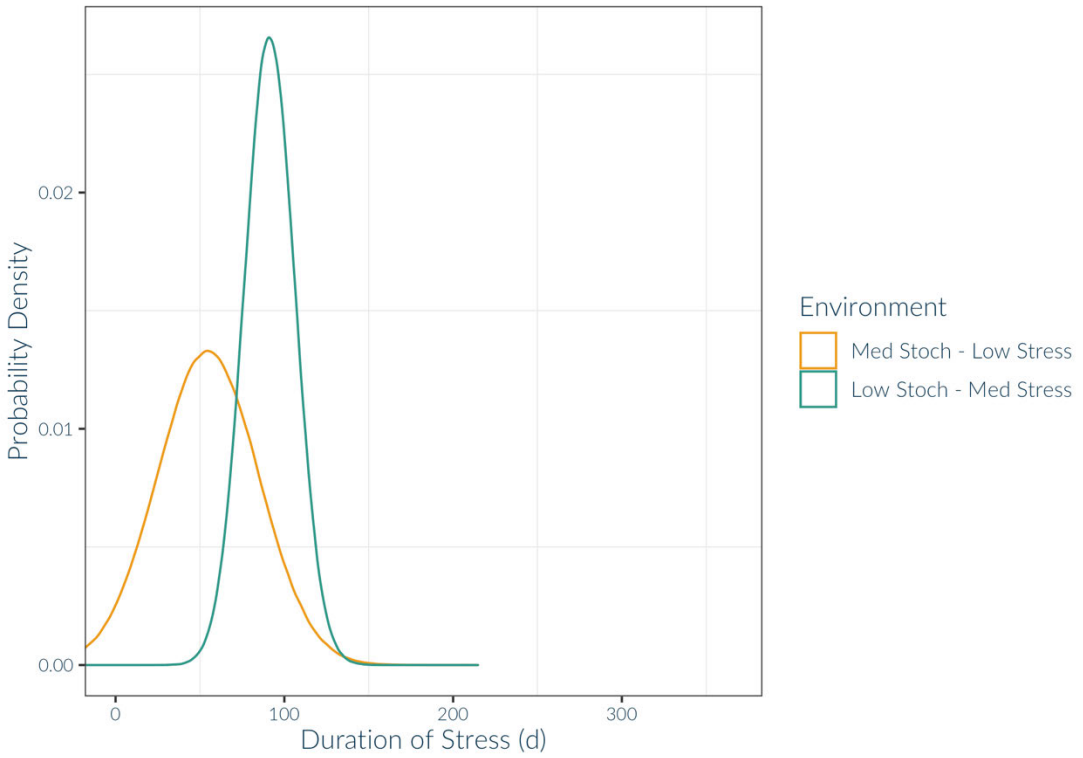

Figure 3-2 The probability density function of for two potential environments: low-stress medium-stochasticity and medium-stress low-stochasticity. The medium stress with low stochasticity (green) is given by a normal distribution: $\mathcal{N}_{s1}(\mu = 91.25d, (15d)^2)$ and the low stress with medium stochasticity (yellow) is given by the normal distribution: $\mathcal{N}_{s2}(\mu = 54.75d, (30d)^2)$. Duration of stress is calculated as (length of year – onset of stress) and units are converted to days as opposed to years to facilitate interpretation. Values that fall at or below 0 are counted as years of no stress. Although the low stress environment has generally shorter stress periods than the medium stress environment, there is a marginally higher likelihood in that environment to encounter years of extreme stress (described as more than 150 days of stress) but likely interspersed with years light and very light stress (< 75 days). In contrast the environment with the medium average stress is less likely to encounter very heavy stress but more likely to encounter heavy stress (105-150 days) with higher likelihood of concurrent years with heavy stress.

3.2.2 Parameter Estimation

3.2.2.1 Plant Allometry, Productivity, Reproduction and Mortality Parameters

Allometric growth parameters were derived principally for *Eucalyptus grandis* using additional data from the related species *Eucalyptus nitens*, *Eucalyptus pilularis*, *Eucalyptus saligna* and *Eucalyptus urophylla*. Data were obtained from the BAAD database (Falster et al., 2015) and relationships were calculated using linear regression with the statistical modelling software R. The database was further used to validate chosen parameters in short (< 20 years) single-plant simulations to ensure allometry was maintained. Where data were not available in the BAAD data base, additional data were extracted from literature where possible or default FF16 model parameters were used. Simulations established optimal parameters for parameters without simple physiological counterparts. Table 3-1 provides full details of parameter values and origin.

Table 3-1 Parameters used in the model. Source indicates what data were used in the parameter derivation. "Simulations" indicates model testing on individual plants throughout model development and FF16 refers to the parent strategy described in (Falster et al., 2016). All other sources are citations to papers. Where a source is missing, a further explanation is included in the main text.

Description	Symbol	Unit	Value	Source
Plant Storage				
Switch time	t_s	y	*varies*	-
Rate of storage conversion to biomass (storage utilisation rate)	α_s	$\mathrm{kg\,kg^{1}\,y^{-1}}$	*varies*	-
Initial storage concentration following germination	β_{s1}	$\mathrm{kg\,kg^{1}}$	0.1	(Martínez-Vilalta et al., 2016)
Coefficient of the rate of transition between growth and no-growth periods	β_{s2}	$\mathrm{y^{1}}$	120	Simulations
Plant Construction				
Crown-shape parameter	η		5	Simulations

Leaf mass per area	ϕ	$kg\ m^{2}$	0.1242302	(Falster et al., 2015)
Wood density	ρ	$kg\ m^{3}$	505	(Falster et al., 2015)
Sapwood mass per unit leaf area	θ	$kg\ m^{2}$	0.0001508 9	(Falster et al., 2015)
Parameter for relationship of height of plant with leaf area	α_{l1}	m	-0.56936	(Drake et al., 2019; Falster et al., 2015)
Exponent of relationship between height and leaf area	α_{l2}		1.48185	(Drake et al., 2019; Falster et al., 2015)
Root mass per unit leaf area	α_{r1}	$kg\ m^{2}$	0.027691	(Falster et al., 2015)
Ratio of bark cross-sectional area to sapwood area	α_{b1}	$m^2\ m^{-2}$	0.3768273	(Falster et al., 2015)
Production				
Leaf photosynthesis per area	α_{p1}	$mol\ m^{2}\ y^{1}$	82.34303	Simulations
Saturation of leaf photosynthesis per area	α_{p2}	-	0.1072532	Simulations
Canopy openness at the top of the canopy	$E_a(z \quad \text{top})$	-	1	FF16
Yield = fraction of carbon fixed converted into mass	α_y	$g\ g^{1}$	0.7	FF16
Biomass per mol carbon	α_{bio}	$kg\ mol^{1}$	0.0245	FF16

Leaf respiration per mass	r_l	$\mathrm{mol\ y^{1}kg^{1}}$	175.8027	FF16 (hyper-parameterisation)
Fine-root respiration per mass	r_r	$\mathrm{mol\ y^{1}kg^{1}}$	217	FF16
Sapwood respiration per mass	r_s	$\mathrm{mol\ y^{1}kg^{1}}$	2.412504	(Medlyn et al., 2005)
Bark respiration per mass	r_b	$\mathrm{mol\ y^{1}kg^{1}}$	4.825008	(Medlyn et al., 2005)
Portion of respiration maintained through stress	r_{min}	$\mathrm{mol\ mol^{-1}}$	0.5	Simulations
Turnover rate for leaves	k_l	$\mathrm{y^{1}}$	1.012133	FF16
Turnover rate for sapwood	k_s	$\mathrm{y^{1}}$	0.06	(Jeffreys, 1999)
Turnover rate for bark	k_b	$\mathrm{y^{1}}$	0.06	(Jeffreys, 1999)
Turnover rate for fine roots	k_r	$\mathrm{y^{1}}$	1	FF16
Fecundity				
Seed mass (mass allocated to single offspring)	Ω	kg C	0.1	Simulations
Height at maturation	H_{mat}	m	30	Simulations
Maximum allocation to reproduction	α_{f1}		0.05	Simulations
Parameter determining rate of change in $\mathrm{d}F/\mathrm{d}t$ around H_{mat}	α_{f2}		50	FF16
Accessory cost per seed	α_{f3}	kg	0.000114	FF16
Mortality				
Survival probability during dispersal	S_D		0.25	FF16

Parameter influencing survival through germination	α_{D0}	$\mathrm{kg\ y^{-1} m^{-2}}$	0.1	FF16
Intrinsic or growth-independent mortality	d_I	$\mathrm{y^{-1}}$	0.01	FF16
Baseline rate for productivity-dependent mortality	α_{DP1}	$\mathrm{y^{-1}}$	0.25	Simulations
Risk coefficient for dry-mass production per unit leaf area in productivity-dependent mortality	α_{DP2}	$\mathrm{y\ kg^{-1} m^{-2}}$	20	Simulations
Baseline rate for storage-dependent mortality	α_{DS1}	$\mathrm{y^{-1}}$	3	Simulations
Risk coefficient for storage concentration in storage-dependent mortality	α_{DS2}	$\mathrm{y\ m^{-2}}$	300	Simulations

3.2.2.2 Parameter Estimation for Competing Strategies

Two parameters govern the allocation strategy: (1) switch time, t_s, and (2) storage utilisation rate, α_s. Together, these two parameters form a growth-storage trade-off. Later switch time and higher storage utilisation rate confer larger growth but higher respiration costs and lower available storage which may lead to higher mortality during stress. Conversely, an earlier switch time and lower storage utilisation rate allow for larger storage pools which may increase survival during stress but at a cost of decreased growth and higher likelihood of shading by taller plants.

I chose two contrasting values for the two parameters, which in combination gave four competing strategies. The values were chosen using a sensitivity analysis for each parameter across a range of plant heights and storage concentrations. Sensitivity analysis simulations were run for a single plant, for one year with no light-limitation and with stress

duration of 91.25 and 54.75 days (corresponding to the average t_{crit} values of 0.85 y and 0.75 y used in model simulations). Any simulations where the storage became negative were excluded from the simulation.

The switch time, t_s, can be varied to either maximise storage (MaxS) or maximise biomass (MaxM) (Chapter 2, p 37). Here I varied t_s from 0 to 0.75 y to find the values such that the total live biomass or storage carbon pool was maximised at the end of the year (Figure 3-3). The storage translocation parameter, α_s, was varied from 0.1 to 0.4 kgC kgC-1 d-1 and the relative growth rate of height and storage concentration were plotted for a range of parameter values and initial plant sizes (Figure 3-4).

From these simulations, two values for each parameter were chosen for a total of four contrasting allocation strategies. The strategies were named as follows: the "Risky - Safe" spectrum represents the switch time, t_s, varying from high to low; and the "Fast – Slow" spectrum represents the storage utilisation rate, α_s varying from high to low. The four strategies are therefore:

- *Fast-Risky* ($t_s = 0.5$ y, $\alpha_s = 0.3$ kg C kg ^{1}C d ^{1})
- *Fast-Safe* ($t_s = 0.25$ y, $\alpha_s = 0.3$ kg C kg ^{1}C d ^{1})
- *Slow-Risky* ($t_s = 0.5$ y, $\alpha_s = 0.1$ kg C kg ^{1}C d ^{1}) and
- *Slow-Safe* ($t_s = 0.25$ y, $\alpha_s = 0.1$ kg C kg ^{1}C d ^{1}).

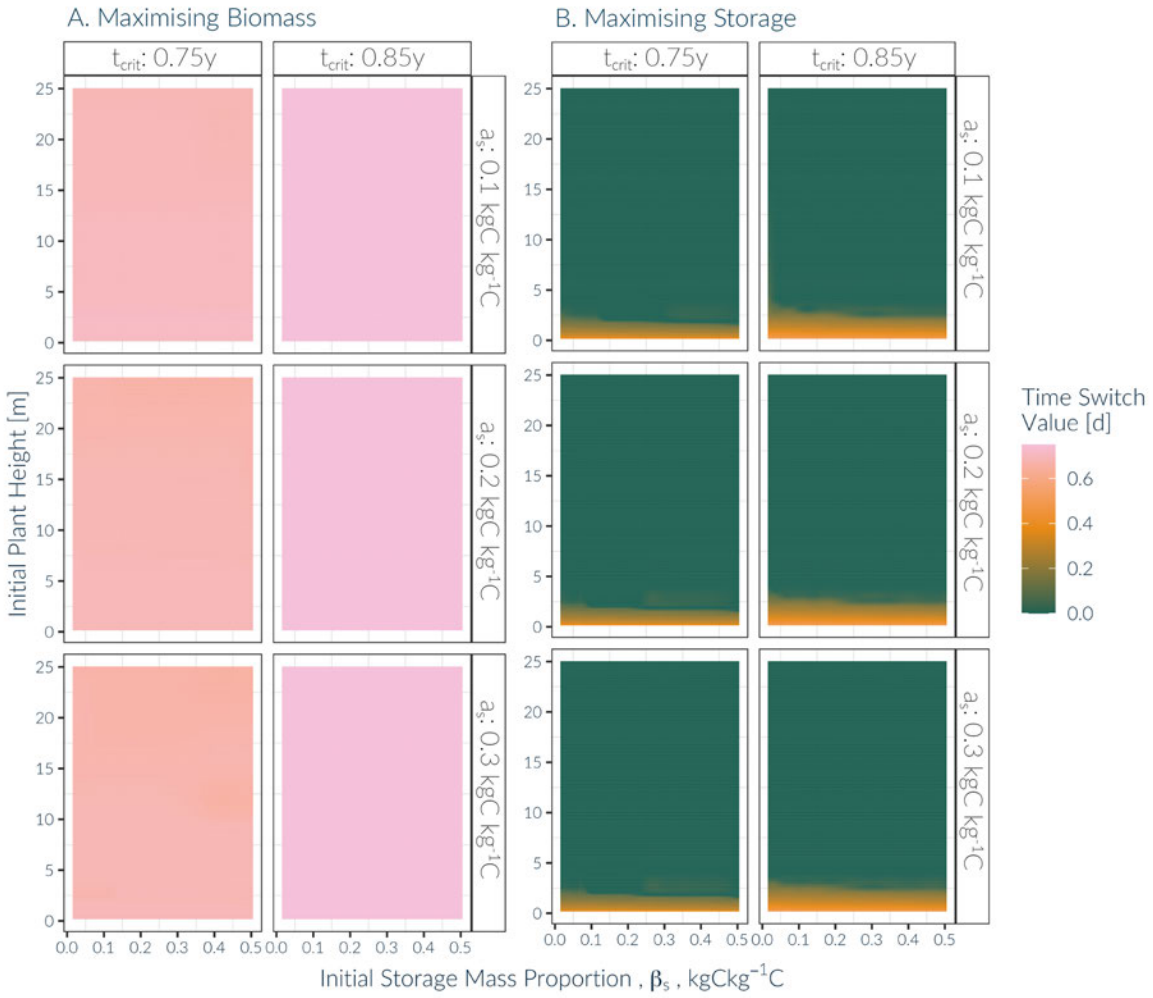

Figure 3-3 Sensitivity analysis of a simulated individual to the switch time parameter t_s for a range of initial plant heights (y-axis) and storage mass proportions (x-axis) and three values of α_s. The colours indicate the value of t_s that maximises the live mass of the plant at the end of the year (A) or the storage mass at the end of the year (B).

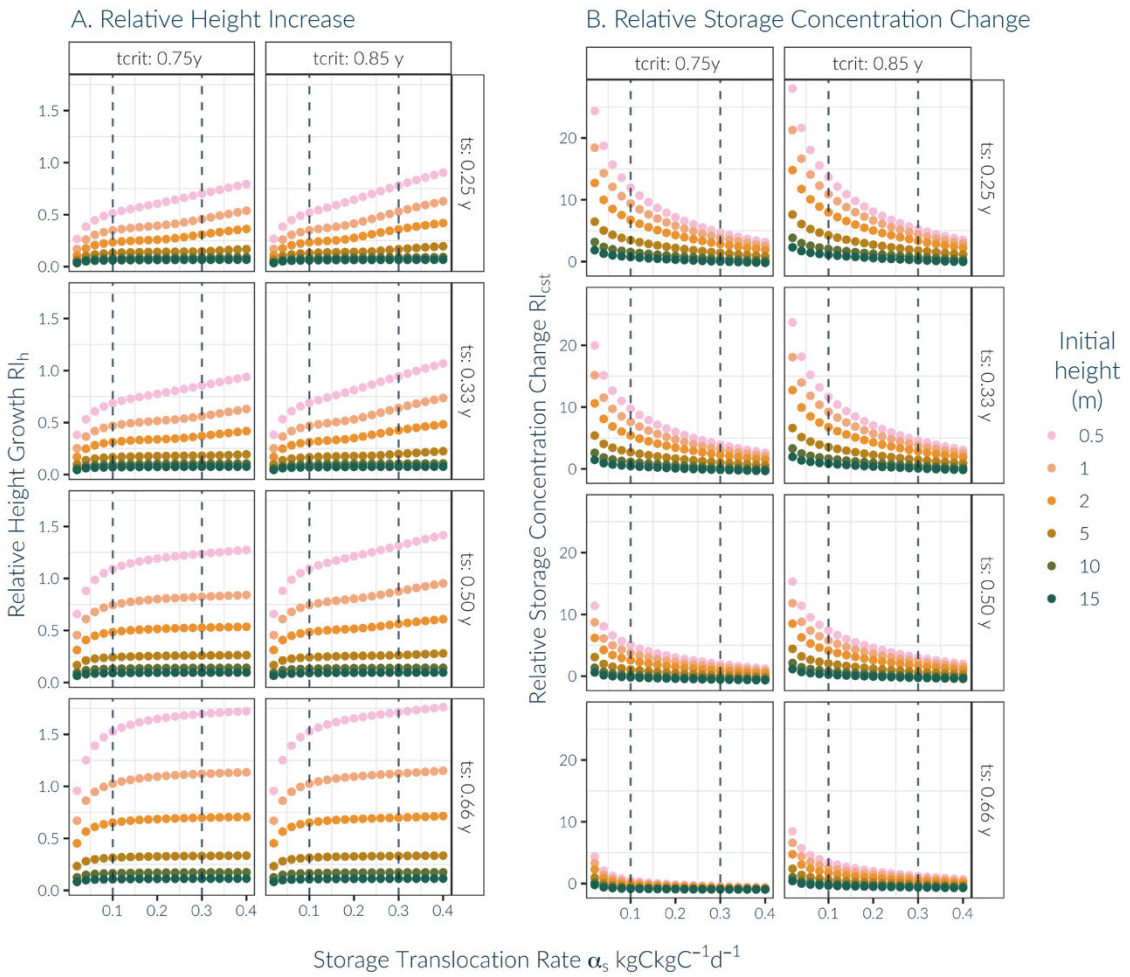

Figure 3-4 Sensitivity of growth of an individual plant for one year to the storage utilisation rate parameter (x-axis) for different environmental stress treatments (columns), time switch parameters (rows), and initial heights (colours). Dashed lines indicate the two values chosen as parameters. Panel A shows the relative increase in height and Panel B shows the relative change in carbon storage concentration.

To test the effect of these strategies on growth in the absence of competition, a single plant of each strategy was simulated for a 100-year period in an environment with no light competition and for the three average stress durations used in the model (Figure 3-5): no stress, 54.75 days and 91.25 days. Both the strategy and the duration of stress affected the final size of an individual. The Risky-Safe spectrum has a much larger effect on the final plant size than the Fast-Slow spectrum. The reasons for these impacts can be seen by zooming in on one year (Figure 3-6). The later switch time (longer growth duration) of Risky strategies contributes more to growth than the storage utilisation rate α_s (Figure 3-6A). The significant difference in the plants of the Fast-Slow strategy spectrum comes during the recovery period when height growth is halted in favour of recovering allometric balance in the plant: the Fast strategy allows plants to recover their growth faster than those with the

Slow strategy. The trade-off is that the Fast strategy also results in a smaller annual minimum of the NSC pool and, therefore, a higher potential for mortality during those periods (Figure 3-6B).

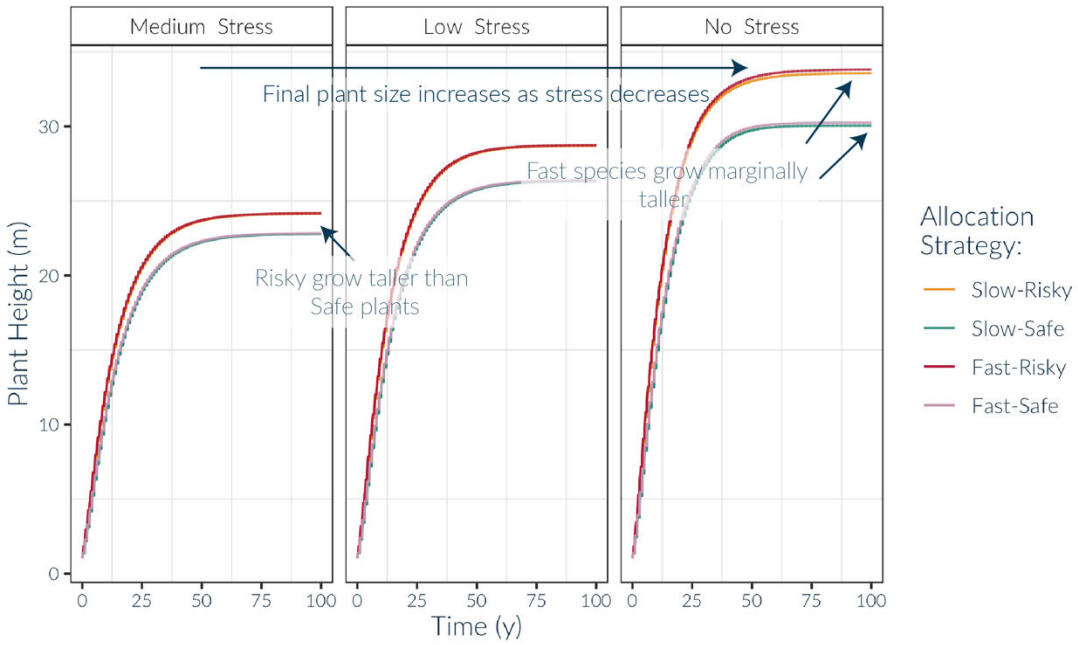

Figure 3-5 Trajectory of plant height for a single plant using each allocation trajectory and growing without competition under different deterministic stress regimes over a 100 year period. Each box represents a different stress regime: medium stress (left, 0.75 of the year is photosynthetically active), low stress (middle, 0.85 of the year is photosynthetically active) and no stress (right, plants can photosynthesise for the entire year). Each colour represents a different allocation strategy: slow-risky (yellow), slow-safe (green), fast-risky (red) and fast-safe (pink) with Risky strategies outcompeting the Safe ones and the Fast-Risky reaching the tallest heights and Slow-Safe being the shortest of the individuals. The trajectory of plant height is similar for all strategies with plants reaching a plateau after a period of relatively fast growth. This plateau increases with number of photosynthetically active years. Differences between the strategies also become more pronounced with a decrease in stress.

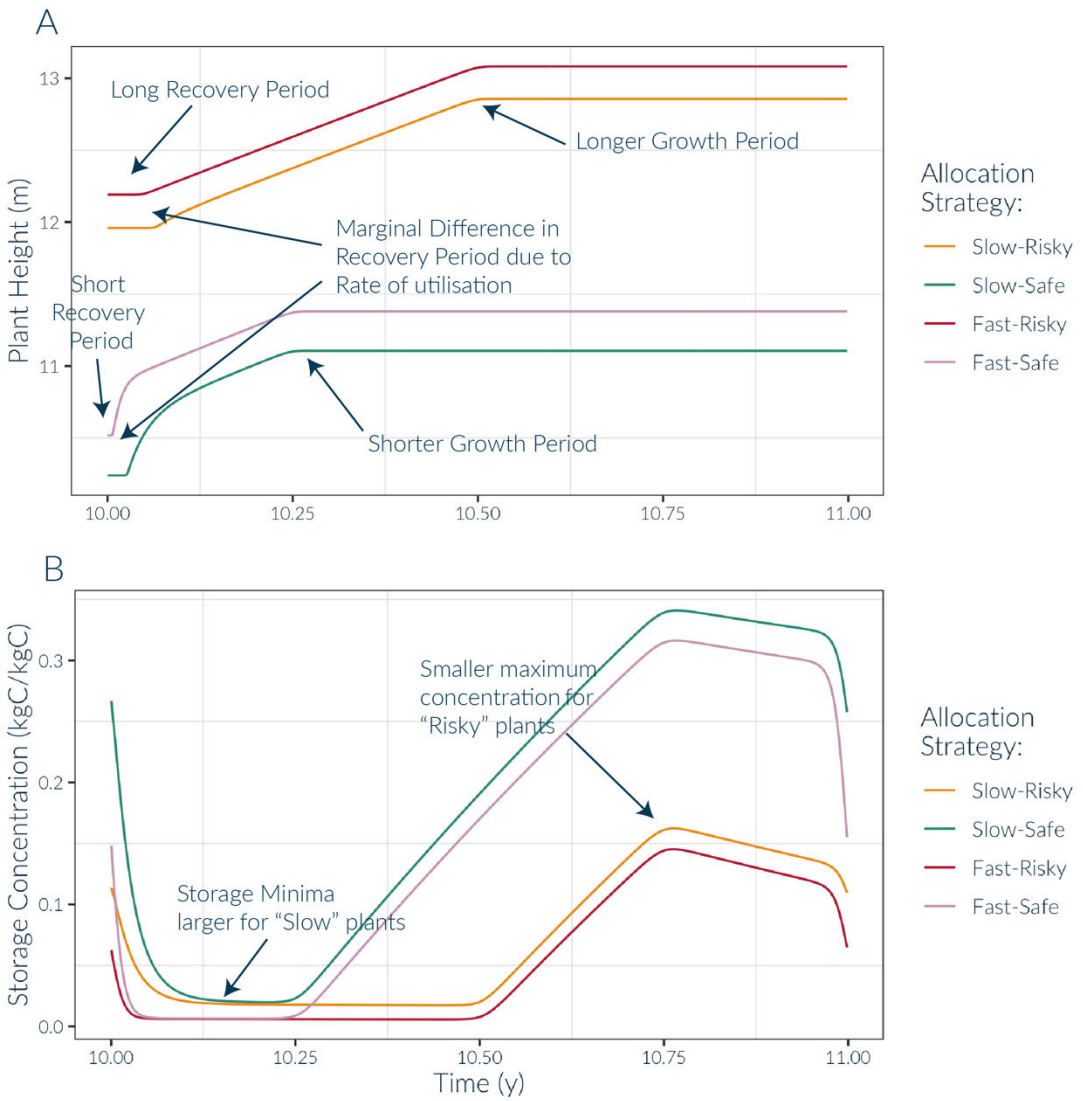

Figure 3-6 Illustration of variability in intra-annual height growth (A) and storage concentration (B) between strategies for a sample year. Strategies are represented by different colours: slow-risky (yellow), slow-safe (green), fast-risky (red) and fast-safe (pink). A: Initial lack of growth (the recovery period) is due to loss of allometric scaling over the previous stress season which leads to lack of vertical growth at the beginning of the year while missing pools are replenished. The Safe strategies have a shorter recovery period with a Fast translocation rate leading to marginally faster recovery period as opposed to Slow translocation rate strategies. The likely larger carbon pools of safe strategies lead to faster initial growth before achieving a constant rate, whereas Risky plants maintain a relatively stable growth rate for their entire height growth period. Most differences between strategies can be attributed to the difference between the switch time, that is to the Safe-Risky strategy spectrum. B: Due to a shorter growing period Safe plants exhibit a larger concentration of carbon as opposed to Risky plants and therefore a larger maximum at the start of the stress period. The minimum of storage concentration is governed by the differences between translocation rates, α_s rather than the switch time leading to a higher minimum of storage concentration for Slow strategies. The highest drawdown of carbon from storage can be attributed to growth rather than maintenance expenditure during the stress period.

The four strategies affecting the Growth-Storage trade-offs are illustrated in Figure 3-7.

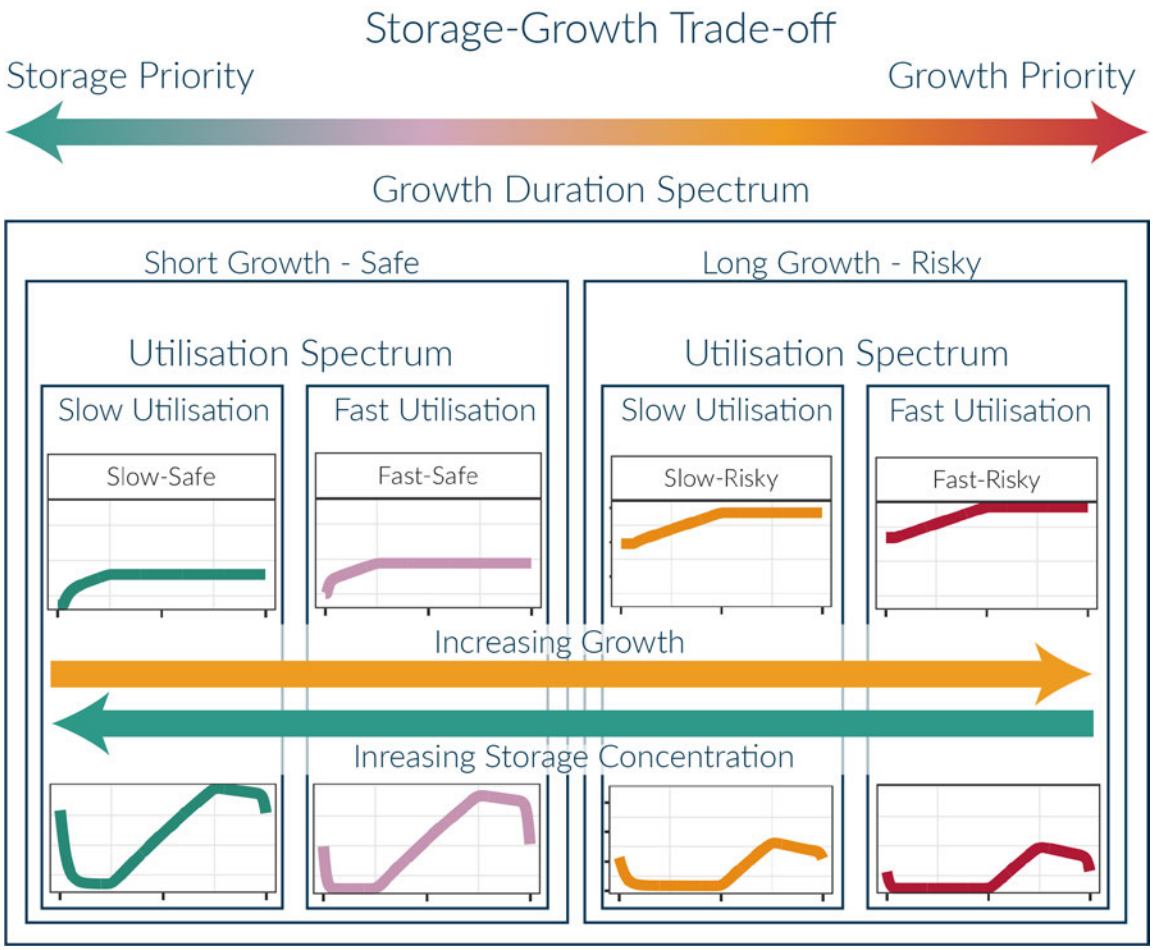

Figure 3-7 Storage-Growth Trade-offs as represented by the four strategies. Graphs illustrate the rough shape of intra-annual height growth. The largest differences are represented by the switch time through the parameter t_s, with shorter growth (smaller t_s values) representing a storage-prioritising plant and longer growth (larger t_s values) representing a growth-prioritising plant. For each growth-duration category a further distinction can be made by looking at storage translocation rates a_s with slower rates being on the storage priority end of the spectrum and faster rates on the growth priority end.

3.2.3 Simulations

With the four strategies defined, the model was run repeatedly for 100 years with all strategies present to investigate outcome of competition. An adaptive time-step was used with a range of 10^{-6} to 10^{-1}y. The environment treatments varied between stress intensity and stress stochasticity.

The environmental stress was varied for each run as follows. A total of 8 environment treatments were chosen, with two average stress intensities crossed with four levels of stochasticity from no stochasticity to high stochasticity. For each environment treatment, five random stress sequences were generated from the probability distribution defining that treatment (only one for the treatments with no stress stochasticity). The

model was run four times for each of the stress sequences to account for model stochasticity associated with germination and mortality (from hereon, referred to as stress-sequence repetitions). Additionally, a control simulation was run with no stress ($t_{crit} = 1$), no stochasticity and no storage-related mortality. A summary of these simulations is given in Table 3-2.

Table 3-2 Summary of Environmental Treatments. Mean growth is the mean duration of growth (y), SD growth indicates the standard deviation of the stress duration, num stress is number of stress-treatment repetitions, num seq is number of stress-sequence repetition (see text), num tot is the total number of repetition for that treatment.

Name	Mean growth	SD Growth	Num Stress	Num Seq	Num Tot	Notes
Control	1	0	1	4	4	No storage-related mortality
Low Stress-No Stochasticity	0.85	0	1	4	4	-
Medium Stress-No Stochasticity	0.75	0	1	4	4	-
Low Stress-Low Stochasticity	0.85	15	5	4	20	-
Medium Stress-Low Stochasticity	0.75	15	5	4	20	-
Low Stress-Medium Stochasticity	0.85	30	5	4	20	-
Medium Stress-Medium Stochasticity	0.75	30	5	4	20	-
Low Stress-High Stochasticity	0.85	60	5	4	20	-
Medium Stress-High Stochasticity	0.75	60	5	4	20	-

The size of the patch was set to be 100 m^2 following Bugmann (2001).

An initial simulation (for a high stochasticity environment) was run for 400 years to find the optimal number of years after which the outcome of competition is clear (although due to the stochastic nature of the stress and simulations themselves, no equilibrium or steady-state can be fully observed).

Each environmental treatment had all 4 allocation strategies present, with each strategy given an equal seed rain (0.5 seeds m^{-2} yr^{-1}) which was calculated from the FF16 deterministic model with the parameters used in the simulation. The simulations were run on a high performance, high memory server cluster with an average simulation duration of 3 days. The high-intensity of the simulation is attributed to the number of trees in each patch that need to be tracked including deceased plants which are kept track of in the algorithm.

3.2.4 Analysis of Simulation Results

All data transformation and analysis were performed using the R statistical programming software (R Core Team, 2018) and the package tidyverse (Wickham et al., 2019). Each

simulation was pre-processed to remove trees with a diameter smaller than 5cm. This was done due to the large number of small trees which did not survive the first few days of analysis and to maturity but were still present in the data resulting in a more computationally feasible analysis. Time series outputs were averaged using a rolling average for observation and a time-series of 20 y < t < 100 y was examined for indicators of relationships between strategy successional status.

To analyse final outcomes, basal area values in the last 10 years of the simulation (90 y < t < 100 y) were averaged for each run. Treatment means and standard deviations were then calculated. To analyse the effect of environmental stress on the final yield, a linear regression, accounting for individual strategies and treatment, was performed. To assist with interpretation of those results, an omega squared, ω^2, value was used to calculate the effect size based on the comparison between proportions of variance of predicting variables (LeCroy & Krysik, 2007) which was interpreted using measures described in (Field, 2013). Both operations were done using the R package *effectsize* (Ben-Shachar et al., 2020).

The differences between the repetitions of the 'stress treatment' and the 'stress sequence' did not need to be considered as any effect would be negligible.

All the result analysis can be found in the following repository: https://github.com/foxeswithdata/storage_plant_simulation_analysis, kept separate from the simulation model code to assist with modularity.

3.3 Results

3.3.1 Effect of stress on final basal area

In each environment, only two of the four strategies are viable. In the control simulation, where there is no stress and no mortality associated with low carbohydrate storage, the Fast-Risky and Slow-Risky strategies outcompeted both Safe strategies, as a result of the longer growing period of the Risky strategies (Figure 3-8). Once stress is introduced, only the Slow approaches are viable, indicating there is an advantage to lowering the rate of storage utilisation, α_S.

The Fast-Safe strategy fails in all environments. Under the no-stress scenario, the benefit of the faster utilisation rate is outweighed by the earlier switch time (shorter growth

duration), and the strategy is outcompeted by Risky strategies. When stress is introduced, the faster utilisation rate creates a higher mortality risk early in the season. The plants are outcompeted by both the Slow-Risky strategy plants, which can grow faster and shade them, and the Slow-Safe strategy which has a larger buffer against stress.

Introducing stress and storage-related mortality into the simulations reduces final basal area by between 30% and 50% (Figure 3-8) which is larger than the 15% and 25% reduction in photosynthetic days. However, the maximum height that an individual plant reaches decreases proportionally with the number of photosynthetic days (Figure 3-5). If the reduction in basal area was caused only by the decreased photosynthetic period, the basal area reduction between control and stress treatments would likely be comparable to that of a decrease in individual plant size. However, the basal area reduction in a patch between stressed and unstressed treatments (Figure 3-8) is close to twice the reduction in the size of a single individual due to stress (Figure 3-5). Therefore, the effect of introducing stress and competitive interaction must play a role beyond loss of photosynthetic uptake. The

processes contributing to this decline are further examined in Sections 3.3.3 and 3.3.4.

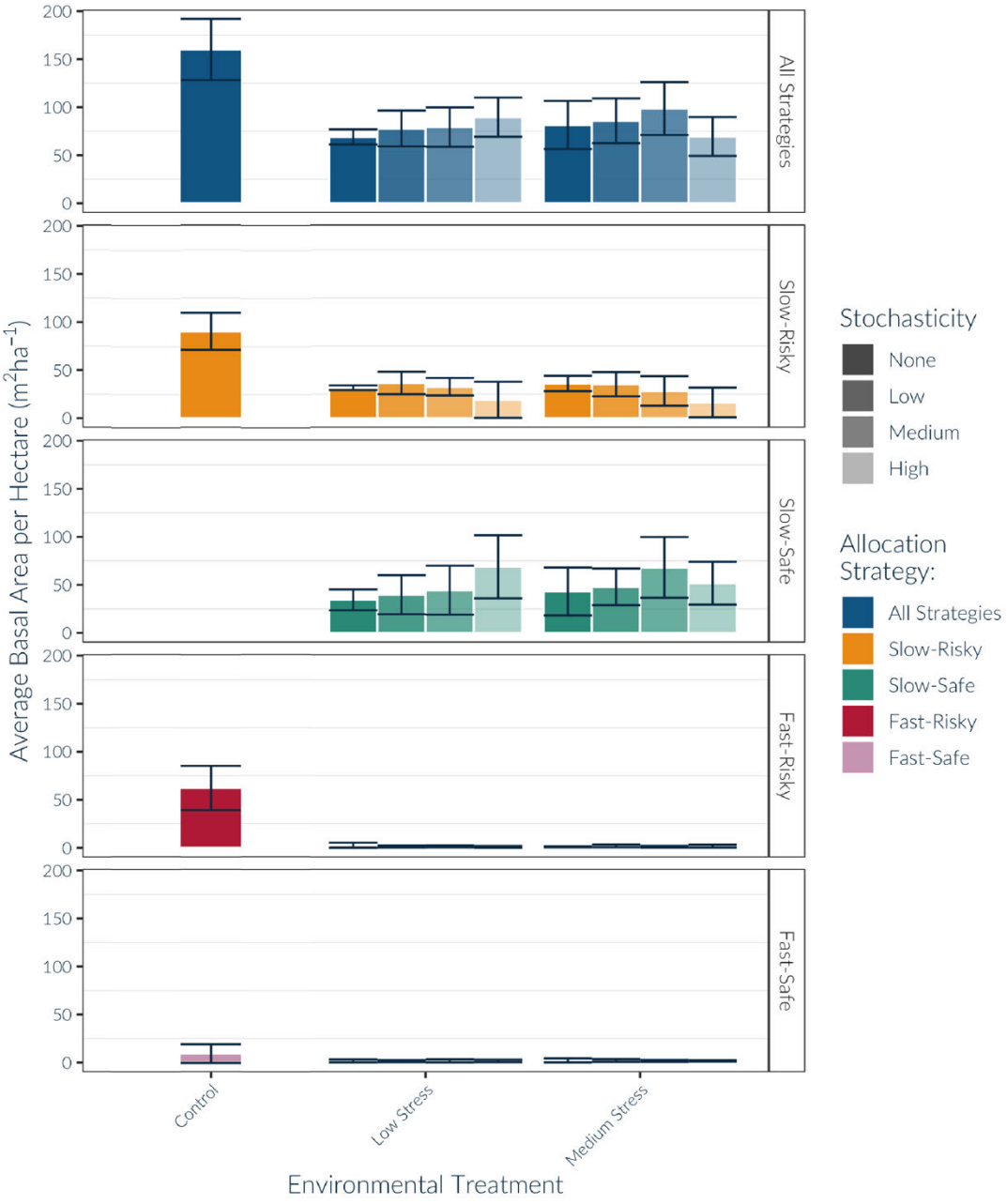

Figure 3-8 Final yield as determined by the basal area averaged first across each time point in years 90-100 of data and then by environmental repetition (N = 4 in control treatments with no stochasticity and N = 20 in treatments with stochasticity > 0). Error bars represent the standard deviation across environmental repetitions. Rows represent strategies with the first row combining all strategies across the plot. Shading represents the stochasticity of the environment with the darkest colours representing environments with no stochasticity and lightest colours showing environments with the highest stochasticity.

3.3.2 Environment treatment effect on final basal area

Table 3-3 and Figure 3-9A show that stress stochasticity affects the competitive dominance. As stochasticity increases, there is a decreasing basal area of the Slow-Risky strategy ("large effect" in Table 3-3) and an increasing basal area of the Slow-Safe strategy ("medium effect"). Plants using the Fast strategy are uncompetitive and exhibit no or a small change in basal area.

In contrast, the average stress duration does not have a consistent effect on competitive outcome (Table 3-4, Figure 3-9B). The basal area of the Slow-Safe strategy is increased with increasing stress duration ("small effect" for all levels of stochasticity and low stochasticity and "medium effect" for medium stochasticity in Table 3-4) but this trend is reversed when plants are subjected to high stochasticity. With medium stress and high stochasticity, there can be years with extreme environmental stress that can significantly inhibit all strategies. There is a small decrease in basal area of Slow-Risky plants with increasing stress, with mostly a "very small" effect. However, this decrease may be enough for the Slow-Safe strategy to become more successful, thereby increasing its overall basal area. The effect may also be affected by the response at high stochasticity when both Slow-Risky and Slow-Safe decrease in basal area which is likely caused by increased mortality due to an increased number of high and very high stress years.

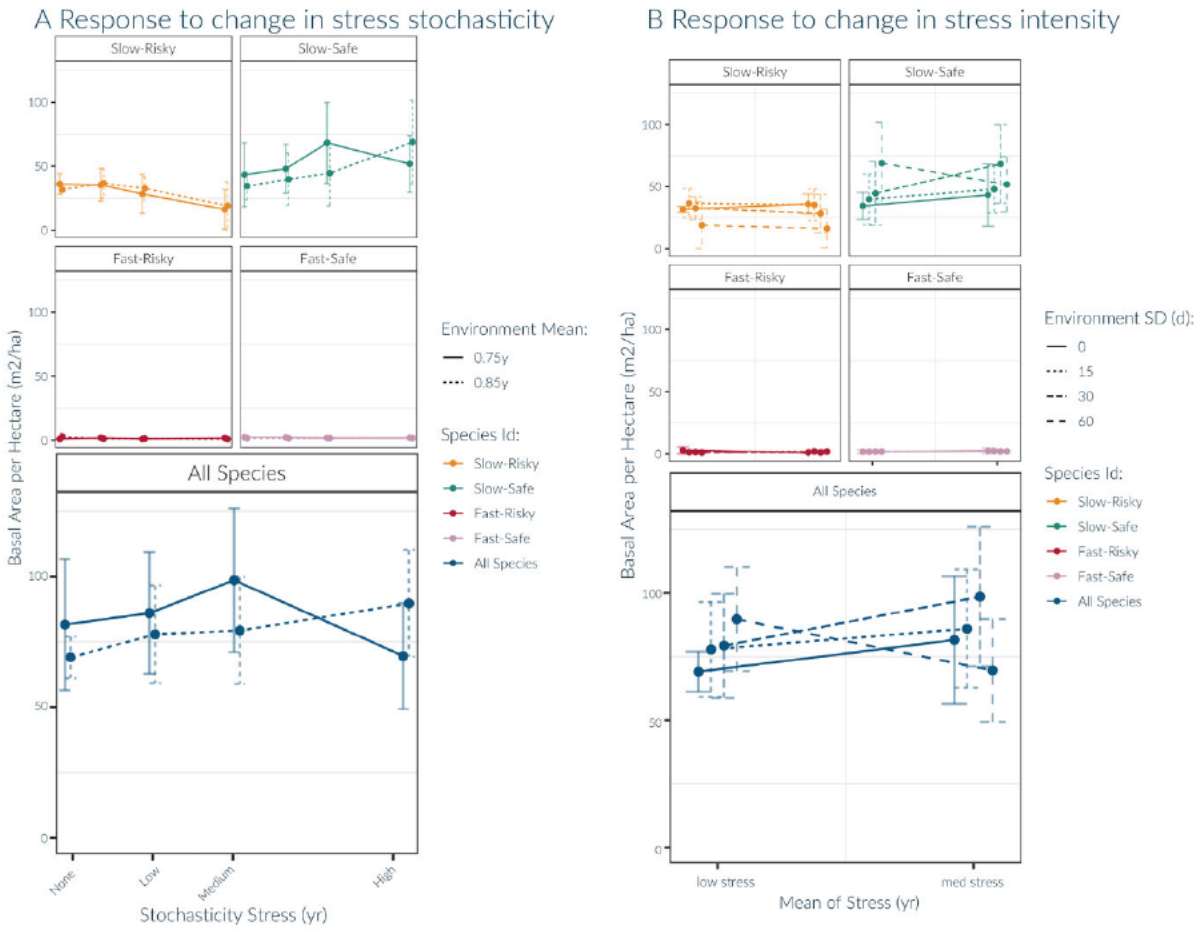

Figure 3-9 Effect of the stress stochasticity (A) and intensity (B) on the final basal area (= mean BA of last 10 years of simulation) for different strategies (top 4 panels) and all strategies combined (large bottom panel). Points and error bars show mean and standard deviation of basal area across environmental repetition (N = 4 in treatments with no stochasticity and N = 20 in treatments with stochasticity). Error bars represent the standard deviation across environmental repetitions.

*Table 3-3 Effect of stochasticity on the log of the final basal area (m2/ha) for each strategy with stochasticity (as explained by the standard deviation around the mean of onset of stress). Each model was run for a subset of mean stress duration (either low stress or medium stress) and for the combined data. Significance of each model parameter is given in brackets ('***': p <= 0.001, '**': p <= 0.01; '*' p <= 0.0; '.': p <= 0.1; '-' p > 0.1). Additionally, an ω^2 value was calculated to measure the effect size and an interpretation of the value is given based on interpretation guidelines from Field (2013).*

Species	Stress Dur Mean	Parameter Value		ω^2	Field 2013
		log(intercept)	A (yr)		
Slow-Risky	All Means	3.88 (***)	-0.03 (***)	0.25	large
	Low Stress	3.94 (***)	-0.03 (***)	0.30	large
	Medium Stress	3.82 (***)	-0.03 (***)	0.22	large

Slow-Safe	All Means	3.57 (***)	0.01 (**)	0.05	small
	Low Stress	3.82 (***)	0.00 (-)	-0.01	very small
	Medium Stress	3.33 (***)	0.01 (***)	0.12	medium
Fast-Risky	All Means	0.14 (-)	0.00 (-)	0.00	very small
	Low Stress	0.01 (-)	0.00 (.)	-0.01	very small
	Medium Stress	0.30 (.)	-0.01 (**)	0.06	small
Fast-Safe	All Means	0.31 (***)	0.00 (-)	0.00	very small
	Low Stress	0.45 (***)	0.00 (-)	-0.01	very small
	Medium Stress	0.16 (-)	0.00 (-)	-0.02	very small

*Table 3-4 Effect of stress mean on the log of the final basal area per hectare (m2/ha) for each strategy calculated using a log-linear model with the negative of the stress mean taken as a continuous variable. Each model was run for a subset of stochasticities (from no stochasticity to high stochasticity) and for all stochasticities combined. Significance of each model parameter is given in brackets as explained by the p-value ('***': p <= 0.001, '**': p <= 0.01; '*' p <= 0.0; '.': p <= 0.1; '-' p > 0.1). Additionally, an omega-squared value was calculated to measure the effect size and an interpretation of the value is given based on interpretation guidelines from Field 2013.*

Strategy	**Stress Stochasticity**	**Parameter Value**		ω^2	**Field 2013**
		Log (intercept)	a(-yr)		
Slow-Risky	All Stochasticity	1.33 (-)	-2.14 (***)	0.00	very small
	No	4.43 (***)	1.15 (-)	-0.01	very small
	Low	3.15 (***)	-0.47 (-)	-0.02	very small
	Medium	-0.49 (-)	-4.63 (-)	0.04	small
	High	0.71 (-)	-1.96 (-)	-0.02	very small
Slow-Safe	All Stochasticity	5.12 (***)	1.64 (-)	0.01	small
	No	3.72 (-)	0.26 (-)	-0.14	very small
	Low	5.83 (***)	2.72 (-)	0.03	small
	Medium	7.74 (***)	4.85(**)	0.12	medium
	High	2.07 (-)	-2.38 (-)	0.03	small
Fast-Risky	All Stochasticity	1.38 (-)	1.68 (-)	0.00	very small
	No	-5.94 (-)	-7.79 (-)	0.11	medium

	Low	2.51 (-)	2.95 (-)	0.00	very small
	Medium	-1.99 (-)	-2.42 (-)	0.00	very small
	High	4.94 (**)	6.25 (*)	0.10	medium
Fast-Safe	All Stochasticity	2.70 (**)	2.93 (*)	0.03	small
	No	2.90 (-)	3.14 (-)	-0.10	very small
	Low	2.87 (-)	3.13 (-)	0.01	very small
	Medium	2.24 (-)	2.45 (-)	-0.01	very small
	High	2.96 (*)	3.12 (-)	0.03	small

3.3.3 Drivers of competitive outcome

One example run was selected from the Low-stress, Medium-stochasticity treatment to illustrate the progression of the model. The height distribution for each strategy is shown in Figure 3-10. The Slow strategy trees show a much higher success compared to the Fast strategy trees. After the initial 20-years of the simulation, the Fast approaches perform below the average across the patch, and there are three long periods during which no Fast-Risky trees are observed (19-24 y, 55-66 y and 77-95 y) and one during which no Fast-Safe plants were present (84-96 y). The maximum height reached by the Fast-Risky strategy is 15.5 m and by the Fast-Safe it is 14.2 m. The Slow-Risky strategy reaches heights of 20.1 m and the Slow-Safe strategy 21.5 m. It can also be noted that many plants with the Slow strategy survive much longer when shaded, compared to those with the Fast strategy. Moreover, although the Slow-Safe and Slow-Risky strategies maintain a relatively similar average height, the Slow-Safe strategy is most successful in terms of Net Carbon Uptake (Figure 3-11), being responsible for up to three quarters of NCU across the patch.

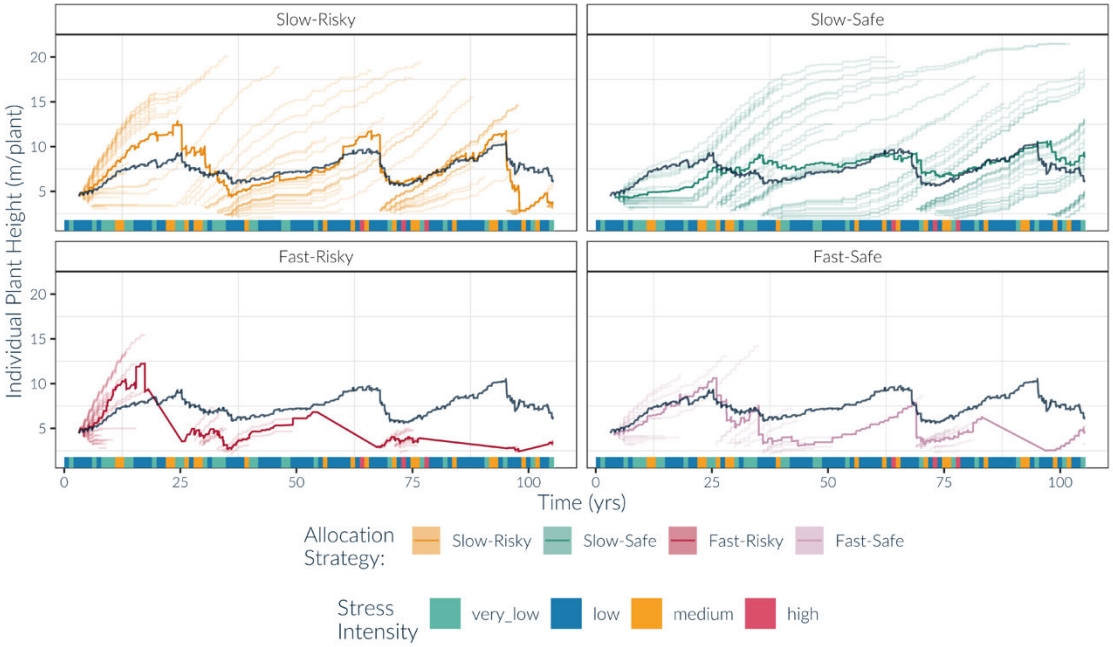

Figure 3-10 Height distribution of individuals over 100 years on a 100 m^2 patch. Each panel shows one allocation strategy in the population ((a) slow-risky, (b): slow-safe, (c): fast-risky and (d): fast-safe). Pale lines show individual trees; darker lines of each colour show the average for all individuals of that species; dark blue line shows average height for the entire population. The rug on each figure shows the duration of the stress in a given year (green for very low stress intensity <30d, blue for low (30 to 75d), yellow for medium (75 to 105d) and red for high (105 to 150d)). Periods of no height increase in an individual can be explained by an allometric mismatch after the period of stress. During the recovery period, growth is prioritised in the plant components that are most imbalanced until allometric relationships are regained.

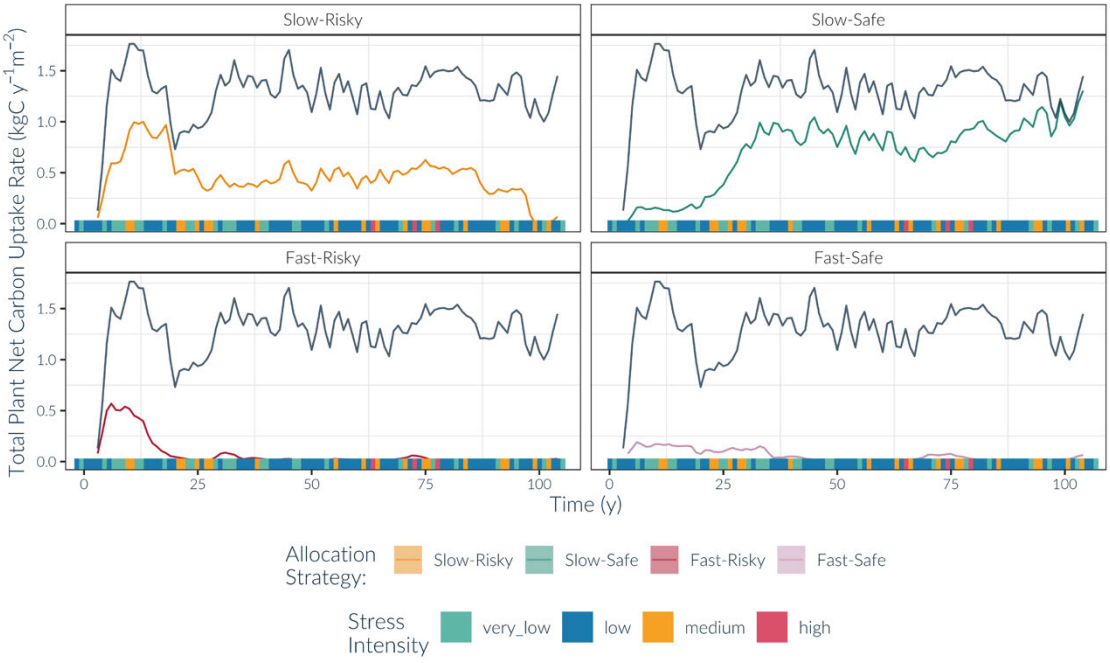

Figure 3-11 Total Net Carbon Uptake (NCU) summed across all individuals in a patch of a given strategy across a 100-year time scale on a 100m2 patch. Dark blue line shows the sum of NCU for the entire population regardless of strategy. The rug on each figure shows the intensity of the stress in a given year as described by the length of the stress (green for very low stress intensity <30d, blue for low (30 to 75d), yellow for medium (75 to 105d) and red for high (105 to 150d)). Periods of no height increase in an individual can be explained by an allometric mismatch: since plants don't grow for a proportion of the year growth is prioritised in those components that are most imbalanced until balance can be regained.

The dominance of the Slow strategy species is visible in the *height* (Figure 3-10) and *productivity* (Figure 3-11) of the individual plants and in the *number* of individual plants (Figure 3-12). Apart from the higher densities during stand establishment in the initial 20 years, the Slow strategies reach a maximum of 26 (for the Slow-Risky) and 31 (for the Slow-Safe) individuals per patch, with an average of 14.0 (Slow-Risky) and 23.6 (Slow-Safe) individuals being simultaneously present on the patch. When compared to the Fast strategies, which reach a maximum of only 10 (Fast-Risky) and 14 (Fast-Safe) individuals and an average of 3.4 (Fast-Risky) and 3.9 (Fast-Safe) individuals, I conclude that the Slow strategies are more successful in competition than Fast strategies. There is a small number of individuals that reach the sapling stage (diameter at breast height, DBH > 5cm). In addition, the low average height of Fast strategies indicates there is a low survival rate for trees that do reach the sapling stage.

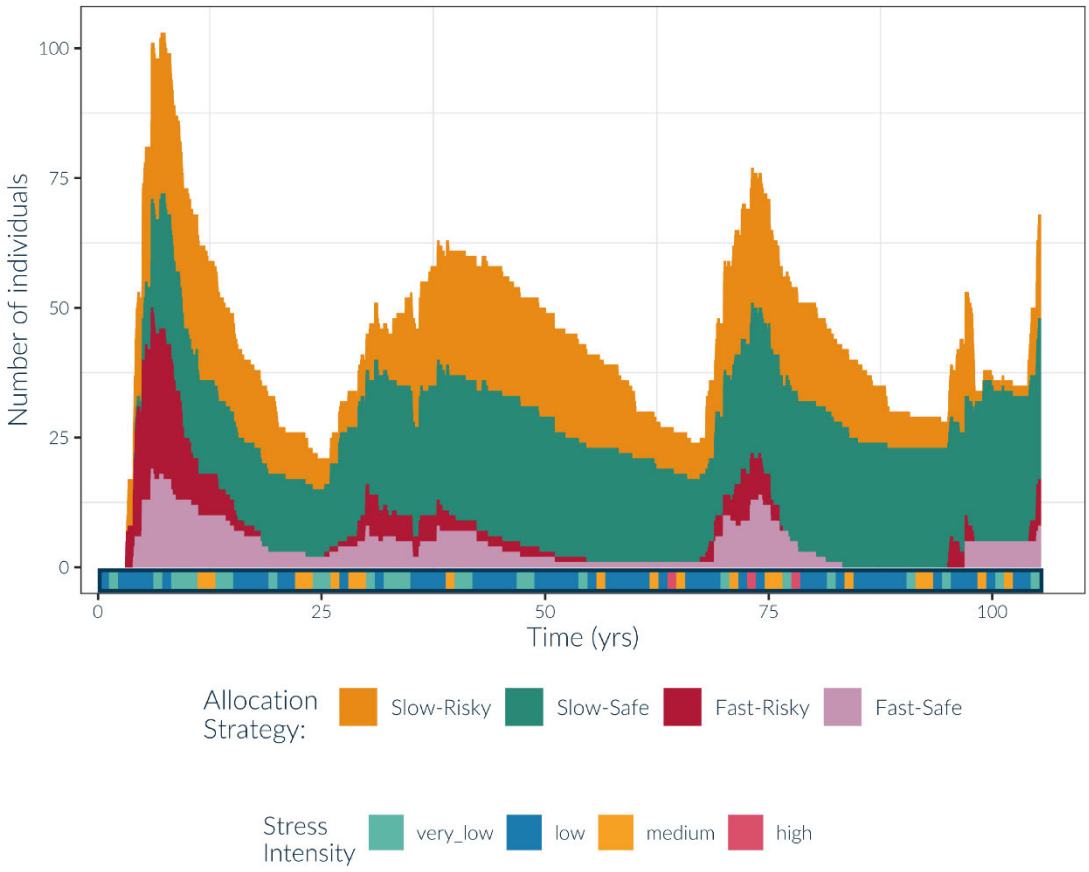

Figure 3-12 Number of individuals of each strategy living on the 100 m^2 patch over time. The rug shows the intensity of the stress in a given year as described by the length of the stress (green for very low stress intensity <30d, blue for low (30 to 75d), yellow for medium (75 to 105d) and red for high (105 to 150d)).

Tree mortality in the model occurs when storage is low (storage-dependent mortality, Equation 3-13), such as when a plant is subjected to a prolonged stress, or when net mass production per leaf area is low (productivity-dependent mortality, Equation 3-12); e.g., when a plant is shaded. In the initial 20 years of the simulation, there is little shading and, therefore, all plants grow at their intrinsic growth rates. In those initial years, the Slow-Safe strategy performs the worst because it has the lowest intrinsic growth rate. Subsequently, however, there is a decline of the Fast strategies, especially the Fast-Risky strategy plants. Two factors are likely influential in this decline. First, during long stress periods, the plants need stored carbon to survive and recover from the stress. Risky plants have lower survival over these periods as evidenced by decreased mean height (Figure 3-10) and NCU (Figure 3-11) as well as lower average storage concentrations (Figure 3-13). Second, Fast strategies have lower minimum storage concentrations compared to Slow

strategies (Figure 3-6 and Figure 3-13) indicating that insufficient productivity under shading may be a contributing factor controlling mortality of this strategy. Since most Fast-Safe individuals occupy the lower parts of the canopy (Figure 3-10), they may have insufficient carbon uptake which, combined with lower carbon store minima, increases the mortality of these individuals. Since the Slow-Safe plants survive to reach the top of the canopy despite being shaded for much of the initial 100 years, inadequate carbon stores under shade must be the ultimate cause of the mortality of the Fast-Safe individuals.

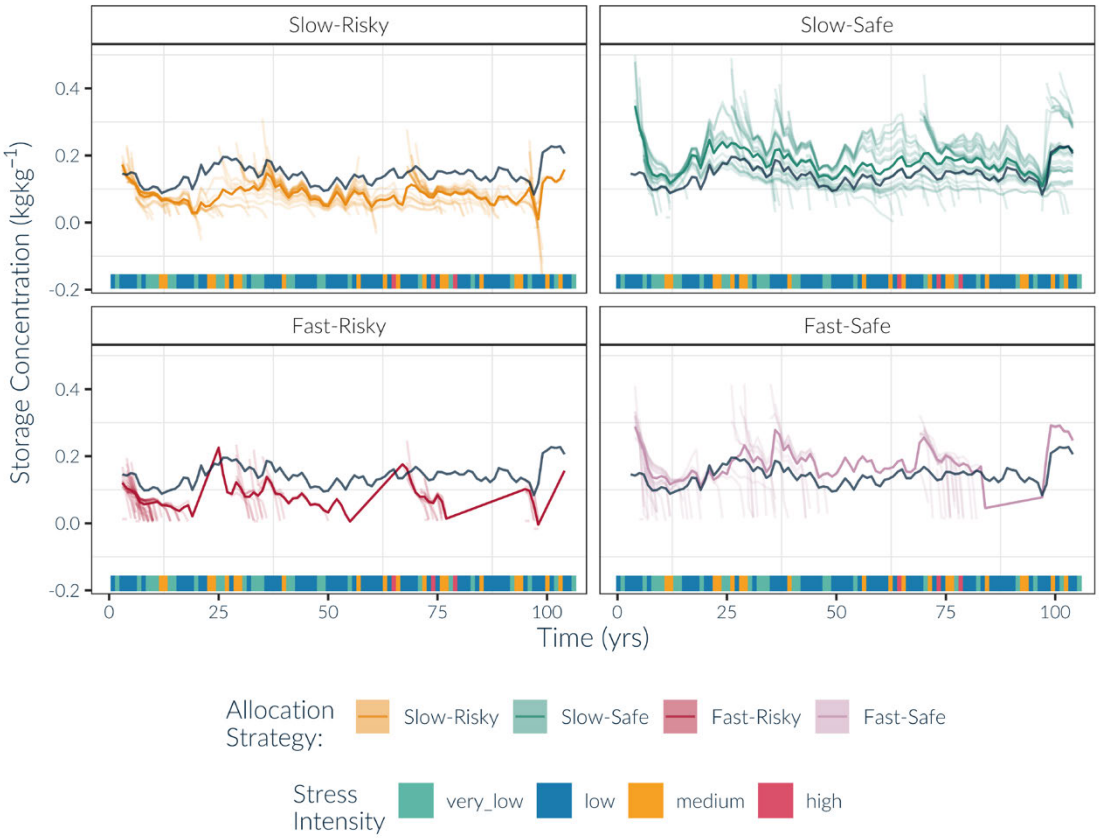

Figure 3-13 Stored carbon concentration in individual plants as a rolling 2-year average. Legend follows Figure 3-10.

3.3.4 Stress and Mortality

The stress and shade contributions to mortality can be further examined by looking at mortality during stress periods and under canopy shading across all simulated environments which include stress.

During the stress period, productivity-dependent mortality is switched off, and trees only die because of storage-dependent mortality. The proportion of deaths during stress can

be calculated for each strategy as the number of plants of the strategy which die in a given stress period, divided by the total number of plants of that strategy which were alive during that period. The proportion of deaths during stress increases with the duration of the stress in a logistic relationship (Figure 3-14). While there is noise in the model output due to the stochastic nature of the mortality function (Equation 3-14), there is still a visible pattern in that the proportion of deaths remains steady until it starts to rapidly increase. For Risky strategies, 50% of plant mortality occurs when stress is 165 days (Fast-Risky) and 172 days (Slow-Risky), while for the Safe strategies these numbers are 266 days (Fast-Safe) and 299 days (Slow-Safe), although this pattern is less clear in the Fast-Safe strategy due to the lower number of individuals.

Outside of the stress period, productivity-dependent mortality can occur in addition to storage-dependent mortality. The proportion of deaths in the population is shown as a function of canopy openness (the percent of light reaching the top of the plant, with 0 being total darkness and 1 being full light) in Figure 3-15. Here trees are grouped by canopy openness and the proportion of trees in each canopy openness group that die that year is calculated. The proportion of deaths has an exponential decay relationship with canopy openness (Figure 3-15). The higher the light level, the lower the proportion of deaths, with differences driven by the rate of carbon utilisation (Fast-Slow) spectrum. Slow strategy plants tolerate shade better than Fast strategy species (showing a faster decline of mortality with increased light). The mortality of Fast strategies under shade may be a combination of increased productivity-dependent mortality due to inadequate carbon supply and storage-dependent mortality due to their lower storage concentration minima (Figure 3-6). This would agree with the hypothesis that the Fast-Safe strategy cannot survive the shade and, therefore, becomes outcompeted by the other strategies.

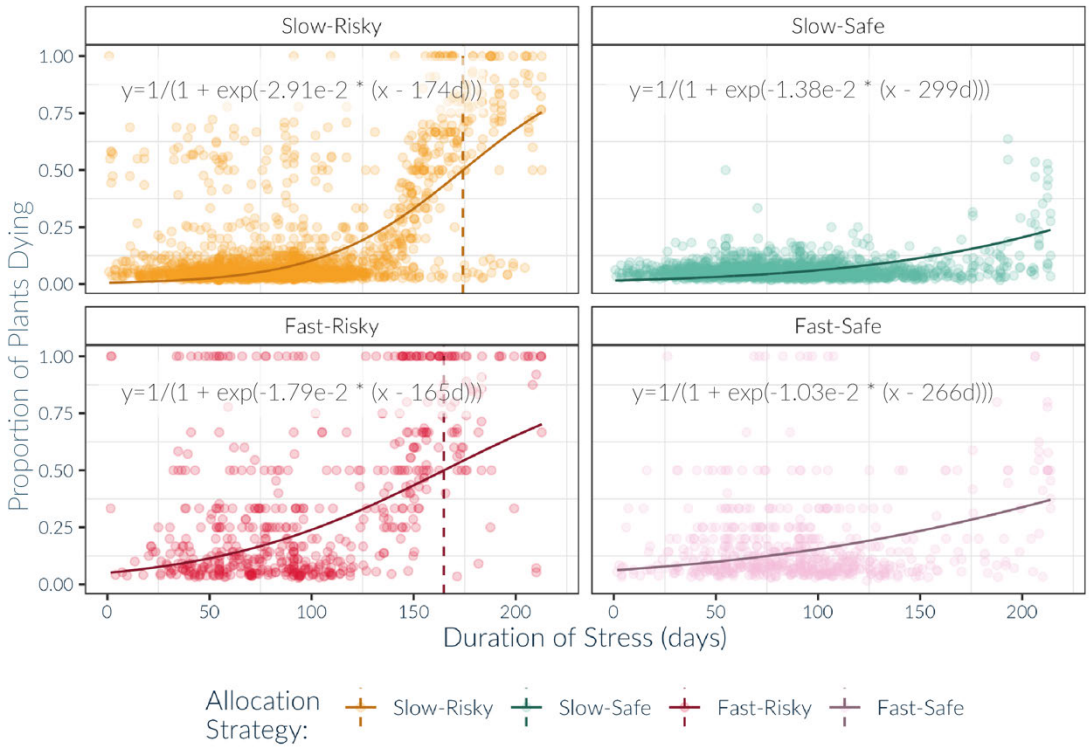

Figure 3-14 Proportion of population dying during a stress period (all simulations), as a function of stress duration. The proportion is calculated as the number of deaths of a given strategy divided by the total number of individuals of that strategy alive during the stress period, with each point signifying a single simulated year. Deaths outside of the stress period are not considered. A logistic equation is fitted to the data and the point of 50% death for each strategy is indicated by the vertical dashed line and indicated in the formula for that fitting (not shown for the Slow-Safe and Fast-Safe strategies for which this point is beyond the data observed).

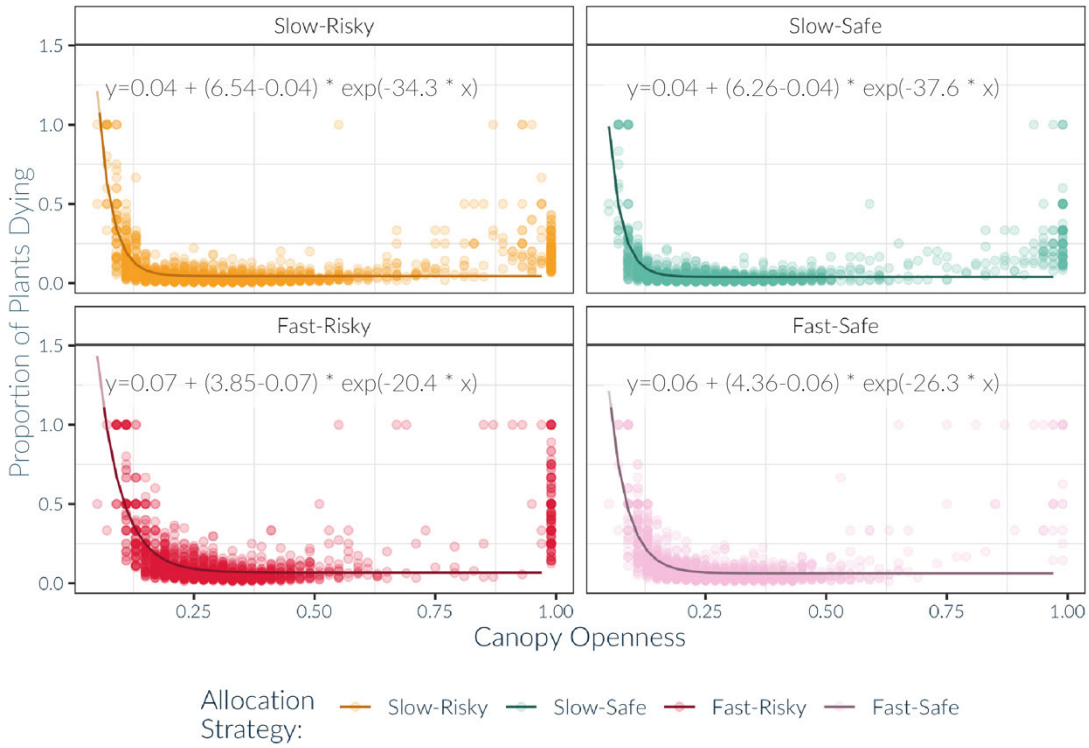

Figure 3-15 Relationship between population mortality and light competition for all simulations. The proportion of plant mortality is calculated as the number of deaths of plants of a given strategy which live in a given light environment divided by the total number of individuals of that strategy alive in that same light environment, with each point signifying a single simulated year. Deaths during the stress period are not included because productivity-driven mortality is assumed to be zero during stress. The light environment is represented by canopy openness, calculated as the proportion of incident light available at the plant height. Deaths with canopy openness = 1 were removed, and an exponential decay function was fitted to each set of data (solid line and equation in each panel).

3.4 Discussion

In this work I have explored the long-term impacts of different carbon storage utilisation strategies using a gap model, which includes both environmental stochasticity and competition between individuals. I simulated the response of a community of trees to varying strategies on the growth-storage trade-off spectrum. The trees grew for 100 years in environments with and without stress, as well as with and without environmental stochasticity. The four strategies varied in two parameters: the speed of carbon utilisation (Slow-Fast utilisation spectrum) and length of the growth period determined by the growth-storage switch point (Safe-Risky spectrum, short to long growth period). The strategies differed only in these traits, so the primary factor determining the outcome of competition

was differential mortality rates: a long growth period (Risky strategy) reduced the chance of survival during a stress period, and a fast carbon utilisation rate (Fast strategy) reduced the size of the carbon storage pool, thereby reducing the shade-tolerance of an individual tree. In general, the Slow-Safe strategy may benefit a secondary succession species, while the Fast-Risky strategy may benefit a pioneer species. Additionally, the Slow-Risky strategy allowed trees to survive both as a pioneer species, but also in more stressful environments, while the Fast-Risky strategy exposed trees to potential mortality. In contrast, trees in the Fast-Safe strategy were not successful in early succession, when they are outcompeted by longer growing and therefore taller individuals, nor in secondary succession because they were not shade tolerant. A summary of the four strategies and their differences is shown in Figure 3-16.

When seasonal stress was absent from the model, the successful strategies were the two Risky strategies. There was no stress-related mortality in the no-stress environment, so the primary cause of mortality was productivity-based mortality, which is dependent on the degree of shading, rather than on the size of the carbon storage pool. Trees in the Risky strategy grew longer and thus outcompeted trees in the Safe strategies by overtopping and shading them. The speed of utilisation of carbon had little effect in the no-stress environment.

When stress was introduced, the tree strategy shifted to the Slow-Safe and Slow-Risky strategies. However, the reason behind the survival of trees in each of the two strategies was different. The trees were subjected to both an annual seasonal stress and shade stress. Trees in the Slow-Safe strategy could survive extended periods of time in shade with limited photosynthesis (Figure 3-10), likely due to higher carbon storage minima offsetting the low photosynthetic gain. Once taller trees died due to annual seasonal stress, trees in the Slow-Safe strategy could grow to the top of the canopy. On the other hand, the Slow-Risky trees were more susceptible during the seasonal stress due to lower carbon stores, but could grow rapidly and outcompete other plants for light. As with the Slow-Safe strategy, Slow-Risky trees also had a high carbon storage minimum (Figure 3-6), which facilitated the survival of small saplings in the shade. The failure of the Fast-Risky strategy was strongly associated with stress-related mortality exacerbated by the inability of trees to

survive in shade. The Fast-Safe strategy also failed, predominantly due to the lack of shade-tolerance in trees, which led to mortality before a canopy gap became available.

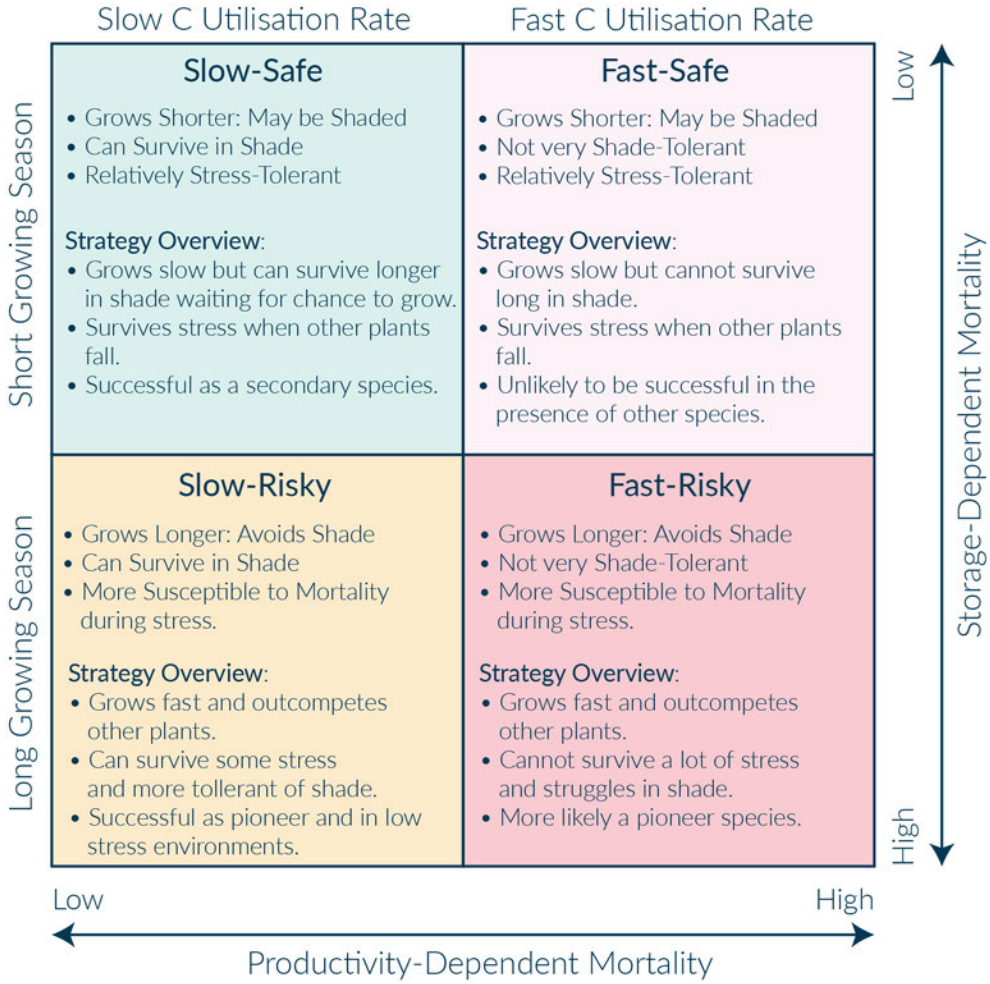

Figure 3-16 Summary of model outcomes by plant strategy. Storage-dependent mortality differentiates between strategies on the Safe-Risky spectrum, with Safe strategies being more tolerant of stress conditions. Productivity-dependent mortality differentiates between strategies on the Slow-Fast spectrum of carbon utilisation, with Slow strategies being more tolerant of shaded conditions.

The results obtained in this study showed a community shift towards storage-prioritising strategies, as seen in the shift from Slow-Risky to Slow-Safe plants with increased stochasticity and stress intensity (Figure 3-9). As carbon storage strategy may be adapted to local conditions (e.g., Blumstein & Hopkins, 2021), the increased variability of local weather conditions and more extreme disturbances associated with climate change (IPCC, 2021) may contribute to significant shifts in community composition. Traits conferring drought- and heat-resistance have been increasingly emerging as contributors to plant survival in ecosystems worldwide. Shifts in community composition have been observed in tropical ecosystems towards increased representation of drought-resistance trees (Feeley et al.,

2011) and shifts in plant trait representation towards decreased specific leaf area and increased wood density, which are indicative of increased hydraulic resistance (Swenson et al., 2020). Long-term vegetation shifts towards more drought-resistant individuals have also been observed after severe droughts in south-western USA (Mueller et al., 2005). However, changes in species composition may not occur if there is a plastic change over time in the strategy of an individual.

Trait plasticity was not considered in this study but may be important in further work examining NSC strategies to climate change. For example, seedlings may acclimate to repeated stress by increasing storage of non-structural carbohydrates (Myers & Kitajima, 2007). Trait plasticity may be an important factor in trees under increasingly intense and varied environmental stress (Gallagher et al., 2019; Lanuza et al., 2020; Lecina-Diaz et al., 2021).

3.4.1 Effect of environmental stress

In addition to its effect on community composition, stress led to a significant decrease in carbon sequestration, as determined by the total basal area of the plants (Figure 3-8). Moreover, stress affected the outcome of competition among strategies (between Slow-Risky and Slow-Safe), with stochasticity having a more pronounced effect than the mean stress duration (Figure 3-9). Increasing stochasticity of the stress led to an increase in the number of Slow-Safe strategy trees and a decrease in Slow-Risky trees. Rather than average intensity, the presence of extreme events affected the decline of trees in the Slow-Risky strategy in the high stochasticity environments.

In order to evaluate the predicted response to stress duration, we need to identify seasonal and non-seasonal environments with similar climatic conditions, such as temperature and water availability. To evaluate the predicted response to stress stochasticity, examining stochastic variation in an environment would be greatly beneficial, although it is not estimated directly in many studies. Measures such as the rainfall seasonality index (Markham, 1970), which can assist in defining the constancy of an environment, and other measures of environmental variability (Katz & Brown, 1992), would be valuable in assessing predicted responses to environmental stress (Lemoine, 2021). Furthermore, identifying species with different NSC dynamics, including variations in intra-

annual NSC concentration and rate of storage accumulation, is needed for comparisons between storage in trees and model results. Unfortunately, there are few datasets available against which to evaluate model predictions, as NSC concentrations are rarely (although increasingly) measured, while utilisation of stored carbon does not have an equivalent measurement which can be used on whole-tree scales.

In one valuable recent study, Signori-Müller et al. (2021) measured NSC concentrations during the wet and dry seasons in tropical forests with varying dry season lengths. Trees in strongly seasonal and non-seasonal tropical forests showed a similar NSC concentration during the wet season, with variation among trees in storage concentrations attributed primarily to species differences (Signori-Müller et al., 2021). During the dry season, trees at sites with an extended dry season showed a different NSC composition, with a transition from higher starch content during the wet season to higher soluble sugar content during the dry season (Signori-Müller et al., 2021), as compared to sites with a shorter dry season. Starch is a long-term NSC storage compound, while soluble sugar is actively used in metabolism and may be mobilised during stress (Dietze, Sala, et al., 2014). The shift in intra-annual NSC-dynamics along the observed seasonality gradient, may suggest a shift between growth-prioritisation and storage-prioritisation to survive stress during the dry season. There is evidence for similar shifts from growth-prioritising strategies to storage-prioritising strategies within species across environmental stress gradients, including rainfall (Bachofen et al., 2018; Hao et al., 2021) and elevation gradients (Wang et al., 2018). In the model developed in this chapter, water dynamics are not included, but shifts in storage along stress gradients may be comparable to the shift from Risky plants to Slow-Safe plants in the model with rising stress duration.

3.4.2 Modelling Carbon Storage Parameters

Beyond improving model realism, the representation of carbon storage in models is important for two reasons: capturing accurate mortality mechanisms (McDowell et al., 2008) and removing the direct coupling between photosynthesis and growth (Keane et al., 2001). Without carbon storage, models assume that all growth is supported by carbon gain within the same timestep, a dynamic which is unrealistic on smaller time steps (Fatichi et al., 2014, 2019; Piper, 2020). Although the number of models implementing carbon storage is

increasing, there are still no consistent guidelines for modelling carbon storage (Dietze, Sala, et al., 2014). While some studies have looked at sensitivity of single carbon storage parameters (Fisher et al., 2010; Jones et al., 2020) or the effects of model structure (Jones et al., 2020; Richardson et al., 2013; Trumbore et al., 2015), further examination of the sensitivity of more complex allocation strategies is needed. In this work I demonstrate that different storage parameters can have nuanced effects on plant mortality. Firstly, the rate of carbon utilisation strongly affected tree shade tolerance during periods of no stress. Trees with the Slow strategy had higher shade tolerance because they maintained higher minimum carbon storage concentrations (Figure 3-6), which, in turn, increased the probability of surviving in low-light conditions (Figure 3-15). The relationship between shade tolerance and carbon storage has been strongly supported by model (Kobe, 1997) and experimental studies (Atkinson et al., 2014; Myers & Kitajima, 2007; Rose et al., 2009).

Similarly, the switch time parameter was found to affect survival during seasonal stress (Figure 3-14). Experimental studies have shown similar decreases in growth along an environmental stress gradient (Wang et al., 2018) and as an acclimatory response of tree seedlings to past stress (Vander Mijnsbrugge et al., 2019), thereby supporting the role of decreased growth duration in mitigating stress periods. While mechanisms of tree mortality under stress are often complex, involving a number of contributing factors, including susceptibility to hydraulic damage, herbivory or pathogens, these model predictions support the theory that stored carbon plays an important role in buffering the damage caused by stress (McDowell et al., 2008). Even though additional factors such as drought or herbivory dynamics were not included in the model, the presence of storage in the model still allowed for a range of behaviours to be captured.

Improving the representation of carbon storage in models should be considered a priority (Merganičová et al., 2019) and one avenue is to examine the relationships between storage strategies and plant traits. In this study, I demonstrated that a more nuanced storage utilisation strategy, adopting variation in only two parameters, increases the range of observable behaviours. However, I assumed that all other traits were constant, whereas many other plant traits may influence plant strategy and growth to the same degree as the two storage traits examined in this study. For example, shade-tolerance in the model is

associated with low carbon utilisation-rate (α_S), but plants have a range of other traits associated with shade tolerance such as leaf economic traits (e.g. lower leaf mass per area or leaf nitrogen content) and hydraulic traits (higher stomatal density) (Abbasi et al., 2021; Zhu et al., 2018). Plants with high shade tolerance often have lower leaf nitrogen concentration (Kitajima, 1994; Kruse et al., 2020) and may be placed on the conservative end of the leaf economic spectrum, a continuum between resource acquisitive and conservative species (Reich, 2014; Wright et al., 2004). While nitrogen variation was not considered in the model, increased nitrogen concentration in modelled plants could contribute to shade tolerance by diminishing their effect.

The few studies which do compare plant traits and storage allocation do not appear to show clear relationships between storage patterns and other plant traits. In some studies, no distinct relationships were found between storage levels and plant traits such as potential tree size, mean growth, mortality rates and wood density (Signori-Müller et al., 2021). A synthesis examining plant drought mortality found a relationship in gymnosperms between storage and hydraulic traits, such as embolism resistance at mortality and hydraulic safety margin, but because data from one species may have significantly influenced this result, the relationship may not be generalised across all gymnosperm species (Adams et al., 2017). Comparisons of NSC concentration with root traits, however, showed NSC relationships strongly associated with root morphological traits such as specific root length and average diameter (Ji et al., 2020), while soluble sugar concentrations in branches were negatively associated with wood density (Dickman et al., 2019) and phenological traits captured intra-annual NSC dynamics in three Mediterranean crop species (Tixier et al., 2020). While this list is not exhaustive, it shows contrasting relationships between traits and carbon storage, thereby warranting further examination of the relationship between modelled carbon storage parameters and observable plant traits, which could significantly aid in improving modelling accuracy of carbon storage.

Moreover, modelling carbon allocation strategies may be complicated due to their dynamic nature, which is not considered in the model presented here. Age and shade can affect the strategy parameters. It would be of interest to explore the effect of age and size in model parameterisation. For example, the storage utilisation rate has been found to vary

with plant age in a model-data-assimilation study (Mahmud et al., 2018). Diurnal NSC concentrations within a plant also have been shown to change between seedlings and mature plants of the same study (Baber et al., 2014) and differences between carbon allocation strategies were found in trees of different heights (Sala & Hoch, 2009; Woodruff & Meinzer, 2011). It would be valuable in future work to relax assumptions about the static nature of plant traits to examine a wider range of strategies.

In addition to the assumption about trait variation between strategies, several other aspects of the model limited the results presented in this chapter. Most importantly, the lack of reproductive feedback is likely to have affected community composition and model outcomes. At any given time, each strategy has an equal chance of establishing in the plot. For a 100-year simulation this assumption is an acceptable simplification, but it would be valuable to explore feedbacks via changing seed production over longer time periods.

3.5 Conclusions

This model provided an evaluation of the effect of environmental stress and stochasticity on the performance and survival of plants with different carbon storage strategies. The representation of carbon storage strategy by two traits allowed a nuanced response to different types of stress to be captured and highlighted the role of carbon storage in tree survival. Shifts in modelled community assembly of trees in response to increased environmental stochasticity and intensity supports previous observations of shifts of community composition towards more stress-resilient plants. Further examination of the effect of other plant traits, and the inclusion of reproductive activity, in the model would help further elucidate the relationship between modelled plant carbon storage traits and observable plant traits.

3.6 Appendix: List of Functions

Table 3-5 List of functions used in the model with references to where they are introduced in the chapter. Where an equation was not introduced in this chapter, a citation of the original paper and the equation number in the original are provided.

Variable	Function	Document Reference
Carbon Exchange		
Average Photosynthesis per leaf area	$\bar{p}\left(x, H, E_a, E_s(t)\right) = E_s(t) \int_0^H p\left(x, E_a(z)\right) q(z, H) dz$	3-1
Photosynthesis at height z	$p\left(x, E_a(z)\right) = \frac{\alpha_{p1}}{E_a(z) + \alpha_{p2}}$	Falster et al (1)
Respiration of component i	$\frac{dR}{dt} = \left(r_{min} + \frac{E_s(t)}{2}\right) \sum_{i=l,b,s,r} M_i r_i$	3-2
Carbon Allocation		
Change in live biomass	$\frac{dM_a}{dt} = \begin{cases} t_y < t_s & \Rightarrow \quad a_s M_{st} \\ t_y \geq t_s & \Rightarrow \quad 0 \end{cases}$	3-3
Height Growth	$\frac{dH}{dt} = \frac{dH}{dA_l} \times \frac{dA_l}{dM_a} \times \frac{dM_a}{dt}$	3-4
Cost of deploying leaf area	$\frac{dA_l}{dM_a} = \left(\frac{dM_l}{dA_l} + \frac{dM_r}{dA_l} + \frac{dM_s}{dA_l} + \frac{dM_r}{dA_l}\right)^{-1}$	3-5
Change in component i	$\frac{dM_i}{dt} = \frac{dM_i}{dA_l} \times \frac{dA_l}{dM_a} \times \frac{dM_a}{dt} - k_i M_i$	3-6
Allometry adjusted component change with leaf area	$\frac{dM_i}{dA_l} = c_i(H, A_l, M_i) \frac{dM_i{}'}{dA_l}$	3-7
Allometric calibration of component i	$c_i(H, A_l, M_i) = \frac{2}{1 + \exp\left(-c_k(M_i'(H, A_l) - M_i\right)}$	3-8

Change in leaf mass with leaf area	$\frac{dM_l}{dA_l} = \Phi$	Falster Table 2
Change in sapwood mass with leaf area	$\frac{dM_s}{dA_l} = \rho\theta\eta_c\left(H + A_l\frac{dH}{dA_l}\right)$	Falster Table 2
Change in bark mass with leaf area	$\frac{dM_b}{dA_l} = \alpha_{b1}\rho\theta\eta_c\left(H + A_l\frac{dH}{dA_l}\right)$	Falster Table 2
Change in root mass with leaf area	$\frac{dM_r}{dA_l} = \alpha_{r1}$	Falster Table 2
Change in height with leaf area	$\frac{dH}{dA_l} = \alpha_{l1}\alpha_{l2}(A_l)^{\alpha_{l2}-1}$	Falster Table 2
Change in sapwood area with leaf area	$\frac{dA_s}{dA_l} = \theta$	Falster Table 2
Change in bark area with leaf area	$\frac{dA_b}{dA_l} = \alpha_{b1}\theta$	Falster Table 2
Reproduction		
Reproduction Allocation	$\frac{dF}{dt} = \frac{\alpha_{f1}}{1+\exp\left(\alpha_{f2}\left(1-\frac{H}{H_{mat}}\right)\right)}\mathrm{M_{st}}$	Falster (6)
Seed Production	$f(x,H,E_a,E_s) = \frac{\frac{dF}{dt}}{\omega+\alpha_{f3}}$	Falster (10)
Leaf Area Distribution		
Cumulative fraction of plant's leaves above z	$Q(z,H) = \left(1-\left(\frac{z}{H}\right)^{\eta}\right)^2$	Falster (12)
Leaf area at height z of plant of height H	$q(z,H) = 2\frac{\eta}{H}\left(1-\left(\frac{z}{H}\right)^{\eta}\right)\left(\frac{z}{H}\right)^{\eta-1}$	Falster (13)
Storage Allocation		

Change in storage pool	$\frac{dM_{st}}{dt} = \frac{dB}{dt} - \frac{dM_a}{dt} - \frac{dF}{dt}$	3-9
Net Mass Production	$\frac{dB}{dt} = \alpha_{bio}\alpha_y \left(A_l \bar{p} - \frac{dR}{dt}\right)$	3-10
Diameter Growth		
Growth in basal area	$\frac{dA_{st}}{dt} = \frac{dA_b}{dt} + \frac{dA_s}{dt} + \frac{dA_h}{dt}$	Falster (7)
Diameter growth	$\frac{dD}{dt} = (\pi A_{st})^{-0.5} \frac{dA_{st}}{dt}$	Falster (8)
Mortality		
Mortality Rate	$d(x, H, M_{st}, E_a, E_s, t) = d_I + d_P(x, H, E_a, E_s, t) + d_S(x, M_{st})$	3-11
Productivity-dependent mortality rate	$d_P(x, H, E_a, E_s, t) = E_s(t)\alpha_{\mathrm{dP1}} \exp\left(-\alpha_{dP2} \frac{\frac{dB}{dt}}{dA_l}\right)$	3-12
Storage-dependent mortality rate	$d_S(x, H, M_{st}) = \alpha_{\mathrm{dS1}} \exp\left(-\alpha_{dS2} \frac{M_{st}}{M_a}\right)$	3-13
Probability of Mortality	$p_D(t) = 1 - \exp(-d\,(x, H, M_{st}, E_a, E_s, t))$	3-14
Germination		
Probability of plant survival through germination	$S_G(x', H_0, E_{a0}) = \frac{1}{1 + \left(a_{d0} \frac{A_l}{\frac{dB}{dt}}\right)^2}$	Falster (21)
Size of initial storage pool	$M_{st0} = \beta_s M_{a0}(H_0)$	3-15
Environment		

Environmental stress	$E_s(t_y) = \begin{cases} t_y < t_{crit} & \Rightarrow & 1 \\ t_y \geq t_{crit} & \Rightarrow & 0 \end{cases}$	3-16

3.7 Appendix: Smoothing piecewise step functions

The piecewise step function:

$$E_s(t_y) = \begin{cases} t_y < t_{crit} & \Rightarrow & 1 \\ t_y \geq t_{crit} & \Rightarrow & 0 \end{cases} \quad (3\text{-}17)$$

Is implemented in the model as:

$$E_s(t_y) = \begin{cases} t_y < \left(\frac{t_{crit}(t)}{2}\right) & \Rightarrow & \frac{1}{1+\exp(-k_s t_y)} \\ t_y \geq \left(\frac{t_{crit}(t)}{2}\right) \wedge t_y < \left(\frac{1-t_{crit}(t)}{2}\right) & \Rightarrow & \frac{1}{1+\exp(k_s(t_y - t_{crit}(t)))} \\ t_y > \left(\frac{1-t_{crit}(t)}{2}\right) & \Rightarrow & \frac{1}{1+\exp(-k_s(t_y-1))} \end{cases} \quad (3\text{-}18)$$

This allows a smooth stress transition which assists in the model solver. This is further illustrated in the following figure:

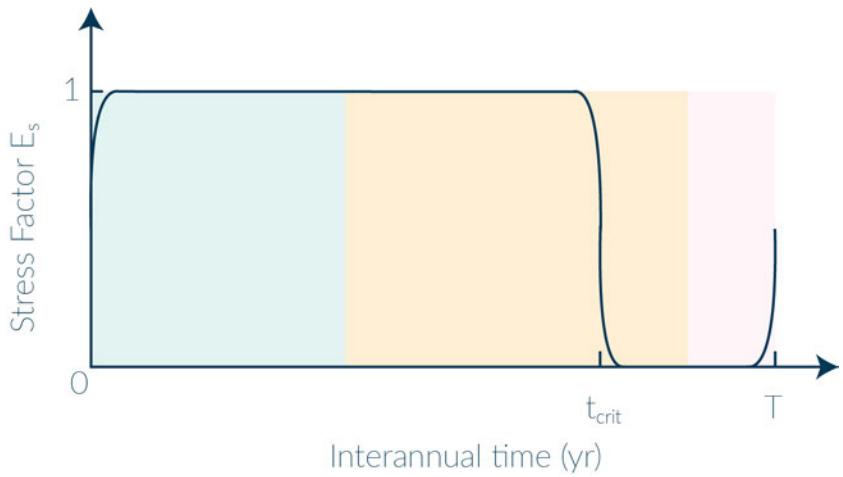

Figure 3-17 A representation of the dynamic function that determines the stress factor for a hypothetical year. 0 and T indicate the beginning and end of the year. The differently coloured sections are the three conditions in Equation 3-18 which correspond to the different step functions. Because the t_{crit} value is different each year, the precise shape will vary.

4 Iterative Predictive Optimisation of Carbon Storage Allocation

Abstract

As climate change progresses, plants are expected to experience increasingly stressful environmental conditions. Up to certain thresholds, plants can survive and recover from stress by storing carbon, which is theorised to have evolved as a locally optimised process. One challenge in defining these thresholds is that environmental stress is typically highly stochastic. Here, I explore optimal plant responses to stochastic stress by developing a new framework which iteratively computes an optimal storage trajectory and updates it to respond to changing conditions. The framework applies model predictive control (MPC) to a simple plant model, coupled with an environmental model consisting of semi-random rainfall modelled as a Markov Process. I explore how the model performs with a range of optimisation goals and compare it with the more traditional optimisation framework (optimal control theory, OCT) described in Chapter 2. Under both the OCT and MPC frameworks, goal functions maximising storage proved unrealistic and had no or minimal biomass allocation. When maximising biomass, both frameworks had a similar allocation pattern, but MPC maintained a significant storage buffer. The changes in MPC framework properties (forecasting prediction and memory windows) exhibited a positive correlation with the size of the storage buffer, but at the cost of a lower fitness. Overall, the MPC framework successfully imitated the optimisation framework, but also allowed an exploration of the relationship between stress and the carbon storage buffer. Future expansion of the framework would allow for forecasting optimal plant response to changing environments.

4.1 Introduction

Climate change is driving increased extreme stress on the environment (IPCC, 2021). Increased and prolonged droughts (Dai, 2013), heatwaves (Cowan et al., 2014), frost events (Zohner et al., 2020) and other climatic extremes, as well as their combinations (Gampe et al., 2021; Vanoni et al., 2016), are becoming more common. These changes can have a profound effect on individual trees and forests as trees are increasingly pushed beyond their tolerance limits. The stress exerted by climate change will lead to increased individual mortality and demographic shifts (Adams et al., 2017; Allen et al., 2010; Anderegg et al.,

2015). A crucial part of predicting regional and global effects of climate change is predicting the response of tree growth and mortality to future stress because of the role that forests play in the global carbon balance (Bonan, 2008; Huntzinger et al., 2017; Le Quéré et al., 2009; Sitch et al., 2015). Vegetation models are widely used to predict forest responses to climate change (Clark et al., 2016; Fisher et al., 2018; Medlyn, Duursma, & Zeppel, 2011; Reichstein et al., 2019). However, there is increasing awareness that these models may not capture all the key processes that determine the predicted stress response (Merganičová et al., 2019), particularly processes leading to mortality (Adams et al., 2013; Davi & Cailleret, 2017).

Carbon storage is one of the key mechanisms which plants use to survive stress periods. Carbon is usually stored in the form of starch and soluble sugars, commonly referred to as non-structural carbohydrates (NSC) (Hoch et al., 2003). Stored NSC can be used to maintain plant function during stress periods, and to rebuild tissues following stress. Despite increasing attention over the last 10 years, there are significant challenges in both quantifying and modelling carbon storage (Merganičová et al., 2019; Quentin et al., 2015). Plants can store carbon in all their organs, including leaves, stems and roots (Kozlowski, 1992) but different species adopt varying strategies for allocation and use of stored carbon through time (e.g., Mitchell, O'Grady, Hayes, et al., 2014; Tixier et al., 2020) and across different tissues (Hartmann & Trumbore, 2016). Moreover, carbon storage allocation is dynamic and allocation strategies can change with plant age (Baber et al., 2014), environmental conditions (Hao et al., 2021; Hoch et al., 2002; Signori-Müller et al., 2021), and individual life history (Atkinson et al., 2014). In trees, carbon is acquired and used at different times of year, particularly in deciduous species (Sala et al., 2012; Wiley & Helliker, 2012). Mobilisation of stored carbon can occur within days, months (Richardson et al., 2013, 2015), or several years after it was acquired (Vargas et al., 2009). These different time periods for storage and use act to buffer the plant against stress operating at different time scales – daily, seasonal, and interannual.

There is increasing evidence for adaptation of the carbon storage strategy in more stressful environments. For example, a recent study on black cottonwood demonstrated heritability of non-structural carbohydrate concentrations. Provenance affected the

proportion of stored starch (more ideal for long term use) *versus* stored sugar (better for short term use); in more stressful environments, this genetic component was more pronounced (Blumstein & Hopkins, 2021). This variation among provenances indicates selective pressure, with tree capacity to survive stressful conditions improved when NSC storage is adapted to the local environment (Bachofen et al., 2018; DeSoto et al., 2016; Piper et al., 2017; Reyes-Bahamonde et al., 2021). At shorter time scales, plants can also acclimate to local conditions by varying how and when carbon - and other limiting resources – are distributed. For example, during a stress period the tree distributes resources from its storage pools to meet critical metabolic needs, as well as functions specific to the stress response (such as tissue repair) (Chapin et al., 1990). Conversely, when stress is absent, photosynthate is readily available for use by the plant. In such conditions, the plant can use both recently acquired and stored carbon for growth and metabolic requirements (Carbone et al., 2013; Keel et al., 2006; von Felten et al., 2007). Therefore, stored carbon becomes a critical resource which can either be spent or saved, i.e. in the language of economics, storing carbon presents an opportunistic cost to growth and thus creates – in economic terms - a growth-storage trade-off (e.g., Atkinson et al., 2014; Myers & Kitajima, 2007).

To predict forest responses to climate change requires models that can predict the availability of NSC to buffer increasing stress, but developing such models is challenging. One tool that has been used to explore allocation strategies is dynamic optimisation modelling (Franklin et al., 2012; Iwasa, 2000) such as optimal control theory (OCT). OCT models have successfully predicted some of the carbon allocation dynamics in annual herbaceous plants (Chiariello & Roughgarden, 1984). Moreover, general patterns of allocation predicted by these models - such as clearly delineated periods of growth, storage, and reproductive activity - can be observed in an annual plant's rapid shifts from growth to reproduction (e.g., bolting, the rapid elongation of reproductive structures, Aronson et al., 1992). However, it is more difficult to use OCT for prediction of behaviour in perennial plants and trees because annual dynamics may be insufficient to capture the complexity of long-lived species. When optimal allocation during a stress period or over a seasonal time-course is modelled, the plant will be predicted to fully deplete its stored carbon at the end of the stress period or season, when maximising biomass growth (Chapter 2) or

reproductive output (Iwasa & Cohen, 1989). In reality, trees tend to maintain large NSC minima (Martínez-Vilalta et al., 2016). If, instead, total storage is maximised, the OCT approach predicts that little to no carbon will be allocated to growth, leading to a biologically unrealistic storage-to-biomass ratio (Chapter 2).

This disparity between observation and model outcomes occur because the OCT models are deterministic, assuming that both the environmental conditions and the length of the stress period are known (e.g., Iwasa & Cohen, 1989; Iwasa & Roughgarden, 1984). In reality, there is usually stochasticity in the stress. Accounting for variable stress risk can have a significant effect on predicted carbon allocation strategies. When stochastic dynamic programming (SDP) – an extension of OCT that allows for stochasticity - is used, a relationship between risk and allocation emerges. For example, stochastic and destructive local events, such as fire, affect the optimal storage-to-foliage ratio (Iwasa & Kubo, 1997), which influences the capacity of the plant to recover. Likewise, dynamic models for estimating optimal allocation strategies to reproduction have been derived using SDP (Iwasa, 1991). However, SDP requires assumptions regarding equilibrium dynamics that may not hold when examining stress responses for trees. For example, the embedded statistical tools focus on the average individual tree response to average conditions. As conditions are likely to change within an individual lifetime, SDP may not fully capture the biologically realistic dynamics involved in plant acclimation to stress. If our aim is to model the acclimation of tree carbon storage strategy to changing conditions, it is important to create a framework that can capture how plant response may vary in a stochastic environment. The system must be able to extrapolate potential future conditions from present ones (i.e., able to forecast) in a manner that imitates some predictive, or anticipatory, capability (Rosen, 2012, pp. 339–351). This framework should make use of OCT and SDP properties of anticipating both present and future benefits, thereby accounting for present and forecasted risk.

In this chapter, I attempt to develop such a framework. In order to better reflect risk (i.e., stochastic variation in stress), I consider feedforward and feedback responses to explore their effects on NSC storage and allocation strategies. To achieve this, I employ a feedback-loop system that uses a “memory” parameter that captures the incidence of past

events to complement knowledge of present conditions. In addition, I implement a feedforward response by using another method in the OCT/SDP family called model predictive control (MPC).

Like OCT, MPC creates a short-term prediction of optimal behaviour over a time window. However, where OCT only models this period as a single prediction, MPC first uses a short(er) term prediction to initialise the model, and then uses a sliding time window – updated with any new events - to explore the optimal behaviour over a longer time frame. Therefore, a framework which uses MPC will have an updating model of predicted conditions, which can capture a changing environment. Moreover, a memory of past conditions can be also incorporated, enabling the prediction of optimal behaviour to be updated as conditions change. This system allows me to construct a model that is adaptive, forecasting, and anticipatory, enabling the identification of the strategy that directs the plant towards a particular optimal fitness outcome, while also capturing plant capacity to respond to stochastic conditions. I implement this framework using a "toy" model (introduced in Chapter 2) to investigate broad patterns of behaviour without attempting to account for the full complexity of the biological reality. The environment is represented with slightly more complexity: it is assumed there are two seasons (wet and dry) with stochastic rainfall determined by different parameters in each season. This chapter has the following aims:

1) Evaluate how the predicted allocation behaviour using an MPC approach compares to the OCT approach presented in Chapter 2;
2) Identify how the predicted allocation behaviour varies depending on the specified optimisation goal;
3) Evaluate the sensitivity of the model to changing control framework parameters such as predictive time window and length of environmental memory.

4.2 Methodology

The model framework consists of three distinct components: 1) the plant model which describes plant growth given allocation parameters, 2) the environment model which describes rainfall inputs over time, and 3) the control architecture which determines the allocation parameters given plant and environmental constraints.

4.2.1 Plant model

The plant model is the same as that used in Chapter 2. Briefly, the plant has two carbon pools: a biomass pool (M) and a storage pool (S) and all processes are represented as linear processes dependent either on the biomass pool (respiration, R, photosynthesis, A, and evapotranspiration, E), or the storage pool (growth, G). Further details of the model can be found in Chapter 2 Methodology.

4.2.2 Environment model

The plant is assumed to experience two seasons in the simulation: the rainy season and the dry season. Water input each day is determined by a rain model, which has different parameters for each season.

The rain model consists of two elements: 1) a Markov Chain (MC) determining whether or not there is rain input that day; and 2) a Chi-square distribution ($\mathcal{X}^2(k)$) which controls how much rain falls that day. The use of an MC adds some predictability into the system allowing rain days to be more likely followed by other rain days and dry days to be more likely followed by other dry days, i.e., a simplified weather system. If there is rain on a given day, the Chi-squared distribution determines the amount of water input, i_t, that day ($i_t = \mathcal{X}^2(k)$, where k specifies the degrees of freedom in the distribution). Using a Chi-Squared distribution to determine the amount of water input allows for rain input to be random, while also skewed towards less rain and with extreme values possible, though unlikely.

The rain input is therefore given by:

$$I_t = f(\pi_t, i_t) \quad (4\text{-}1)$$

where π_t is the Environment state, which can be either Dry ($\pi_t = S_D$) or Rain ($\pi_t = S_R$). When the plant is in the dry state, $\pi_t = S_D$, there is no water input and, therefore, $I_t = 0$. On the other hand, when the model is in the rain state, $\pi_t = S_R$, there is water input as determined by the Chi-Squared Distribution ($i_t = \mathcal{X}^2(k = 40)$, Figure 4-1).

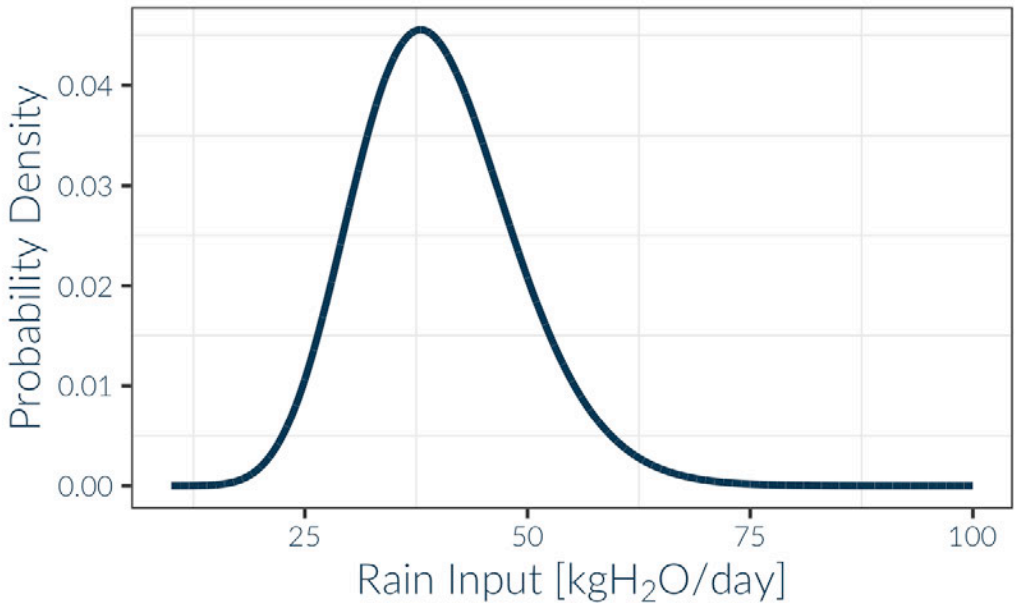

Figure 4-1 The Chi-Square distribution, $X^2(k = 40)$, determining the likelihood of the amount of rain input in a day. Rain input is expressed in kg per plant per day. If a stocking density of 1000 stems ha^{-1} is assumed, these values can be converted to mm d^{-1} by dividing by 10.

The environment state is generated from two Markov Chains (MC) with the same states, but different state transition probabilities. The first Markov Chain model represents the Rainy Season (RS-MC), and the second Markov Chain represents the Dry Season (DS-MC; Figure 4-2). The transition from the Rain Season to the Dry Season occurs at time $t = t_{crit}$. The value of t_{crit} was chosen from several putative values used in test simulations. The final value was chosen such that there was significant growth, as well as a severe but not critical drought. The state transition and steady state probabilities for the Rainy Season MC are given in Table 4-1 and for the Dry Season MC in Table 4-2. Both MC have stable probabilities which meant that the steady state probabilities could be numerically computed. The steady state probabilities indicate the independent likelihood of each state occurring in that season.

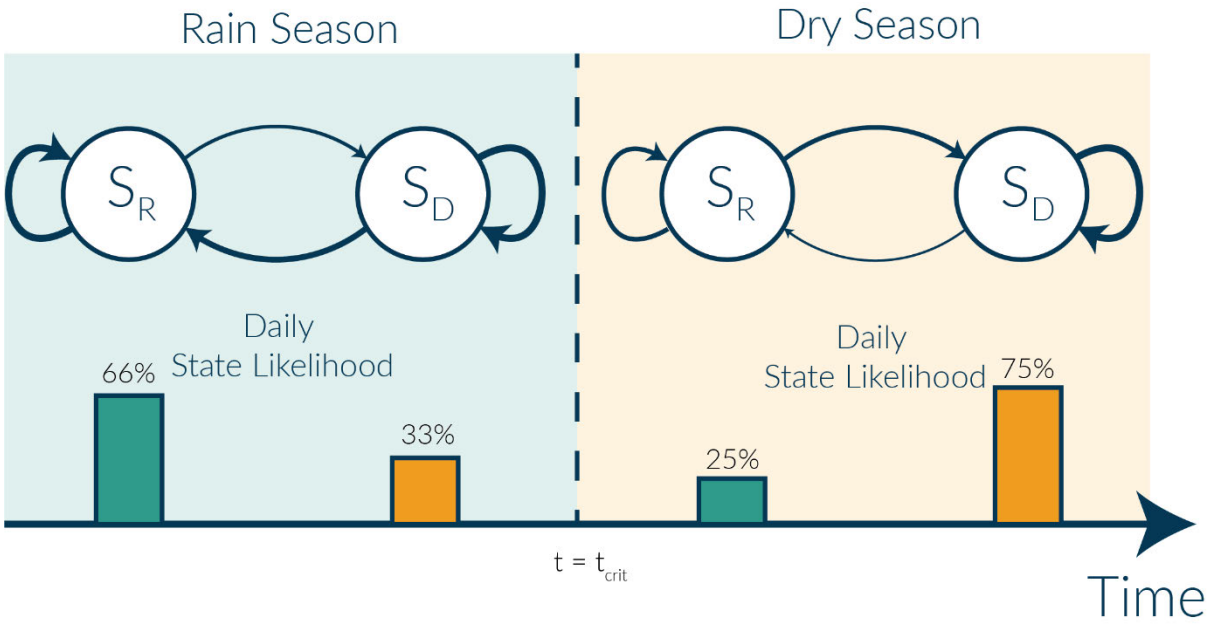

Figure 4-2 An illustration of the Rain Model for the Rain Season (left) and the Dry Season (right). The transition from the Rain Season to the Dry Season occurs at time $t = t_{crit}$ *indicated on the x axis. Within each season, a Markov Chain (MC) is used to determine the state transition from one day to the next. The two states used in both models are the dry state,* S_D *and the rain state,* S_R*. The arrows between the states signify allowable transitions (fully connected MC) with arrow thickness indicating the likelihood of transition. The bars indicate the steady state for each of the states of the Markov Chains (*S_R*: green;* S_D*: orange) with the values given atop each bar. The steady state values indicate the likelihood of each state to occur independent of the past states.*

Table 4-1: The Markov chain used for the rainy season with two states: S_D and S_R. Each number indicates the probability of transitioning from the state represented by the row to the state represented by the column. The bottom row indicates the steady state probability for each state.

		x_{t+1}	
		S_D	S_R
x_t	S_D	0.60	0.40
	S_R	0.20	0.80
Steady State		0.33	0.67

Table 4-2: The Markov chain used for the dry season with two states: S_D and S_R. Each number indicates the probability of transitioning from the state represented by the row to the state represented by the column. The bottom row indicates the steady state probability for each state.

		x_{t+1}	
		S_D	S_R
x_t	S_D	0.85	0.15
	S_R	0.45	0.55
Steady State		0.75	0.25

4.2.3 Control Framework

To find the approximate optimal storage utilisation trajectory, $\boldsymbol{u_t}$, with respect to a fitness goal, a control architecture framework (Control Framework) is implemented. Briefly, the Control Framework consists of implementing a model predictive control (MPC) method which computes an optimal storage utilisation trajectory over a short time horizon (t_w) and implements the first optimal step of that trajectory. This process is then iterated until the simulation is completed. Thus, at each time step, new information derived from stochasticity in the system can be observed and accounted for in the model. In contrast, the more widely used optimal control theory (OCT), implemented in Chapter 2, assumes that the system is deterministic and computes the exact optimal storage utilisation trajectory for the entire simulation period in a single computation step.

I further divide this framework into three distinct elements: 1) 'goal-seeking', 2) 'memory', and 3) 'prediction'.

The plant is assumed to be able to accurately sense its own mass and storage pools as well as the available water pool at any given point.

I specify the goal function as an integral of the combination of storage size and biomass size:

$$\Phi_{kf} = \max_{u_t} \int_t^{t+t_w} k_f M_\tau + \left(1 - k_f\right) S_\tau \mathrm{d}\tau \qquad (4\text{-}2)$$

with constraints placed on the plant biomass and storage to ensure that neither of them can become negative:

$$M_t \geq 0 \qquad (4\text{-}3)$$

$$S_t \geq 0 \qquad (4\text{-}4)$$

In other words, the plant maximises the integral of its mass size (M) and storage size (S). This differs from the goal function of Chapter 2 in which an end point value was used. While functionally the two approaches are similar, the use of an integral complements the continuous nature of the control architecture framework used in this chapter. To simplify presentation of the large values that result from using this new fitness goal, results are presented as the fitness output (i.e., the value of Φ_{kf}) normalized by prediction time horizon (t_w) to give a daily average size of Φ_{kf} and help with interpretation.

The fitness goal parameter, k_f, takes a value between 0 and 1 and signifies the plant's prioritisation between storage and biomass (see Chapter 2). In the special case of $k_f = 0$ the plant maximises the total storage integral (MaxS), and in the case of $k_f = 1$ the plant maximises the total biomass integral (MaxM).

The iterative nature of the MPC method suggests that adopting intermediate k_f values will influence the behaviour exhibited by the plant: priority will likely shift between the MaxM and MaxS behaviour depending on the plant size and environmental conditions.

The optimal behaviour is calculated over a forward time window, t_w. To compute this optimal behaviour, an estimate of the environmental state over the forward time window is required. To distinguish this estimate from the actual environment state I_t, I denote the predicted environmental state as $\boldsymbol{I'_{t\,(t+t_w)}}$.

The simplest prediction method that can be applied is to assume that the water input will be the same over the coming days as it is on the current day:

$$\boldsymbol{I'_{t\,(t+t_w)}} = \left[I'_t = I_t, I'_{t+1} = I_t, \ldots, I'_{t+t_w} = I_t\right] \qquad (4\text{-}5)$$

An alternative method of prediction uses information from past experience by adding a memory mechanism. In this way, when the plant encounters a single dry day during the rainy season, its behaviour won't be immediately affected (and vice versa).

The plant model can remember the rain pattern for the last t_m days and use these in its predicted water input ($\boldsymbol{I_{t\ (t+t_w)}}$). If the time window is longer than the memory period, the memorised rain pattern is repeated to fill the full space of the time window:

$$\boldsymbol{I'_{t\ (t+t_w)}} = \left[I'_t = I_{t-t_m}, I'_{t+1} = I_{t-t_m+1}, \dots, I'_{t+t_w} = I_t\right] \quad (4\text{-}6)$$

4.2.4 Simulations

The model is implemented through a combination of Matlab (Version R2020b, Mathworks) and R (version 3.6.3, R Core Team, 2018). The constrained nonlinear multivariable Matlab function *fmincon* is used to compute the short-term optimisation over the predicted time window. This function uses a nonlinear programming solver and was used with the interior-point algorithm which solves a constrained minimization problem by attempting to solve a sequence of approximate minimization problems (MathWorks, n.d. and the sources therein). The short-term optimisation computes the set of values $\boldsymbol{u_{t\ t+tw}} = [u_t \dots u_{t+tw}]$ that maximises the objective function over the prediction window, t_w. All values of the predicted $\boldsymbol{u_{t\ t+tw}}$ are allowed to vary independently from each other within the limits of 0 and a maximum rate of utilisation of stored carbon to growth, k_s. Furthermore, k_s follows mass-balance constraints which means it can never exceed 1:

$$0 \leq u_t \leq k_s \leq 1 \quad (4\text{-}7)$$

The remainder of the framework and result analysis are performed in R with the assistance of the *tidyverse* package (Wickham et al., 2019). The repository containing code can be found in the following link: https://github.com/foxeswithdata/recursive_learning. Additionally, to assist with comparison between the MPC and OCT methods the OCT simulations are performed using code developed in Chapter 2 (repository: https://github.com/foxeswithdata/StoringForDrought).

4.2.4.1 Parameters

The parameters used in the model are derived from an experimental study by Drake et al. (2019). The 15-month long experiment exposed young *Eucalyptus tereticornis* trees to factorial warming x rainfall reduction treatments in whole-tree chambers. Parameters are given here for completeness, but details of parameter derivation can be found in Chapter 2.

Table 4-3 List of parameters and variables used in simulation.

SYMBOL	UNITS	VALUE	DESCRIPTION
CARBON AND WATER POOLS			
S_t	g C plant ^{1}	-	Storage Carbon Pool.
S_0	g C plant ^{1}	550	Initial Storage Carbon Pool.
M_t	g C plant ^{1}	-	Biomass Carbon Pool.
M_0	g C plant ^{1}	3300	Initial Biomass Carbon Pool.
W_t	kg H_2O plant ^{1}	-	Available Soil Water Pool.
W_0	kg H_2O plant ^{1}	50	Initial Available Soil Water Pool.
TIME PARAMETERS			
T	d	250	Simulated Period Length.
t_s	d	-	Time of switch from allocating carbon to biomass to allocating carbon to storage (outcome of OCT model).
t_{crit}	d	variable	Time of switch between Rain and Dry Seasons.
t_w	d	variable	Prediction Time Window Length.
t_m	d	variable	Memory Window Length
PROCESS PARAMETERS			
k_p	gCg ^{1}Cd ^{1}	-	Photosynthesis Parameter.
k_p^*	gCg ^{1}Cd ^{1}	0.014	Maximum value of the photosynthetic parameter.
k_r	gCg ^{1}Cd ^{1}	0.004	Respiration parameter.
k_w	kgH_2Og ^{1}Cd ^{1}	0.4	Water use parameter.
k_s	gCg ^{1}Cd ^{1}	0.06	Maximum value of the storage utilisation rate parameter.
u_t	gCg ^{1}Cd ^{1}	variable	Storage utilisation rate(derived through the model).
k_f		variable	Fitness Goal Parameter

4.2.4.2 *Sensitivity of Control Architecture*

A number of simulations are performed to examine the response of the plant to varying parameters of the control framework. Five different rain regimes were generated to represent the stochasticity of the environment experienced by the plant. As a point of comparison, for each of these rain regimes, additional deterministic simulations were conducted using OCT and a brute-force optimisation to find the optimal storage utilisation trajectory, u_t. The OCT simulations used an initial water availability equal to the total water available throughout the original simulation (an average of 5365±245 kg H_2O plant ^{1}, the exact number corresponding to specific simulated rainfall regimes) but did not include additional rainfall throughout the analysed period. As presented in Chapter 2, the OCT model optimises final pool size. The brute-force optimisation (computed using the *fmincon*

function, a nonlinear programming solver over the entire simulated period of 250 d) had the same rainfall input as the control framework simulation and aimed to maximise the integral form of the goal function (Equation 4-2). Additionally, the brute-force optimisation solution was run five times with random initial conditions for each goal function and rainfall regi me combination, using the maximum fitness solution. I cannot guarantee that the global optimum is always found, but this approach does account for potential local minima.

The effect of the optimisation target was investigated by specifying a number of k_f values: $k_f = \{0,0.45,0.5,0.55,0.6,0.65,0.75,1\}$. For a single rainfall regime, the range of k_f values was further expanded to cover the full spectrum of possible values. The two edge cases of MaxM ($k_f = 1$) and MaxS ($k_f = 0$) are captured as well as several intermediate k_f values, which appear near the MaxS-MaxM behaviour boundary shown in Chapter 2. Moreover, a comparison between no memory ($t_m = 0d$) and 5 day memory ($t_m = 5d$) was conducted. Finally, the effect of the prediction time window was investigated by looking at a range of time windows from short (10 days) to long (25 days): $t_w = \{10d, 15d, 20d, 25d\}$. All possible combinations of the above are examined for five rainfall patterns with the switch between rain and dry season at $t_{crit} = 150d$ for a total of 320 simulations. An example of a rainfall simulation can be found in Figure 4-3. Because of the time required for each simulation (up to 6 hours of High Performance Computing time) the simulations had to be limited to the 64 simulation settings described above.

4.3 Results

4.3.1 Comparison of prediction methods

A sample state trajectory for a single rainfall simulation (Figure 4-3; 113 days with no rain and 73 days which fall in the dry period) can be found in Figure 4-4. In this example, the figure shows the optimal state trajectory for the deterministic OCT model, brute-force optimisation solution and the control architecture framework results for the two extreme strategies of MaxM and MaxS and two in-between strategies ($k_f = 0.45$ and $k_f = 0.65$) for the control architecture only.

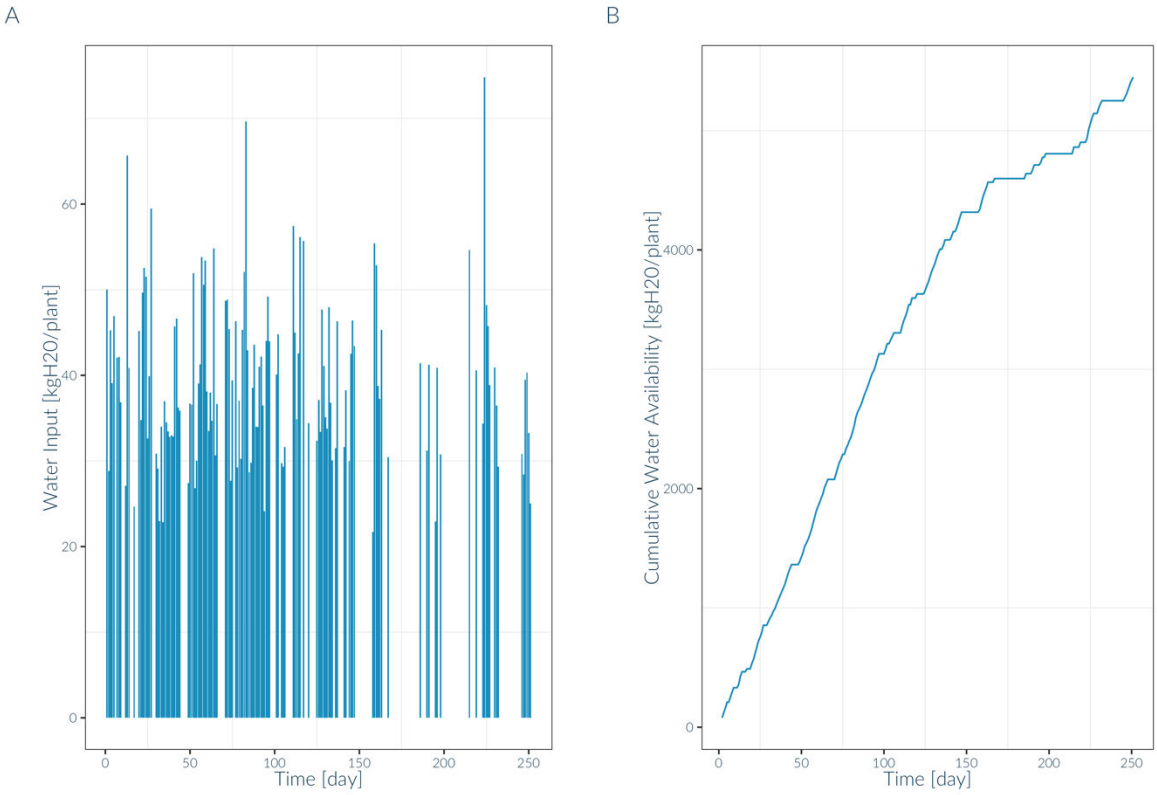

Figure 4-3 A: Randomly generated rainfall used in evaluating simulations. B: Cumulative water available to the plant with random rainfall.

The MaxS strategies show the same, or nearly the same, behaviour under all simulations in that the plant utilises minimal (Figure 4-4B and C) or no carbon for biomass growth (Figure 4-4A). This is consistent with an analytical OCT solution in that a plant which maximises storage may benefit from some growth, but must spend most of its effort storing carbon (Chapter 2). The MPC control framework cannot predict the slight benefit that is gained from a short growing period at the beginning of the simulation, likely linked to the prediction window which is too small to account for benefits of growth. Moreover, while the MaxS fitness objective may be valid for a short severely stressed period, it is unlikely that this objective corresponds to whole-plant fitness in the long term.

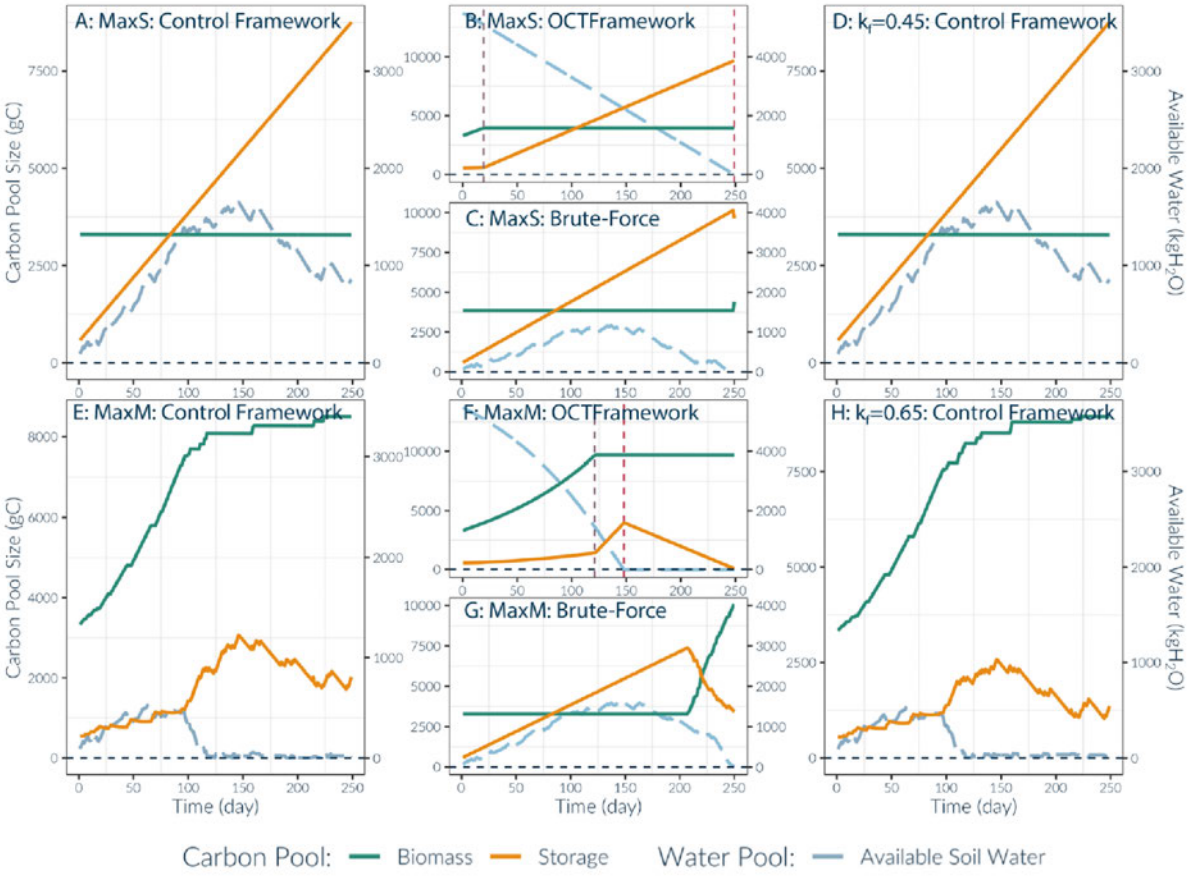

Figure 4-4 Carbon and water pool trajectories obtained from running simulations for the OCT, brute-force optimisation and control frameworks (with time window of $t_w = 25d$). Shown here are the extreme-cases of k_f (MaxS and MaxM; OCT framework: B and F respectively; Brute-Force Optimisation: C and G respectively; Control Framework: A and E respectively) and two example intermediate values of k_f ($k_f = 0.45$ and $k_f = 0.65$; Control framework only: D and H respectively). For MaxS and MaxS equivalent ($k_f = 0.45$) strategies the response of all three frameworks is similar with no or minimal storage utilisation for biomass growth. MaxM strategies show some variation with the general shape of the solution: the OCT and the control framework are similar with an initial period of growth followed by storage; and the Brute-Force Optimisation framework showing a contrasting behaviour of storing all available carbon and rapidly growing towards the end of the simulation. Of note is that although the OCT and control framework solutions are similar, the control framework maintains a buffer of stored carbon, whereas the OCT framework finishes the simulation with no stored carbon.

For the MaxM fitness objective, there is some consistency in behaviour predicted by the MPC and OCT methodologies, but the Brute-Force approach yields a very different response. While the MPC control framework for MaxM strategies gives a state trajectory shape that is similar to that obtained with deterministic OCT, there are differences in the values of the states, with the Control Framework generally yielding smaller values than the deterministic OCT solution for both final and averaged daily pool sizes (Figure 4-5). On the other hand, the MaxM brute-force yields an alternative behaviour in which allocation is delayed until the end of the simulation (Figure 4-4G). This behaviour minimises respiration

costs rather than maximising carbon uptake, while simultaneously avoiding water depletion. The accumulated storage is then used to promote rapid growth at the end of the simulation. However, when the integral-form of the goal function (Equation 4-2) is considered, the brute-force MaxM and MaxM-equivalent solutions are suboptimal, when compared to their OCT and Control Framework counterparts (Figure 4-5A).

The observed differences between the different models can be confirmed when examining the size of the plants as determined by their biomass. Final and average daily biomass size was largest for the OCT solution (Figure 4-6) across all scenarios. The final biomass of the Brute-Force MaxM solution was comparable with that of the equivalent OCT solution, but the average daily biomass size was not. On the other hand, the average daily and final biomass of the MPC models was lower than that of the optimal control solution.

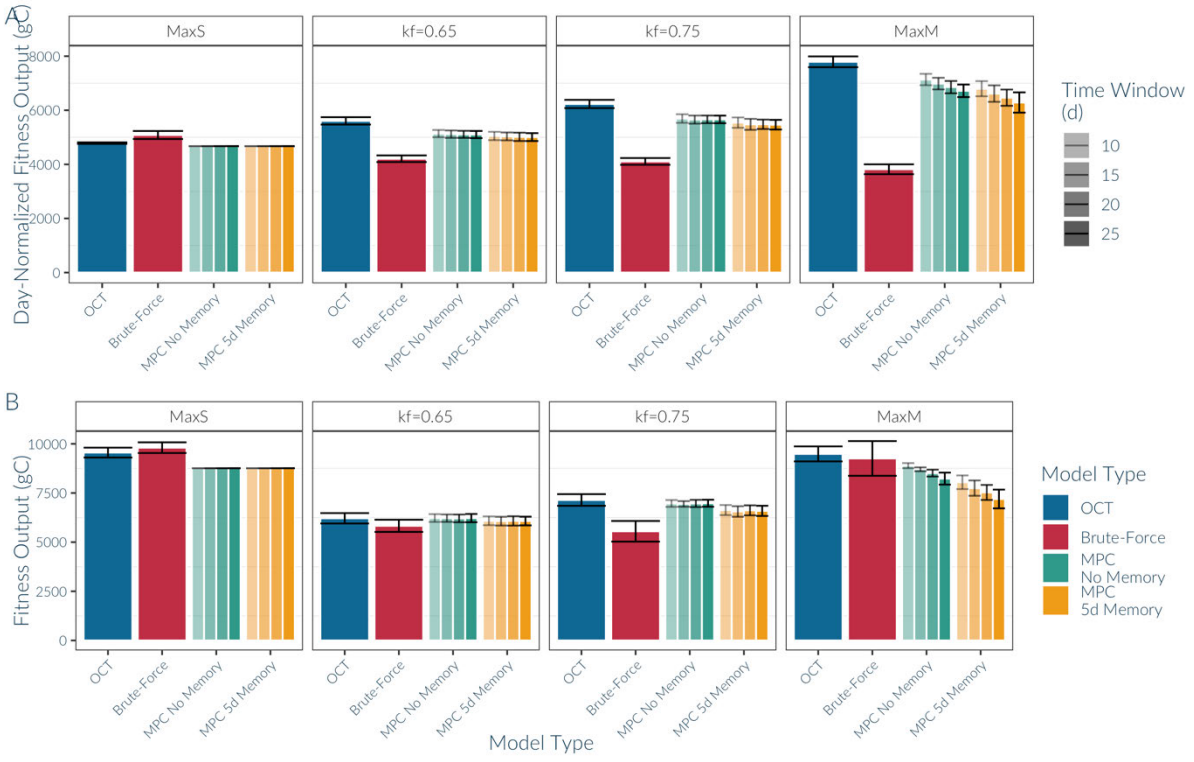

Figure 4-5 Fitness output evaluation for different model settings with four different goal functions. Fitness is evaluated as the average daily fitness goal output, Φ_{kf}, (A) and carbon pool size (calculated as $k_f M_T + (1 - k_f) S_T$) at the end of the simulation (B). The value of k_f is given above each box with MaxS indicating k_f=0 (maximising storage) and MaxM indicating $k_f = 1$ (maximising biomass). Error bars indicate standard deviation for each group (N=5). Colours indicate different model types: Optimal Control Theory solution (OCT: blue), Brute-Force optimisation solution (red), control framework with no memory (MPC no memory, green) and control framework with a 5 day memory (MPC 5d Memory: yellow). For MPC outputs, shade intensity indicates the size of the forward prediction time window, t_w (with lighter shade indicating shorter time window).

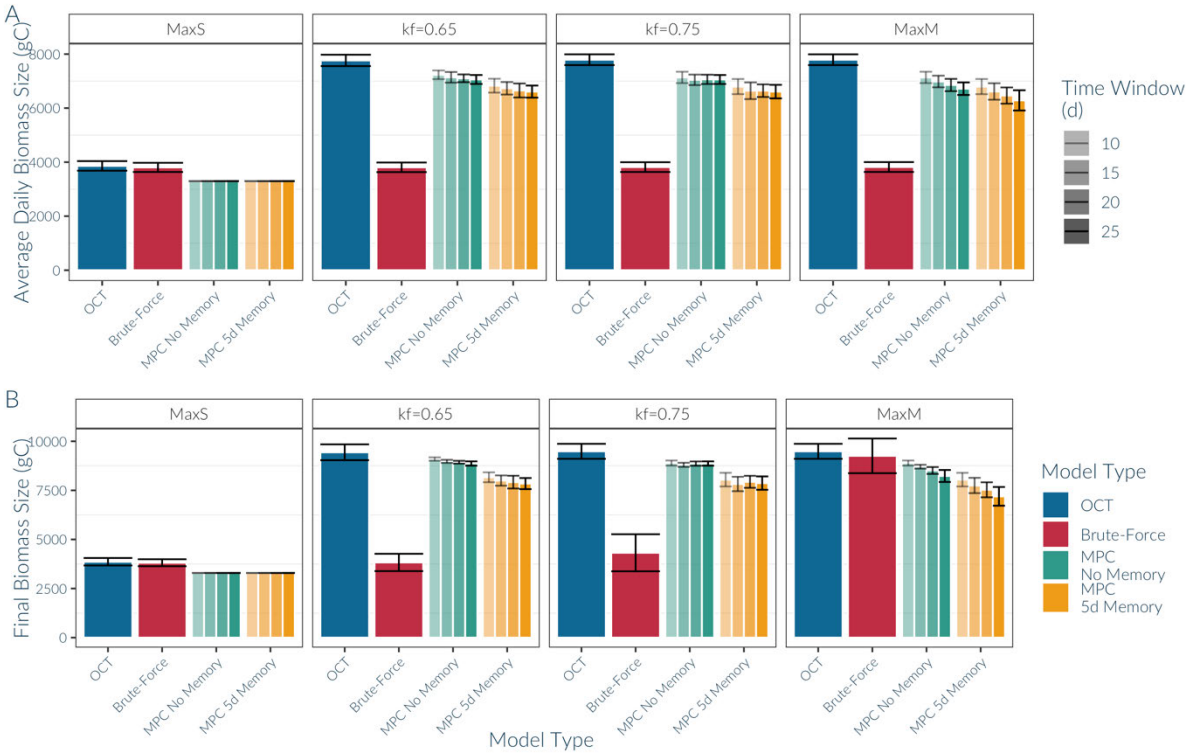

Figure 4-6 Biomass pool size as a daily average over the simulation (A) and at the end of the simulation (B) for different models and with different fitness goals. Legend as in Figure 4-5.

The difference between models can be explained by analysing the computed allocation trajectories for a single rainfall regime (Figure 4-7). The OCT and Control framework solutions follow a bang-bang response dynamic, in which the storage utilisation rate, u_t, switches between its maximum and minimum values. The OCT solution has one such switch distinguishing between a growth and storage phase (at t=10 for the MaxS solution and at t=113 for the MaxM and MaxM-equivalent solutions). The Control framework solution also has two phases, growth and storage, but in each phase, there can be multiple start and stop growth switches. The last day of growth in the first phase is t=143 for the $k_f = 0.65$ solution and t=115 for the MaxM solution. Compared to the OCT solution, the number of growing days is significantly reduced: 58 days for the $k_f = 0.65$ solution and 47 days for the MaxM solution. However, this decrease in growing days does not translate to an equivalent decrease in biomass; there is an average of 25% decrease in the final biomass of the control framework solution compared to OCT (Figure 4-6). This can be attributed to the fact that the plant accumulates storage over the days when it does not grow; thereby, the absolute value of stored carbon utilised for growth becomes larger on

the days when the plant does grow. The same pattern explains why the final biomass of the brute-force solution may be comparable to that of the OCT solution: in the MaxM solution, the plant only grows in the last 30 days but the final biomass is comparable to that of the OCT solution (Figure 4-6) because the storage accumulated over the first part of the simulation can be quickly mobilised.

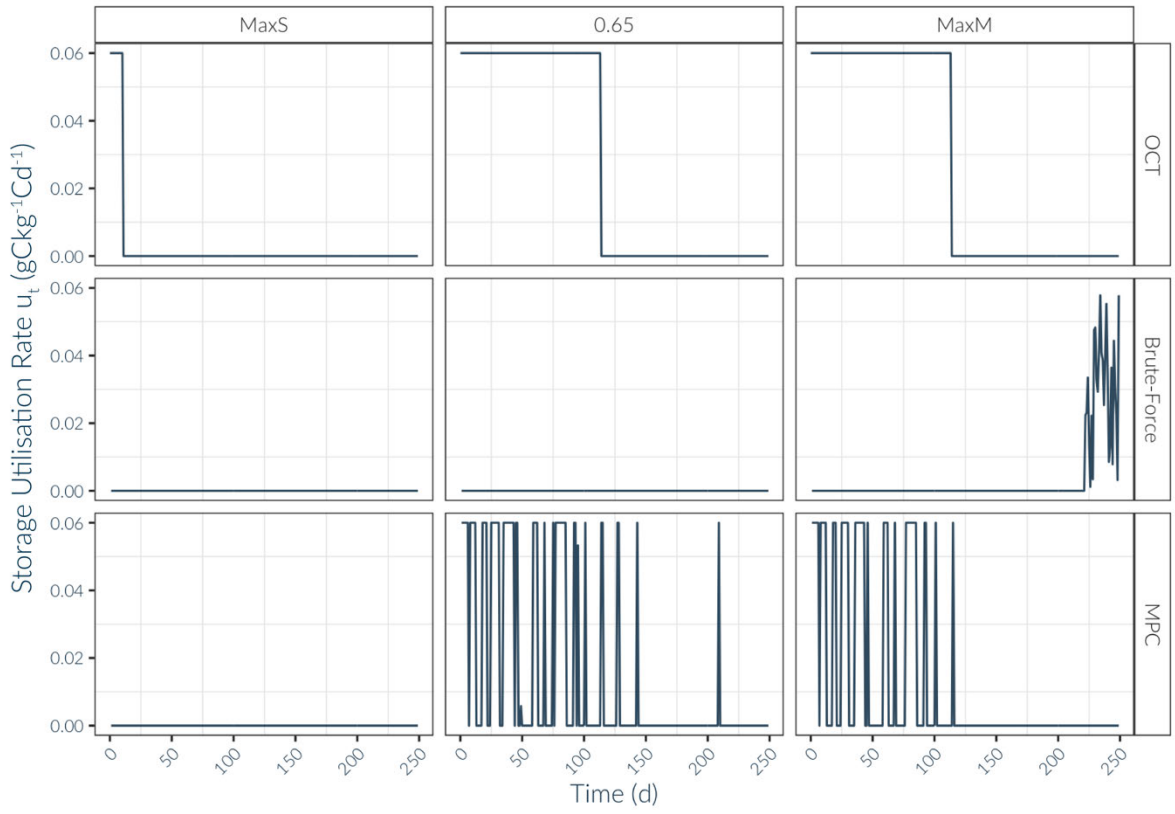

Figure 4-7 Shape of the storage utilisation trajectory over time computed for different models used in the study and across different values of k_f. Values are for one rainfall simulation only. The models correspond to Optimal Control Theory (OCT), Brute-Force and Control Framework with a time window of 25 days and a memory window of 5 days (MPC). Fitness goal parameters range between MaxS ($k_f = 0$, left), MaxM-equivalent ($k_f = 0.65$, middle) and MaxM ($k_f = 1$, right).

The difference within the control framework solutions is attributed to changing the size of the memory of previous rain patterns and the prediction window (Figure 4-8). The overall shape of the response does not change (two growth phases are still observed in the Control Framework simulations: growth and storage, as well as a third phase of water stress during the dry season). However, the strategy adopted changes as the memory and time windows are increased, leading to a decrease in final biomass size (Figure 4-6) and fitness (Figure 4-5), although the effect is less profound for smaller values of k_f. The shape of the

storage utilisation trajectory explains these differences. When memory is introduced, the modelled plant has a shorter growing period and does not grow during the dry period (Figure 4-8). This pattern occurs because the plant model does not use memory, so that the predicted rain pattern is either rain every day or no rain at all, whereas when memory is used the predicted rain pattern is more variable. Including a memory function allows the model to discern between rain season and dry season. Next, increasing the size of the forward prediction time window decreases the number of days on which growth occurs (Figure 4-8), also leading to a decrease in final biomass. The pattern of decreased growth is different between the no-memory and memory model. When there is no memory, there is an increase in the number of "storage breaks" in the growth period (days in which the plant stores during the growth period), whereas when memory is used the length of those breaks increases in addition to there being an overall shorter growth phase. This pattern occurs because a longer prediction window requires a larger store of carbon to allow survival over a longer period.

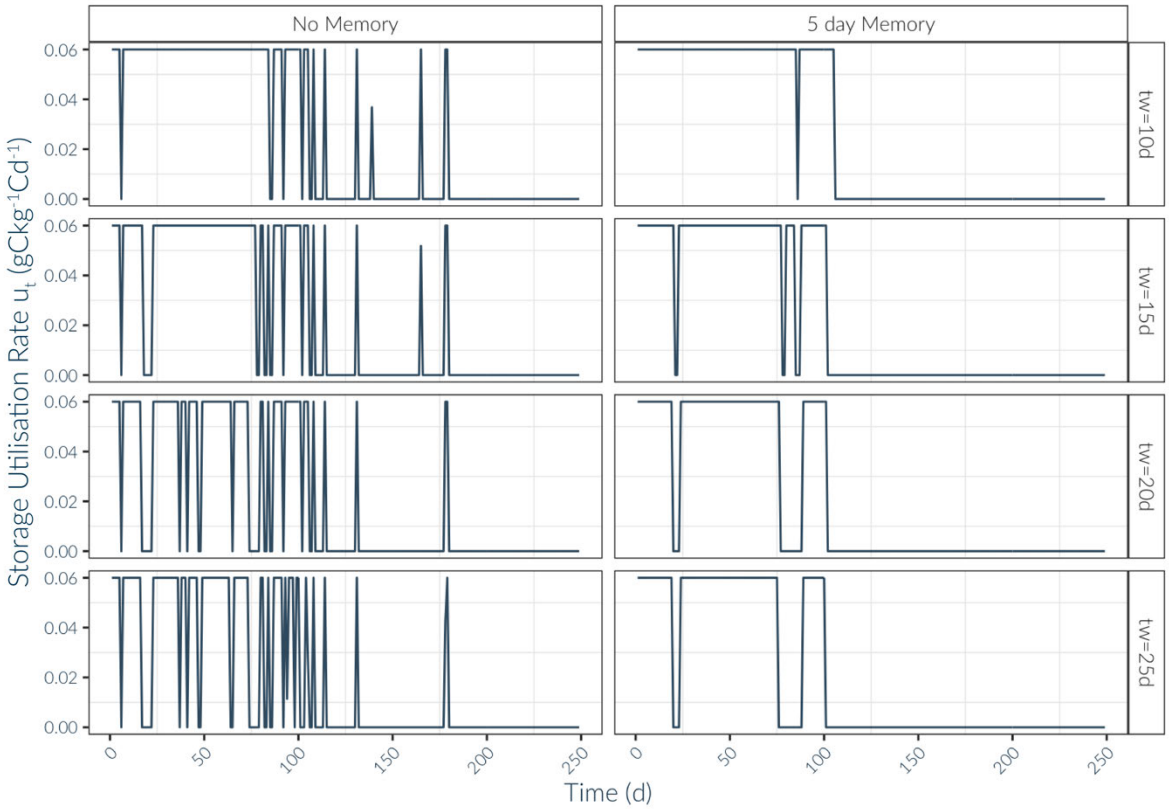

Figure 4-8 Shape of the storage utilisation trajectory over the simulated period computed for different control framework parameters. Only the MaxM solution for a single rain simulation is presented above. Columns correspond to different values of the memory window, t_m (left: no memory, right: 5 day memory) and the rows correspond to increasing sizes of the prediction window, t_w.

4.3.2 Equivalence of Goal Functions

When OCT is used to find the optimal storage utilisation trajectory, the predicted response is equivalent either to a MaxM or MaxS solution, irrespective of the chosen value of k_f (Chapter 2, Figure 2-7, p 54). Analogously, the utilisation trajectory predicted by the control framework on each day will predict behaviour that is equivalent to either the MaxS- or MaxM goal function. However, the predicted behaviour switches between a MaxM- or MaxS-equivalent on a daily scale. Depending on the value of k_f chosen, the proportion of days for which the predicted behaviour is equivalent to a MaxM strategy versus a MaxS strategy will vary (Figure 4-9A).

When $k_f \leq 0.5$, the predicted behaviour is entirely equivalent to that predicted for the MaxS goal function (with 0% of days equivalent to the predicted MaxM behaviour). At $k_f = 0.55$ the predicted behaviour switches to more MaxM-like behaviour, with 45 to 75%

of days with behaviour equivalent to the predicted MaxM behaviour. Only at $k_f = 1$ (i.e., MaxM) does the predicted behaviour follow 100% MaxM-like behaviour. During the transition phase, the percentage of MaxM equivalent days does not vary for different k_f values, but it does vary with the control parameters (Figure 4-9B). Increasing the prediction time window, t_w, and memory window, t_m, both increase the percentage of MaxM equivalent days.

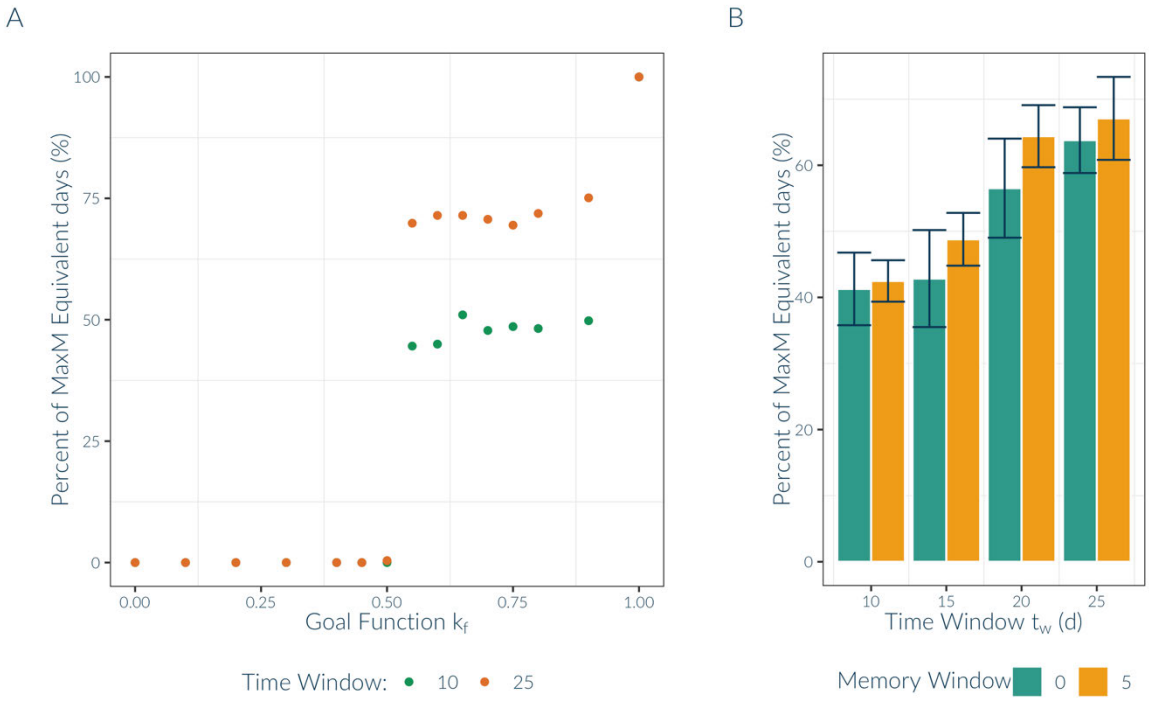

Figure 4-9 Proportion of MaxM-like behaviour predicted for different goal functions $\boldsymbol{k_f}$, calculated as the percentage of simulation days for which the predicted $\boldsymbol{u(t)}$ value is closer to the value predicted for the MaxM goal function ($\boldsymbol{k_f = 1}$) than the MaxS goal function ($\boldsymbol{k_f = 0}$). That is, each day's prediction is counted as being MaxM-like if $\boldsymbol{|(u_{kf}(t) - u_1(t)| < |u_{kf}(t) - u_0(t)|}$, where $\boldsymbol{u_{kf}(t)}$ is the predicted trajectory for goal function $\boldsymbol{k_f}$at time $\boldsymbol{t}$, $\boldsymbol{u_1(t)}$ is the predicted trajectory for the MaxM goal function and $\boldsymbol{u_0(t)}$ is the predicted trajectory for the MaxM goal function. (A) Proportion of MaxM-like behaviour is shown for a range of $\boldsymbol{k_f}$ values, for two time windows ($\boldsymbol{t_w = 10d}$ and $\boldsymbol{t_w = 25d}$) and memory window, $\boldsymbol{t_m = 0d}$ = 0 and a single rainfall scenario. (B) Average percentage of MaxM-equivalent days for simulated MaxM-equivalent strategies (that is strategies with $\boldsymbol{0.50 < k_f < 1}$ according to A). The average is computed across all rainfall scenarios and variable fitness goal parameters, $\boldsymbol{k_f}$, within the above-mentioned limits on $\boldsymbol{k_f}$ (N=20). Error bars indicate the standard deviation. Averages are computed for varying time windows, $\boldsymbol{t_w}$ (x-axis) and memory windows (green: $\boldsymbol{t_m = 0d}$, yellow: $\boldsymbol{t_m = 5d}$).

4.3.3 Storage Buffer

The optimal behaviour predicted by the OCT method for the MaxM goal function depletes its entire pool of storage by the end of the simulation period (Figure 4-4F). In contrast, the behaviour predicted by the MPC framework for the MaxM goal function does not, thereby

maintaining a small buffer throughout the dry season (Figure 4-4E). Notably, the storage buffer is predicted to be larger for the MaxM goal function than goal functions which prioritise some portion of storage ($k_f < 1$; eg. $k_f = 0.65$, Figure 4-4D).

Increasing the time window for forward predictions and the memory window for past environmental conditions, will increase the size of the storage pool (Figure 4-10). The increase in the size of the storage pool is larger than the increase in total plant size, resulting in an increase in final storage concentration, as shown in Figure 4-11 for the MaxM fitness goal. The size of the time window corresponds to the length of time during which the plant needs to survive, so the storage buffer size will increase with a larger time window to accommodate the difference between the number of days over which the plant may need to support maintenance using stored carbon.

On the other hand, the increase in the storage buffer size with introducing memory is associated with the increased capacity of the model to distinguish between the dry and rain periods: when no memory is used the occasional dry day during the rain period may be interpreted by the model to be the start of a dry season and vice versa. In contrast, when a prediction is made using the 5 days memory window as opposed to a single day only when no memory is present, the rain and dry seasons can be distinguished with more accuracy.

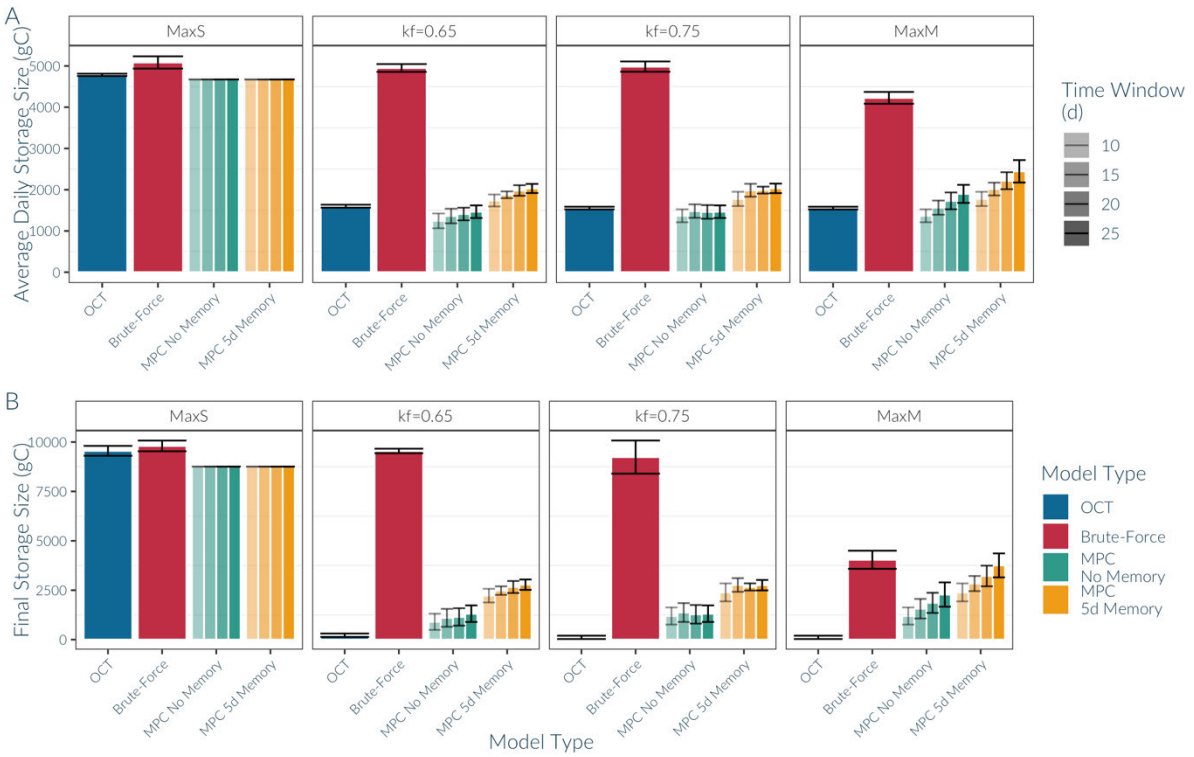

Figure 4-10 Storage pool size as a daily average over the simulation (A) and at the end of the simulation (B) for different models and with different fitness goals. Legend as in Figure 4-5.

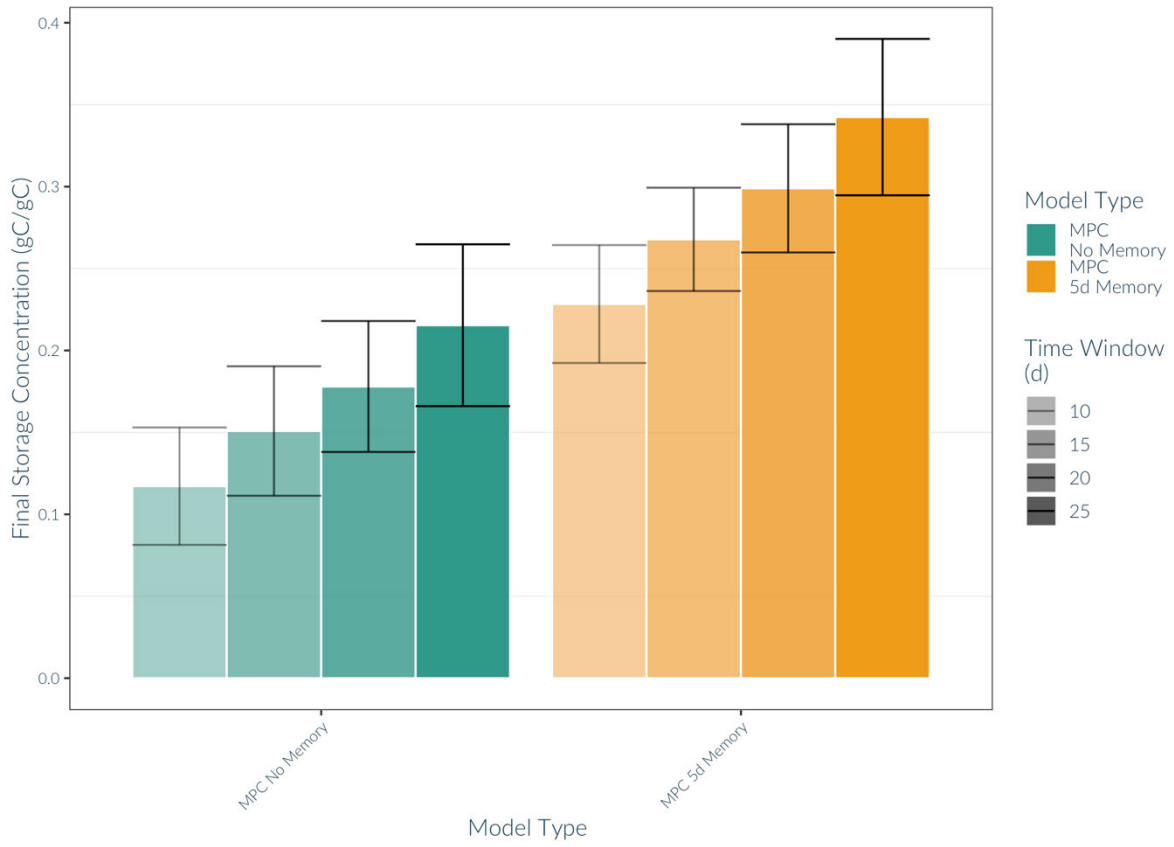

Figure 4-11 Storage pool concentration (calculated as Storage/(Storage + Biomass)) at the end of the simulation, for the MaxM ($k_f = 1$) fitness goal.. Error bars indicate standard deviation for each group (N=5). Colours indicate different memory sizes (green: no memory and yellow: 5 day memory). Shade intensity indicates the size of the forward prediction time window, t_w (with lighter shade indicating shorter time window).

4.4 Discussion

The idea that natural selection tends to select for organisms with higher fitness in a given environment is one of the central tenets of ecology (Parker & Smith, 1990). Modelling natural selection through optimisation modelling, including modelling plant behaviour (Iwasa, 2000; McGill & Brown, 2007), is thus attractive to capture the outcomes of evolutionary processes. However, as plants also adopt short-term acclimation responses to environmental variability, modelling the process of dynamic acclimation is necessary in understanding plant responses to their environment. In this work, I have created a framework for examining plant short-term plastic responses to changing environmental risks. This "Control Framework", which uses model predictive control (MPC), assumes the plant can change behaviour relatively rapidly as the risk profile of a stress changes. The predicted behaviour was compared with results obtained from OCT deterministic

optimisation models under a range of fitness proxies from the goal spectrum of 'maximising storage' to 'maximising biomass'. Here I found that the predicted behaviour did not change between the control framework and OCT solutions when plants were assumed to maximise storage. When maximising the biomass pool, the MPC framework predicts a similar allocation pattern to the OCT solution: large initial growth, followed by a storage period and a stress period. However, the OCT solution resulted in the depletion of stored carbon at the end of the simulation but the MPC solution maintained a sizable buffer of stored carbon. Moreover, the size of this buffer was dependent on the properties of the Control Framework. The storage buffer increased with a longer prediction time window and with the introduction of memory to the model. This difference between the OCT and MPC solutions can be attributed to the continuous re-evaluation of environmental conditions in the MPC solution. Each day a new optimal response is calculated and, therefore, the plant must always have enough stored carbon to survive over the predicted time window. If the conditions rapidly change, causing increased plant stress, the MPC methodology can capture the flexibility of the response.

In this chapter, I assumed the existence of a rainy and dry season to capture analogy between the MPC and OCT frameworks. This allowed for more stochastic rainfalls to be simulated. The continuous updating of the model can be applied to predict behaviour in any rainfall or stress scenario. Hence, the Control Framework can be used to predict behaviour in more predictable environments, more stochastic environments, or even extreme stress environments.

4.4.1 Comparing strategies: capturing realism and CF/MPC viability

While the behaviour predicted by the MPC approach is ultimately suboptimal, yielding a lower mean value of the optimisation target than the OCT approach, it is nonetheless more realistic, i.e., aligns more with observations from experiments (e.g., the maintenance of a carbon storage buffer, Martínez-Vilalta et al., 2016). With the MaxM fitness goal, the plant is predicted to grow for a period of time during the wet season, before switching to storage in response to water availability and increased maintenance costs due to size. During the remainder of the simulation, including the dry season, the plant maintains a sizable storage pool which can be used by the plant when stressed. In contrast, a deterministic approach

using OCT predicts the storage pool would be fully depleted by the end of the observed period, which disagrees with most observations in which plants maintain minimum storage concentrations (Martínez-Vilalta et al., 2016). Even less realistic was the brute-force optimisation model, which predicted that growth should be delayed until late into the simulation, followed by rapid late growth from an over-sized storage pool. While this approach provides the optimal solution in terms of final biomass size, the brute-force optimisation behaviour has not been observed in plant growth. While plant storage can be substantial, with extremes of up to 300 mg/g dry matter (Martínez-Vilalta et al., 2016) they do not reach storage pool sizes seen in the simulations (for a maximum of 31%, 41% and 70% of the plant biomass for the OCT, MPC and Brute-Force models, respectively).

4.4.2 Parameter sensitivity: storage buffer response

The most pronounced response to varying framework parameters was in the size of the storage concentration. The maintenance of a storage buffer can be interpreted as a mechanism of adaptation to stressful conditions (Sala et al., 2012; Wiley & Helliker, 2012). In fact, plants rarely deplete their stored carbon under stress (Adams et al., 2017; Mitchell et al., 2013; Wiley, 2020) and higher non-structural carbohydrate (NSC) concentrations can be associated with survival (Kitajima, 1994; Kobe, 1997; Piper & Paula, 2020; Wiley & Helliker, 2012). In fact, carbon storage buffers can be large enough to replenish an individual's foliage several times (Gholz & Cropper Jr., 1991; Hoch et al., 2003; Würth et al., 2005).

The storage buffer differed between different framework parameters, much as plant NSC concentration can vary largely between individuals (e.g., Bansal & Germino, 2010; Hao et al., 2021), species (e.g., Aguadé et al., 2015; Furze et al., 2019; Han et al., 2020; Tixier et al., 2020), and biomes (Martínez-Vilalta et al., 2016). However, differences between NSC patterns have yet to be conclusively linked to physical and functional traits, which often provide a context in which individuals and species can be compared (e.g., Chave et al., 2009; Osnas et al., 2013; Reich, 2014). For example, wood density, potential size or growth rate were not related to plant NSC concentration in a study across tropical rainfall gradients (Signori-Müller et al., 2021). Moreover, in a synthesis of drought-tolerance Adams *et al.*,

(2017) found that while there is some correlation between NSC values and hydraulic traits those results may not be significant for all species.

In the Control Framework, variation in NSC concentration can be clearly attributed to control parameters. When the time window size is increased, the plant must store enough carbon to survive a longer period, thereby increasing the required carbon storage concentration with the time window size. On the other hand, when memory is implemented, the prediction of optimal behaviour is based on a larger amount of information about the current rainfall pattern. However, these parameters (prediction time window, memory length) do not have a clear link with known physiological traits and can be more associated with perceived risks rather than purely physical characteristics. As such, studies of hormone response to stress (Mund et al., 2020; Sopory, 2019, pp. 238–239), in addition to physiological responses, may shed additional light into variation between plant carbon storage.

4.4.3 Limitations

Several biological processes have been simplified or omitted in this work, any of which could have affected the behaviour of the plant. Importantly, the processes represented in the model were simplified through the use of linear relationships. In nature, these processes are often non-linear and their behaviour changes in response to resource abundance. For example, photosynthesis slows with decreased water availability (Fatichi et al., 2014) instead of stopping abruptly as I have implemented in this model. Moreover, photosynthesis is not always linearly dependent on biomass size. Instead, as the size of the plant and the number of leaves increase, the plant begins to shade itself, thereby, decreasing the efficiency of photosynthesis per leaf (Ackerly, 1999) which results in asymptotic behaviour. Respiration can also be represented in more complex and realistic ways. For instance, respiration has two components: maintenance respiration which ensures the survival of the plant (Amthor, 1984), and growth respiration, which provides energy to support the growth of new cells (Johnson, 1990). Considering non-linear dynamics, such as the ones described above, is important because it may change the optimal response of the plant. Asymptotic limits on resource allocation processes may lead to very different results in the calculated optimal trajectory. As the plant grows, the marginal return of photosynthesis will decrease,

while the marginal cost will increase due to higher respiration. Under such circumstances the optimal behaviour may be to stop growing in a non-linear model. In contrast, in the linear model used in this study, the cost-benefit ratio to growing new biomass does not depend on the plant size and, therefore, the plant is more likely to grow bigger in such a model.

Moreover, only short timescales were evaluated in this work and post-stress recovery was not examined. It was further assumed that the fitness goal remained unchanged throughout the simulation. However, the carbon allocation strategy of a plant may change over the lifetime of an individual (Niinemets, 2010) or through lagged responses (e.g., "drought memory", Alves et al., 2020). Moreover, plants can experience long-term effects of stress by decreased growth (Huang et al., 2018) or in some cases delayed mortality (Trugman et al., 2018). To fully evaluate the mechanisms of plant carbon storage response to stress, different timescales would have to be considered.

4.5 Conclusions and future work

The model and framework introduced in this chapter presents a new way of capturing allocation trajectories in plant response to stochastic stress. When applied to a problem of a plant subjected to drought, the MPC framework predicted a growth trajectory that imitated an optimal control solution while maintaining flexibility in the response to changing conditions. The iterative nature of the computation led to the maintenance of a storage buffer to account for the continuously increasing time required for plant survival. The strategy and subsequently the storage buffer which resulted from the simulated behaviour was sensitive to the length of the forecast used in daily predictions as well as the implementation of memory which decreased sensitivity to daily fluctuations in environmental conditions.

This work serves as the proof of concept for the Control Framework as a methodology of examining the acclimation of carbon storage and other processes to changing environments. Beyond addressing the limitations stated above, future work can involve exploring more complex plant models and submodules to evaluate the methodology in more realistic scenarios. Crucial to this endeavour would be access to carefully collected experimental data that can assist defining what are realistic results. In parallel, the

framework itself can be improved by implementing new modules such as “learning”, updating the model to further aid with acclimation, and examining sensitivity to longer-term adaptation. Further work on comparing optimisation models and MPC, especially in the conditions under which plant responses to stress begin to vary or diverge between species and individuals. However, using the modelling framework presented in this chapter, these extensions are achievable and would greatly aid in expanding our understanding of plant climate change acclimation.

5 Synthesis and Future Directions

This thesis study has explored the growth–storage trade-offs involved in the storage of carbon by trees under stress. I have used a range of modelling approaches in order to better understand the optimal storage utilisation trajectory (OSUT). First, I investigated the OSUT for a tree subjected to a range of drought regimes using two life history strategies: prioritisation of growth (MaxM) and prioritisation of storage (MaxS). Second, I explored the growth and survival under these alternative growth and storage strategies of a community of trees living in stochastic (random) environments. Third, I investigated the emergence of an OSUT from a feedback-and-feedforward framework in a stochastic environment. This approach provided a novel way to model optimal carbon storage by highlighting the importance of capturing the trade-offs between growth and storage while considering the effects of a more realistic and stochastic environment on the process of carbon storage.

5.1 Shape of the optimal storage utilisation trajectory: recommendations for the representation of carbon storage in models

I have observed that patterns of allocation of carbon storage in plants can represent an active, rather than passive, storage utilisation strategy by mathematically characterising the shape of the OSUT under stress (Chapter 2). The OSUT is comprised of three stages: (1) an initial period when soil moisture is high and growth is prioritised; (2) an intermediate period when the plant switches to prioritising carbon storage and thus no growth occurs; and (3) a stress period when photosynthesis is inhibited and thus key metabolic activities such as respiration must be supported with stored carbon. Crucially, I have found that the OSUT can be characterised by the switch point when the plant stops growing (t_s). This occurs before the plant becomes fully stressed and upon switching from growth, the plant must prioritise accumulating carbon in its storage pool. This pattern of growth followed by storage is commonly observed in plants during drought (Körner, 2015; Mitchell, O'Grady, Tissue, et al., 2014), but it is typically associated with passive storage, where storage accumulation begins due to sink limitation rather than a storage-prioritising strategy (Körner, 2003). However, this same pattern of growth and storage also emerges from the optimisation analysis in which storing carbon prior to full stress is necessary for plant survival. The implication from

this work is, therefore, that the mechanism of carbon storage is more likely to be an active process than a passive one.

Using the growth–storage patterns characterised in Chapter 2, I have determined how alternative growth versus storage strategies performed over the long term in a community of plants living in an environment subjected to stress in a stochastic way (Chapter 3). Using a gap model, I simulated the growth of plants along a spectrum of two carbon storage–related traits, the carbon utilisation rate and the growth-storage time switch period under different stress conditions. Notably, while optimisation modelling can provide insight into the evolution of carbon storage strategies, the success of these strategies was found to be further dependent on ecological parameters, specifically the randomness of the environment and the competitive effect of other plants. Moreover, the key factor found to determine the outcome of competition was differential mortality rates. A short growth period reduced the chance of survival during a stress period and a fast carbon utilisation rate reduced the minimum level of the annual carbon storage pool during the growth period, thereby reducing the shade tolerance of an individual tree. Furthermore, as stress stochasticity increased, plants with a more conservative storage strategy (slower growth and a shorter growing period) began to dominate the community in terms of both number and overall size. They became more dominant in the environment, highlighting the importance of having the right storage strategy for surviving stochastic stress.

This work lays the foundation for realistically modelling the effects of climate change on plant communities across time and space by modelling carbon storage processes. However, this study represents the initial stages in exploring the utility of mathematical characterisation of carbon storage for plant communities. As such, future work on modelling carbon storage should consider the following two recommendations:

1. Carbon storage should be modelled as an active (not passive) process and carbon allocation models should consider the effects of competition between carbon pools.
2. The variation in active carbon storage allocation strategies can be modelled using two parameters: i) a switch time point, which captures phenological elements of the process and can indicate a shift between the growth and storage dynamics in plants; and ii) a carbon utilisation parameter, which reflects the rate at which stored carbon is used to support plant growth.

Having established the need to model realistic environments, in Chapter 4 I have addressed the assumptions that the environment is static and that a plant is locally adapted to a single, predictable environmental niche (as defined in Chapter 2). Here, I formulated a framework that approximates a long-term optimal response and allows acclimatisation to occur over time even in stochastic conditions. By using the method of model predictive control (MPC), I iteratively computed short-term optimal trajectories for allocating carbon storage and partially solved each trajectory before reassessment under new conditions. This approach successfully approximated the optimal dynamics model developed in Chapter 2. Crucially, the new computed strategy has shown that a substantial carbon storage buffer was created based on the repeated re-evaluation of current and predicted stochastic environmental conditions to ensure optimal plant performance, thereby simulating acclimatisation. Therefore, I recommend adopting the MPC methodology to examine the realistic acclimatisation responses of plants in scenarios of high randomness such as the future environments expected under climate change and global heating.

5.2 Linking carbon storage strategies with plant functional traits and other processes

The work presented here highlights potential future lines of inquiry into linking carbon storage processes in plants with other functional traits. In general, the relationships between carbohydrate storage in plants and their functional traits are yet to be properly characterised, with plant experiments so far yielding conflicting accounts of these relationships. This study foregrounds the importance of considering carbon storage strategies as time-sensitive processes. Because of the time element, in evaluating a carbon storage strategy the relationship between carbon storage and functional traits is unlikely to encompass a straightforward reactive process and, therefore, unlikely to be adequately characterisable through correlations between parameters at a single time point. Instead, an explicit mathematical modelling analysis is essential and experimental researchers should be guided by robust mathematical frameworks in order to successfully interpret their data with respect to time dynamics. Given that an optimal storage strategy may be identified by both the time of switching between storage and growth, and the rate of carbon storage utilisation when the plant is growing, I recommend that these two traits form the basis for experimental exploration of the relationships between plant functional traits.

First, the relationship between the switch time and hydraulic traits should be explored. The optimal strategy adopted by plants under drought (Chapter 2) relates to the carbon safety margin, which in turn relates to the hydraulic safety margin (Mencuccini, 2014; Mitchell, O'Grady, Tissue, et al., 2014). The relationship between hydraulic traits and carbon storage concentrations is unclear; for example, normalised non-structural carbohydrate (NSC) concentrations are related to embolism resistance in gymnosperms, but not in angiosperms (Adams et al., 2017). A key insight from this study is that if a carbon storage strategy is defined by the factors that affect the switch between growth and storage in addition to carbohydrate storage concentration, then the relationship between hydraulic traits and carbon storage may be more important than previously thought.

Second, the time of switching from growth to storage is key to plant tolerance to abiotic stress. It may be that stress is mitigated by an earlier switch and, crucially, this phenological event can be identified in experiments, creating a link between mathematical modelling and experimental science. As Chapter 3 has shown, the two storage traits (the time of switching between storage and growth, and the rate of carbon storage utilisation) are key to influencing plant tolerance to abiotic stress. I showed that this is due to higher carbon concentrations during the processes of annual photosynthesis inhibition (e.g. winter) and during growth, which leads to shade tolerance. Carbon storage can have a positive effect on plant survival during stress and other studies have shown that shade-tolerant plants have higher NSC concentrations than shade-intolerant upper-canopy plants (Atkinson et al., 2014), while plants that live in more stressful (e.g. drier) environments may stop growth sooner (Kagawa et al., 2003). However, attributes such as shade tolerance can also be attributed to other traits such as nitrogen content or specific leaf area (Abbasi et al., 2021; Reich, 2014). Therefore, further experimental studies that explore the relationships between the traits of carbon storage strategies and recognised physiological traits will be important in modelling the carbon behaviour of plants during stress events.

This research arc has been further explored in Chapter 4, where the focus shifted from characterising functional traits to considering 'behavioural' traits, specifically two traits related to the 'memory' and 'predictive capacity' of a plant to assess future stress risks. While these concepts do not have physiological equivalents, I showed that they may be

proxies for risk perception and response. Chapter 4 has illustrated the value of exploring physiological relationships in order to enable us to characterise the thresholds for plant stress response. For example, by extending the predictive capacity of a modelled plant, the plant's optimal storage buffer size may increase, in turn allowing the plant to survive longer and more intense stress periods. In contrast, a plant with a lower predictive capacity may be categorisable as risk-taking, relying on a steady supply of carbon to survive, making it more susceptible to stress. Exploration of how plants sense risk through investigating thresholds of hormonal and signalling responses to stress may, therefore, be a worthwhile pursuit in order to identify traits related to the acclimatisation of carbon storage strategies. With better understanding of such acclimatisation mechanisms and traits, we can improve the modelling and forecasting of how diverse communities of plants respond to the rapidly changing conditions enforced by anthropogenic climate change.

5.3 Representing plant function as an emergent control process

A key development in this thesis study is, therefore, consideration of whether a plant only reacts to immediate stimuli or can actually map – and follow – a trajectory as defined by the OSUT. In Chapters 2 and 3, the OSUT was assumed to be the effect of a locally adapted optimal process. However, the adaptation of traits is a continuous process with a continuously shifting landscape of parameters (Dieckmann et al., 2006). As such, what is considered optimal must also shift along with changing internal and external factors. Therefore, in Chapter 4 I have considered the requirements and mechanisms for acclimatisation regarded as a process which searches for approximately optimal solutions. Interpretation of the methods used in Chapter 4 requires a shift away from using an anthropomorphic approach to terminology, implying the existence of a neurological system capable of making decisions, towards engaging with counterparts from computer and complexity science which focus on the emergent complex behaviour of simple subsystems.

While the control framework used in Chapter 4 employs the use of prediction and evaluation mechanisms, these are defined here based on computer science terminology and do not require that plants have some kind of centralised processing system capable of forecasting. In biological literature it has generally been assumed that the capacity to forecast conditions requires an individual to possess a centralised nervous system and a

‘perceptual forecasting machine’ (e.g., a brain); this machine uses information from ‘sensors’ and ‘regulators’ to decide how the ‘actuator’ components behave (e.g., Bridgeman, 1995). In other words, forecasting has been assumed to require a system that can perceive the environment (e.g., the eyes sensing danger), compute potential behaviours (e.g. the brain assessing risk and evaluating possible courses of action) and then enact behaviour in response (e.g., the limbs making the body jump away from the danger). However, this anthropocentric view confuses machines with consciousness and ignores the highly complex feedback-loop systems with multiple sensor, regulator and actuator components that exist throughout nature (Wiener, 2019). For example, consider the molecular fuel of plasticity: in spite of every cell hosting the same DNA sequence, protein production is performed at the cellular level and independently by each cell. Gene expression regulates this production, responding to cellular environmental cues as well as metadata such as the developmental identity of the cell and associated tissue. These elements work in concert to optimise the cell’s behaviour in relation to the perceived environment, leading to the observation of computation-like behaviour at the molecular level (Eagleman, 2020 and the examples within; Lyon, 2015; Mitchell & Pilpel, 2011; Tagkopoulos et al., 2008; Wu et al., 2009). This capacity of the cell to conduct complex tasks when the individual parts of the system cannot be considered or predicted in isolation from each other, but only in terms of their collected behaviour and relationships, is defined as emergent behaviour. Emergence is a central thesis in the biomathematics field of systems biology and was a major conceptual hindrance for biologists (Lazebnik, 2002) until the development of systems biology.

Plants operate without a nervous system, but do display emergent behaviour that seems to coordinate the responses of a plant and its components to present and future stimuli. While it is unarguable that some plant processes are purely reactive to environmental stimuli (e.g. photoperiod and temperature; Gauzere *et al.*, 2019), the coordination of processes across the entirety of the plant may also require complex responses in relation to the expected abiotic conditions and behaviours of other organisms (Post, 2019, pp. 47–48). Models of optimal plant behaviour predict that when plant components (e.g., shoots and roots) are distributed and optimised independently, the

whole plant will show emergent optimal behaviour despite the relative independence of the subsystems (Ledder et al., 2020). Moreover, plant components such as branches may display independent allocation strategies under non-stressed conditions but begin to display coordinated allocation responses when stressed (Obeso, 2002; Sprugel et al., 1991). It follows, therefore, that mechanisms such as prediction and evaluation, as used in Chapter 4, may be emergent from the collective behaviour of subsystems which imitate coordination mechanisms normally attributed to systems that do have nervous systems and can make decisions. In turn, these internal models of coordination allow the plant to adopt long-term, 'predictive', goal-seeking behaviour capable of acclimatising to future risk. Therefore, progressing from traditional optimisation techniques and adopting methods such as MPC that can imitate this coordination process may help us in addressing the challenges of modelling plant responses to an increasingly variable climate.

Bibliography

Abbasi, U. A., You, W.-H., & Yan, E.-R. (2021). Correlations between leaf economics, hydraulic, and shade-tolerance traits among co-occurring individual trees. *Acta Oecologica*, *110*, 103673. https://doi.org/10.1016/j.actao.2020.103673

Ackerly, D. (1999). Self-shading, carbon gain and leaf dynamics: A test of alternative optimality models. *Oecologia*, *119*(3), 300–310. https://doi.org/10.1007/s004420050790

Adams, H. D., Collins, A. D., Briggs, S. P., Vennetier, M., Dickman, L. T., Sevanto, S. A., Garcia-Forner, N., Powers, H. H., & McDowell, N. G. (2015). Experimental drought and heat can delay phenological development and reduce foliar and shoot growth in semiarid trees. *Global Change Biology*, *21*(11), 4210–4220. https://doi.org/10.1111/gcb.13030

Adams, H. D., Germino, M. J., Breshears, D. D., Barron-Gafford, G. A., Guardiola-Claramonte, M., Zou, C. B., & Huxman, T. E. (2013). Nonstructural leaf carbohydrate dynamics of Pinus edulis during drought-induced tree mortality reveal role for carbon metabolism in mortality mechanism. *New Phytologist*, *197*(4), 1142–1151. https://doi.org/10.1111/nph.12102

Adams, H. D., Macalady, A. K., Breshears, D. D., Allen, C. D., Stephenson, N. L., Saleska, S. R., Huxman, T. E., & McDowell, N. g. (2010). Climate-Induced Tree Mortality: Earth System Consequences. *Eos, Transactions American Geophysical Union*, *91*(17), 153. https://doi.org/10.1029/2010EO170003

Adams, H. D., Williams, A. P., Xu, C., Rauscher, S. A., Jiang, X., & McDowell, N. G. (2013). Empirical and process-based approaches to climate-induced forest mortality models. *Frontiers in Plant Science*, *4*. https://doi.org/10.3389/fpls.2013.00438

Adams, H. D., Zeppel, M. J. B., Anderegg, W. R. L., Hartmann, H., Landhäusser, S. M., Tissue, D. T., Huxman, T. E., Hudson, P. J., Franz, T. E., Allen, C. D., Anderegg, L. D. L., Barron-Gafford, G. A., Beerling, D. J., Breshears, D. D., Brodribb, T. J., Bugmann, H., Cobb, R. C., Collins, A. D., Dickman, L. T., … McDowell, N. G. (2017). A multi-species synthesis of physiological mechanisms in drought-induced tree mortality. *Nature Ecology & Evolution*, *1*(9), 1285–1291. https://doi.org/10.1038/s41559-017-0248-x

Adams, M. A. (2013). Mega-fires, tipping points and ecosystem services: Managing forests and woodlands in an uncertain future. *Forest Ecology and Management*, *294*, 250–261. https://doi.org/10.1016/j.foreco.2012.11.039

Aguade, D., Poyatos, R., Gomez, M., Oliva, J., & Martinez-Vilalta, J. (2015). The role of defoliation and root rot pathogen infection in driving the mode of drought-related physiological decline in Scots pine (Pinus sylvestris L.). *Tree Physiology*, *35*(3), 229–242. https://doi.org/10.1093/treephys/tpv005

Aguadé, D., Poyatos, R., Rosas, T., & Martínez-Vilalta, J. (2015). Comparative Drought Responses of Quercus ilex L. and Pinus sylvestris L. in a Montane Forest Undergoing a Vegetation Shift. *Forests*, *6*(12), 2505–2529. https://doi.org/10.3390/f6082505

Ahrens, C. W., Andrew, M. E., Mazanec, R. A., Ruthrof, K. X., Challis, A., Hardy, G., Byrne, M., Tissue, D. T., & Rymer, P. D. (2020). Plant functional traits differ in adaptability and

are predicted to be differentially affected by climate change. *Ecology and Evolution*, *10*(1), 232–248. https://doi.org/10.1002/ece3.5890

Ahrens, C. W., Rymer, P. D., & Tissue, D. T. (2021). Intra-specific trait variation remains hidden in the environment. *New Phytologist*, 1183–1185. https://doi.org/10.1111/nph.16959

Albrecht, T., & Argueso, C. T. (2016). Should I fight or should I grow now? The role of cytokinins in plant growth and immunity and in the growth–defence trade-off. *Annals of Botany*, mcw211. https://doi.org/10.1093/aob/mcw211

Alexander, L. V. (2016). Global observed long-term changes in temperature and precipitation extremes: A review of progress and limitations in IPCC assessments and beyond. *Weather and Climate Extremes*, *11*, 4–16. https://doi.org/10.1016/j.wace.2015.10.007

Allen, C. D., Macalady, A. K., Chenchouni, H., Bachelet, D., McDowell, N., Vennetier, M., Kitzberger, T., Rigling, A., Breshears, D. D., Hogg, E. H. (Ted), Gonzalez, P., Fensham, R., Zhang, Z., Castro, J., Demidova, N., Lim, J.-H., Allard, G., Running, S. W., Semerci, A., & Cobb, N. (2010). A global overview of drought and heat-induced tree mortality reveals emerging climate change risks for forests. *Forest Ecology and Management*, *259*(4), 660–684. https://doi.org/10.1016/j.foreco.2009.09.001

Allen, M. T., Prusinkiewicz, P., & DeJong, T. M. (2005). Using L-systems for modeling source–sink interactions, architecture and physiology of growing trees: The L-PEACH model. *New Phytologist*, *166*(3), 869–880. https://doi.org/10.1111/j.1469-8137.2005.01348.x

Alves, R. D. F. B., Menezes-Silva, P. E., Sousa, L. F., Loram-Lourenço, L., Silva, M. L. F., Almeida, S. E. S., Silva, F. G., Perez de Souza, L., Fernie, A. R., & Farnese, F. S. (2020). Evidence of drought memory in Dipteryx alata indicates differential acclimation of plants to savanna conditions. *Scientific Reports*, *10*(1), 16455. https://doi.org/10.1038/s41598-020-73423-3

Amthor, J. S. (1984). The role of maintenance respiration in plant growth. *Plant, Cell & Environment*, *7*(8), 561–569. https://doi.org/10.1111/1365-3040.ep11591833

An, R., Hu, J., & Wen, L. (2021). A Nonlinear Model Predictive Control Model Aimed at the Epidemic Spread with Quarantine Strategy. *Journal of Theoretical Biology*, 110915. https://doi.org/10.1016/j.jtbi.2021.110915

Anderegg, W. R. L., Hicke, J. A., Fisher, R. A., Allen, C. D., Aukema, J., Bentz, B., Hood, S., Lichstein, J. W., Macalady, A. K., McDowell, N., Pan, Y., Raffa, K., Sala, A., Shaw, J. D., Stephenson, N. L., Tague, C., & Zeppel, M. (2015). Tree mortality from drought, insects, and their interactions in a changing climate. *New Phytologist*, *208*(3), 674–683. https://doi.org/10.1111/nph.13477

Anderegg, W. R. L., Klein, T., Bartlett, M., Sack, L., Pellegrini, A. F. A., Choat, B., & Jansen, S. (2016). Meta-analysis reveals that hydraulic traits explain cross-species patterns of drought-induced tree mortality across the globe. *Proceedings of the National Academy of Sciences*, *113*(18), 5024–5029. https://doi.org/10.1073/pnas.1525678113

Anderegg, W. R. L., Trugman, A. T., Badgley, G., Konings, A. G., & Shaw, J. (2020). Divergent forest sensitivity to repeated extreme droughts. *Nature Climate Change*, *10*(12), 1091–1095. https://doi.org/10.1038/s41558-020-00919-1

Anderson, L. O., Ribeiro Neto, G., Cunha, A. P., Fonseca, M. G., Mendes de Moura, Y., Dalagnol, R., Wagner, F. H., & de Aragão, L. E. O. e C. (2018). Vulnerability of Amazonian forests to repeated droughts. *Philosophical Transactions of the Royal Society B: Biological Sciences*, *373*(1760), 20170411. https://doi.org/10.1098/rstb.2017.0411

Aria, M., & Cuccurullo, C. (2017). Bibliometrix: An R tool for comprehensive analysis of scientific literature. *Journal of Informetrics*, *11*, 959–975.

Aronson, J., Kigel, J., Shmida, A., & Klein, J. (1992). Adaptive phenology of desert and Mediterranean populations of annual plants grown with and without water stress. *Oecologia*, *89*(1), 17–26. https://doi.org/10.1007/BF00319010

Aspinwall, M. J., Drake, J. E., Campany, C., Vårhammar, A., Ghannoum, O., Tissue, D. T., Reich, P. B., & Tjoelker, M. G. (2016). Convergent acclimation of leaf photosynthesis and respiration to prevailing ambient temperatures under current and warmer climates in *Eucalyptus tereticornis*. *New Phytologist*, *212*(2), 354–367. https://doi.org/10.1111/nph.14035

Atkinson, R. R. L., Burrell, M. M., Osborne, C. P., Rose, K. E., & Rees, M. (2012). A non-targeted metabolomics approach to quantifying differences in root storage between fast- and slow-growing plants. *New Phytologist*, *196*(1), 200–211. https://doi.org/10.1111/j.1469-8137.2012.04274.x

Atkinson, R. R. L., Burrell, M. M., Rose, K. E., Osborne, C. P., & Rees, M. (2014). The dynamics of recovery and growth: How defoliation affects stored resources. *Proceedings of the Royal Society B: Biological Sciences*, *281*(1783), 20133355. https://doi.org/10.1098/rspb.2013.3355

Ayub, G., Smith, R. A., Tissue, D. T., & Atkin, O. K. (2011). Impacts of drought on leaf respiration in darkness and light in *Eucalyptus saligna* exposed to industrial-age atmospheric CO $_2$ and growth temperature. *New Phytologist*, *190*(4), 1003–1018. https://doi.org/10.1111/j.1469-8137.2011.03673.x

Baber, O., Slot, M., Celis, G., & Kitajima, K. (2014). Diel patterns of leaf carbohydrate concentrations differ between seedlings and mature trees of two sympatric oak species. *Botany*, *92*(7), 535–540. https://doi.org/10.1139/cjb-2014-0032

Bachofen, C., Moser, B., Hoch, G., Ghazoul, J., & Wohlgemuth, T. (2018). No carbon "bet hedging" in pine seedlings under prolonged summer drought and elevated CO2. *Journal of Ecology*, *106*(1), 31–46. https://doi.org/10.1111/1365-2745.12822

Bahn, M., Lattanzi, F. A., Hasibeder, R., Wild, B., Koranda, M., Danese, V., Brüggemann, N., Schmitt, M., Siegwolf, R., & Richter, A. (2013). Responses of belowground carbon allocation dynamics to extended shading in mountain grassland. *New Phytologist*, *198*(1), 116–126. https://doi.org/10.1111/nph.12138

Bahn, M., Reichstein, M., Dukes, J. S., Smith, M. D., & Mcdowell, N. G. (2014). Climate-biosphere interactions in a more extreme world. *New Phytologist*, *202*(2), 356–359. https://doi.org/10.1111/nph.12662

Bansal, S., & Germino, M. J. (2010). Unique responses of respiration, growth, and non-structural carbohydrate storage in sink tissue of conifer seedlings to an elevation gradient at timberline. *Environmental and Experimental Botany*, *69*(3), 313–319. https://doi.org/10.1016/j.envexpbot.2010.05.002

Bansal, S., Reinhardt, K., & Germino, M. J. (2011). Linking carbon balance to establishment patterns: Comparison of whitebark pine and Engelmann spruce seedlings along an herb cover exposure gradient at treeline. *Plant Ecology*, *212*(2), 219–228. https://doi.org/10.1007/s11258-010-9816-8

Barbaroux, C., & Breda, N. (2002). Contrasting distribution and seasonal dynamics of carbohydrate reserves in stem wood of adult ring-porous sessile oak and diffuse-porous beech trees. *Tree Physiology*, *22*(17), 1201–1210. https://doi.org/10.1093/treephys/22.17.1201

Barry, K. M., Quentin, A., Eyles, A., & Pinkard, E. A. (2012). Consequences of resource limitation for recovery from repeated defoliation in Eucalyptus globulus Labilladiere. *Tree Physiology*, *32*(1), 24–35. https://doi.org/10.1093/treephys/tpr128

Bart, R. R., Kennedy, M. C., Tague, C. L., & McKenzie, D. (2020). Integrating fire effects on vegetation carbon cycling within an ecohydrologic model. *Ecological Modelling*, *416*, 108880. https://doi.org/10.1016/j.ecolmodel.2019.108880

Bartlett, M. K., Scoffoni, C., & Sack, L. (2012). The determinants of leaf turgor loss point and prediction of drought tolerance of species and biomes: A global meta-analysis. *Ecology Letters*, *15*(5), 393–405. https://doi.org/10.1111/j.1461-0248.2012.01751.x

Bartlett, M. K., Zhang, Y., Kreidler, N., Sun, S., Ardy, R., Cao, K., & Sack, L. (2014). Global analysis of plasticity in turgor loss point, a key drought tolerance trait. *Ecology Letters*, *17*(12), 1580–1590. https://doi.org/10.1111/ele.12374

Bastos, A. (2020). *Diverging impacts of extreme summers on European C-cycling from different regional and seasonal compensation effects*. EGU General Assembly Conference Abstracts. https://doi.org/10.5194/egusphere-egu2020-3476

Bastos, A., O'Sullivan, M., Ciais, P., Makowski, D., Sitch, S., Friedlingstein, P., Chevallier, F., Rödenbeck, C., Pongratz, J., Luijkx, I. T., Patra, P. K., Peylin, P., Canadell, J. G., Lauerwald, R., Li, W., Smith, N. E., Peters, W., Goll, D. S., Jain, A. K., … Zaehle, S. (2020). Sources of Uncertainty in Regional and Global Terrestrial CO_2 Exchange Estimates. *Global Biogeochemical Cycles*, *34*(2). https://doi.org/10.1029/2019GB006393

Batllori, E., Lloret, F., Aakala, T., Anderegg, W. R. L., Aynekulu, E., Bendixsen, D. P., Bentouati, A., Bigler, C., Burk, C. J., Camarero, J. J., Colangelo, M., Coop, J. D., Fensham, R., Floyd, M. L., Galiano, L., Ganey, J. L., Gonzalez, P., Jacobsen, A. L., Kane, J. M., … Zeeman, B. (2020). Forest and woodland replacement patterns following drought-related mortality. *Proceedings of the National Academy of Sciences*, *117*(47), 29720–29729. https://doi.org/10.1073/pnas.2002314117

Bazot, S., Barthes, L., Blanot, D., & Fresneau, C. (2013). Distribution of non-structural nitrogen and carbohydrate compounds in mature oak trees in a temperate forest at four key phenological stages. *Trees - Structure and Function*, *27*(4), 1023–1034. Scopus. https://doi.org/10.1007/s00468-013-0853-5

Bennett, A. C., McDowell, N. G., Allen, C. D., & Anderson-Teixeira, K. J. (2015). Larger trees suffer most during drought in forests worldwide. *Nature Plants*, *1*(10), 15139. https://doi.org/10.1038/nplants.2015.139

Ben-Shachar, M. S., Lüdecke, D., & Makowski, D. (2020). {e}ffectsize: Estimation of Effect Size Indices and Standardized Parameters. *Journal of Open Source Software*, *5*(56), 2815. https://doi.org/10.21105/joss.02815

Bierhuizen, J. F., & Slatyer, R. O. (1965). Effect of atmospheric concentration of water vapour and CO2 in determining transpiration-photosynthesis relationships of cotton leaves. *Agricultural Meteorology*, *2*(4), 12.

Birami, B., Gattmann, M., Heyer, A. G., Grote, R., Arneth, A., & Ruehr, N. K. (2018). Heat Waves Alter Carbon Allocation and Increase Mortality of Aleppo Pine Under Dry Conditions. *Frontiers in Forests and Global Change*, *1*, 8. https://doi.org/10.3389/ffgc.2018.00008

Bloom, A. J. (1986). Plant economics. *Trends in Ecology & Evolution*, *1*(4), 98–100. https://doi.org/10.1016/0169-5347(86)90033-9

Bloom, A. J., Chapin III, F. S., & Mooney, H. A. (1985). Resource limitation in plants—An economic analogy. *Annual Review of Ecology and Systematics. Vol. 16*, 363–392. Scopus. https://www.scopus.com/inward/record.uri?eid=2-s2.0-0022165116&partnerID=40&md5=fcbe5419bbe9338e690be03df1b087f2

Blum, A., & Tuberosa, R. (2018). Dehydration survival of crop plants and its measurement. *Journal of Experimental Botany*, *69*(5), 975–981. https://doi.org/10.1093/jxb/erx445

Blumenthal, D. M., Mueller, K. E., Kray, J. A., Ocheltree, T. W., Augustine, D. J., & Wilcox, K. R. (2020). Traits link drought resistance with herbivore defence and plant economics in semi-arid grasslands: The central roles of phenology and leaf dry matter content. *Journal of Ecology*, *108*(6), 2336–2351. https://doi.org/10.1111/1365-2745.13454

Blumstein, M., & Hopkins, R. (2021). Adaptive variation and plasticity in non-structural carbohydrate storage in a temperate tree species. *Plant, Cell & Environment*, *44*(8), 2494–2505. https://doi.org/10.1111/pce.13959

Bogeat-Triboulot, M.-B., Brosché, M., Renaut, J., Jouve, L., Le Thiec, D., Fayyaz, P., Vinocur, B., Witters, E., Laukens, K., Teichmann, T., Altman, A., Hausman, J.-F., Polle, A., Kangasjärvi, J., & Dreyer, E. (2007). Gradual Soil Water Depletion Results in Reversible Changes of Gene Expression, Protein Profiles, Ecophysiology, and Growth Performance in *Populus euphratica* , a Poplar Growing in Arid Regions. *Plant Physiology*, *143*(2), 876–892. https://doi.org/10.1104/pp.106.088708

Bojórquez, A., Álvarez-Yépiz, J. C., Búrquez, A., & Martínez-Yrízar, A. (2019). Understanding and predicting frost-induced tropical tree mortality patterns. *Global Change Biology*, *25*(11), 3817–3828. https://doi.org/10.1111/gcb.14775

Boltyanskii, V. G., Gamkrelidze, R. V., & Pontryagin, L. S. (1960). *The theory of optimal processes. I. The maximum principle*. TRW SPACE TECHNOLOGY LABS LOS ANGELES CALIF.

Bonan, G. B. (2008). Forests and climate change: Forcings, feedbacks, and the climate benefits of forests. *Science*, *320*(5882), 1444–1449. Scopus. https://doi.org/10.1126/science.1155121

Bond, W. J., & Midgley, G. F. (2000). A proposed CO2-controlled mechanism of woody plant invasion in grasslands and savannas. *Global Change Biology*, *6*(8), 865–869. https://doi.org/10.1046/j.1365-2486.2000.00365.x

Botkin, D. B., Janak, J. F., & Wallis, J. R. (1972). Some Ecological Consequences of a Computer Model of Forest Growth. *Journal of Ecology*, *60*(3), 849–872. https://doi.org/10.2307/2258570

Bradshaw, C. J. A., & Warkentin, I. G. (2015). Global estimates of boreal forest carbon stocks and flux. *Global and Planetary Change*, *128*, 24–30. https://doi.org/10.1016/j.gloplacha.2015.02.004

Brando, P. M., Paolucci, L., Ummenhofer, C. C., Ordway, E. M., Hartmann, H., Cattau, M. E., Rattis, L., Medjibe, V., Coe, M. T., & Balch, J. (2019). Droughts, Wildfires, and Forest Carbon Cycling: A Pantropical Synthesis. *Annual Review of Earth and Planetary Sciences*, *47*(1), 555–581. https://doi.org/10.1146/annurev-earth-082517-010235

Bridgeman, B. (1995). A review of the role of efference copy in sensory and oculomotor control systems. *Annals of Biomedical Engineering*, *23*(4), 409–422. https://doi.org/10.1007/BF02584441

Brum, M., Saleska, S., Alves, L. F., Penha, D., Ivanov, V., Restrepo-Coupe, N., Albert, L., Oliveira-Junior, R., Moura, J. M., Mião, S., Signori-Müller, C., Prohaska, N., Aragão, L., & Oliveira, R. (2021). *Mapping seasonal and interannual Non-Structural Carbohydrate variation to drought-resistance strategies in eastern Amazon tree species* [Preprint]. Preprints. https://doi.org/10.22541/au.161662321.19984685/v1

Bryant, E. H. (1971). Life History Consequences of Natural Selection: Cole's Result. *The American Naturalist*, *105*(941), 75–76. https://doi.org/10.1086/282703

Buckley, T. N. (2005). The control of stomata by water balance. *New Phytologist*, *168*(2), 275–292. https://doi.org/10.1111/j.1469-8137.2005.01543.x

Buckley, T. N. (2021). Optimal carbon partitioning helps reconcile the apparent divergence between optimal and observed canopy profiles of photosynthetic capacity. *New Phytologist*, *230*(6), 2246–2260. https://doi.org/10.1111/nph.17199

Bugmann, H. (2001). A Review of Forest Gap Models. *Climatic Change*, *51*(3), 259–305.

Bugmann, H. K. M. (1996). A Simplified Forest Model to Study Species Composition Along Climate Gradients. *Ecology*, *77*(7), 2055–2074. https://doi.org/10.2307/2265700

Cailleret, M., Nourtier, M., Amm, A., Durand-Gillmann, M., & Davi, H. (2014). Drought-induced decline and mortality of silver fir differ among three sites in Southern France. *Annals of Forest Science*, *71*(6), 643–657. https://doi.org/10.1007/s13595-013-0265-0

Caldararu, S., Purves, D. W., & Palmer, P. I. (2014). Phenology as a strategy for carbon optimality: A global model. *Biogeosciences*, *11*(3), 763–778. https://doi.org/10.5194/bg-11-763-2014

Camisón, Á., Ángela Martín, M., Dorado, F. J., Moreno, G., & Solla, A. (2020). Changes in carbohydrates induced by drought and waterlogging in Castanea sativa. *Trees*, *34*(2), 579–591. https://doi.org/10.1007/s00468-019-01939-x

Cao, Y., Li, Y., & Chen, Y. (2018). Non-structural carbon, nitrogen, and phosphorus between black locust and chinese pine plantations along a precipitation gradient on the Loess Plateau, China. *Trees*, *32*(3), 835–846. https://doi.org/10.1007/s00468-018-1676-1

Carbone, M. S., Czimczik, C. I., Keenan, T. F., Murakami, P. F., Pederson, N., Schaberg, P. G., Xu, X., & Richardson, A. D. (2013). Age, allocation and availability of nonstructural carbon in mature red maple trees. *New Phytologist*, *200*(4), 1145–1155. https://doi.org/10.1111/nph.12448

Carnicer, J., Coll, M., Ninyerola, M., Pons, X., Sanchez, G., & Penuelas, J. (2011). Widespread crown condition decline, food web disruption, and amplified tree mortality with increased climate change-type drought. *Proceedings of the National Academy of Sciences*, *108*(4), 1474–1478. https://doi.org/10.1073/pnas.1010070108

Ceballos-Núñez, V., Richardson, A. D., & Sierra, C. A. (2018). Ages and transit times as important diagnostics of model performance for predicting carbon dynamics in terrestrial vegetation models. *Biogeosciences*, *15*(5), 1607–1625. https://doi.org/10.5194/bg-15-1607-2018

Chapin, F. S., Bloom, A. J., Field, C. B., & Waring, R. H. (1987). Plant Responses to Multiple Environmental Factors. *BioScience*, *37*(1), 49–57. https://doi.org/10.2307/1310177

Chapin, F. S., Randerson, J. T., McGuire, A. D., Foley, J. A., & Field, C. B. (2008). Changing feedbacks in the climate–biosphere system. *Frontiers in Ecology and the Environment*, *6*(6), 313–320. https://doi.org/10.1890/080005

Chapin, F. S., Schulze, E.-D., & Mooney, H. A. (1990). The ecology and economics of storage in plants. *Annual Review of Ecology and Systematics*, *21*(1), 423–447. https://doi.org/10.1146/annurev.es.21.110190.002231

Charrier, G., Martin-StPaul, N., Damesin, C., Delpierre, N., Hänninen, H., Torres-Ruiz, J. M., & Davi, H. (2021). Interaction of drought and frost in tree ecophysiology: Rethinking the timing of risks. *Annals of Forest Science*, *78*(2), 40. https://doi.org/10.1007/s13595-021-01052-5

Chave, J., Coomes, D., Jansen, S., Lewis, S. L., Swenson, N. G., & Zanne, A. E. (2009). Towards a worldwide wood economics spectrum. *Ecology Letters*, *12*(4), 351–366. https://doi.org/10.1111/j.1461-0248.2009.01285.x

Chaves, M. M., Flexas, J., & Pinheiro, C. (2009). Photosynthesis under drought and salt stress: Regulation mechanisms from whole plant to cell. *Annals of Botany*, *103*(4), 551–560. https://doi.org/10.1093/aob/mcn125

Chen, X., Zhao, P., Ouyang, L., Zhu, L., Ni, G., & Schäfer, K. V. R. (2020). Whole-plant water hydraulic integrity to predict drought-induced Eucalyptus urophylla mortality under drought stress. *Forest Ecology and Management*, *468*, 118179. https://doi.org/10.1016/j.foreco.2020.118179

Chiariello, N., & Roughgarden, J. (1984). Storage Allocation in Seasonal Races of an Annual Plant: Optimal Versus Actual Allocation. *Ecology*, *65*(4), 1290–1301. https://doi.org/10.2307/1938334

Choat, B., Jansen, S., Brodribb, T. J., Cochard, H., Delzon, S., Bhaskar, R., Bucci, S. J., Feild, T. S., Gleason, S. M., Hacke, U. G., Jacobsen, A. L., Lens, F., Maherali, H., Martínez-

Vilalta, J., Mayr, S., Mencuccini, M., Mitchell, P. J., Nardini, A., Pittermann, J., … Zanne, A. E. (2012). Global convergence in the vulnerability of forests to drought. *Nature*, *491*(7426), 752–755. https://doi.org/10.1038/nature11688

Clark, J. S., Dietze, M., Chakraborty, S., Agarwal, P. K., Ibanez, I., LaDeau, S., & Wolosin, M. (2007). Resolving the biodiversity paradox. *Ecology Letters*, *10*(8), 647–659. https://doi.org/10.1111/j.1461-0248.2007.01041.x

Clark, J. S., Iverson, L., Woodall, C. W., Allen, C. D., Bell, D. M., Bragg, D. C., D'Amato, A. W., Davis, F. W., Hersh, M. H., Ibanez, I., Jackson, S. T., Matthews, S., Pederson, N., Peters, M., Schwartz, M. W., Waring, K. M., & Zimmermann, N. E. (2016). The impacts of increasing drought on forest dynamics, structure, and biodiversity in the United States. *Global Change Biology*, *22*(7), 2329–2352. https://doi.org/10.1111/gcb.13160

Clarke, P. J., Manea, A., & Leishman, M. R. (2016). Are fire resprouters more carbon limited than non-resprouters? Effects of elevated CO2 on biomass, storage and allocation of woody species. *Plant Ecology*, *217*(6), 763–771. https://doi.org/10.1007/s11258-015-0528-y

Cochard, H. (2019). *A new mechanism for tree mortality due to drought and heatwaves* [Preprint]. Plant Biology. https://doi.org/10.1101/531632

Coumou, D., & Rahmstorf, S. (2012). A decade of weather extremes. *Nature Climate Change*, *2*(7), 491–496. https://doi.org/10.1038/nclimate1452

Cowan, I., & Farquhar, G. D. (1977). Stomatal function in relation to leaf metabolism and environment. In *Integration of Activity in the Higher Plant* (pp. 471–505). Cambridge University Press.

Cowan, T., Purich, A., Perkins, S., Pezza, A., Boschat, G., & Sadler, K. (2014). More Frequent, Longer, and Hotter Heat Waves for Australia in the Twenty-First Century. *Journal of Climate*, *27*(15), 5851–5871. https://doi.org/10.1175/JCLI-D-14-00092.1

Craine, J. M., Engelbrecht, B. M. J., Lusk, C. H., McDowell, N. G., & Poorter, H. (2012). Resource limitation, tolerance, and the future of ecological plant classification. *Frontiers in Plant Science*, *3*. https://doi.org/10.3389/fpls.2012.00246

da Costa, A. C. L., Galbraith, D., Almeida, S., Portela, B. T. T., da Costa, M., de Athaydes Silva Junior, J., Braga, A. P., de Gonçalves, P. H. L., de Oliveira, A. A., Fisher, R., Phillips, O. L., Metcalfe, D. B., Levy, P., & Meir, P. (2010). Effect of 7 yr of experimental drought on vegetation dynamics and biomass storage of an eastern Amazonian rainforest. *New Phytologist*, *187*(3), 579–591. https://doi.org/10.1111/j.1469-8137.2010.03309.x

Dai, A. (2013). Increasing drought under global warming in observations and models. *Nature Climate Change*, *3*(1), 52–58. https://doi.org/10.1038/nclimate1633

Damour, G., Simonneau, T., Cochard, H., & Urban, L. (2010). An overview of models of stomatal conductance at the leaf level: Models of stomatal conductance. *Plant, Cell & Environment*, no-no. https://doi.org/10.1111/j.1365-3040.2010.02181.x

D'Andrea, E., Scartazza, A., Battistelli, A., Collalti, A., Proietti, S., Rezaie, N., Matteucci, G., & Moscatello, S. (2021). Unravelling resilience mechanisms in forests: Role of non-

structural carbohydrates in responding to extreme weather events. *Tree Physiology*, *tpab044*. https://doi.org/10.1093/treephys/tpab044

Davi, H., & Cailleret, M. (2017). Assessing drought-driven mortality trees with physiological process-based models. *Agricultural and Forest Meteorology*, *232*, 279–290. eih. https://doi.org/10.1016/j.agrformet.2016.08.019

De Kauwe, M. G., Medlyn, B. E., Knauer, J., & Williams, C. A. (2017). Ideas and perspectives: How coupled is the vegetation to the boundary layer? *Biogeosciences*, *14*(19), 4435–4453. https://doi.org/10.5194/bg-14-4435-2017

De Schepper, V., & Steppe, K. (2010). Development and verification of a water and sugar transport model using measured stem diameter variations. *Journal of Experimental Botany*, *61*(8), 2083–2099. https://doi.org/10.1093/jxb/erq018

De Schepper, V., & Steppe, K. (2011). Tree girdling responses simulated by a water and carbon transport model. *Annals of Botany*, *108*(6), 1147–1154. https://doi.org/10.1093/aob/mcr068

Delgado, M., Zúñiga-Feest, A., & Piper, F. I. (2018). Does carbon storage confer waterlogging tolerance? Evidence from four evergreen species of a temperate rainforest. *Australian Journal of Botany*, *66*(1), 74. https://doi.org/10.1071/BT17104

Deng, X., Xiao, W., Shi, Z., Zeng, L., & Lei, L. (2019). Combined Effects of Drought and Shading on Growth and Non-Structural Carbohydrates in Pinus massoniana Lamb. Seedlings. *Forests*, *11*(1), 18. https://doi.org/10.3390/f11010018

Deslauriers, A., Caron, L., & Rossi, S. (2015). Carbon allocation during defoliation: Testing a defense-growth trade-off in balsam fir. *Frontiers in Plant Science*, *6*. https://doi.org/10.3389/fpls.2015.00338

DeSoto, L., Olano, J. M., & Rozas, V. (2016). Secondary Growth and Carbohydrate Storage Patterns Differ between Sexes in Juniperus thurifera. *Frontiers in Plant Science*, *7*. https://doi.org/10.3389/fpls.2016.00723

Dewar, R. C., Franklin, O., Mäkelä, A., McMurtrie, R. E., & Valentine, H. T. (2009). Optimal Function Explains Forest Responses to Global Change. *BioScience*, *59*(2), 127–139. https://doi.org/10.1525/bio.2009.59.2.6

Dickman, L. T., McDowell, N. G., Grossiord, C., Collins, A. D., Wolfe, B. T., Detto, M., Wright, S. J., Medina-Vega, J. A., Goodsman, D., Rogers, A., Serbin, S. P., Wu, J., Ely, K. S., Michaletz, S. T., Xu, C., Kueppers, L., & Chambers, J. Q. (2019). Homoeostatic maintenance of nonstructural carbohydrates during the 2015–2016 El Niño drought across a tropical forest precipitation gradient. *Plant, Cell & Environment*, *42*(5), 1705–1714. https://doi.org/10.1111/pce.13501

Dickman, L. T., Mcdowell, N. G., Sevanto, S., Pangle, R. E., & Pockman, W. T. (2015). Carbohydrate dynamics and mortality in a piñon-juniper woodland under three future precipitation scenarios: Carbohydrate dynamics in piñon-juniper woodland. *Plant, Cell & Environment*, *38*(4), 729–739. https://doi.org/10.1111/pce.12441

Dieckmann, U., Heino, M., & Parvinen, K. (2006). The adaptive dynamics of function-valued traits. *Journal of Theoretical Biology*, *241*(2), 370–389. https://doi.org/10.1016/j.jtbi.2005.12.002

Dietze, M. C., Matthes, J. H., & Arnone, J. (2014). A general ecophysiological framework for modelling the impact of pests and pathogens on forest ecosystems. *Ecology Letters*, *17*(11), 1418–1426. eih. https://doi.org/10.1111/ele.12345

Dietze, M. C., Sala, A., Carbone, M. S., Czimczik, C. I., Mantooth, J. A., Richardson, A. D., & Vargas, R. (2014). Nonstructural Carbon in Woody Plants. *Annual Review of Plant Biology*, *65*(1), 667–687. https://doi.org/10.1146/annurev-arplant-050213-040054

Doerner, P. (2020). Extreme environments: Crucibles of potent abiotic stress tolerance. *Journal of Experimental Botany*, *71*(13), 3761–3764. https://doi.org/10.1093/jxb/eraa269

Dolezal, J., Jandova, V., Macek, M., & Liancourt, P. (2021). Contrasting biomass allocation responses across ontogeny and stress gradients reveal plant adaptations to drought and cold. *Functional Ecology*, *35*(1), 32–42. https://doi.org/10.1111/1365-2435.13687

Drake, J. E., Tjoelker, M. G., Aspinwall, M. J., Reich, P. B., Pfautsch, S., & Barton, C. V. M. (2019). The partitioning of gross primary production for young *Eucalyptus tereticornis* trees under experimental warming and altered water availability. *New Phytologist*, *222*(3), 1298–1312. https://doi.org/10.1111/nph.15629

Drewniak, B., & Gonzalez-Meler, M. (2017). Earth System Model Needs for Including the Interactive Representation of Nitrogen Deposition and Drought Effects on Forested Ecosystems. *Forests*, *8*(8), 267. https://doi.org/10.3390/f8080267

Duan, H., Chaszar, B., Lewis, J. D., Smith, R. A., Huxman, T. E., & Tissue, D. T. (2018). CO2 and temperature effects on morphological and physiological traits affecting risk of

drought-induced mortality. *Tree Physiology*, *38*(8), 1138–1151. eih. https://doi.org/10.1093/treephys/tpy037

Duan, H., Li, Y., Xu, Y., Zhou, S., Liu, J., Tissue, D. T., & Liu, J. (2019). Contrasting drought sensitivity and post-drought resilience among three co-occurring tree species in subtropical China. *Agricultural and Forest Meteorology*, *272–273*, 55–68. https://doi.org/10.1016/j.agrformet.2019.03.024

Dybzinski, R., Farrior, C., Wolf, A., Reich, P. B., & Pacala, S. W. (2011). Evolutionarily Stable Strategy Carbon Allocation to Foliage, Wood, and Fine Roots in Trees Competing for Light and Nitrogen: An Analytically Tractable, Individual-Based Model and Quantitative Comparisons to Data. *The American Naturalist*, *177*(2), 153–166. https://doi.org/10.1086/657992

Eagleman, D. (2020). *Livewired: The inside story of the ever-changing brain*. Canongate Books.

Eller, C. B., de V. Barros, F., R.L. Bittencourt, P., Rowland, L., Mencuccini, M., & S. Oliveira, R. (2018). Xylem hydraulic safety and construction costs determine tropical tree growth: Tree growth vs hydraulic safety trade-off. *Plant, Cell & Environment*, *41*(3), 548–562. https://doi.org/10.1111/pce.13106

Engelbrecht, B. M. J., Comita, L. S., Condit, R., Kursar, T. A., Tyree, M. T., Turner, B. L., & Hubbell, S. P. (2007). Drought sensitivity shapes species distribution patterns in tropical forests. *Nature*, *447*(7140), 80–82. https://doi.org/10.1038/nature05747

Engen, S., & Saether, B.-E. (1994). Optimal allocation of resources to growth and reproduction. *Theoretical Population Biology*, *46*(2), 232–248.

Eziz, A., Yan, Z., Tian, D., Han, W., Tang, Z., & Fang, J. (2017). Drought effect on plant biomass allocation: A meta-analysis. *Ecology and Evolution*, *7*(24), 11002–11010. https://doi.org/10.1002/ece3.3630

Falster, D. S., Brännström, Å., Dieckmann, U., & Westoby, M. (2011). Influence of four major plant traits on average height, leaf-area cover, net primary productivity, and biomass density in single-species forests: A theoretical investigation: Influence of functional traits on emergent vegetation properties. *Journal of Ecology*, *99*(1), 148–164. https://doi.org/10.1111/j.1365-2745.2010.01735.x

Falster, D. S., Duursma, R. A., Ishihara, M. I., Barneche, D. R., FitzJohn, R. G., Vårhammar, A., Aiba, M., Ando, M., Anten, N., Aspinwall, M. J., Baltzer, J. L., Baraloto, C., Battaglia, M., Battles, J. J., Bond-Lamberty, B., van Breugel, M., Camac, J., Claveau, Y., Coll, L., … York, R. A. (2015). BAAD: A Biomass And Allometry Database for woody plants: *Ecological Archives* E096-128. *Ecology*, *96*(5), 1445–1445. https://doi.org/10.1890/14-1889.1

Falster, D. S., FitzJohn, R. G., Brännström, Å., Dieckmann, U., & Westoby, M. (2016). plant: A package for modelling forest trait ecology and evolution. *Methods in Ecology and Evolution*, *7*(2), 136–146. https://doi.org/10.1111/2041-210X.12525

Fatichi, S., Ivanov, V. Y., & Caporali, E. (2012). A mechanistic ecohydrological model to investigate complex interactions in cold and warm water-controlled environments: 1. Theoretical framework and plot-scale analysis. *Journal of Advances in Modeling Earth Systems*, *4*(2), n/a-n/a. https://doi.org/10.1029/2011MS000086

Fatichi, S., Leuzinger, S., & Körner, C. (2014). Moving beyond photosynthesis: From carbon source to sink-driven vegetation modeling. *New Phytologist*, *201*(4), 1086–1095. https://doi.org/10.1111/nph.12614

Fatichi, S., Pappas, C., Zscheischler, J., & Leuzinger, S. (2019). Modelling carbon sources and sinks in terrestrial vegetation. *New Phytologist*, *221*(2), 652–668. https://doi.org/10.1111/nph.15451

Feeley, K. J., Davies, S. J., Perez, R., Hubbell, S. P., & Foster, R. B. (2011). Directional changes in the species composition of a tropical forest. *Ecology*, *92*(4), 871–882. https://doi.org/10.1890/10-0724.1

Feldpausch, T. R., Phillips, O. L., Brienen, R. J. W., Gloor, E., Lloyd, J., Lopez-Gonzalez, G., Monteagudo-Mendoza, A., Malhi, Y., Alarcón, A., Álvarez Dávila, E., Alvarez-Loayza, P., Andrade, A., Aragao, L. E. O. C., Arroyo, L., Aymard C., G. A., Baker, T. R., Baraloto, C., Barroso, J., Bonal, D., … Vos, V. A. (2016). Amazon forest response to repeated droughts. *Global Biogeochemical Cycles*, *30*(7), 964–982. https://doi.org/10.1002/2015GB005133

Ferner, E., Rennenberg, H., & Kreuzwieser, J. (2012). Effect of flooding on C metabolism of flood-tolerant (Quercus robur) and non-tolerant (Fagus sylvatica) tree species. *Tree Physiology*, *32*(2), 135–145. https://doi.org/10.1093/treephys/tps009

Field, A. (2013). *Discovering statistics using IBM SPSS STATISTICS* (4th ed., Vol. 43, Issue 06). SAGE. https://doi.org/10.5860/choice.43-3433

Field, C. (1983). Allocating leaf nitrogen for the maximization of carbon gain: Leaf age as a control on the allocation program. *Oecologia*, *56*(2–3), 341–347. https://doi.org/10.1007/BF00379710

Field, C. B., Lobell, D. B., Peters, H. A., & Chiariello, N. R. (2007). Feedbacks of Terrestrial Ecosystems to Climate Change. *Annual Review of Environment and Resources*, *32*(1), 1–29. https://doi.org/10.1146/annurev.energy.32.053006.141119

Fine, P. V. A., Miller, Z. J., Mesones, I., Irazuzta, S., Appel, H. M., Stevens, M. H. H., Sääksjärvi, I., Schultz, J. C., & Coley, P. D. (2006). The growth–defense trade-off and habitat specialization by plants in Amazonian forests. *Ecology*, *87*(sp7), S150–S162. https://doi.org/10.1890/0012-9658(2006)87[150:TGTAHS]2.0.CO;2

Fisher, R. A., Koven, C. D., Anderegg, W. R. L., Christoffersen, B. O., Dietze, M. C., Farrior, C. E., Holm, J. A., Hurtt, G. C., Knox, R. G., Lawrence, P. J., Lichstein, J. W., Longo, M., Matheny, A. M., Medvigy, D., Muller-Landau, H. C., Powell, T. L., Serbin, S. P., Sato, H., Shuman, J. K., … Moorcroft, P. R. (2018). Vegetation demographics in Earth System Models: A review of progress and priorities. *Global Change Biology*, *24*(1), 35–54. https://doi.org/10.1111/gcb.13910

Fisher, R., McDowell, N., Purves, D., Moorcroft, P., Sitch, S., Cox, P., Huntingford, C., Meir, P., & Ian Woodward, F. (2010). Assessing uncertainties in a second-generation dynamic vegetation model caused by ecological scale limitations. *New Phytologist*, *187*(3), 666–681. https://doi.org/10.1111/j.1469-8137.2010.03340.x

Franklin, O. (2007). Optimal nitrogen allocation controls tree responses to elevated CO_2. *New Phytologist*, *174*(4), 811–822. https://doi.org/10.1111/j.1469-8137.2007.02063.x

Franklin, O., Johansson, J., Dewar, R. C., Dieckmann, U., McMurtrie, R. E., Brannstrom, A., & Dybzinski, R. (2012). Modeling carbon allocation in trees: A search for principles. *Tree Physiology*, *32*(6), 648–666. https://doi.org/10.1093/treephys/tpr138

Friend, A. D., Stevens, A. K., Knox, R. G., & Cannell, M. G. R. (1997). A process-based, terrestrial biosphere model of ecosystem dynamics (Hybrid v3.0). *Ecological Modelling*, *95*(2–3), 249–287. https://doi.org/10.1016/S0304-3800(96)00034-8

Furze, M. E., Huggett, B. A., Aubrecht, D. M., Stolz, C. D., Carbone, M. S., & Richardson, A. D. (2019). Whole-tree nonstructural carbohydrate storage and seasonal dynamics in five temperate species. *New Phytologist*, *221*(3), 1466–1477. https://doi.org/10.1111/nph.15462

Galiano, L., Martínez-Vilalta, J., & Lloret, F. (2011). Carbon reserves and canopy defoliation determine the recovery of Scots pine 4 yr after a drought episode. *New Phytologist*, *190*(3), 750–759. https://doi.org/10.1111/j.1469-8137.2010.03628.x

Galiano, L., Timofeeva, G., Saurer, M., Siegwolf, R., Martínez-Vilalta, J., Hommel, R., & Gessler, A. (2017). The fate of recently fixed carbon after drought release: Towards unravelling C storage regulation in *Tilia platyphyllos* and *Pinus sylvestris*: The fate of recently fixed C after drought release. *Plant, Cell & Environment*, *40*(9), 1711–1724. https://doi.org/10.1111/pce.12972

Gallagher, R. V., Allen, S., & Wright, I. J. (2019). Safety margins and adaptive capacity of vegetation to climate change. *Scientific Reports*, *9*(1), 8241. https://doi.org/10.1038/s41598-019-44483-x

Gampe, D., Zscheischler, J., Reichstein, M., O'Sullivan, M., Smith, W. K., Sitch, S., & Buermann, W. (2021). Increasing impact of warm droughts on northern ecosystem productivity over recent decades. *Nature Climate Change*, 1–8. https://doi.org/10.1038/s41558-021-01112-8

García, C. E., Prett, D. M., & Morari, M. (1989). Model predictive control: Theory and practice—A survey. *Automatica*, *25*(3), 335–348. https://doi.org/10.1016/0005-1098(89)90002-2

Gaudinski, J. B., Torn, M. S., Riley, W. J., Swanston, C., Trumbore, S. E., Joslin, J. D., Majdi, H., Dawson, T. E., & Hanson, P. J. (2009). Use of stored carbon reserves in growth of temperate tree roots and leaf buds: Analyses using radiocarbon measurements and modeling. *Global Change Biology*, *15*(4), 992–1014. https://doi.org/10.1111/j.1365-2486.2008.01736.x

Gauzere, J., Lucas, C., Ronce, O., Davi, H., & Chuine, I. (2019). Sensitivity analysis of tree phenology models reveals increasing sensitivity of their predictions to winter chilling temperature and photoperiod with warming climate. *Ecological Modelling*, *411*, 108805. https://doi.org/10.1016/j.ecolmodel.2019.108805

Ghil, M., Yiou, P., Hallegatte, S., Malamud, B. D., Naveau, P., Soloviev, A., Friederichs, P., Keilis-Borok, V., Kondrashov, D., Kossobokov, V., Mestre, O., Nicolis, C., Rust, H. W., Shebalin, P., Vrac, M., Witt, A., & Zaliapin, I. (2011). Extreme events: Dynamics,

statistics and prediction. *Nonlinear Processes in Geophysics*, *18*(3), 295–350. https://doi.org/10.5194/npg-18-295-2011

Gholz, H. L., & Cropper Jr., W. P. (1991). Carbohydrate dynamics in mature Pinuselliottii var. Elliottii trees. *Canadian Journal of Forest Research*, *21*(12), 1742–1747. https://doi.org/10.1139/x91-240

Gough, C. M., Flower, C. E., Vogel, C. S., Dragoni, D., & Curtis, P. S. (2009). Whole-ecosystem labile carbon production in a north temperate deciduous forest. *Agricultural and Forest Meteorology*, *149*(9), 1531–1540. https://doi.org/10.1016/j.agrformet.2009.04.006

Graham, D., & Patterson, B. D. (1982). Responses of Plants to Low, Nonfreezing Temperatures: Proteins, Metabolism and Acclimation. *Annual Review of Plant Physiology*, *33*, 347–372.

Grossman, Y. L., & DeJong, T. M. (1994). PEACH: A simulation model of reproductive and vegetative growth in peach trees. *Tree Physiology*, *14*(4), 329–345. https://doi.org/10.1093/treephys/14.4.329

Guillemot, J., Francois, C., Hmimina, G., Dufrêne, E., Martin-StPaul, N. K., Soudani, K., Marie, G., Ourcival, J., & Delpierre, N. (2017). Environmental control of carbon allocation matters for modelling forest growth. *New Phytologist*, *214*(1), 180–193. https://doi.org/10.1111/nph.14320

Guo, Q., Li, J., Zhang, Y., Zhang, J., Lu, D., Korpelainen, H., & Li, C. (2016). Species-specific competition and N fertilization regulate non-structural carbohydrate contents in two

Larix species. *Forest Ecology and Management*, *364*, 60–69. https://doi.org/10.1016/j.foreco.2016.01.007

Han, H., He, H., Wu, Z., Cong, Y., Zong, S., He, J., Fu, Y., Liu, K., Sun, H., Li, Y., Yu, C., & Xu, J. (2020). Non-Structural Carbohydrate Storage Strategy Explains the Spatial Distribution of Treeline Species. *Plants*, *9*(3), 384. https://doi.org/10.3390/plants9030384

Hao, B., Hartmann, H., Li, Y., Liu, H., Shi, F., Yu, K., Li, X., Li, Z., Wang, P., Allen, C. D., & Wu, X. (2021). Precipitation Gradient Drives Divergent Relationship between Non-Structural Carbohydrates and Water Availability in Pinus tabulaeformis of Northern China. *Forests*, *12*(2), 133. https://doi.org/10.3390/f12020133

Harrison, R. D. (2001). Drought and the consequences of El Niño in Borneo: A case study of figs. *Population Ecology*, *43*(1), 63–75. https://doi.org/10.1007/PL00012017

Hartmann, H., Adams, H. D., Hammond, W. M., Hoch, G., Landhäusser, S. M., Wiley, E., & Zaehle, S. (2018). Identifying differences in carbohydrate dynamics of seedlings and mature trees to improve carbon allocation in models for trees and forests. *Environmental and Experimental Botany*, *152*, 7–18. https://doi.org/10.1016/j.envexpbot.2018.03.011

Hartmann, H., Bahn, M., Carbone, M., & Richardson, A. D. (2020). Plant carbon allocation in a changing world – challenges and progress: Introduction to a Virtual Issue on carbon allocation: Introduction to a virtual issue on carbon allocation. *New Phytologist*, *227*(4), 981–988. https://doi.org/10.1111/nph.16757

Hartmann, H., McDowell, N. G., & Trumbore, S. (2015). Allocation to carbon storage pools in Norway spruce saplings under drought and low CO2. *Tree Physiology*, *35*(3), 243–252. eih. https://doi.org/10.1093/treephys/tpv019

Hartmann, H., Moura, C. F., Anderegg, W. R. L., Ruehr, N. K., Salmon, Y., Allen, C. D., Arndt, S. K., Breshears, D. D., Davi, H., Galbraith, D., Ruthrof, K. X., Wunder, J., Adams, H. D., Bloemen, J., Cailleret, M., Cobb, R., Gessler, A., Grams, T. E. E., Jansen, S., … O'Brien, M. (2018). Research frontiers for improving our understanding of drought-induced tree and forest mortality. *New Phytologist*, *218*(1), 15–28. https://doi.org/10.1111/nph.15048

Hartmann, H., & Trumbore, S. (2016). Understanding the roles of nonstructural carbohydrates in forest trees – from what we can measure to what we want to know. *New Phytologist*, *211*(2), 386–403. https://doi.org/10.1111/nph.13955

Hinman, E. D., & Fridley, J. D. (2018). To spend or to save? Assessing energetic growth-storage tradeoffs in native and invasive woody plants. *Oecologia*, *188*(3), 659–669. https://doi.org/10.1007/s00442-018-4177-4

Hoch, G. (2007). Cell wall hemicelluloses as mobile carbon stores in non-reproductive plant tissues. *Functional Ecology*, *21*(5), 823–834. https://doi.org/10.1111/j.1365-2435.2007.01305.x

Hoch, G. (2015). Carbon Reserves as Indicators for Carbon Limitation in Trees. In U. Luttge & W. Beyschlag (Eds.), *Progress in Botany 76* (Vol. 76, Issue 4833, p. 1023). Springer US. https://doi.org/10.1038/1941023a0

Hoch, G., Popp, M., & Körner, C. (2002). Altitudinal increase of mobile carbon pools in *Pinus cembra* suggests sink limitation of growth at the Swiss treeline. *Oikos*, *98*(3), 361–374. https://doi.org/10.1034/j.1600-0706.2002.980301.x

Hoch, G., Richter, A., & Körner, Ch. (2003). Non-structural carbon compounds in temperate forest trees: Non-structural carbon compounds in temperate forest trees. *Plant, Cell & Environment*, *26*(7), 1067–1081. https://doi.org/10.1046/j.0016-8025.2003.01032.x

Huang, J., Hammerbacher, A., Weinhold, A., Reichelt, M., Gleixner, G., Behrendt, T., van Dam, N. M., Sala, A., Gershenzon, J., Trumbore, S., & Hartmann, H. (2019). Eyes on the future—Evidence for trade-offs between growth, storage and defense in Norway spruce. *New Phytologist*, *222*(1), 144–158. https://doi.org/10.1111/nph.15522

Huang, J., Kautz, M., Trowbridge, A. M., Hammerbacher, A., Raffa, K. F., Adams, H. D., Goodsman, D. W., Xu, C., Meddens, A. J. H., Kandasamy, D., Gershenzon, J., Seidl, R., & Hartmann, H. (2020). Tree defence and bark beetles in a drying world: Carbon partitioning, functioning and modelling. *New Phytologist*, *225*(1), 26–36. https://doi.org/10.1111/nph.16173

Huang, M., Wang, X., Keenan, T. F., & Piao, S. (2018). Drought timing influences the legacy of tree growth recovery. *Global Change Biology*, *24*(8), 3546–3559. https://doi.org/10.1111/gcb.14294

Huntzinger, D. N., Michalak, A. M., Schwalm, C., Ciais, P., King, A. W., Fang, Y., Schaefer, K., Wei, Y., Cook, R. B., Fisher, J. B., Hayes, D., Huang, M., Ito, A., Jain, A. K., Lei, H., Lu, C., Maignan, F., Mao, J., Parazoo, N., … Zhao, F. (2017). Uncertainty in the response

of terrestrial carbon sink to environmental drivers undermines carbon-climate feedback predictions. *Scientific Reports*, *7*(1), 4765. https://doi.org/10.1038/s41598-017-03818-2

Ichie, T., Igarashi, S., Yoshida, S., Kenzo, T., Masaki, T., & Tayasu, I. (2013). Are stored carbohydrates necessary for seed production in temperate deciduous trees? *Journal of Ecology*, *101*(2), 525–531. https://doi.org/10.1111/1365-2745.12038

IPCC. (2021). *Climate Change 2021: The Physical Science Basis. Contribution of Working Group I to the Sixth Assessment Report of the Intergovernmental Panel on Climate Change* (V. Masson-Delmotte, P. Zhai, A. Pirani, C. Péan, S. Berger, N. Caud, Y. Chen, L. Goldfarb, M. I. Gomis, M. Huang, K. Leitzell, E. Lonnoy, J. B. R. Matthews, T. K. Maycock, T. Waterfield, O. Yelekçi, R. Yu, & B. Zhou, Eds.). Cambridge University Press.

Iwasa, Y. (1991). Pessimistic plant: Optimal growth schedule in stochastic environments. *Theoretical Population Biology*, *40*(2), 246–268. https://doi.org/10.1016/0040-5809(91)90055-K

Iwasa, Y. (2000). Dynamic optimization of plant growth. *Evolutionary Ecology Research*, *2*(4), 437–455.

Iwasa, Y., & Cohen, D. (1989). Optimal Growth Schedule of a Perennial Plant. *The American Naturalist*, *133*(4), 480–505. http://www.jstor.org/stable/2462084

Iwasa, Y., & Kubo, T. (1997). Optimal size of storage for recovery after unpredictable disturbances. *Evolutionary Ecology*, *11*(1), 41–65. https://doi.org/10.1023/A:1018483429029

Iwasa, Y., & Levin, S. A. (1995). The Timing of Life History Events. *Journal of Theoretical Biology*, *172*(1), 10.

Iwasa, Y., & Roughgarden, J. (1984). Shoot/root balance of plants: Optimal growth of a system with many vegetative organs. *Theoretical Population Biology*, *25*(1), 78–105. https://doi.org/10.1016/0040-5809(84)90007-8

Janni, M., Gullì, M., Maestri, E., Marmiroli, M., Valliyodan, B., Nguyen, H. T., & Marmiroli, N. (2020). Molecular and genetic bases of heat stress responses in crop plants and breeding for increased resilience and productivity. *Journal of Experimental Botany*, *71*(13), 3780–3802. https://doi.org/10.1093/jxb/eraa034

Jeffreys, M. P. (1999). *Dynamics of Stemwood Nitrogen in Pinus radiata with Modelled Implications for Forest Productivity Under Elevated Atmospheric Carbon Dioxide*.

Ji, L., Attaullah, K., Wang, J., Yu, D., Yang, Y., Yang, L., & Lu, Z. (2020). Root Traits Determine Variation in Nonstructural Carbohydrates (NSCs) under Different Drought Intensities and Soil Substrates in Three Temperate Tree Species. *Forests*, *11*(4), 415. https://doi.org/10.3390/f11040415

Johansson, J., Brännström, Å., Metz, J. A. J., & Dieckmann, U. (2018). Twelve fundamental life histories evolving through allocation-dependent fecundity and survival. *Ecology and Evolution*, *8*(6), 3172–3186. https://doi.org/10.1002/ece3.3730

Johnson, I. R. (1990). Plant respiration in relation to growth, maintenance, ion uptake and nitrogen assimilation. *Plant, Cell and Environment*, *13*(4), 319–328. https://doi.org/10.1111/j.1365-3040.1990.tb02135.x

Jones, S., Rowland, L., Cox, P., Hemming, D., Wiltshire, A., Williams, K., Parazoo, N. C., Liu, J., da Costa, A. C. L., Meir, P., Mencuccini, M., & Harper, A. B. (2020). The impact of a simple representation of non-structural carbohydrates on the simulated response of tropical forests to drought. *Biogeosciences*, *17*(13), 3589–3612. https://doi.org/10.5194/bg-17-3589-2020

Kagawa, A., Naito, D., Sugimoto, A., & Maximov, T. C. (2003). Effects of spatial and temporal variability in soil moisture on widths and δ13C values of eastern Siberian tree rings. *Journal of Geophysical Research: Atmospheres*, *108*(D16). https://doi.org/10.1029/2002JD003019

Kannenberg, S. A., Schwalm, C. R., & Anderegg, W. R. L. (2020). Ghosts of the past: How drought legacy effects shape forest functioning and carbon cycling. *Ecology Letters*, *23*(5), 891–901. https://doi.org/10.1111/ele.13485

Katz, R. W., & Brown, B. G. (1992). Extreme events in a changing climate: Variability is more important than averages. *Climatic Change*, *21*(3), 289–302. https://doi.org/10.1007/BF00139728

Kayler, Z. E., De Boeck, H. J., Fatichi, S., Grünzweig, J. M., Merbold, L., Beier, C., McDowell, N., & Dukes, J. S. (2015). Experiments to confront the environmental extremes of climate change. *Frontiers in Ecology and the Environment*, *13*(4), 219–225. https://doi.org/10.1890/140174

Keane, R. E., Austin, M., Field, C., Huth, A., Lexer, M. J., Peters, D., Solomon, A., & Wyckoff, P. (2001). Tree mortality in gap models: Application to climate change. *Climatic Change*, *51*(3–4), 509–540. Scopus. https://doi.org/10.1023/A:1012539409854

Keel, S. G., Siegwolf, R. T. W., & Körner, C. (2006). Canopy CO $_2$ enrichment permits tracing the fate of recently assimilated carbon in a mature deciduous forest. *New Phytologist*, *172*(2), 319–329. https://doi.org/10.1111/j.1469-8137.2006.01831.x

Kitajima, K. (1994). Relative importance of photosynthetic traits and allocation patterns as correlates of seedling shade tolerance of 13 tropical trees. *Oecologia*, *98*(3–4), 419–428. https://doi.org/10.1007/BF00324232

Kitajima, K. (2002). Do shade-tolerant tropical tree seedlings depend longer on seed reserves? Functional growth analysis of three Bignoniaceae species: *Seed-reserve dependency*. *Functional Ecology*, *16*(4), 433–444. https://doi.org/10.1046/j.1365-2435.2002.00641.x

Kobe, R. K. (1997). Carbohydrate Allocation to Storage as a Basis of Interspecific Variation in Sapling Survivorship and Growth. *Oikos*, *80*(2), 226. https://doi.org/10.2307/3546590

Körner, C. (2003). Carbon limitation in trees. *Journal of Ecology*, *91*(1), 4–17. https://doi.org/10.1046/j.1365-2745.2003.00742.x

Körner, C. (2015). Paradigm shift in plant growth control. *Current Opinion in Plant Biology*, *25*, 107–114. https://doi.org/10.1016/j.pbi.2015.05.003

Koshkin, S., Zalles, Z., Tobin, M. F., Toumbacaris, N., & Spiess, C. (2021). Optimal allocation in annual plants with density-dependent fitness. *Theory in Biosciences*, *140*(2), 177–196. https://doi.org/10.1007/s12064-021-00343-9

Kozłowski, J., & Uchmanski, J. (1987). Optimal individual growth and reproduction in perennial species with indeterminate growth. *Evolutionary Ecology*, *1*(3), 214–230. https://doi.org/10.1007/BF02067552

Kozłowski, J., & Wiegert, R. G. (1987). Optimal age and size at maturity in annuals and perennials with determinate growth. *Evolutionary Ecology*, *1*(3), 231–244. https://doi.org/10.1007/BF02067553

Kozlowski, T. T. (1992). Carbohydrate Sources and Sinks in Woody Plants. *Botanical Review*, *58*(2,), 107–222. http://www.jstor.org/stable/4354186

Kreuzwieser, J., & Rennenberg, H. (2014). Molecular and physiological responses of trees to waterlogging stress: Responses of tree to waterlogging. *Plant, Cell & Environment*, n/a-n/a. https://doi.org/10.1111/pce.12310

Kruse, J., Turnbull, T., Rennenberg, H., & Adams, M. A. (2020). Plasticity of Leaf Respiratory and Photosynthetic Traits in Eucalyptus grandis and E. regnans Grown Under Variable Light and Nitrogen Availability. *Frontiers in Forests and Global Change*, *3*, 5. https://doi.org/10.3389/ffgc.2020.00005

Lanuza, O. R., Espelta, J. M., Peñuelas, J., & Peguero, G. (2020). Assessing intraspecific trait variability during seedling establishment to improve restoration of tropical dry forests. *Ecosphere*, *11*(2). https://doi.org/10.1002/ecs2.3052

Laurance, W. F., & Williamson, G. B. (2001). Positive Feedbacks among Forest Fragmentation, Drought, and Climate Change in the Amazon. *Conservation Biology*, *15*(6), 1529–1535. https://doi.org/10.1046/j.1523-1739.2001.01093.x

Lazebnik, Y. (2002). Can a biologist fix a radio?—Or, what I learned while studying apoptosis. *Cancer Cell*, *2*(3), 179–182. https://doi.org/10.1016/S1535-6108(02)00133-2

Le Quéré, C., Raupach, M. R., Canadell, J. G., Marland, G., Bopp, L., Ciais, P., Conway, T. J., Doney, S. C., Feely, R. A., Foster, P., Friedlingstein, P., Gurney, K., Houghton, R. A., House, J. I., Huntingford, C., Levy, P. E., Lomas, M. R., Majkut, J., Metzl, N., … Woodward, F. I. (2009). Trends in the sources and sinks of carbon dioxide. *Nature Geoscience*, *2*(12), 831–836. https://doi.org/10.1038/ngeo689

Le Roux, X., Lacointe, A., Escobar-Gutiérrez, A., & Le Dizès, S. (2001). Carbon-based models of individual tree growth: A critical appraisal. *Annals of Forest Science*, *58*(5), 469–506. https://doi.org/10.1051/forest:2001140

Lecina-Diaz, J., Martínez-Vilalta, J., Alvarez, A., Banqué, M., Birkmann, J., Feldmeyer, D., Vayreda, J., & Retana, J. (2021). Characterizing forest vulnerability and risk to climate-change hazards. *Frontiers in Ecology and the Environment*, *19*(2), 126–133. https://doi.org/10.1002/fee.2278

LeCroy, C. W., & Krysik, J. (2007). Understanding and interpreting effect size measures. *Social Work Research*, *31*(4), 243–248. https://doi.org/10.1093/swr/31.4.243

Ledder, G., Russo, S. E., Muller, E. B., Peace, A., & Nisbet, R. M. (2020). Local control of resource allocation is sufficient to model optimal dynamics in syntrophic systems. *Theoretical Ecology*, *13*(4), 481–501. https://doi.org/10.1007/s12080-020-00464-9

Lemoine, N. P. (2021). Unifying ecosystem responses to disturbance into a single statistical framework. *Oikos*, *130*(3), 408–421. https://doi.org/10.1111/oik.07752

Lenhart, S., & Workman, J. T. (2007). *Optimal control applied to biological models*. Chapman and Hall/CRC.

Lerdau, M. (1992). Future Discounts and Resource Allocation in Plants. *Functional Ecology*, *6*(4), 371. https://doi.org/10.2307/2389273

Leuzinger, S., Manusch, C., Bugmann, H., & Wolf, A. (2013). A sink-limited growth model improves biomass estimation along boreal and alpine tree lines: Sink limitation in vegetation modelling. *Global Ecology and Biogeography*, *22*(8), 924–932. https://doi.org/10.1111/geb.12047

Lexer, M. J., & Hönninger, K. (2001). A modified 3D-patch model for spatially explicit simulation of vegetation composition in heterogeneous landscapes. *Forest Ecology and Management*, *144*(1–3), 43–65.

Li, M.-H., Jiang, Y., Wang, A., Li, X., Zhu, W., Yan, C.-F., Du, Z., Shi, Z., Lei, J., Schönbeck, L., He, P., Yu, F.-H., & Wang, X. (2018). Active summer carbon storage for winter persistence in trees at the cold alpine treeline. *Tree Physiology*, *38*(9), 1345–1355. https://doi.org/10.1093/treephys/tpy020

Liao, C.-Y., & Bassham, D. C. (2020). Combating stress: The interplay between hormone signaling and autophagy in plants. *Journal of Experimental Botany*, *71*(5), 1723–1733. https://doi.org/10.1093/jxb/erz515

Linder, S., & Troeng, E. (1980). Photosynthesis and Transpiration of 20-Year-Old Scots Pine. *Ecological Bulletins*, *32*, 165–181.

Litton, C. M., Raich, J. W., & Ryan, M. G. (2007). Carbon allocation in forest ecosystems. *Global Change Biology*, *13*(10), 2089–2109. https://doi.org/10.1111/j.1365-2486.2007.01420.x

Liu, Q., Peng, C., Schneider, R., Cyr, D., Liu, Z., Zhou, X., & Kneeshaw, D. (2021). TRIPLEX-Mortality model for simulating drought-induced tree mortality in boreal forests: Model development and evaluation. *Ecological Modelling*, *455*, 109652. https://doi.org/10.1016/j.ecolmodel.2021.109652

Lyon, P. (2015). The cognitive cell: Bacterial behavior reconsidered. *Frontiers in Microbiology*, *6*, 264. https://doi.org/10.3389/fmicb.2015.00264

Ma, Z., Peng, C., Zhu, Q., Chen, H., Yu, G., Li, W., Zhou, X., Wang, W., & Zhang, W. (2012). Regional drought-induced reduction in the biomass carbon sink of Canada's boreal forests. *Proceedings of the National Academy of Sciences*, *109*(7), 2423–2427. https://doi.org/10.1073/pnas.1111576109

MacAllister, S., Mencuccini, M., Sommer, U., Engel, J., Hudson, A., Salmon, Y., & Dexter, K. G. (2019). Drought-induced mortality in Scots pine: Opening the metabolic black box. *Tree Physiology*, *39*(8), 1358–1370. https://doi.org/10.1093/treephys/tpz049

Mackay, D. S., Roberts, D. E., Ewers, B. E., Sperry, J. S., McDowell, N. G., & Pockman, W. T. (2015). Interdependence of chronic hydraulic dysfunction and canopy processes can improve integrated models of tree response to drought: MODELING CHRONIC HYDRAULIC DYSFUNCTION AND CANOPY PROCESSES. *Water Resources Research*, *51*(8), 6156–6176. https://doi.org/10.1002/2015WR017244

Maguire, A. J., & Kobe, R. K. (2015). Drought and shade deplete nonstructural carbohydrate reserves in seedlings of five temperate tree species. *Ecology and Evolution*, *5*(23), 5711–5721. https://doi.org/10.1002/ece3.1819

Mahmud, K., Medlyn, B. E., Duursma, R. A., Campany, C., & De Kauwe, M. G. (2018). Inferring the effects of sink strength on plant carbon balance processes from experimental measurements. *Biogeosciences*, *15*(13), 4003–4018. https://doi.org/10.5194/bg-15-4003-2018

Mäkelä, A., Berninger, F., & Hari, P. (1996). Optimal Control of Gas Exchange during Drought: Theoretical Analysis. *Annals of Botany*, *77*(5), 461–468. https://doi.org/10.1006/anbo.1996.0056

Mäkelä, A., & Sievänen, R. (1992). Height growth strategies in open-grown trees. *Journal of Theoretical Biology*, *159*(4), 443–467. https://doi.org/10.1016/S0022-5193(05)80690-3

Mäkelä, A., Valentine, H. T., & Helmisaari, H. (2008). Optimal co-allocation of carbon and nitrogen in a forest stand at steady state. *New Phytologist*, *180*(1), 114–123. https://doi.org/10.1111/j.1469-8137.2008.02558.x

Manzoni, S., Vico, G., Katul, G., Fay, P. A., Polley, W., Palmroth, S., & Porporato, A. (2011). Optimizing stomatal conductance for maximum carbon gain under water stress: A meta-analysis across plant functional types and climates: Optimal leaf gas exchange under water stress. *Functional Ecology*, *25*(3), 456–467. https://doi.org/10.1111/j.1365-2435.2010.01822.x

Markham, C. G. (1970). SEASONALITY OF PRECIPITATION IN THE UNITED STATES. *Annals of the Association of American Geographers*, *60*(3), 593–597. https://doi.org/10.1111/j.1467-8306.1970.tb00743.x

Marler, T. E., & Cascasan, A. N. J. (2018). Carbohydrate Depletion during Lethal Infestation of *Aulacaspis yasumatsui* on *Cycas revoluta*. *International Journal of Plant Sciences*, *179*(6), 497–504. https://doi.org/10.1086/697929

Martínez-Vilalta, J., Sala, A., Asensio, D., Galiano, L., Hoch, G., Palacio, S., Piper, F. I., & Lloret, F. (2016). Dynamics of non-structural carbohydrates in terrestrial plants: A global synthesis. *Ecological Monographs*, *86*(4), 495–516. https://doi.org/10.1002/ecm.1231

MathWorks. (n.d.). *MATLAB fmincon*. Retrieved March 23, 2022, from https://uk.mathworks.com/help/optim/ug/fmincon.html#References

McDowell, N. G. (2011). Mechanisms Linking Drought, Hydraulics, Carbon Metabolism, and Vegetation Mortality. *Plant Physiology*, *155*(3), 1051–1059. https://doi.org/10.1104/pp.110.170704

McDowell, N. G., Fisher, R. A., Xu, C., Domec, J. C., Hölttä, T., Mackay, D. S., Sperry, J. S., Boutz, A., Dickman, L., Gehres, N., Limousin, J. M., Macalady, A., Martínez-Vilalta, J., Mencuccini, M., Plaut, J. A., Ogée, J., Pangle, R. E., Rasse, D. P., Ryan, M. G., … Pockman, W. T. (2013). Evaluating theories of drought-induced vegetation mortality using a multimodel–experiment framework. *New Phytologist*, *200*(2), 304–321. https://doi.org/10.1111/nph.12465

McDowell, N., Pockman, W. T., Allen, C. D., Breshears, D. D., Cobb, N., Kolb, T., Plaut, J., Sperry, J., West, A., Williams, D. G., & Yepez, E. A. (2008). Mechanisms of plant survival and mortality during drought: Why do some plants survive while others succumb to drought? *New Phytologist*, *178*(4), 719–739. https://doi.org/10.1111/j.1469-8137.2008.02436.x

McGill, B. J., & Brown, J. S. (2007). Evolutionary Game Theory and Adaptive Dynamics of Continuous Traits. *Annual Review of Ecology, Evolution, and Systematics*, *38*(1), 403–435. https://doi.org/10.1146/annurev.ecolsys.36.091704.175517

McLaughlin, J., & Webster, K. (2014). Effects of climate change on peatlands in the far north of Ontario, Canada: A synthesis. *Arctic, Antarctic, and Alpine Research*, *46*(1), 84–102. eih. https://doi.org/10.1657/1938-4246-46.1.84

McMahon, S. M., Arellano, G., & Davies, S. J. (2019). The importance and challenges of detecting changes in forest mortality rates. *Ecosphere*, *10*(2). https://doi.org/10.1002/ecs2.2615

McMorris, D. (2020). *Optimal Allocation of Two Resources in Annual Plants*.

McMurtrie, R. E., Norby, R. J., Medlyn, B. E., Dewar, R. C., Pepper, D. A., Reich, P. B., & Barton, C. V. M. (2008). Why is plant-growth response to elevated CO2 amplified when water is limiting, but reduced when nitrogen is limiting? A growth-optimisation hypothesis. *Functional Plant Biology*, *35*(6), 521. https://doi.org/10.1071/FP08128

McNickle, G. G., Gonzalez-Meler, M. A., Lynch, D. J., Baltzer, J. L., & Brown, J. S. (2016). The world's biomes and primary production as a triple tragedy of the commons foraging

game played among plants. *Proceedings of the Royal Society B: Biological Sciences*, *283*(1842), 20161993. https://doi.org/10.1098/rspb.2016.1993

Medlyn, B. E., Berbigier, P., Clement, R., Grelle, A., Loustau, D., Linder, S., Wingate, L., Jarvis, P. G., Sigurdsson, B. D., & McMurtrie, R. E. (2005). Carbon balance of coniferous forests growing in contrasting climates: Model-based analysis. *Agricultural and Forest Meteorology*, *131*(1–2), 97–124. https://doi.org/10.1016/j.agrformet.2005.05.004

Medlyn, B. E., Duursma, R. A., Eamus, D., Ellsworth, D. S., Prentice, I. C., Barton, C. V. M., Crous, K. Y., De Angelis, P., Freeman, M., & Wingate, L. (2011). Reconciling the optimal and empirical approaches to modelling stomatal conductance. *Global Change Biology*, *17*(6), 2134–2144. https://doi.org/10.1111/j.1365-2486.2010.02375.x

Medlyn, B. E., Duursma, R. A., & Zeppel, M. J. B. (2011). Forest productivity under climate change: A checklist for evaluating model studies. *WIREs Climate Change*, *2*(3), 332–355. https://doi.org/10.1002/wcc.108

Medvigy, D., Wofsy, S. C., Munger, J. W., Hollinger, D. Y., & Moorcroft, P. R. (2009). Mechanistic scaling of ecosystem function and dynamics in space and time: Ecosystem Demography model version 2. *Journal of Geophysical Research*, *114*(G1), G01002. https://doi.org/10.1029/2008JG000812

Meir, P., Mencuccini, M., & Dewar, R. C. (2015). Drought-related tree mortality: Addressing the gaps in understanding and prediction. *New Phytologist*, *207*(1), 28–33. https://doi.org/10.1111/nph.13382

Mencuccini, M. (2014). Temporal scales for the coordination of tree carbon and water economies during droughts. *Tree Physiology*, *34*(5), 439–442. https://doi.org/10.1093/treephys/tpu029

Merganičová, K., Merganič, J., Lehtonen, A., Vacchiano, G., Sever, M. Z. O., Augustynczik, A. L. D., Grote, R., Kyselová, I., Mäkelä, A., Yousefpour, R., Krejza, J., Collalti, A., & Reyer, C. P. O. (2019). Forest carbon allocation modelling under climate change. *Tree Physiology*, *39*(12), 1937–1960. https://doi.org/10.1093/treephys/tpz105

Minchin, P. E. H. (2007). Mechanistic modelling of carbon partitioning. *Frontis*, 113–122. https://library.wur.nl/ojs/index.php/frontis/article/view/1376

Mitchell, A., & Pilpel, Y. (2011). A mathematical model for adaptive prediction of environmental changes by microorganisms. *Proceedings of the National Academy of Sciences*, *108*(17), 7271–7276. https://doi.org/10.1073/pnas.1019754108

Mitchell, P. J., O'Grady, A. P., Hayes, K. R., & Pinkard, E. A. (2014). Exposure of trees to drought-induced die-off is defined by a common climatic threshold across different vegetation types. *Ecology and Evolution*, *4*(7), 1088–1101. https://doi.org/10.1002/ece3.1008

Mitchell, P. J., O'Grady, A. P., Tissue, D. T., White, D. A., Ottenschlaeger, M. L., & Pinkard, E. A. (2013). Drought response strategies define the relative contributions of hydraulic dysfunction and carbohydrate depletion during tree mortality. *New Phytologist*, *197*(3), 862–872. https://doi.org/10.1111/nph.12064

Mitchell, P. J., O'Grady, A. P., Tissue, D. T., Worledge, D., & Pinkard, E. A. (2014). Co-ordination of growth, gas exchange and hydraulics define the carbon safety margin

in tree species with contrasting drought strategies. *Tree Physiology*, *34*(5), 443–458. https://doi.org/10.1093/treephys/tpu014

Moeller, H. V., & Neubert, M. G. (2016). Multiple Friends with Benefits: An Optimal Mutualist Management Strategy? *The American Naturalist*, *187*(1), E1–E12. https://doi.org/10.1086/684103

Mori, S., Yamaji, K., Ishida, A., Prokushkin, S. G., Masyagina, O. V., Hagihara, A., Hoque, A. T. M. R., Suwa, R., Osawa, A., Nishizono, T., Ueda, T., Kinjo, M., Miyagi, T., Kajimoto, T., Koike, T., Matsuura, Y., Toma, T., Zyryanova, O. A., Abaimov, A. P., … Umari, M. (2010). Mixed-power scaling of whole-plant respiration from seedlings to giant trees. *Proceedings of the National Academy of Sciences*, *107*(4), 1447–1451. https://doi.org/10.1073/pnas.0902554107

Morin, X., Bugmann, H., de Coligny, F., Martin-StPaul, N., Cailleret, M., Limousin, J.-M., Ourcival, J.-M., Prevosto, B., Simioni, G., Toigo, M., Vennetier, M., Catteau, E., & Guillemot, J. (2021). Beyond forest succession: A gap model to study ecosystem functioning and tree community composition under climate change. *Functional Ecology*, *35*(4), 955–975. https://doi.org/10.1111/1365-2435.13760

Mrad, A., Sevanto, S., Domec, J.-C., Liu, Y., Nakad, M., & Katul, G. (2019). A Dynamic Optimality Principle for Water Use Strategies Explains Isohydric to Anisohydric Plant Responses to Drought. *Frontiers in Forests and Global Change*, *2*, 49. https://doi.org/10.3389/ffgc.2019.00049

Mueller, R. C., Scudder, C. M., Porter, M. E., Talbot Trotter, R., Gehring, C. A., & Whitham, T. G. (2005). Differential tree mortality in response to severe drought: Evidence for

long-term vegetation shifts: Drought-induced differential tree mortality. *Journal of Ecology*, *93*(6), 1085–1093. https://doi.org/10.1111/j.1365-2745.2005.01042.x

Muller, B., Pantin, F., Génard, M., Turc, O., Freixes, S., Piques, M., & Gibon, Y. (2011). Water deficits uncouple growth from photosynthesis, increase C content, and modify the relationships between C and growth in sink organs. *Journal of Experimental Botany*, *62*(6), 1715–1729. https://doi.org/10.1093/jxb/erq438

Muller-Landau, H. C. (2010). The tolerance-fecundity trade-off and the maintenance of diversity in seed size. *Proceedings of the National Academy of Sciences*, *107*(9), 4242–4247. https://doi.org/10.1073/pnas.0911637107

Mund, M., Herbst, M., Knohl, A., Matthäus, B., Schumacher, J., Schall, P., Siebicke, L., Tamrakar, R., & Ammer, C. (2020). It is not just a 'trade-off': Indications for sink- and source-limitation to vegetative and regenerative growth in an old-growth beech forest. *New Phytologist*, *226*(1), 111–125. https://doi.org/10.1111/nph.16408

Munné-Bosch, S., & Alegre, L. (2004). Die and let live: Leaf senescence contributes to plant survival under drought stress. *Functional Plant Biology*, *31*(3), 203. https://doi.org/10.1071/FP03236

Myers, J. A., & Kitajima, K. (2007). Carbohydrate storage enhances seedling shade and stress tolerance in a neotropical forest. *Journal of Ecology*, *95*(2), 383–395. https://doi.org/10.1111/j.1365-2745.2006.01207.x

Nadeau, C. P., & Urban, M. C. (2019). Eco-evolution on the edge during climate change. *Ecography*, ecog.04404. https://doi.org/10.1111/ecog.04404

Niinemets, Ü. (2010). Responses of forest trees to single and multiple environmental stresses from seedlings to mature plants: Past stress history, stress interactions, tolerance and acclimation. *Forest Ecology and Management*, *260*(10), 1623–1639. https://doi.org/10.1016/j.foreco.2010.07.054

Norby, R. J., Ogle, K., Curtis, P. S., Badeck, F.-W., Huth, A., Hurtt, G. C., Kohyama, T., & Peñuelas, J. (2001). Aboveground growth and competition in forest gap models: An analysis for studies of climatic change. *Climatic Change*, *51*(3–4), 33. Scopus. https://doi.org/10.1023/A:1012510619424

Nordhaus, W. D. (1993). Rolling the 'DICE': An optimal transition path for controlling greenhouse gases. *Resource and Energy Economics*, *15*(1), 27–50. https://doi.org/10.1016/0928-7655(93)90017-O

Obeso, J. R. (2002). The costs of reproduction in plants. *New Phytologist*, *155*(3), 321–348. https://doi.org/10.1046/j.1469-8137.2002.00477.x

O'Brien, M. J., Burslem, D. F. R. P., Caduff, A., Tay, J., & Hector, A. (2015). Contrasting nonstructural carbohydrate dynamics of tropical tree seedlings under water deficit and variability. *New Phytologist*, *205*(3), 1083–1094. https://doi.org/10.1111/nph.13134

Oddou-Muratorio, S., Davi, H., & Lefèvre, F. (2020). Integrating evolutionary, demographic and ecophysiologicalprocesses to predict the adaptive dynamics of forest tree populations under globalchange. *Tree Genetics & Genomes*, *16*(5), 67. https://doi.org/10.1007/s11295-020-01451-1

Oddou-Muratorio, S., Petit-Cailleux, C., Journé, V., Lingrand, M., Magdalou, J.-A., Hurson, C., Garrigue, J., Davi, H., & Magnanou, E. (2018). *Crown defoliation decreases reproduction and wood growth in a marginal European beech population* [Preprint]. Ecology. https://doi.org/10.1101/474874

Ogaya, R., & Peñuelas, J. (2004). Phenological patterns of *Quercus ilex, Phillyrea latifolia* , and *Arbutus unedo* growing under a field experimental drought. *Écoscience*, *11*(3), 263–270. https://doi.org/10.1080/11956860.2004.11682831

Onoda, Y., Wright, I. J., Evans, J. R., Hikosaka, K., Kitajima, K., Niinemets, Ü., Poorter, H., Tosens, T., & Westoby, M. (2017). Physiological and structural tradeoffs underlying the leaf economics spectrum. *New Phytologist*, *214*(4), 1447–1463. https://doi.org/10.1111/nph.14496

Osnas, J. L. D., Lichstein, J. W., Reich, P. B., & Pacala, S. W. (2013). Global Leaf Trait Relationships: Mass, Area, and the Leaf Economics Spectrum. *Science*, *340*(6133), 741–744. https://doi.org/10.1126/science.1231574

O'sullivan, O. S., Heskel, M. A., Reich, P. B., Tjoelker, M. G., Weerasinghe, L. K., Penillard, A., Zhu, L., Egerton, J. J. G., Bloomfield, K. J., Creek, D., Bahar, N. H. A., Griffin, K. L., Hurry, V., Meir, P., Turnbull, M. H., & Atkin, O. K. (2017). Thermal limits of leaf metabolism across biomes. *Global Change Biology*, *23*(1), 209–223. https://doi.org/10.1111/gcb.13477

Palacio, S., Paterson, E., Hester, A. J., Nogués, S., Lino, G., Anadon-Rosell, A., Maestro, M., & Millard, P. (2020). No preferential carbon-allocation to storage over growth in

clipped birch and oak saplings. *Tree Physiology*, *40*(5), 621–636. https://doi.org/10.1093/treephys/tpaa011

Parker, G. A., & Smith, J. M. (1990). Optimality theory in evolutionary biology. *Nature*, *348*(6296), 27–33. https://doi.org/10.1038/348027a0

Phillips, O. L., Aragao, L. E. O. C., Lewis, S. L., Fisher, J. B., Lloyd, J., Lopez-Gonzalez, G., Malhi, Y., Monteagudo, A., Peacock, J., Quesada, C. A., van der Heijden, G., Almeida, S., Amaral, I., Arroyo, L., Aymard, G., Baker, T. R., Banki, O., Blanc, L., Bonal, D., … Torres-Lezama, A. (2009). Drought Sensitivity of the Amazon Rainforest. *Science*, *323*(5919), 1344–1347. https://doi.org/10.1126/science.1164033

Piper, F. I. (2020). Decoupling between growth rate and storage remobilization in broadleaf temperate tree species. *Functional Ecology*, *34*(6), 1180–1192. https://doi.org/10.1111/1365-2435.13552

Piper, F. I., & Fajardo, A. (2016). Carbon dynamics of *Acer pseudoplatanus* seedlings under drought and complete darkness. *Tree Physiology*, treephys;tpw063v1. https://doi.org/10.1093/treephys/tpw063

Piper, F. I., Fajardo, A., & Hoch, G. (2017). Single-provenance mature conifers show higher non-structural carbohydrate storage and reduced growth in a drier location. *Tree Physiology*, *37*(8), 1001–1010. https://doi.org/10.1093/treephys/tpx061

Piper, F. I., & Paula, S. (2020). The Role of Nonstructural Carbohydrates Storage in Forest Resilience under Climate Change. *Current Forestry Reports*, *6*(1), 1–13. https://doi.org/10.1007/s40725-019-00109-z

Piper, F. I., & Reyes, A. (2020). Does microwaving or freezing reduce the losses of non-structural carbohydrates during plant sample processing? *Annals of Forest Science*, *77*(2), 34. https://doi.org/10.1007/s13595-020-00935-3

Poorter, L., & Kitajima, K. (2007). Carbohydrate storage and light requirements of tropical moist and dry forest tree species. *Ecology*, *88*(4), 1000–1011. https://doi.org/10.1890/06-0984

Post, E. (2019). *Time in ecology*. Princeton University Press.

Pugliese, A., & Kozlowski, J. (1990). Optimal patterns of growth and reproduction for perennial plants with persisting or not persisting vegetative parts. *Evolutionary Ecology*, *4*(1), 75–89. https://doi.org/10.1007/BF02270717

Qi, Y., Wei, W., Chen, C., & Chen, L. (2019). Plant root-shoot biomass allocation over diverse biomes: A global synthesis. *Global Ecology and Conservation*, *18*, e00606. https://doi.org/10.1016/j.gecco.2019.e00606

Qie, L., Lewis, S. L., Sullivan, M. J. P., Lopez-Gonzalez, G., Pickavance, G. C., Sunderland, T., Ashton, P., Hubau, W., Abu Salim, K., Aiba, S.-I., Banin, L. F., Berry, N., Brearley, F. Q., Burslem, D. F. R. P., Dančák, M., Davies, S. J., Fredriksson, G., Hamer, K. C., Hédl, R., … Phillips, O. L. (2017). Long-term carbon sink in Borneo's forests halted by drought and vulnerable to edge effects. *Nature Communications*, *8*(1), 1966. https://doi.org/10.1038/s41467-017-01997-0

Quentin, A. G., Pinkard, E. A., Ryan, M. G., Tissue, D. T., Baggett, L. S., Adams, H. D., Maillard, P., Marchand, J., Landhäusser, S. M., Lacointe, A., Gibon, Y., Anderegg, W. R. L., Asao, S., Atkin, O. K., Bonhomme, M., Claye, C., Chow, P. S., Clément-Vidal, A., Davies, N.

W., … Woodruff, D. R. (2015). Non-structural carbohydrates in woody plants compared among laboratories. *Tree Physiology*, tpv073. https://doi.org/10.1093/treephys/tpv073

R Core Team. (2018). *R: A Language and Environment for Statistical Computing*. R Foundation for Statistical Computing. https://www.R-project.org/

Raupach, M. (2005). 19 Dynamics and Optimality in Coupled Terrestrial Energy, Water, Carbon and Nutrient Cycles. *Predictions in Ungauged Basins: International Perspectives on the State of the Art and Pathways Forward*, *301*, 223.

Reich, P. B. (2014). The world-wide 'fast-slow' plant economics spectrum: A traits manifesto. *Journal of Ecology*, *102*(2), 275–301. https://doi.org/10.1111/1365-2745.12211

Reichstein, M., Bahn, M., Ciais, P., Frank, D., Mahecha, M. D., Seneviratne, S. I., Zscheischler, J., Beer, C., Buchmann, N., Frank, D. C., Papale, D., Rammig, A., Smith, P., Thonicke, K., van der Velde, M., Vicca, S., Walz, A., & Wattenbach, M. (2013). Climate extremes and the carbon cycle. *Nature*, *500*(7462), 287–295. https://doi.org/10.1038/nature12350

Reichstein, M., Camps-Valls, G., Stevens, B., Jung, M., Denzler, J., Carvalhais, N., & Prabhat. (2019). Deep learning and process understanding for data-driven Earth system science. *Nature*, *566*(7743), 195–204. https://doi.org/10.1038/s41586-019-0912-1

Reyes-Bahamonde, C., Piper, F. I., & Cavieres, L. A. (2021). Carbon allocation to growth and storage depends on elevation provenance in an herbaceous alpine plant of Mediterranean climate. *Oecologia*, *195*(2), 299–312. https://doi.org/10.1007/s00442-020-04839-x

Reynolds, J. F., & Thornley, J. H. M. (1982). A shoot: Root partitioning model. *Annals of Botany*, *49*(September 1981), 585–597.

Richardson, A. D., Carbone, M. S., Huggett, B. A., Furze, M. E., Czimczik, C. I., Walker, J. C., Xu, X., Schaberg, P. G., & Murakami, P. (2015). Distribution and mixing of old and new nonstructural carbon in two temperate trees. *New Phytologist*, *206*(2), 590–597. https://doi.org/10.1111/nph.13273

Richardson, A. D., Carbone, M. S., Keenan, T. F., Czimczik, C. I., Hollinger, D. Y., Murakami, P., Schaberg, P. G., & Xu, X. (2013). Seasonal dynamics and age of stemwood nonstructural carbohydrates in temperate forest trees. *New Phytologist*, *197*(3), 850–861. https://doi.org/10.1111/nph.12042

Rosas, T., Galiano, L., Ogaya, R., Peñuelas, J., & Martínez-Vilalta, J. (2013). Dynamics of non-structural carbohydrates in three Mediterranean woody species following long-term experimental drought. *Frontiers in Plant Science*, *4*. https://doi.org/10.3389/fpls.2013.00400

Rose, K. E., Atkinson, R. L., Turnbull, L. A., & Rees, M. (2009). The costs and benefits of fast living. *Ecology Letters*, *12*(12), 1379–1384. https://doi.org/10.1111/j.1461-0248.2009.01394.x

Rosen, R. (2000). *Essays on life itself*. Columbia University Press.

Rosen, R. (2012). Anticipatory Systems. In R. Rosen (Ed.), *Anticipatory Systems: Philosophical, Mathematical, and Methodological Foundations* (pp. 313–370). Springer. https://doi.org/10.1007/978-1-4614-1269-4_6

Rowland, L., da Costa, A. C. L., Galbraith, D. R., Oliveira, R. S., Binks, O. J., Oliveira, A. A. R., Pullen, A. M., Doughty, C. E., Metcalfe, D. B., Vasconcelos, S. S., Ferreira, L. V., Malhi, Y., Grace, J., Mencuccini, M., & Meir, P. (2015). Death from drought in tropical forests is triggered by hydraulics not carbon starvation. *Nature*, *528*(7580), 119–122. https://doi.org/10.1038/nature15539

Roy, S., & Mathur, P. (2021). Delineating the mechanisms of elevated CO2 mediated growth, stress tolerance and phytohormonal regulation in plants. *Plant Cell Reports*. https://doi.org/10.1007/s00299-021-02738-w

Ruehr, N. K., Grote, R., Mayr, S., & Arneth, A. (2019). Beyond the extreme: Recovery of carbon and water relations in woody plants following heat and drought stress. *Tree Physiology*, *39*(8), 1285–1299. https://doi.org/10.1093/treephys/tpz032

Ruelland, E., Vaultier, M. N., Zachowski, A., & Hurry, V. (2009). Chapter 2 Cold Signalling and Cold Acclimation in Plants. In *Advances in Botanical Research* (1st ed., Vol. 49, Issue C). Elesvier Ltd. https://doi.org/10.1016/S0065-2296(08)00602-2

Rüger, N., Comita, L. S., Condit, R., Purves, D., Rosenbaum, B., Visser, M. D., Wright, S. J., & Wirth, C. (2018). Beyond the fast–slow continuum: Demographic dimensions structuring a tropical tree community. *Ecology Letters*, *21*(7), 1075–1084. https://doi.org/10.1111/ele.12974

Rüger, N., Condit, R., Dent, D. H., DeWalt, S. J., Hubbell, S. P., Lichstein, J. W., Lopez, O. R., Wirth, C., & Farrior, C. E. (2020). Demographic trade-offs predict tropical forest dynamics. *Science*, *368*(6487), 165–168. https://doi.org/10.1126/science.aaz4797

Running, S. W., & Coughlan, J. C. (1988). A general model of forest ecosystem processes for regional applications I. Hydrologic balance, canopy gas exchange and primary production processes. *Ecological Modelling*, *42*(2), 125–154. https://doi.org/10.1016/0304-3800(88)90112-3

Ryan, M. G. (2011). Tree responses to drought. *Tree Physiology*, *31*(3), 237–239. https://doi.org/10.1093/treephys/tpr022

Sala, A., & Hoch, G. (2009). Height-related growth declines in ponderosa pine are not due to carbon limitation. *Plant, Cell & Environment*, *32*(1), 22–30. https://doi.org/10.1111/j.1365-3040.2008.01896.x

Sala, A., Piper, F., & Hoch, G. (2010). Physiological mechanisms of drought-induced tree mortality are far from being resolved. *New Phytologist*, *186*(2), 274–281. https://doi.org/10.1111/j.1469-8137.2009.03167.x

Sala, A., Woodruff, D. R., & Meinzer, F. C. (2012). Carbon dynamics in trees: Feast or famine? *Tree Physiology*, *32*(6), 764–775. https://doi.org/10.1093/treephys/tpr143

Schwalm, C. R., Anderegg, W. R. L., Michalak, A. M., Fisher, J. B., Biondi, F., Koch, G., Litvak, M., Ogle, K., Shaw, J. D., Wolf, A., Huntzinger, D. N., Schaefer, K., Cook, R., Wei, Y., Fang, Y., Hayes, D., Huang, M., Jain, A., & Tian, H. (2017). Global patterns of drought recovery. *Nature*, *548*(7666), 202–205. https://doi.org/10.1038/nature23021

Sheffield, J., & Wood, E. F. (2008). Projected changes in drought occurrence under future global warming from multi-model, multi-scenario, IPCC AR4 simulations. *Climate Dynamics*, *31*(1), 79–105. https://doi.org/10.1007/s00382-007-0340-z

Shinozaki, K., Yoda, K., Hozumi, K., & Kira, T. (1964). A quantitative analysis of plant form-the pipe model theory: I. Basic analyses. *Japanese Journal of Ecology*, *14*(3), 97–105.

Shugart, H. H., & Noble, I. R. (1981). A computer model of succession and fire response of the high-altitude Eucalyptus forest of the Brindabella Range, Australian Capital Territory. *Austral Ecology*, *6*(2), 149–164. https://doi.org/10.1111/j.1442-9993.1981.tb01286.x

Signori-Müller, C., Oliveira, R. S., Barros, F. de V., Tavares, J. V., Gilpin, M., Diniz, F. C., Zevallos, M. J. M., Yupayccana, C. A. S., Acosta, M., Bacca, J., Chino, R. S. C., Cuellar, G. M. A., Cumapa, E. R. M., Martinez, F., Mullisaca, F. M. P., Nina, A., Sanchez, J. M. B., da Silva, L. F., Tello, L., … Galbraith, D. (2021). Non-structural carbohydrates mediate seasonal water stress across Amazon forests. *Nature Communications*, *12*(1), 2310. https://doi.org/10.1038/s41467-021-22378-8

Silpi, U., Lacointe, A., Kasempsap, P., Thanysawanyangkura, S., Chantuma, P., Gohet, E., Musigamart, N., Clement, A., Ameglio, T., & Thaler, P. (2007). Carbohydrate reserves as a competing sink: Evidence from tapping rubber trees. *Tree Physiology*, *27*(6), 881–889. https://doi.org/10.1093/treephys/27.6.881

Sinclair, T. R., Tanner, C. B., & Bennett, J. M. (1984). Water-Use Efficiency in Crop Production. *BioScience*, *34*(1), 36–40. https://doi.org/10.2307/1309424

Sitch, S., Friedlingstein, P., Gruber, N., Jones, S. D., Murray-Tortarolo, G., Ahlström, A., Doney, S. C., Graven, H., Heinze, C., Huntingford, C., Levis, S., Levy, P. E., Lomas, M., Poulter, B., Viovy, N., Zaehle, S., Zeng, N., Arneth, A., Bonan, G., … Myneni, R. (2015).

Recent trends and drivers of regional sources and sinks of carbon dioxide. *Biogeosciences*, *12*(3), 653–679. https://doi.org/10.5194/bg-12-653-2015

Skelton, R. P., West, A. G., & Dawson, T. E. (2015). Predicting plant vulnerability to drought in biodiverse regions using functional traits. *Proceedings of the National Academy of Sciences*, *112*(18), 5744–5749. https://doi.org/10.1073/pnas.1503376112

Smith, & Maynard, J. (1978). Optimization Theory In Evolution. *Annual Review of Ecology and Systematics*, *9*, 31–56. https://doi.org/10.1007/b130886

Smith, W. K., Biederman, J. A., Scott, R. L., Moore, D. J. P., He, M., Kimball, J. S., Yan, D., Hudson, A., Barnes, M. L., MacBean, N., Fox, A. M., & Litvak, M. E. (2018). Chlorophyll Fluorescence Better Captures Seasonal and Interannual Gross Primary Productivity Dynamics Across Dryland Ecosystems of Southwestern North America. *Geophysical Research Letters*, *45*(2), 748–757. https://doi.org/10.1002/2017GL075922

Sopory, S. (Ed.). (2019). *Sensory Biology of Plants*. Springer Singapore. https://doi.org/10.1007/978-981-13-8922-1

Sperry, J. S., & Love, D. M. (2015). What plant hydraulics can tell us about responses to climate-change droughts. *New Phytologist*, *207*(1), 14–27. https://doi.org/10.1111/nph.13354

Sperry, J. S., & Sullivan, J. E. M. (1992). Xylem Embolism in Response to Freeze-Thaw Cycles and Water Stress in Ring-Porous, Diffuse-Porous, and Conifer Species. *Plant Physiology*, *100*(2), 605–613. https://doi.org/10.1104/pp.100.2.605

Sprugel, D. G., Hinckley, T. M., & Schaap, W. (1991). The theory and practice of branch autonomy. *Annual Review of Ecology and Systematics*, *22*(1), 309–334.

Stearns, S. C. (1989). Trade-Offs in Life-History Evolution. *Functional Ecology*, *3*(3), 259. https://doi.org/10.2307/2389364

Stengel, R. F. (2012). *Optimal Control and Estimation*. Dover.

Swenson, N. G., Hulshof, C. M., Katabuchi, M., & Enquist, B. J. (2020). Long-term shifts in the functional composition and diversity of a tropical dry forest: A 30-yr study. *Ecological Monographs*, *90*(3). https://doi.org/10.1002/ecm.1408

Tagkopoulos, I., Liu, Y.-C., & Tavazoie, S. (2008). Predictive Behavior Within Microbial Genetic Networks. *Science*, *320*(5881), 1313–1317. https://doi.org/10.1126/science.1154456

Tardieu, F., Granier, C., & Muller, B. (2011). Water deficit and growth. Co-ordinating processes without an orchestrator? *Current Opinion in Plant Biology*, *14*(3), 283–289. https://doi.org/10.1016/j.pbi.2011.02.002

Tardieu, F., & Simonneau, T. (1998). Variability among species of stomatal control under fluctuating soil water status and evaporative demand: Modelling isohydric and anisohydric behaviours. *Journal of Experimental Botany*, *49*(SPEC. ISS.), 419–432. Scopus. https://www.scopus.com/inward/record.uri?eid=2-s2.0-0031918674&partnerID=40&md5=3eea820f81c9e887186a9412f88e73ec

Thomas, R. Q., & Williams, M. (2014). A model using marginal efficiency of investment to analyze carbon and nitrogen interactions in terrestrial ecosystems (ACONITE Version

1). *Geoscientific Model Development*, *7*(5), 2015–2037. https://doi.org/10.5194/gmd-7-2015-2014

Thornley, J. H. M. (1972). A Model to Describe the Partitioning of Photosynthate during Vegetative Plant Growth. *Annals of Botany*, *36*(2), 419–430. https://doi.org/10.1093/oxfordjournals.aob.a084601

Tixier, A., Gambetta, G. A., Godfrey, J., Orozco, J., & Zwieniecki, M. A. (2019). Non-structural Carbohydrates in Dormant Woody Perennials; The Tale of Winter Survival and Spring Arrival. *Frontiers in Forests and Global Change*, *2*, 18. https://doi.org/10.3389/ffgc.2019.00018

Tixier, A., Guzmán-Delgado, P., Sperling, O., Amico Roxas, A., Laca, E., & Zwieniecki, M. A. (2020). Comparison of phenological traits, growth patterns, and seasonal dynamics of non-structural carbohydrate in Mediterranean tree crop species. *Scientific Reports*, *10*(1), 347. https://doi.org/10.1038/s41598-019-57016-3

Tomasella, M., Casolo, V., Aichner, N., Petruzzellis, F., Savi, T., Trifilò, P., & Nardini, A. (2019). Non-structural carbohydrate and hydraulic dynamics during drought and recovery in Fraxinus ornus and Ostrya carpinifolia saplings. *Plant Physiology and Biochemistry*, *145*, 1–9. https://doi.org/10.1016/j.plaphy.2019.10.024

Tomasella, M., Häberle, K.-H., Nardini, A., Hesse, B., Machlet, A., & Matyssek, R. (2017). Post-drought hydraulic recovery is accompanied by non-structural carbohydrate depletion in the stem wood of Norway spruce saplings. *Scientific Reports*, *7*(1), 14308. https://doi.org/10.1038/s41598-017-14645-w

Tomasella, M., Petrussa, E., Petruzzellis, F., Nardini, A., & Casolo, V. (2020). The Possible Role of Non-Structural Carbohydrates in the Regulation of Tree Hydraulics. *International Journal of Molecular Sciences*, *21*(1), 144. https://doi.org/10.3390/ijms21010144

Trugman, A. T., Detto, M., Bartlett, M. K., Medvigy, D., Anderegg, W. R. L., Schwalm, C., Schaffer, B., & Pacala, S. W. (2018). Tree carbon allocation explains forest drought-kill and recovery patterns. *Ecology Letters*, *21*(10), 1552–1560. https://doi.org/10.1111/ele.13136

Trumbore, S., Czimczik, C. I., Sierra, C. A., Muhr, J., & Xu, X. (2015). Non-structural carbon dynamics and allocation relate to growth rate and leaf habit in California oaks. *Tree Physiology*, *35*(11), 1206–1222. Scopus. https://doi.org/10.1093/treephys/tpv097

Tyree, M. T., & Sperry, J. S. (1989). Vulnerability of Xylem to Cavitation and Embolism. *Annual Review of Plant Biology*, *40*(1), 20.

Vacchiano, G., Ascoli, D., Berzaghi, F., Lucas-Borja, M. E., Caignard, T., Collalti, A., Mairota, P., Palaghianu, C., Reyer, C. P. O., Sanders, T. G. M., Schermer, E., Wohlgemuth, T., & Hacket-Pain, A. (2018). Reproducing reproduction: How to simulate mast seeding in forest models. *Ecological Modelling*, *376*, 40–53. https://doi.org/10.1016/j.ecolmodel.2018.03.004

van der Werf, A., Visser, A. J., Schieving, F., & Lambers, H. (1993). Evidence for Optimal Partitioning of Biomass and Nitrogen at a Range of Nitrogen Availabilities for a Fast- and Slow-Growing Species. *Functional Ecology*, *7*(1), 63. https://doi.org/10.2307/2389868

Vander Mijnsbrugge, K., Turcsan, A., Moreels, S., Van Goethem, M., Meeus, S., & Van der Aa, B. (2019). Does Drought Stress on Seedlings Have Longer Term Effects on Sapling Phenology, Reshooting, Growth and Plant Architecture in Quercus robur, Q. petraea and Their Morphological Intermediates? *Forests*, *10*(11), 1012. https://doi.org/10.3390/f10111012

Vanoni, M., Bugmann, H., Nötzli, M., & Bigler, C. (2016). Drought and frost contribute to abrupt growth decreases before tree mortality in nine temperate tree species. *Forest Ecology and Management*, *382*, 51–63. https://doi.org/10.1016/j.foreco.2016.10.001

Vargas, R., Trumbore, S. E., & Allen, M. F. (2009). Evidence of old carbon used to grow new fine roots in a tropical forest. *New Phytologist*, *182*(3), 710–718. https://doi.org/10.1111/j.1469-8137.2009.02789.x

Vieira, T. O., Santiago, L. S., Pestana, I. A., Ávila-Lovera, E., Silva, J. L. A., & Vitória, A. P. (2021). Species-specific performance and trade-off between growth and survival in the early-successional light-demanding group. *Photosynthetica*, *59*(1), 203–214. https://doi.org/10.32615/ps.2021.013

Vincent, T. L., & Pulliam, H. R. (1980). Evolution of life history strategies for an asexual annual plant model. *Theoretical Population Biology*, *17*(2), 215–231. https://doi.org/10.1016/0040-5809(80)90007-6

von Felten, S., Hättenschwiler, S., Saurer, M., & Siegwolf, R. (2007). Carbon allocation in shoots of alpine treeline conifers in a CO2 enriched environment. *Trees*, *21*(3), 283–294. https://doi.org/10.1007/s00468-006-0118-7

Walters, M. B., & Reich, P. B. (1996). Are Shade Tolerance, Survival, and Growth Linked? Low Light and Nitrogen Effects on Hardwood Seedlings. *Ecology*, *77*(3), 841–853. https://doi.org/10.2307/2265505

Wang, A.-Y., Han, S.-J., Zhang, J.-H., Wang, M., Yin, X.-H., Fang, L.-D., Yang, D., & Hao, G.-Y. (2018). The interaction between nonstructural carbohydrate reserves and xylem hydraulics in Korean pine trees across an altitudinal gradient. *Tree Physiology*, *38*(12), 1792–1804. Scopus. https://doi.org/10.1093/treephys/tpy119

Weinstein, D. A., Beloin, M., & Yanai, R. Q. (1991). Modeling changes in red spruce carbon balance and allocation in response to interacting ozone and nutrient stresses. *Tree Physiology*, *9*(1–2), 21.

Wenk, E. H., & Falster, D. S. (2015). Quantifying and understanding reproductive allocation schedules in plants. *Ecology and Evolution*, *5*(23), 5521–5538. https://doi.org/10.1002/ece3.1802

Wermelinger, B., Baumgärtner, J., & Gutierrez, A. P. (1991). A demographic model of assimilation and allocation of carbon and nitrogen in grapevines. *Ecological Modelling*, *53*, 1–26. https://doi.org/10.1016/0304-3800(91)90138-Q

Wickham, H., Averick, M., Bryan, J., Chang, W., McGowan, L., François, R., Grolemund, G., Hayes, A., Henry, L., Hester, J., Kuhn, M., Pedersen, T., Miller, E., Bache, S., Müller, K., Ooms, J., Robinson, D., Seidel, D., Spinu, V., … Yutani, H. (2019). Welcome to the Tidyverse. *Journal of Open Source Software*, *4*(43), 1686. https://doi.org/10.21105/joss.01686

Wiener, N. (2019). *Cybernetics or Control and Communication in the Animal and the Machine*. MIT press.

Wiley, E. (2020). Do Carbon Reserves Increase Tree Survival during Stress and Following Disturbance? *Current Forestry Reports*, *6*(1), 14–25. https://doi.org/10.1007/s40725-019-00106-2

Wiley, E., & Helliker, B. (2012). A re-evaluation of carbon storage in trees lends greater support for carbon limitation to growth. *New Phytologist*, *195*(2), 285–289. https://doi.org/10.1111/j.1469-8137.2012.04180.x

Wiley, E., Hoch, G., & Landhäusser, S. M. (2017). Dying piece by piece: Carbohydrate dynamics in aspen (Populus tremuloides) seedlings under severe carbon stress. *Journal of Experimental Botany*, *68*(18), 5221–5232. https://doi.org/10.1093/jxb/erx342

Wilkinson, S., & Davies, W. J. (2002). ABA-based chemical signalling: The co-ordination of responses to stress in plants: ABA-based chemical signalling. *Plant, Cell & Environment*, *25*(2), 195–210. https://doi.org/10.1046/j.0016-8025.2001.00824.x

Williams, A. P., Allen, C. D., Macalady, A. K., Griffin, D., Woodhouse, C. A., Meko, D. M., Swetnam, T. W., Rauscher, S. A., Seager, R., Grissino-Mayer, H. D., Dean, J. S., Cook, E. R., Gangodagamage, C., Cai, M., & McDowell, N. G. (2013). Temperature as a potent driver of regional forest drought stress and tree mortality. *Nature Climate Change*, *3*(3), 292–297. https://doi.org/10.1038/nclimate1693

Wolf, A., Anderegg, W. R. L., & Pacala, S. W. (2016). Optimal stomatal behavior with competition for water and risk of hydraulic impairment. *Proceedings of the National*

Academy of Sciences, *113*(46), E7222–E7230. https://doi.org/10.1073/pnas.1615144113

Woodruff, D. R., & Meinzer, F. C. (2011). Water stress, shoot growth and storage of non-structural carbohydrates along a tree height gradient in a tall conifer: Growth, water stress and carbohydrate storage. *Plant, Cell & Environment*, *34*(11), 1920–1930. https://doi.org/10.1111/j.1365-3040.2011.02388.x

Wright, I. J., Reich, P. B., Westoby, M., Ackerly, D. D., Baruch, Z., Bongers, F., Cavender-Bares, J., Chapin, T., Cornelissen, J. H. C., Diemer, M., Flexas, J., Garnier, E., Groom, P. K., Gulias, J., Hikosaka, K., Lamont, B. B., Lee, T., Lee, W., Lusk, C., … Villar, R. (2004). The worldwide leaf economics spectrum. *Nature*, *428*(6985), 821–827. https://doi.org/10.1038/nature02403

Wu, X., Du, X., Fang, S., Kang, J., Xia, Z., & Guo, Q. (2020). Impacts of competition and nitrogen addition on plant stoichiometry and non-structural carbohydrates in two larch species. *Journal of Forestry Research*. https://doi.org/10.1007/s11676-020-01236-1

Wu, Y., Kaiser, A. D., Jiang, Y., & Alber, M. S. (2009). Periodic reversal of direction allows Myxobacteria to swarm. *Proceedings of the National Academy of Sciences*, *106*(4), 1222–1227. https://doi.org/10.1073/pnas.0811662106

Würth, M. K. R., Peláez-Riedl, S., Wright, S. Joseph., & Körner, C. (2005). Non-structural carbohydrate pools in a tropical forest. *Oecologia*, *143*(1), 11–24. https://doi.org/10.1007/s00442-004-1773-2

Yang, B., Peng, C., Zhu, Q., Zhou, X., Liu, W., Duan, M., Wang, H., Liu, Z., Guo, X., & Wang, M. (2019). The effects of persistent drought and waterlogging on the dynamics of nonstructural carbohydrates of Robinia pseudoacacia L. seedlings in Northwest China. *Forest Ecosystems*, *6*(1), 23. https://doi.org/10.1186/s40663-019-0181-3

Yang, Y., Saatchi, S. S., Xu, L., Yu, Y., Choi, S., Phillips, N., Kennedy, R., Keller, M., Knyazikhin, Y., & Myneni, R. B. (2018). Post-drought decline of the Amazon carbon sink. *Nature Communications*, *9*(1), 3172. https://doi.org/10.1038/s41467-018-05668-6

Yiou, P., & Viovy, N. (2020). *Modelling the Ruin of Forests under Climate Hazards* [Preprint]. Earth system interactions with the biosphere: ecosystems. https://doi.org/10.5194/esd-2020-78

Zhang, P., Zhou, X., Fu, Y., Shao, J., Zhou, L., Li, S., Zhou, G., Hu, Z., Hu, J., Bai, S. H., & McDowell, N. G. (2020). Differential effects of drought on nonstructural carbohydrate storage in seedlings and mature trees of four species in a subtropical forest. *Forest Ecology and Management*, *469*, 118159. https://doi.org/10.1016/j.foreco.2020.118159

Zhu, S.-D., Chen, Y.-J., Ye, Q., He, P.-C., Liu, H., Li, R.-H., Fu, P.-L., Jiang, G.-F., & Cao, K.-F. (2018). Leaf turgor loss point is correlated with drought tolerance and leaf carbon economics traits. *Tree Physiology*, *38*(5), 658–663. https://doi.org/10.1093/treephys/tpy013

Zhu, S.-D., Song, J.-J., Li, R.-H., & Ye, Q. (2013). Plant hydraulics and photosynthesis of 34 woody species from different successional stages of subtropical forests: Hydraulics

and photosynthesis of subtropical plants. *Plant, Cell & Environment*, *36*(4), 879–891. https://doi.org/10.1111/pce.12024

Zohner, C. M., Mo, L., Renner, S. S., Svenning, J.-C., Vitasse, Y., Benito, B. M., Ordonez, A., Baumgarten, F., Bastin, J.-F., Sebald, V., Reich, P. B., Liang, J., Nabuurs, G.-J., de-Miguel, S., Alberti, G., Antón-Fernández, C., Balazy, R., Brändli, U.-B., Chen, H. Y. H., … Crowther, T. W. (2020). Late-spring frost risk between 1959 and 2017 decreased in North America but increased in Europe and Asia. *Proceedings of the National Academy of Sciences*, *117*(22), 12192–12200. https://doi.org/10.1073/pnas.1920816117